

TWO-PHASE FLOW MODELING IN
CIRCULAR PIPES

MOHAMED MAHMOUD AWAD





Library and
Archives Canada

Bibliothèque et
Archives Canada

Published Heritage
Branch

Direction du
Patrimoine de l'édition

395 Wellington Street
Ottawa ON K1A 0N4
Canada

395, rue Wellington
Ottawa ON K1A 0N4
Canada

Your file *Votre référence*
ISBN: 978-0-494-33469-0
Our file *Notre référence*
ISBN: 978-0-494-33469-0

NOTICE:

The author has granted a non-exclusive license allowing Library and Archives Canada to reproduce, publish, archive, preserve, conserve, communicate to the public by telecommunication or on the Internet, loan, distribute and sell theses worldwide, for commercial or non-commercial purposes, in microform, paper, electronic and/or any other formats.

The author retains copyright ownership and moral rights in this thesis. Neither the thesis nor substantial extracts from it may be printed or otherwise reproduced without the author's permission.

AVIS:

L'auteur a accordé une licence non exclusive permettant à la Bibliothèque et Archives Canada de reproduire, publier, archiver, sauvegarder, conserver, transmettre au public par télécommunication ou par l'Internet, prêter, distribuer et vendre des thèses partout dans le monde, à des fins commerciales ou autres, sur support microforme, papier, électronique et/ou autres formats.

L'auteur conserve la propriété du droit d'auteur et des droits moraux qui protègent cette thèse. Ni la thèse ni des extraits substantiels de celle-ci ne doivent être imprimés ou autrement reproduits sans son autorisation.

In compliance with the Canadian Privacy Act some supporting forms may have been removed from this thesis.

Conformément à la loi canadienne sur la protection de la vie privée, quelques formulaires secondaires ont été enlevés de cette thèse.

While these forms may be included in the document page count, their removal does not represent any loss of content from the thesis.

Bien que ces formulaires aient inclus dans la pagination, il n'y aura aucun contenu manquant.


Canada



**Memorial University of Newfoundland
Faculty of Engineering and Applied Science
Department of Mechanical Engineering**

**TWO-PHASE FLOW MODELING IN
CIRCULAR PIPES**

**By
@ Mohamed Mahmoud Awad
(B. Sc., M. Sc.)**

**Submitted to the School of Graduate Studies in partial
fulfillment of the requirements for the degree of Doctoral
Philosophy**

**Faculty of Engineering and Applied Science
Memorial University of Newfoundland
St. John's, Newfoundland
Canada, A1B 3X5
2007**

ABSTRACT

This thesis reviews the two-phase frictional pressure gradient and void fraction models available in the literature. New research is proposed in the area of two-phase frictional pressure gradient and void fraction, specifically, the development of new models which will enable the prediction of pressure drop and void fraction characteristics, which are important design parameter in many engineering applications such as chemical industry, nuclear industry, petroleum industry, refrigeration and air-conditioning applications, and space station applications. The new models will be simple but accurate at the same time.

Results for developing new definitions of two-phase viscosity that can be used to compute the two-phase frictional pressure gradient using the homogeneous model, giving a simple asymptotic compact model for two-phase frictional pressure gradient in horizontal pipes as well as bounds on two-phase frictional pressure gradient and void fraction in circular pipes are presented.

It is shown that the new definitions of two-phase viscosity can be used to analyze the experimental data of two-phase frictional pressure gradient in circular pipes using the homogeneous model.

It is observed that the new models accurately predict the experimental data contained in the literature and are much simpler than other empirical models, which are presently available in the literature.

ACKNOWLEDGMENTS

The author acknowledges Dr. Yuri S. Muzychka who introduced me to the possibilities of analytical modeling. Also, he has been a constant source of advice and inspiration throughout the work and to whom grateful thanks are due.

The author acknowledges Dr. Thormod E. Johansen and Dr. Mahmoud R. Haddara for their guide.

The author acknowledges the financial support of Natural Sciences and Engineering Research Council of Canada (NSERC).

Finally, the author likes to express his special respect to his family, especially parents, who contributed more than anyone to his overall education. Many thanks for their unwavering love, support, encouragement, and understanding throughout the years.

During the years at Memorial University of Newfoundland (MUN), the author discovered a new country, a new culture, and a new society. So, these years have enriched the author's life.

CONTENTS

ABSTRACT	ii
ACKNOWLEDGMENTS	iii
LIST OF TABLES	vii
LIST OF FIGURES	ix
NOMENCLATURE	xii
1. INTRODUCTION	1
1.1 What is Two-Phase Flow?	1
1.2 Basic Definitions and Terminology	3
1.3 Flow Patterns in Two-Phase Flow	7
1.3.1 Flow Patterns in a Horizontal Two-Phase Flow	7
1.3.2 Flow Patterns in a Vertical Two-Phase Flow	9
1.4 Flow Pattern Maps	11
1.4.1 Flow Pattern Map in a Horizontal Two-Phase Flow	12
1.4.2 Flow Pattern Map in a Vertical Two-Phase Flow	13
1.5 Pressure Drop in Two-Phase Flow	14
1.5.1 Two-Phase Frictional Multiplier	17
1.5.2 Some Forms of Dimensionless Two-Phase Frictional Pressure Drop (Δp_f^*)	18
1.6 Methods of Analysis	20
1.6.1 Correlations	21
1.6.2 Phenomenological Models	22
1.6.3 Simple Analytical Models	23
1.6.3.1 The Homogeneous Flow Model	23
1.6.3.2 The Separated Flow Model	23
1.6.3.3 The Drift Flux Model	25
1.6.4 Other Methods	26
1.6.4.1 Integral Analysis	26
1.6.4.2 Differential Analysis	26
1.6.4.3 Computational Fluid Dynamics (CFD)	26
1.6.4.4 Artificial Neural Network (ANN)	27
1.7 Research Objectives	28
1.8 Outline of Thesis	29
2. LITERATURE REVIEW OF FRICTIONAL PRESSURE GRADIENT	31
2.1 Introduction	31
2.2 Review of Two-Phase Frictional Pressure Gradient Models and their Limitations	31
2.2.1 Separated Flow	31
2.2.2 The Homogeneous Model	54
2.2.2.1 The Homogeneous Model with Correction for Two-Dimensional	

CONTENTS

Effects	72
2.2.3 Other Correlations	73
2.2.4 Experimental Study	86
2.2.5 Computer Study	112
2.3 Comparison of Selected Two-Phase Frictional Pressure Gradient Flow Models	114
2.4 Summary	117
3. LITERATURE REVIEW OF VOID FRACTION	127
3.1 Introduction	127
3.2 Review of Two-Phase Void Fraction Models and their Limitations	127
3.3 Comparison of Selected Two-Phase Flow Void Fraction Models	174
3.4 Summary	176
4. HOMOGENEOUS TWO-PHASE FLOW PROPERTIES	183
4.1 Introduction	183
4.2 Proposed Methodology	189
4.3 Results and Discussion	193
4.3.1 Fanning friction factor (f_m) versus Reynolds number (Re_m) in Circular Pipes	194
4.3.2 Fanning friction factor (f_m) versus Reynolds number (Re_m) in Minichannels and Microchannels	197
4.4 Summary	201
5. ASYMPTOTIC METHODS IN TWO-PHASE FLOW	202
5.1 Introduction	202
5.2 The Separate Cylinders Model of Two-Phase Flow	202
5.3 Asymptotic Analysis	212
5.3.1 Asymptotic Behavior	212
5.3.2 Superposition of Asymptotes	214
5.4 Asymptotic Methods in Two-Phase Flow	216
5.4.1 Single-Phase Frictional Pressure Gradient Equations	218
5.5 Results and Discussion	220
5.5.1 Comparison of the Present Asymptotic Model with Data	220
5.5.2 Effect of Mass Flux on the Frictional Pressure Gradient	223
5.5.3 Comparison of the Present Asymptotic Model [200] with Other Correlations	224
5.5.4. ϕ_l and ϕ_g versus Lockhart-Martinelli Parameter (X) in Circular Pipes	227
5.5.5. ϕ_l and ϕ_g versus Lockhart-Martinelli Parameter (X) in Minichannels and Microchannels	233
5.6 Summary	237
6. BOUNDS ON TWO-PHASE FLOW	239
6.1 Introduction	239
6.2 Development of Bounds on Two-Phase Frictional Pressure Gradient in Circular Pipes	239

CONTENTS

6.2.1 Large Circular Pipes	240
6.2.1.1 The Lower Bound	241
6.2.1.2 The Upper Bound	243
6.2.1.3 Mean Model	244
6.2.2 Small Circular Pipes	245
6.2.2.1 The Lower Bound	245
6.2.2.2 The Upper Bound	248
6.2.2.3 Mean Model	249
6.2.3 Results and Discussion	250
6.2.3.1 Two-Phase Frictional Pressure Gradient	250
6.2.3.2 ϕ_l and ϕ_g versus Lockhart-Martinelli Parameter (X)	255
6.3 Development of Bounds on Two-Phase Void Fraction in Circular Pipes	266
6.3.1 The Lower Bound	266
6.3.2 The Upper Bound	267
6.3.3 Mean Model	268
6.3.4 Results and Discussion	268
6.3.4.1 Comparison of the Present Model with Data	269
6.3.4.2 α and $(1-\alpha)$ versus Lockhart-Martinelli Parameter (X)	272
6.4 Summary	276
7. SUMMARY AND CONCLUSIONS	278
7.1 Summary of Present Research	278
7.2 Areas for Future Research	280
REFERENCES	283
APPENDIX A: LIST OF RESEARCH PAPERS	309

LIST OF TABLES

Table 1.1 Definitions of Different Two-Phase Frictional Multipliers	18
Table 2.1 Values of the Exponent (n) and the Constants C_l and C_g for Different Flow Conditions	34
Table 2.2 Equations to Calculate the Parameter (X) under Different Flow Conditions	35
Table 2.3 Values of Exponent (n) for Different Flow Types	39
Table 2.4 Values of Chisholm Constant (C) for Different Flow Types	40
Table 2.5 Values of Coefficient (B) for Smooth Tubes	44
Table 2.6 Values of a , b , and c for Different Flow Mechanisms	53
Table 2.7 A Set of Suggested Values of K and n	62
Table 2.8 Effects of Pipe Diameter and Liquid Viscosity on C	87
Table 2.9 Effect of Pipe Roughness on C , for Air-Gas Oil in 50 mm Pipes	88
Table 2.10 Summary of Pressure Drop Studies	118
Table 3.1 Values of C_A as a function of Z	134
Table 3.2 Constants for Beggs and Brill Equation for Predicting Liquid Holdup	149
Table 3.3 Values of c , q , r , and s for Different Models and Correlations	152
Table 3.4 Values of K , a , b and c for Ideal Stratified Flow	158
Table 3.5 Values of W_1 and ω_1 for Gas-Liquid, Turbulent-Laminar Ideal Stratified Flow	159
Table 3.6 Values of W_2 and ω_2 for Gas-Liquid, Laminar-Turbulent Ideal Stratified Flow	160
Table 3.7 Values of K , a , b and c for Ideal Annular Flow	160
Table 3.8 Parameters of the Universal Composite Correlations for Holdup	172
Table 3.9 Summary of Void Fraction Studies	177
Table 4.1 Analogy between Thermal Conductivity in Porous Media and Viscosity in Two-Phase Flow	190
Table 5.1 Expressions of ϕ_l^2 for Different Flow Conditions	206
Table 5.2 Expressions of ϕ_g^2 for Different Flow Conditions	207
Table 5.3 Expressions of α for Different Flow Conditions	210
Table 5.4 Expressions of $(1-\alpha)$ for Different Flow Conditions	210
Table 5.5 Comparison of Different Models with Dukler Data [202]	221
Table 5.6 Comparison of Different Models with Chisholm Data [200]	223
Table 5.7 Values of the Asymptotic Parameter (p) in Circular Pipes at Different Conditions	231
Table 5.8 Values of the Asymptotic Parameter (p) in Minichannels and Microchannels at Different Conditions	236
Table 6.1 Bounds on Two-Phase Frictional Pressure Gradient in Large Circular Pipes	276
Table 6.2 Bounds on Two-Phase Frictional Pressure Gradient in Small	

LIST OF TABLES

Circular Pipes	276
Table 6.3 Bounds on Two-Phase Void Fraction in Circular Pipes	277

LIST OF FIGURES

Figure 1.1 Flow Patterns in a Horizontal Two-Phase Flow [1]	9
Figure 1.2 Flow Patterns in a Vertical Two-Phase Flow [2]	11
Figure 1.3 Baker Flow Pattern Map for Horizontal Flow in a Pipe [5]	13
Figure 1.4 Hewitt and Roberts Flow Pattern Map for Vertical Upflow in a Pipe [2]	14
Figure 2.1 Comparison of Two-Phase Frictional Pressure Gradient Models	115
Figure 2.2 Comparison of Two-Phase Frictional Pressure Gradient Models	116
Figure 2.3 Comparison of Two-Phase Frictional Pressure Gradient Models	116
Figure 2.4 Comparison of Two-Phase Frictional Pressure Gradient Models	117
Figure 3.1 Comparison of Selected Two-Phase Flow Void Fraction Models	174
Figure 3.2 Comparison of Selected Two-Phase Flow Void Fraction Models	175
Figure 3.3 Comparison of Selected Two-Phase Flow Void Fraction Models	175
Figure 3.4 Comparison of Selected Two-Phase Flow Void Fraction Models	176
Figure 4.1 k_e/k_l versus v_2 [176]	191
Figure 4.2 μ_m/μ_l versus x	191
Figure 4.3 f_m versus Re_m in Circular Pipes Using Definition 1 of Two-Phase Viscosity	195
Figure 4.4 f_m versus Re_m in Circular Pipes Using Definition 2 of Two-Phase Viscosity	195
Figure 4.5 f_m versus Re_m in Circular Pipes Using Definition 3 of Two-Phase Viscosity	196
Figure 4.6 f_m versus Re_m in Circular Pipes Using Definition 4 of Two-Phase Viscosity	196
Figure 4.7 f_m versus Re_m in Circular Pipes Using Definition 5 of Two-Phase Viscosity	197
Figure 4.8 f_m versus Re_m in Minichannels and Microchannels Using Definition 1 of Two-Phase Viscosity	198
Figure 4.9 f_m versus Re_m in Minichannels and Microchannels Using Definition 2 of Two-Phase Viscosity	199
Figure 4.10 f_m versus Re_m in Minichannels and Microchannels Using Definition 3 of Two-Phase Viscosity	199
Figure 4.11 f_m versus Re_m in Minichannels and Microchannels Using Definition 4 of Two-Phase Viscosity	200
Figure 4.12 f_m versus Re_m in Minichannels and Microchannels Using Definition 5 of Two-Phase Viscosity	200
Figure 5.1 ϕ_l versus X for Different Flow Conditions	207
Figure 5.2 ϕ_g versus X for Different Flow Conditions	208
Figure 5.3 α versus X for Different Flow Conditions	211
Figure 5.4 $(1-\alpha)$ versus X for Different Flow Conditions	211
Figure 5.5 Comparison of the Asymptotic Model with Dukler's Data [202]	221
Figure 5.6 Comparison of the Asymptotic Model with Chisholm's Data [200]	222

LIST OF FIGURES

Figure 5.7 Effect of Mass Flux on the Frictional Pressure Gradient	224
Figure 5.8 Comparison of the Present Asymptotic Model with Other Correlations at $d = 50.8$ mm	225
Figure 5.9 Comparison of the Present Asymptotic Model with Other Correlations at $d = 27$ mm	226
Figure 5.10 Comparison of the Asymptotic Model with Dukler's Data [202]	227
Figure 5.11 Comparison of the Asymptotic Model with Chisholm's Data [200]	228
Figure 5.12 Comparison of the Present Asymptotic Model with Govier and Omer's Data [203]	228
Figure 5.13 Comparison of the Present Asymptotic Model with Janssen and Kervinen's Data [204]	229
Figure 5.14 Comparison of the Asymptotic Model with Hashizume's Data [79]	229
Figure 5.15 Comparison of the Asymptotic Model with Hashizume's Data [79]	230
Figure 5.16 Comparison of the Present Asymptotic Model with Cicchitti et al.'s Data [46]	230
Figure 5.17 Comparison of the Present Asymptotic Model with Cheremisinoff and Davis's Data [205]	231
Figure 5.18 ϕ_l versus X for Different Sets of Data	232
Figure 5.19 ϕ_g versus X for Different Sets of Data	232
Figure 5.20 Comparison of the Asymptotic Model with Lee and Lee's Data [206]	233
Figure 5.21 Comparison of the Present Asymptotic Model with Chung and Kawaji's Data [207]	234
Figure 5.22 Comparison of the Present Asymptotic Model with Kawaji et al.'s Data [208] (Gas in the Main Channel and Liquid in the Branch)	234
Figure 5.23 Comparison of the Present Asymptotic Model with Kawaji et al.'s Data [208] (Liquid in the Main Channel and Gas in the Branch)	235
Figure 5.24 Comparison of the Present Asymptotic Model with Ohtake et al.'s Data [209]	235
Figure 5.25 ϕ_l versus X for Different Sets of Data	236
Figure 5.26 ϕ_g versus X for Different Sets of Data	237
Figure 6.1 Comparison of the Present Model with Bandel's Data [12]	251
Figure 6.2 Comparison of the Present Model with Hashizume's Data [79]	252
Figure 6.3 Comparison of the Present Model with Hashizume's Data [79]	252
Figure 6.4 Comparison of the Model with Müller-Steinhagen's Data [180]	253
Figure 6.5 Comparison of the Model with Ungar and Cornwell's Data [89]	254
Figure 6.6 Comparison of the Model with Ungar and Cornwell's Data [89]	254
Figure 6.7 Comparison of the Present Model with Hashizume's Data [79]	256
Figure 6.8 Comparison of the Present Model with Hashizume's Data [79]	257
Figure 6.9 Comparison of the Present Model with Govier and Omer's Data [203]	257
Figure 6.10 Comparison of the Present Model with Janssen and Kervinen's Data [204]	258
Figure 6.11 ϕ_l versus X for Different Sets of Data	258
Figure 6.12 Comparison of the Present Model with Lee and Lee's Data [206]	259
Figure 6.13 Comparison of the Model with Chung and Kawaji's Data [207]	259

LIST OF FIGURES

Figure 6.14 Comparison of the Present Model with Kawaji et al.'s Data [208] (Gas in the Main Channel and Liquid in the Branch)	260
Figure 6.15 ϕ_l versus X for Different Sets of Data	260
Figure 6.16 Comparison of the Present Model with Cicchitti et al.'s Data [46]	263
Figure 6.17 Comparison of the Present Model with Cheremisinoff and Davis's Data [205]	263
Figure 6.18 ϕ_g versus X for Different Sets of Data	264
Figure 6.19 Comparison of the Present Model with Kawaji et al.'s Data [208] (Liquid in the Main Channel and Gas in the Branch)	264
Figure 6.20 Comparison of the Present Model with Ohtake et al.'s Data [209]	265
Figure 6.21 ϕ_g versus X for Different Sets of Data	265
Figure 6.22 Comparison of the Present Model with Larson's Data [216]	270
Figure 6.23 Comparison of the Present Model with Hashizume's Data [79]	270
Figure 6.24 Comparison of the Present Model with Hashizume's Data [79]	271
Figure 6.25 Comparison of the Present Model with Wojtan et al.'s Data [217]	271
Figure 6.26 Comparison of the Present Model with Hashizume's Data [79]	272
Figure 6.27 Comparison of the Present Model with Hashizume's Data [79]	273
Figure 6.28 α versus X for Different Sets of Data	273
Figure 6.29 Comparison of the Present Model with Bergelin and Gazley's Data [218]	274
Figure 6.30 Comparison of the Present Model with Baker's Data [3]	275
Figure 6.31 $1-\alpha$ versus X for Different Sets of Data	275

NOMENCLATURE

<i>A</i>	The pipe cross-sectional area, m ²
<i>a</i>	coefficient
<i>a</i>	Churchill parameter, Eq. (5.44)
<i>B</i>	Chisholm parameter
<i>b</i>	exponent
<i>b</i>	Churchill parameter, Eq. (5.45)
<i>B_{gd}</i>	Grönnerud's boiling number = $4q/(Gh_{fg})$
<i>Bo</i>	Bond number = $(g(\rho_l - \rho_g)(d/2)^2)/\sigma$
<i>C</i>	constant
<i>C</i>	Chisholm constant, Eqs. (2.8) and (2.9)
<i>C_A</i>	Armand coefficient, Eq. (3.1)
<i>C_{B1}</i>	Beggs and Brill parameter, Table (3.2)
<i>C_{B2}</i>	Beggs and Brill parameter, Table (3.2)
<i>C_{B3}</i>	Beggs and Brill parameter, Table (3.2)
<i>C_{B4}</i>	Beggs and Brill parameter, Eqs. (3.70)-(3.72)
<i>C_o</i>	Zuber-Findlay coefficient, Eq. (3.44)
<i>c</i>	constant in Butterworth expression, Eq. (3.80)
<i>c</i>	exponent in García et al. expression, Eq. (3.135)
<i>c</i>	constant in asymptotic solution
<i>c₁</i>	function of Froude number or constant, Eqs. (2.165)-(2.167)
<i>c₂</i>	function of Froude number or constant, Eqs. (2.165)-(2.167)
<i>Ce</i>	dimensionless number, Eq. (2.104)
<i>d</i>	pipe diameter, m
<i>d</i>	exponent in García et al. expression, Eq. (3.135)
<i>d*</i>	dimensionless pipe diameter, Eq. (3.123)
<i>E</i>	Friedel parameter, Eq. (2.119)
<i>e</i>	fraction of the liquid entrained as droplets
<i>e</i>	error
<i>E₁</i>	parameter, Eq. (3.53)
<i>E₂</i>	parameter, Eq. (3.54)
<i>E_o</i>	Eötvös number = $g d^2 (\rho_l - \rho_g)/\sigma$
<i>F</i>	Friedel parameter, Eq. (2.120)
<i>f</i>	Fanning friction factor
<i>f₀</i>	Fanning friction factor, Eq. (2.52)
<i>Fr</i>	Froude number = $G^2/(gd\rho^2)$
<i>Ft</i>	Froude rate, Eq. (3.130)
<i>f(A)</i>	function in Serizawa and Michiyoshi correlation
<i>f(B)</i>	function in Serizawa and Michiyoshi correlation, Eq. (2.29)
<i>f(C)</i>	function in Serizawa and Michiyoshi correlation
<i>G</i>	mass flux, kg/m ² .s
<i>g</i>	acceleration due to gravity, m/s ²
<i>H</i>	Friedel parameter, Eq. (2.121)
<i>H_g</i>	gas holdup fraction
<i>H_l</i>	liquid holdup fraction
<i>h_{fg}</i>	heat of evaporation, J/kg

NOMENCLATURE

i	exponent in asymptotic solution for $z \rightarrow 0$
J	mechanical equivalent of heat, 1 in SI units, Eq. (2.60)
J	Müller-Steinhagen and Heck factor, Eq. (2.144)
j	exponent in asymptotic solution for $z \rightarrow \infty$
K	dimensionless flow parameter
k	thermal conductivity, W/m.K
k	index for summation
K_f	Bo Pierre's boiling number, N/kg, Eq. (2.60)
K_2	Olujic two-phase parameter, Eq. (2.133)
K_d^*	Kutateladze number, Eq. (3.122)
k_i	constant in Chen and Spedding holdup correlation, Eq. (3.101)
L	pipe length, m
L_1	Beggs and Brill correlation boundary, Eq. (3.65)
L_2	Beggs and Brill correlation boundary, Eq. (3.66)
La	Laplace number = $\rho_l d \sigma / \mu_l^2$
Lo	dimensionless number, Eq. (2.82)
\overline{Lo}	dimensional group
M	parameter used in Chisholm correlation, Eqs. (2.14) and (2.15)
m	mass flow rate, kg/s
m	exponent
N	number of data points
n	exponent
n	Blasius index
n_1	Olujic two-phase index, Eq. (2.142)
n_2	Olujic two-phase index, Eq. (2.143)
N_d	pipe diameter influence number = $d (\rho_l g / \sigma)^{0.5}$
N_l	liquid viscosity influence number = $\mu_l (g / \rho_l \sigma^3)^{0.25}$
N_{Ug}	gas velocity influence number = $U_g (\rho_l g \sigma)^{0.25}$
N_{Ul}	liquid velocity influence number = $U_l (\rho_l g \sigma)^{0.25}$
p	pressure, Pa
p	fitting parameter
dp/dz	pressure gradient, Pa/m
Δp	pressure drop, Pa
Δp_f^*	dimensionless frictional pressure drop, Pa
Q	The total volumetric rate of flow, m ³ /s
q	The heat flux, W/m ²
q	index, Eq. (3.80)
Re	Reynolds number = Gd/μ
r	index, Eq. (3.80)
r_{ge}	radius of the separate circular cylinder carrying the gas phase
r_{le}	radius of the separate circular cylinder carrying the liquid phase
r_o	radius of the actual pipe
S	slip ratio
s	Beggs and Brill correlating factor, Eq. (2.73)
s	index, Eq. (3.80)
T	temperature, °C
t	constant in García et al. expression, Eq. (3.135)

NOMENCLATURE

U	The superficial velocity of flow, m/s
u	The average velocity of flow, m/s
u_{gj}	mean drift velocity, m/s
v	The specific volume of flow, m ³ /kg
W_1	constant in Chen and Spedding holdup correlation, Eq. (3.103)
W_2	constant in Chen and Spedding holdup correlation, Eq. (3.104)
We	Weber number = $G^2 d / \rho \sigma$
X	Lockhart-Martinelli parameter, Eq. (2.2)
x	mass quality
Y	parameter, Eq. (3.4)
y	distance from the pipe wall, m
y	Beggs and Brill correlation parameter, Eq. (2.72)
y	dependent parameter
Z	parameter, Eq. (3.21)
z	independent parameter

Greek Symbols

α	The void fraction
$\alpha(\lambda)$	ratio of two-phase Fanning friction factor to single-phase Fanning friction factor at two-phase Reynolds number, Eq. (2.53)
B	dimensionless group, Eq. (2.54)
β	The volumetric quality
δ	liquid film thickness, m
δ	constant in Bonnecaze et al. holdup correlation, Eq. (3.59)
δ_g^+	dimensionless liquid film thickness
ε	pipe roughness, m
ε_0	Olujic two-phase flow parameter Eq. (2.138)
ε_1	Olujic two-phase flow parameter Eq. (2.139)
ε_2	Olujic two-phase flow parameter Eq. (2.140)
ρ	density, kg/m ³
μ	dynamic viscosity, kg/m.s
ϕ_g^2	two-phase frictional multiplier for gas alone flow
ϕ_{go}^2	two-phase frictional multiplier for total flow assumed gas
ϕ_l^2	two-phase frictional multiplier for liquid alone flow
ϕ_{lo}^2	two-phase frictional multiplier for total flow assumed liquid
λ	dimensionless parameter used in Baker flow pattern map, Eq. (1.22)
λ	parameter used in Chisholm correlation, Eq. (2.11)
λ	ratio of the liquid volumetric flow rate to the total volumetric flow rate, Eq. (2.57)
ν	kinematic viscosity, m ² /s
ψ	dimensionless parameter used in Baker flow pattern map, Eq. (1.23)
ψ	parameter used in Chisholm correlation, Eq. (2.13)
σ	surface tension, N/m
τ	shear stress, Pa
θ	angle of inclination of pipe to horizontal

NOMENCLATURE

Ω	correction factor
ω	mass fraction of oil, Eq. (2.168)
ω_1	exponent in Chen and Spedding holdup correlation, Eq. (3.103)
ω_2	exponent in Chen and Spedding holdup correlation, Eq. (3.104)
ξ	property index, Eq. (2.30)
Γ	physical property coefficient, Eq. (2.16)
Γ_0	Olujic two-phase parameter, Eq. (2.141)
γ	Bankoff parameter, Eq. (2.109)

Subscripts

0	when $\rho_l = \rho_g$
0	corresponding to very small value
1	component 1
2	component 2
∞	corresponding to very large value
a	acceleration
air	air
asy	asymptotic
atm	atmospheric
av	average
BP	Bo Pierre
Bf	Bankoff
c	critical
$Chawla$	Chawla
e	effective
Fr	Froude
$Friedel$	Friedel
f	frictional
gd	Grønnerud
g	gas
go	gas only (all flow as gas)
$grav$	gravitational
h	hydraulic
i	interfacial
i	inlet
int	intermediate value
l	liquid
ll	laminar liquid-laminar gas flow type
lo	liquid only (all flow as liquid)
$lower$	lower
lt	laminar liquid-turbulent gas flow type
m	homogeneous mixture
max	maximum
o	outlet
oil	oil
$pure$	pure refrigerant

NOMENCLATURE

<i>R</i>	rough pipe
<i>r</i>	reduced
<i>RMS</i>	root mean square
<i>S</i>	smooth pipe
<i>s</i>	saturation
<i>tl</i>	turbulent liquid-laminar gas flow type
<i>tp</i>	two-phase
<i>tt</i>	turbulent liquid-turbulent gas flow type
<i>upper</i>	upper
<i>water</i>	water

Superscripts

$\overline{(\)}$	mean value
-------------------	------------

CHAPTER 1

INTRODUCTION

1.1 What is Two-Phase Flow?

A phase is defined as one of the states of the matter. It can be either a solid, a liquid, or a gas. Multiphase flow is the simultaneous flow of several phases. The study of multiphase flow is very important in energy-related industries and applications. The simplest case of multiphase flow is two-phase flow. Two-phase flow can be solid-liquid flow, liquid-liquid flow, gas-solid flow, and gas-liquid flow. Examples of solid-liquid flow include flow of corpuscles in the plasma, flow of mud, flow of liquid with suspended solids such as slurries, motion of liquid in aquifers. The flow of two immiscible liquids like oil and water, which is very important in oil recovery processes, is an example of liquid-liquid flow. The injection of water into the oil flowing in the pipeline reduces the resistance to flow and the pressure gradient. Thus, there is no need for large pumping units. Immiscible liquid-liquid flow has other industrial applications such as dispersive flows, liquid extraction processes, and co-extrusion flows. In dispersive flows, liquids can be dispersed into droplets by injecting a liquid through an orifice or a nozzle into another continuous liquid. The injected liquid may drip or may form a long jet at the nozzle depending upon the flow rate ratio of the injected liquid and the continuous liquid. If the flow rate ratio is small, the injected liquid may drip continuously at the nozzle outlet. For higher flow rate ratio, the injected liquid forms a

continuous jet at the end of the nozzle. In other applications, the injected liquid could be dispersed as tiny droplets into another liquid to form an emulsion. In liquid extraction processes, solutes dissolved in a liquid solution are separated by contact with another immiscible liquid. Polymer processing industry is an instance of co-extrusion flow where the products are required to manifest a steady interface to obtain superior mechanical properties. Examples of gas-solid flow include fluidized bed, and transport of powdered cement, grains, metal powders, ores, coal, and so on using pneumatic conveying. The main advantages in pneumatic conveying over other systems like conveyor belt are the continuous operation, the relative flexibility of the pipeline location to avoid obstructions or to save space, and the capability to tap the pipeline at any location to remove some or all powder.

Sometimes, the term two-component is used to describe flows in which the phases do not consist of the same chemical substance. Steam-water flow found in nuclear power plants and other power systems is an example of two-phase single-component flow. Argon-water is an instance of two-phase two-component flow. Air-water is an example of two-phase multicomponent flow. Actually, the terms two-component flow and two-phase flow are often used rather loosely in the literature to mean liquid-gas flow and liquid-vapor flow respectively. The engineers developed the terminology rather than the chemists. However, there is little danger of ambiguity.

1.2 Basic Definitions and Terminology

The total mass flow rate (m) (in kg per second) is the sum of the mass flow rate of liquid phase (m_l) and the mass flow rate of gas phase (m_g).

$$m = m_l + m_g \quad (1.1)$$

The total volumetric flow rate (Q) (in cubic meter per second) is the sum of the volumetric flow rate of liquid phase (Q_l) and the volumetric flow rate of gas phase (Q_g).

$$Q = Q_l + Q_g \quad (1.2)$$

The volumetric flow rate of liquid phase (Q_l) is related to the mass flow rate of liquid phase (m_l) as follows:

$$Q_l = \frac{m_l}{\rho_l} \quad (1.3)$$

The volumetric flow rate of gas phase (Q_g) is related to the mass flow rate of gas phase (m_g) as follows:

$$Q_g = \frac{m_g}{\rho_g} \quad (1.4)$$

The total mass flux of the flow (G) is defined the total mass flow rate (m) divided by the pipe cross-sectional area (A).

$$G = \frac{m}{A} \quad (1.5)$$

The quality (dryness fraction) (x) is defined as the ratio of the mass flow rate of gas phase (m_g) to the total mass flow rate (m).

$$x = \frac{m_g}{m} = \frac{m_g}{m_l + m_g} \quad (1.6)$$

The volumetric quality (β) is defined as the ratio of the volumetric flow rate of gas phase (Q_g) to the total volumetric flow rate (Q).

$$\beta = \frac{Q_g}{Q} = \frac{Q_g}{Q_l + Q_g} \quad (1.7)$$

The volumetric quality (β) can be related to the mass quality (x) as follows:

$$\beta = \frac{xv_g}{xv_g + (1-x)v_l} = \frac{1}{1 + \left(\frac{1-x}{x}\right) \left(\frac{\rho_g}{\rho_l}\right)} \quad (1.8)$$

The void fraction (α) is defined as the ratio of the pipe cross-sectional area (or volume) occupied by the gas phase to the pipe cross-sectional area (or volume).

$$\alpha = \frac{A_g}{A} = \frac{A_g}{A_l + A_g} \quad (1.9)$$

The superficial velocity of liquid phase flow (U_l) is the velocity if the liquid is flowing alone in the pipe. It is defined as the volumetric flow rate of liquid phase (Q_l) divided by the pipe cross-sectional area (A).

$$U_l = \frac{Q_l}{A} \quad (1.10)$$

The superficial velocity of gas phase flow (U_g) is the velocity if the gas is flowing alone in the pipe. It is defined as the volumetric flow rate of gas phase (Q_g) divided by the pipe cross-sectional area (A).

$$U_g = \frac{Q_g}{A} \quad (1.11)$$

The mixture velocity of flow (U_m) is defined as the total volumetric flow rate (Q) divided by the pipe cross-sectional area (A).

$$U_m = \frac{Q}{A} \quad (1.12)$$

The mixture velocity of flow (U_m) (in meter per second) can also be expressed in terms of the superficial velocity of liquid phase flow (U_l) and the superficial velocity of gas phase flow (U_g) as follows:

$$U_m = U_l + U_g \quad (1.13)$$

The average velocity of liquid phase flow (u_l) is defined as the volumetric flow rate of liquid phase (Q_l) divided by the pipe cross-sectional area occupied by the liquid phase flow (A_l).

$$u_l = \frac{Q_l}{A_l} = \frac{Q_l}{(1-\alpha)A} = \frac{U_l}{(1-\alpha)} \quad (1.14)$$

The average velocity of gas phase flow (u_g) is defined as the volumetric flow rate of gas phase (Q_g) divided by the pipe cross-sectional area occupied by the gas phase flow (A_g).

$$u_g = \frac{Q_g}{A_g} = \frac{Q_g}{\alpha A} = \frac{U_g}{\alpha} \quad (1.15)$$

In order to characterize a two-phase flow, the slip ratio (S) is frequently used instead of void fraction. The slip ratio is defined as the ratio of the average velocity of gas phase flow (u_g) to the average velocity of liquid phase flow (u_l). The void fraction (α) can be related to the slip ratio (S) as follows:

$$S = \frac{u_g}{u_l} = \frac{Q_g / A \alpha}{Q_l / A (1-\alpha)} = \frac{Q_g (1-\alpha)}{Q_l \alpha} \quad (1.16)$$

$$S = \frac{u_g}{u_l} = \frac{G x / A \alpha \rho_g}{G (1-x) / A (1-\alpha) \rho_l} = \frac{\rho_l x (1-\alpha)}{\rho_g (1-x) \alpha} \quad (1.17)$$

Equations (1.16) and (1.17) can be rewritten in the form:

$$\alpha = \frac{Q_g}{S Q_l + Q_g} \quad (1.18)$$

$$\alpha = \frac{1}{1 + S \left(\frac{1-x}{x} \right) \left(\frac{\rho_g}{\rho_l} \right)} \quad (1.19)$$

From Eqs. (1.7), and (1.18) or from (1.8), and (1.19), it is obvious that the volumetric quality (β) is equivalent to the void fraction (α) when the slip ratio (S) is 1. The void fraction (α) is called the homogeneous void fraction (α_m) when the slip ratio (S) is 1. This means that $\beta = \alpha_m$.

1.3 Flow Patterns in Two-Phase Flow

1.3.1 Flow Patterns in a Horizontal Two-Phase Flow

Many flow patterns have been recognized in a horizontal two-phase flow. Sketches of the different types are shown in Fig. 1.1. Alves [1] has described these different types as follows: "Assume a horizontal pipe with liquid flowing so as to fill the pipe, and consider the types of flow that occur as gas is added in increasing amounts".

i. Bubble Flow: Flow in which bubbles of gas move along the upper part of the pipe at approximately the same velocity as the liquid. This type is similar to froth flow where the entire pipe is filled with froth similar to an emulsion.

ii. Plug Flow: Flow in which alternate plugs of liquid and gas move along the upper part of the pipe.

iii. Stratified Flow: Flow in which the liquid flows along the bottom of the pipe and the gas flows above, over a smooth liquid-gas interface.

iv. Wavy Flow: Flow, which is similar to, stratified flow except that the gas moves at a higher velocity and the interface is disturbed by waves traveling in the direction of flow.

v. Slug Flow: Flow in which a wave is picked up periodically by the more rapidly moving gas to form a frothy slug which passes through the pipe at a much greater velocity than the average liquid velocity.

vi. Annular Flow: Flow in which the liquid forms in a film around the inside wall of the pipe and the gas flows at a high velocity as a central core. Sometimes, it is possible to have all the liquid flowing in the annular film on the pipe wall. This is most likely to happen at low flow rates near the boundary with slug flow. This type of flow is called ideal annular flow.

vii. Spray Flow: Flow in which most or nearly of all of the liquid is entrained as spray by the gas. This has also been called dispersed flow.

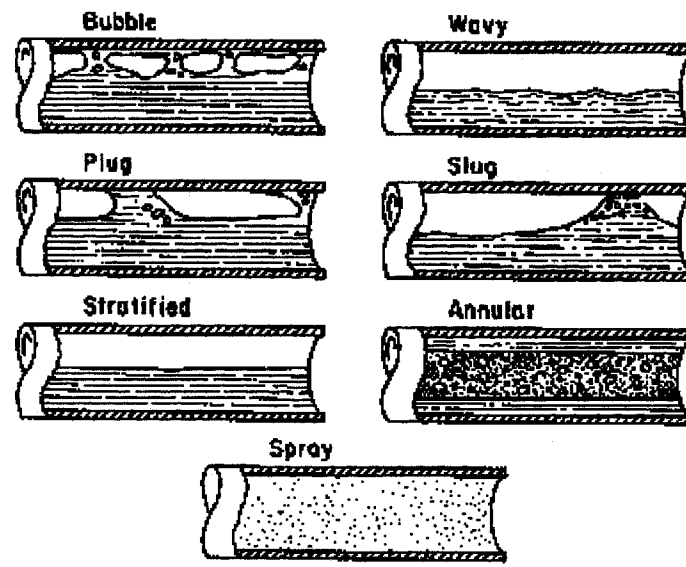


Figure 1.1 Flow Patterns in a Horizontal Two-Phase Flow [1]

1.3.2 Flow Patterns in a Vertical Two-Phase Flow

Many flow patterns have been recognized in a vertical two-phase flow. Sketches of the different types are shown in Fig. 1.2.

i. Bubble Flow: The liquid phase is continuous. The dispersion of bubbles flows within the liquid continuum. The bubbles have variable shapes and sizes, usually distorted spheres.

ii. Slug (Plug) Flow: At higher gas flows, bubbles coalesce and grow to dimensions comparable to the pipe size. When this occurs, large characteristically bullet-shaped bubbles are formed. These bullet-shaped bubbles are commonly called plugs (or gas slugs) or Taylor bubbles. Regions containing dispersions of smaller bubbles, which are

commonly called liquid slugs, may separate these bullet-shaped bubbles. The liquid phase flows down the outside of the large bubbles in the form of a thin falling film, though the net flow of both liquid and gas can be upward.

iii. Churn Flow: When the flow velocity increases, the slug flow bubbles breakdown. This leads to an unstable flow pattern. There is an oscillatory motion of the liquid upward and downward in wide-bore pipes. Thus, this type of flow is called churn flow. The oscillatory motion may not occur in narrow-bore pipes. A smoother transition between the slug flow and annular flow patterns may be observed.

iv. Annular Flow: The gas phase flows along the center of the pipe. The liquid phase flow as a continuous annular film along the walls of pipe. Usually, some of the liquid phase is entrained as small droplets in the gas core. If there is an appreciable degree of entrainment, the term annular-mist flow is used. This happens at high gas rates and the liquid film tends to be quite thin. It is possible (although less common) for bubbles to be entrained in the liquid film. Annular flow is very important in many engineering applications like cooling of nuclear reactors because it gives rise to very high heat transfer coefficients and enables a lot of heat to be removed from the core with a short length of cooling channel passing through the reactor core. For this reason, the designer tries to maximize the fraction of the tube that exhibits annular flow.

v. **Wispy Annular Flow:** When the liquid flow rate increases, the concentration of drops in the gas core increases. Ultimately, droplets coalesce in the gas core. This leads to large lumps or streaks (wisps) of liquid in the gas core. This pattern is characteristic of flows with high mass flux.

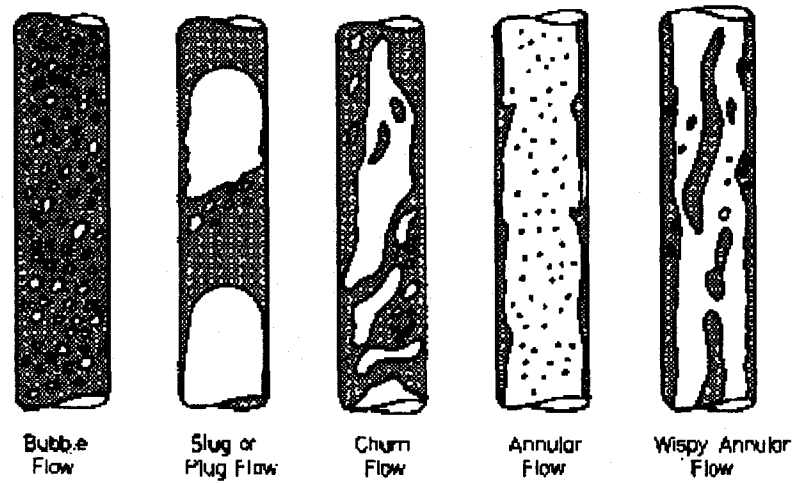


Figure 1.2 Flow Patterns in a Vertical Two-Phase Flow [2]

1.4 Flow Pattern Maps

Flow pattern maps are an attempt, on a two-dimensional graph, to separate the space into areas corresponding to the different flow patterns. Simple flow pattern maps use the same axes for all flow patterns and transitions while complex flow pattern maps use different axes for different transitions. Flow pattern maps exist for both horizontal and vertical flow.

1.4.1 Flow Pattern Map in a Horizontal Two-Phase Flow

The Baker map is an example of flow pattern map for horizontal flow in a pipe. Figure 1.3 shows Baker flow pattern map for horizontal flow in a pipe. This map was first suggested by Baker [3], and was subsequently modified by Scott [4]. The axes are defined in terms of G_g/λ and $G_l\psi$, where

$$G_g = \frac{m_g}{A} \quad (1.20)$$

$$G_l = \frac{m_l}{A} \quad (1.21)$$

$$\lambda = \left(\frac{\rho_g}{\rho_{air}} \frac{\rho_l}{\rho_{water}} \right)^{\frac{1}{2}} \quad (1.22)$$

$$\psi = \frac{\sigma_{water}}{\sigma} \left(\frac{\mu_l}{\mu_{water}} \left[\frac{\rho_{water}}{\rho_l} \right]^2 \right)^{\frac{1}{3}} \quad (1.23)$$

The dimensionless parameters λ and ψ , were introduced to account for variations in the density, surface tension, and dynamic viscosity of the flowing media. These parameters are functions of the fluid properties normalized with respect to the properties of water and air at standard conditions. Both λ and ψ reduce to 1 for water/air mixtures at standard conditions. The Baker map is reasonably well for water/air and oil/gas mixtures in small diameter (< 0.05 m) pipes.

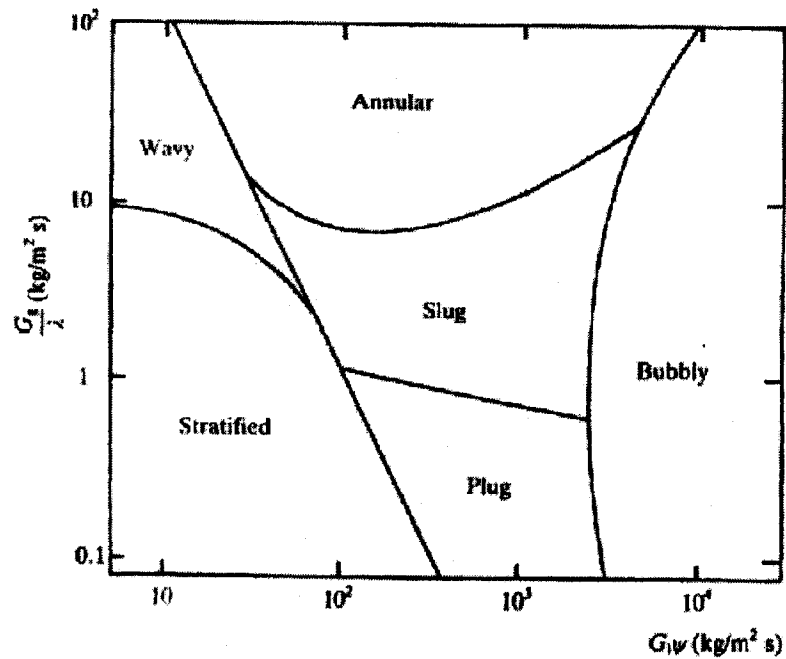


Figure 1.3 Baker Flow Pattern Map for Horizontal Flow in a Pipe [5]

1.4.2 Flow Pattern Map in a Vertical Two-Phase Flow

The Hewitt and Roberts [6] map is an example of flow pattern map for vertical flow in a pipe. Figure 1.4 shows Hewitt and Roberts flow pattern map for vertical upflow in a pipe. Since the axes are defined in terms of G_g/ρ_g and G_l/ρ_l (phase momentum flux). So all the transitions are assumed to depend on the phase momentum fluxes. Wispy annular flow is a sub-category of annular flow that occurs at high mass flux when the entrained drops are said to appear as wisps or elongated droplets. The Hewitt and Roberts map is reasonably well for all water/air and water/steam systems over a range of pressures in small diameter pipes.

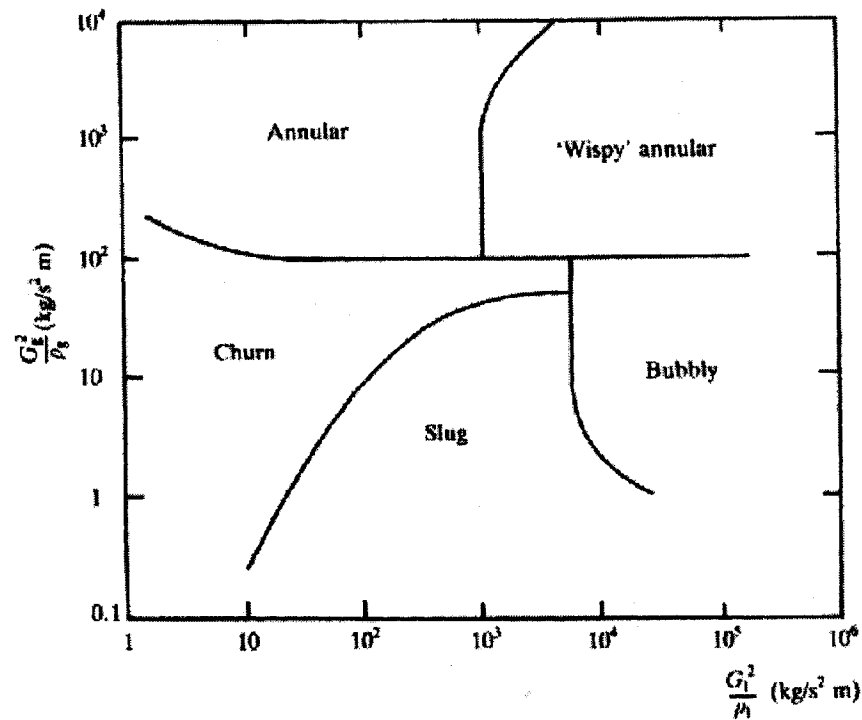


Figure 1.4 Hewitt and Roberts Flow Pattern Map for Vertical Upflow in a Pipe [5]

For both horizontal and vertical maps, it should be noted also that the transitions between adjacent flow patterns do not occur suddenly but over a range of flow rates. So, the lines should really be replaced by rather broad transition bands.

1.5 Pressure Drop in Two-Phase Flow

The pressure drop, which is the change of fluid pressure occurring as a two-phase flow passes through the system. The pressure drop is very important parameter in the design of both adiabatic systems and systems with phase change, like boilers and condensers. In natural circulation systems, the pressure drop dictates the circulation rate,

and hence the other system parameters. In forced circulation systems, the pressure drop governs the pumping requirement.

In addition, the pressure drop is very important in pipelines because co-current flow of liquid and vapor (gas) create design and operational problems due to formation of different types of two-phase flow patterns. Estimation of pressure drop in these cases helps the piping designer in reaching an optimum line size and a better piping system design.

Not only accurate prediction of pressure drop is extremely important when designing both horizontal and vertical two-phase flow systems, but also it is extremely important when designing inclined two-phase flow systems like directional wells or hilly terrain pipelines. Pipe inclination has an appreciable effect on flow patterns, slippage between phases and energy transfer between phases. There is no method for performing these calculations, which is accurate for all flow conditions. Historically, pressure drop in inclined flow has often been calculated using horizontal or vertical two-phase flow correlations. This is often satisfactory if the pipe inclination is very near to the horizontal case or the vertical case. However, this may not be the case in many applications.

The total measured pressure drop in two-phase flow (Δp) consists of three contributions. The first contribution is the frictional pressure drop (Δp_f). The second contribution is the acceleration pressure drop (Δp_a). The third contribution is the gravitational pressure drop (Δp_{grav}).

$$\Delta p = \Delta p_f + \Delta p_a + \Delta p_{grav} \quad (1.24)$$

The acceleration pressure drop (Δp_a) can be neglected in the adiabatic flow. For flow in a horizontal pipe, the gravitational pressure drop (Δp_{grav}) is zero. Thus, the total measured pressure drop (Δp) in the adiabatic experiments in horizontal pipes comes from the frictional pressure drop (Δp_f) only.

To compute the frictional component of pressure drop, either the two-phase friction factor or the two-phase frictional multiplier must be known. It is necessary to know the void fraction (the ratio of gas flow rate to total flow rate) to compute the acceleration, and gravitational components of pressure drop [7].

For the homogeneous model, the frictional component of pressure drop can be computed using the two-phase friction factor (f_{tp}) in two different approaches. In the first approach, the two-phase friction factor (f_{tp}) has been assumed equal to the friction factor occurs when the total flow has been assumed to be all liquid (f_{lo}). The friction factor (f_{lo}) will be a function of the all-liquid Reynolds number (Re_{lo}) and the pipe relative roughness (ϵ/d). The use of f_{lo} in the evaluation of the two-phase frictional pressure drop does not allow extrapolation to the correct value when $x = 1$ (i.e., with single-phase vapor flowing through the pipe). The second approach overcomes this difficulty. In the second approach, the two-phase friction factor (f_{tp}) has been evaluated using the viscosity of two-phase gas-liquid flow based on the homogeneous model (μ_m) in the normal friction factor relationships.

The acceleration component of pressure drop (Δp_a) reflects the change in kinetic energy of the flow. Assuming the vapor and liquid velocities to be uniform in each phase,

the acceleration component of pressure drop can be obtained by the application of a simplified momentum equation in the form:

$$\Delta p_a = G^2 \left\{ \left[\frac{(1-x_o)^2}{\rho_l(1-\alpha_o)} + \frac{x_o^2}{\rho_g \alpha_o} \right] - \left[\frac{(1-x_i)^2}{\rho_l(1-\alpha_i)} + \frac{x_i^2}{\rho_g \alpha_i} \right] \right\} \quad (1.25)$$

The gravitational component of pressure gradient can be expressed in terms of the void fraction as follows:

$$\left(\frac{dp}{dz} \right)_{grav} = g[\alpha \rho_g + (1-\alpha) \rho_l] \sin \theta \quad (1.26)$$

Using Eq. (1.26) and knowing that $\alpha_m = \beta$, the gravitational component of pressure gradient based on the homogeneous model can be expressed as follows:

$$\left(\frac{dp}{dz} \right)_{grav,m} = \frac{g \sin \theta}{\frac{x}{\rho_g} + \frac{1-x}{\rho_l}} \quad (1.27)$$

1.5.1 Two-Phase Frictional Multiplier

The two-phase frictional pressure drop (Δp_f) can be expressed in terms of two-phase frictional multiplier. This representation method is often useful for calculation and comparison needs. For example, the two-phase frictional pressure drop (Δp_f) can be expressed in terms of the single-phase frictional pressure drop for the total flow considered as liquid ($\Delta p_{f,lo}$) using two-phase frictional multiplier for total flow assumed liquid in the pipe (ϕ_{lo}^2). The single-phase frictional pressure drop for the total flow

considered as liquid is computed from the total mass flux (G) and the physical properties of the liquid. The concept of all-liquid frictional pressure drop is useful because it allows the correlation to be tied into single-phase results at one end and eliminates any ambiguity about the physical properties to use, especially viscosity. Moreover, the all-liquid frictional pressure drop is chosen over the all-gas frictional pressure drop, because the liquid density generally does not vary in a problem, while the gas density changes with pressure. Also, the correlation of frictional pressure drop in terms of the parameter (ϕ_{lo}^2) is more convenient for boiling and condensation problems than (ϕ_l^2) . The parameter (ϕ_{lo}^2) was first introduced by Martinelli, and Nelson [8] in 1948. Table 1.1 shows definitions of different two-phase frictional multipliers.

Table 1.1 Definitions of Different Two-Phase Frictional Multipliers

Two-Phase Frictional Multiplier	Mass Flux	Density	Reynolds Number	Symbol
All flow as liquid	$G_l + G_g$	ρ_l	$(G_l + G_g)d/\mu_l$	ϕ_{lo}^2
Liquid fraction only	G_l	ρ_l	$G_l d/\mu_l$	ϕ_l^2
Gas fraction only	G_g	ρ_g	$G_g d/\mu_g$	ϕ_g^2
All flow as gas	$G_l + G_g$	ρ_g	$(G_l + G_g)d/\mu_g$	ϕ_{go}^2

1.5.2 Some Forms of Dimensionless Two-Phase Frictional Pressure Drop (Δp_f^*)

Keilin et al. [9] expressed two-phase frictional pressure drop (Δp_f) in a dimensionless form as follows:

$$\Delta p_f^* = \frac{\Delta p_f}{x\Delta p_{f,go} - (1-x)\Delta p_{f,lo}} \quad (1.28)$$

The above expression satisfies the following limiting conditions:

$$\text{at } x = 0, \Delta p_f = \Delta p_{f,lo} \text{ and } \Delta p_f^* = 0; \quad \text{at } x = 1, \Delta p_f = \Delta p_{f,go} \text{ and } \Delta p_f^* = 1; \quad (1.29)$$

The dimensionless two-phase frictional pressure drop (Δp_f^*) can be expressed as a function of two-phase frictional multipliers as follows:

$$\Delta p_f^* = \frac{\phi_{lo}^2}{1-x+x(\phi_{lo}^2/\phi_{go}^2)} \quad (1.30)$$

For turbulent-turbulent flow, and using the Blasius equation [10] to define the friction factor, the above equation can be expressed as follows:

$$\Delta p_f^* = \frac{\left[1-x+x\left(\frac{\rho_l}{\rho_g}\right)\right] \left[1-x+x\left(\frac{\mu_l}{\mu_g}\right)\right]^{-0.25}}{1-x+x\left(\frac{\rho_l}{\rho_g}\right) \left(\frac{\mu_g}{\mu_l}\right)^{0.25}} \quad (1.31)$$

Borishansky et al. [11] expressed two-phase frictional pressure drop (Δp_f) in a dimensionless form as follows:

$$\Delta p_f^* = \frac{\Delta p_f - \Delta p_{f,lo}}{\Delta p_{f,go} - \Delta p_{f,lo}} \quad (1.32)$$

The above expression satisfies the following limiting conditions:

$$\text{at } x = 0, \Delta p_f = \Delta p_{f,lo} \text{ and } \Delta p_f^* = 0; \quad \text{at } x = 1, \Delta p_f = \Delta p_{f,go} \text{ and } \Delta p_f^* = 1; \quad (1.33)$$

The dimensionless two-phase frictional pressure drop (Δp_f^*) can be expressed as a function of two-phase frictional multipliers as follows:

$$\Delta p_f^* = \frac{\phi_{lo}^2 - 1}{(\phi_{lo}^2 / \phi_{go}^2) - 1} \quad (1.34)$$

For turbulent-turbulent flow, and using the Blasius equation [10] to define the friction factor, the above equation can be expressed as follows:

$$\Delta p_f^* = \frac{\left[1 - x + x \left(\frac{\rho_l}{\rho_g} \right) \right] \left[1 - x + x \left(\frac{\mu_l}{\mu_g} \right) \right]^{-0.25} - 1}{\left(\frac{\rho_l}{\rho_g} \right) \left(\frac{\mu_g}{\mu_l} \right)^{0.25} - 1} \quad (1.35)$$

1.6 Methods of Analysis

Two-phase flows obey all of the basic equations of fluid mechanics (continuity equation, momentum equation, and energy equation). However, the equations for two-phase flows are more complicated than those of single-phase flows. The techniques for analyzing one-dimensional two-phase flows include correlations, the phenomenological models, simple analytical model, and other methods such as integral analysis, differential analysis, computational fluid dynamics (CFD), and artificial neural network (ANN).

1.6.1 Correlations

The basic procedure used in predicting the frictional pressure drop in two-phase flow is developing a general correlation based on statistical evaluation of the data. The main disadvantage of this procedure is the difficulty in deciding on a method of properly weighing the fit in each flow pattern. For example, it is difficult to decide whether a correlation giving a poor fit with stratified flow and a good fit with annular flow is a better correlation than one giving a fair fit for both kinds of flow. Although the researchers that deal with two-phase flow problems still continue to use general correlations, alternate procedures must be developed to improve the ability to predict the pressure drop. In addition, correlations fitted to data banks that contain measurements with a number of liquid-gas combinations for different flow conditions and pipe diameters often have the disadvantage of containing a large number of constants and of being inconvenient in use. The correlation developed by Bandel [12], is an example of this type of correlations.

The prediction of frictional pressure drop in two-phase flow can also be achieved by empirical correlations. Correlating the experimental data in terms of chosen variables is a convenient way of obtaining design equations with a minimum of analytical work. There are a considerable number of empirical correlations for the prediction of frictional pressure drop in two-phase flow. Although the empirical correlations require a minimum of knowledge of the system characteristics, they are limited by the range of data available for correlation construction. Most of these empirical correlations can be used beyond the range of the data from that they were constructed but with poor reliability [13]. Also,

deviations of several hundred percent between predicted and measured values may be found for conditions outside the range of the original data from that these correlations were derived [13].

The prediction of void fraction in two-phase flow can also be achieved by empirical correlations. There are a considerable number of empirical correlations for the prediction of void fraction. The empirical correlations are usually presented in terms of the slip ratio (S).

1.6.2 Phenomenological Models

The phenomenological models can be developed based on the interfacial structure. Including phenomenon specific information like interfacial shear stress and slug frequency is used to obtain a complete picture of the flow. To reduce the dependence on empirical data, modeling on a theoretical basis is used. However, some empiricism is still required. The prediction of pressure gradient, void fraction, and the heat transfer coefficient simultaneously means that the phenomenological model is now preferred. For design purposes, the phenomenological models are often brought together within a framework provided by a flow pattern map such as Taitel, and Dukler [14], flow pattern map. The precision and accuracy of phenomenological models are equal to those of empirical methods, while the probability density function is less sensitive to changes in fluid system [15].

The prediction of void fraction in two-phase flow can also be achieved by using models for specific flow regimes. The Taitel and Dukler [14] model is an example for this type of model.

1.6.3 Simple Analytical Models

Simple analytical models are quite successful method for organizing the experimental results and for predicting the design parameters. Simple analytical models take no account of the details of the flow. Examples of simple analytical models include the homogeneous flow model, the separated flow model, and the drift flux model.

1.6.3.1 The Homogeneous Flow Model

The homogeneous flow model provides the simplest technique for analyzing two-phase (or multiphase) flows. In the homogeneous model, both liquid and vapor phases move at the same velocity (slip ratio = 1). Consequently, the homogeneous model has also been called the zero slip model. The homogeneous model considers the two-phase flow as a single-phase flow having average fluid properties depending on quality. Thus, the frictional pressure drop is calculated by assuming a constant friction coefficient between the inlet and outlet sections of the pipe.

1.6.3.2 The Separated Flow Model

In the separated model, two-phase flow is considered to be divided into liquid and vapor streams. Hence, the separated model has been referred to as the slip flow model.

The separated model was originated from the classical work of Lockhart, and Martinelli [16], that was followed by Martinelli, and Nelson [8]. The Lockhart-Martinelli method is one of the best and simplest procedures for calculating two-phase flow pressure drop and hold up. One of the biggest advantages of the Lockhart-Martinelli method is that it can be used for all flow patterns. However, relatively low accuracy must be accepted for this flexibility. The separated model is popular in the power plant industry. Also, the separated model is relevant for the prediction of pressure drop in heat pump systems and evaporators in refrigeration. The success of the separated model is due to the basic assumptions in the model are closely met by the flow patterns observed in the major portion of the evaporators.

The separated flow model may be developed with different degrees of complexity. In the simplest situation, only one parameter, like velocity, is allowed to differ for the two phases while conservation equations are only written for the combined flow. In the most sophisticated situation, separate equations of continuity, momentum, and energy are written for each phase and these six equations are solved simultaneously, together with rate equations which describe how the phases interact with each other and with the walls of the pipe. Correlations or simplifying assumptions are introduced when the number of variables to be determined is greater than the available number of equations.

For void fraction, the separated model is used by both analytical and semi-empirical methods. In the analytical theories, some quantities like the momentum or the kinetic energy is minimized to obtain the slip ratio (S). The momentum flux model and

the Zivi model [17] are two examples of this technique, where the slip ratio (S) equals $(\rho_l/\rho_g)^{1/2}$ and $(\rho_l/\rho_g)^{1/3}$.

1.6.3.3 The Drift Flux Model

The drift flux model is a type of separated flow model. In the drift flux model, attention is focused on the relative motion rather than on the motion of the individual phases. The drift flux model was developed by Wallis [18]. The drift flux model has widespread application to bubble flow and plug flow. The drift flux model is not particularly suitable to a flow such as annular flow that has two characteristic velocities in one phase: the liquid film velocity and the liquid drop velocity. However, the drift flux model has been used for annular flows, but with no particular success.

The drift flux model is the fifth example of the existing void fraction models. The Rouhani and Axelsson [19] model is an instance for this type of model. In the drift-flux model, the void fraction (α) is a function of the gas superficial velocity (U_g), the total superficial velocity (U), the phase distribution parameter (C_o), and the mean drift velocity (u_{gj}) that includes the effect of the relative velocity between the phases. The form of the drift-flux model is

$$\alpha = \frac{U_g}{C_o U + u_{gj}} \quad (1.36)$$

The drift-flux correlations often present procedures to compute C_o and u_{gj} . Since the expressions of C_o and u_{gj} are usually functions of the void fraction (α), the predictions of the void fraction (α) are calculated using method of solving of non-linear equation.

1.6.4 Other Methods

There are other methods of analysis like integral analysis, differential analysis, computational fluid dynamics (CFD), and artificial neural network (ANN).

1.6.4.1 Integral Analysis

In a one-dimensional integral analysis, the form of certain functions which describe, for instance, the velocity or concentration distribution in a pipe is assumed first. Then, these functions are made to satisfy appropriate boundary conditions and the basic equations of fluid mechanics (continuity equation, momentum equation, and energy equation) in integral form. Single-phase boundary layers are analyzed using similar techniques.

1.6.4.2 Differential Analysis

The velocity and concentration fields are deduced from suitable differential equations. Usually, the equations are written for time-average quantities, like in single-phase theories of turbulence.

1.6.4.3 Computational Fluid Dynamics (CFD)

Two-phase flows are encountered in a wide range of industrial and natural situations. Due to their complexity such flows have been investigated only analytically and experimentally. New computing facilities provide the flexibility to construct computational models that are easily adapted to a wide variety of physical conditions

without constructing a large-scale prototype or expensive test rigs. But there is an inherent uncertainty in the numerical predictions due to stability, convergence and accuracy. The importance of a well-placed mesh is highlighted in the modeling of two-phase flows in horizontal pipelines [20].

1.6.4.4 Artificial Neural Network (ANN)

In recent years, artificial neural network (ANN) has been universally used in many applications related to engineering and science. ANN has the advantage of self-learning and self-organization. ANN can employ the prior acquired knowledge to respond to the new information rapidly and automatically. When the traditional methods are difficult to be carried out or sometimes the specific models of mathematical physics will not be existing thoroughly, the neural network will be considered as a very good tool to tackle these time-consuming and complex nonlinear relations because neural network has the excellent characteristics of parallel processing, calculating for complex computation and self-learning. The development of any ANN model involves three basic steps. First, the generation of data required for training. Second, the training and testing of the ANN model using the information about the inputs to predict the values of the output. Third, the evaluation of the ANN configuration that leads to the selection of an optimal configuration that produces the best results based on some preset measures. The optimum ANN model is also validated using a larger dataset. In the area of two-phase flow, the applications of the ANN include the prediction of pressure drop [21], identifying flow regimes [22] and predicting liquid holdup [22,23].

1.7 Research Objectives

The current research has the following objectives mentioned below.

1. A comprehensive review of different two-phase frictional pressure gradient and void fraction models and their limitations. The research on pressure drop and void fraction in two-phase flow began in the 1940's. Since then, pressure drop and void fraction data have been collected for horizontal, vertical, and inclined gas-liquid systems. From the pressure drop and void fraction data, many attempts have been made to develop general procedures for predicting these quantities.
2. Introducing new definitions for two-phase viscosity to the field of two-phase flow using the analogy between thermal conductivity in porous media and viscosity in two-phase flow. These new definitions of two-phase viscosity can be used to compute the two-phase frictional pressure gradient in circular pipes using the homogeneous model. Expressing of two-phase frictional pressure gradient in a dimensionless form as Fanning friction factor (f_m) versus Reynolds number (Re_m) can also be done.
3. Development of robust models for predicting two-phase frictional pressure gradient flow in circular pipes based upon the asymptotic modeling method. This model may be developed using nonlinear superposition of the asymptotic behavior of the liquid phase and gas phase. The asymptotic modeling method is direct, flexible and simple. This approach has lead to great success in the modeling of complex heat transfer and fluid flow in single-phase flows.

4. Development of lower and upper bounds for two-phase frictional pressure gradient and void fraction in circular pipes. This approach is very useful in design and analysis, as engineers can then use the resulting average and bounding values in predictions of system performance. The approach is also useful when conducting new experiments, since it provides a reasonable envelope for the data to fall within.

The current research deals primarily with adiabatic two-phase gas-liquid flow in smooth horizontal circular pipes at normal conditions. This means that the acceleration component of pressure gradient is negligible and the gravitational component of pressure gradient is zero. As a result, the total pressure gradient is equal to the frictional pressure gradient.

At the last stage of the research, the present proposed models are extended to minichannels and microchannels because the pressure drop in minichannels and microchannels is an important design parameter in many engineering applications like aerospace, bioengineering, compact heat exchangers, electronics cooling and miniature thermal systems.

1.8 Outline of Thesis

The remainder of the thesis is organized as follows. Chapter 2 reviews the currently available models and correlations of two-phase frictional pressure gradient. Chapter 3 reviews the currently available models and correlations of two-phase void fraction. Chapter 4 presents the development of new definitions of two-phase viscosity

and using them to analyze the experimental data of two-phase frictional pressure gradient in circular pipes using the homogeneous model. Chapter 5 presents the development of robust models for predicting two-phase frictional pressure gradient flow in circular pipes based upon the asymptotic modeling method. Chapter 6 outlines the procedures for obtaining lower and upper bounds for two-phase frictional pressure gradient and void fraction. Chapter 7 summarizes the findings and suggests areas that need further examination.

CHAPTER 2

LITERATURE REVIEW OF FRICTIONAL PRESSURE GRADIENT

2.1 Introduction

The research on pressure drop in two-phase flow began in the 1940's. Since then, pressure drop data have been collected for horizontal, vertical, and inclined gas-liquid systems. From the pressure drop data, many attempts have been made to develop general procedures for predicting it. In this chapter, a comprehensive review of different two-phase frictional pressure gradient models and their limitations as well as experimental study and computer study will be presented.

2.2 Review of Two-Phase Frictional Pressure Gradient Models and their Limitations

2.2.1 Separated Flow

Martinelli and Nelson [8] presented a tentative method for the calculation of the pressure drop during forced circulation boiling of water. Their method was based upon the application of pressure drop data, obtained during the isothermal flow of air and different liquids, to the calculation of local pressure gradients during forced circulation boiling. They assumed that the flow regime would always be 'turbulent-turbulent' since any normal forced circulation boiler design for all practical purposes would involve this

flow mechanism only. Also, they assumed that the static pressure drop of the liquid phase was the same as that of the vapor phase. Because of the nature of this assumption, their model would be better suited to annular flow. During the isothermal flow in a horizontal pipe, the frictional pressure drop only was obtained, since no change in the acceleration pressure drop took place. Therefore, the extension of the isothermal data to the case of forced circulation boiling gave the frictional pressure drop. They developed a correlation for calculating ϕ_{lo}^2 . They defined two-phase frictional multiplier for total flow assumed liquid in the pipe (ϕ_{lo}^2) as follows:

$$\phi_{lo}^2 = \frac{(dp/dz)_f}{(dp/dz)_{f,lo}} \quad (2.1)$$

The Martinelli-Nelson correlation was empirical. They presented their correlation in a graphic manner. On the horizontal axis, the independent parameter was the mass quality (x). On the vertical axis, the independent parameter was the ratio of two-phase frictional pressure drop to all-liquid frictional pressure drop (ϕ_{lo}^2). When the flow was all liquid, x was equal to 0, and ϕ_{lo}^2 was equal to 1. When the flow was all gas, x was equal to 1, and ϕ_{lo}^2 was equal to $\Delta p_{f,g}/\Delta p_{f,lo}$, so the pressure drop was equal to $\Delta p_{f,g}$. On the grid, they plotted a family of curves for pressures from 100 psia (6.89 bar) to 3 206 psia (221.2 bar) (the critical pressure). They found that ϕ_{lo}^2 decreased by increasing pressure at a given x , and reached 1 at the critical pressure. From these curves, the frictional pressure drop during forced circulation boiling could be estimated quickly once the exit mass quality, the boiling pressure, and the pressure drop for 100 % liquid were known. They

compared the predicted pressure drop with the measured pressure drop for the pressure range from 18 to 3 000 psia and for the exit mass quality range from 4 to 100 %. The comparison indicated that the method was promising. However, this method was based upon a meager amount of data. So, further experimental verification was needed before this method could be considered valid. If the proposed method was found reliable, extension to the calculation of pressure drop during the condensation or vaporization of liquids other than water should be possible.

Lockhart and Martinelli [16] presented data for the simultaneous flow of air and liquids including benzene, kerosene, water, and different types of oils in pipes varying in diameter from 0.0586 in. to 1.017 in. There were four types of isothermal two-phase, two-component flow. In the first type, flow of both the liquid and the gas were turbulent. In the second type, flow of the liquid was viscous and flow of the gas was turbulent. In the third type, flow of the liquid was turbulent and flow of the gas was viscous. In the fourth type, flow of both the liquid and the gas were viscous. They correlated the pressure drop resulting from these different flow mechanisms by means of the Lockhart-Martinelli parameter (X). The Lockhart-Martinelli parameter (X) was defined as:

$$X^2 = \frac{(dp/dz)_{f,l}}{(dp/dz)_{f,g}} \quad (2.2)$$

In addition, they expressed the two-phase frictional pressure drop in terms of factors, which multiplied single-phase drops. These multipliers were given by:

$$\phi_l^2 = \frac{(dp/dz)_f}{(dp/dz)_{f,l}} \quad (2.3)$$

$$\phi_g^2 = \frac{(dp/dz)_f}{(dp/dz)_{f,g}} \quad (2.4)$$

Using the generalized Blasius form of the Fanning friction factor, the frictional component single-phase pressure gradient could be expressed as

$$\left(\frac{dp}{dz}\right)_{f,l} = \frac{2C_l \mu_l^n U_l^{2-n} \rho_l^{1-n}}{d^{1+n}} \quad (2.5)$$

$$\left(\frac{dp}{dz}\right)_{f,g} = \frac{2C_g \mu_g^n U_g^{2-n} \rho_g^{1-n}}{d^{1+n}} \quad (2.6)$$

Values of the exponent (n) and the constants C_l and C_g for different flow conditions are given in Table 2.1.

Table 2.1 Values of the Exponent (n) and the Constants C_l and C_g for Different Flow Conditions

	turbulent-turbulent	laminar-turbulent	turbulent-laminar	laminar-laminar
n	0.2	1.0	0.2	1.0
C_l	0.046	16	0.046	16
C_g	0.046	0.046	16	16
Re_l	> 2000	< 1000	> 2000	< 1000
Re_g	> 2000	> 2000	< 1000	< 1000

Also, they presented the relationship of ϕ_l and ϕ_g to X in graphical forms. They proposed tentative criteria for the transition of the flow from one type to another. Equations to calculate the parameter (X) under different flow conditions are given in Table 2.2.

Table 2.2 Equations to Calculate the Parameter (X) under Different Flow Conditions

Flow Condition	X
turbulent-turbulent	$X_{tt}^2 = \left(\frac{1-x}{x} \right)^{1.8} \left(\frac{\rho_g}{\rho_l} \right) \left(\frac{\mu_l}{\mu_g} \right)^{0.2}$
laminar-turbulent	$X_{lt}^2 = Re_g^{-0.8} \left(\frac{C_l}{C_g} \right) \left(\frac{1-x}{x} \right) \left(\frac{\rho_g}{\rho_l} \right) \left(\frac{\mu_l}{\mu_g} \right)$
turbulent-laminar	$X_{tl}^2 = Re_l^{0.8} \left(\frac{C_l}{C_g} \right) \left(\frac{1-x}{x} \right) \left(\frac{\rho_g}{\rho_l} \right) \left(\frac{\mu_l}{\mu_g} \right)$
laminar-laminar	$X_{ll}^2 = \left(\frac{1-x}{x} \right) \left(\frac{\rho_g}{\rho_l} \right) \left(\frac{\mu_l}{\mu_g} \right)$

Although the Lockhart-Martinelli correlation related to the adiabatic flow of low pressure air-liquid mixtures, they purposely presented the information in a generalized form to enable the application of the model to single component systems, and, in particular, to steam-water mixtures. Their empirical correlations were shown to be as reliable as any annular flow pressure drop correlation [24]. The disadvantage of this

method was its limit to small-diameter pipes and low pressures because many applications of two-phase flow fell beyond these limits.

Chenoweth and Martin [25] studied pressure drop of gas-liquid mixtures in horizontal pipes. The objective of their study was extending the range used to develop the Lockhart-Martinelli correlation (small diameter pipes and pressures from atmospheric to 50 psi) to include large diameter pipes at higher pressures. This was due to many two-phase applications were found in this range. They made the tests in 1.5 and 3 in. galvanized steel pipes using air and water at pressures from atmospheric to 100 psia. The type of flow was turbulent liquid-turbulent gas flow. They compared their isothermal data with Lockhart-Martinelli correlation. They found that the best agreement was for data taken at atmospheric pressure. The largest deviation was for data taken at 100 psia in the 3 in. pipe. In this case, the predicted pressure was higher than the measured pressure by a factor ranging from 1.4 to 2.5. In general, deviation increased as either pipe diameter or gas density was increased beyond the range of data available when the Lockhart-Martinelli correlation was published. They used the test results to develop an improved correlation for turbulent two-phase flow in horizontal pipes. The correlation was empirical like all earlier correlations. They presented their correlation in a graphic manner. On the horizontal axis, the independent parameter was the superficial liquid volume fraction, or LVF, of the mixture computed from the flow rates and densities of the two phases. On the vertical axis, the dependent parameter was the ratio of two-phase frictional pressure drop to all-liquid frictional pressure drop (ϕ_{lo}^2). When the flow was all liquid, both LVF and ϕ_{lo}^2 had a value of 1. On the other hand, when the flow was all gas,

LVF was equal to 0, and ϕ_{lo}^2 was equal to $\Delta p_{f,g}/\Delta p_{f,lo}$, so the pressure drop was equal to $\Delta p_{f,g}$. On the grid, they plotted a family of curves from 50 to 1 000 for $\Delta p_{f,g}/\Delta p_{f,lo}$, the ratio of all-gas frictional pressure drop to all-liquid frictional pressure drop for the pipe system (i.e. including valves and fittings as well as lengths of straight pipes). They found that the correlation represented all of the experimental data within $\pm 50\%$, and 92% of the data within $\pm 50\%$. Although the correlation was based on the data of air-water mixture, it could be used for any gas-liquid mixture as long as the flow was turbulent. For example, the data of many other investigators correlated equally well. Also, the test results for 3 typical 3 in. fittings showed that single-phase friction coefficients could be used satisfactorily in the correlation to predict two-phase pressure drop.

Thom [26] gave a simplified scheme for the calculation of pressure drop during forced circulation of a two-phase mixture of boiling water and steam. His method followed that proposed by Martinelli and Nelson [8], which had been extended to include the gravitational term in vertical evaporating tubes. He assumed that water entering the tube was at saturation temperature. Thus evaporation, with net generation of steam, started at once. He gave curves from which frictional, acceleration, and gravitational losses could be estimated provided the outlet mass quality had been calculated from a heat balance. He based these curves directly on the experimental result of the boiler circulation research sponsored at the University of Cambridge by the Water-Tube Boilermakers' Association. He compared his calculated values with the later data of Haywood, et al. [27], for a vertical tube. The deviation for the comparison was 10%.

Baroczy [28] described a systematic correlation for the prediction of two-phase friction pressure drop for both single component flow, and two-component flow. The correlation considered fluid properties, mixture quality, and mass flux. The correlation was based on data for steam, water-air, and mercury-nitrogen for a wide range of quality, and mass flux. He called liquid to gas viscosity and density ratio $((\mu_l/\mu_g)^{0.2}/(\rho_l/\rho_g))$ as the property index. The property index had the advantage of not requiring knowledge of the critical pressure and temperature in order to establish the property ratios at the critical point, where they had a value of 1. By similar reasoning, it could be used to establish the analogous condition for two-phase, two-component flow, that was, equal viscosity and density for each phase. Thus, the physical properties of single and two-component, two-phase fluids could be described on the common basis. The two-phase frictional multiplier if the total flow assumed liquid in the pipe (ϕ_{lo}^2) was shown to be a function of property index, mixture quality, and mass flux. He varied the property index from critical pressure to five decades below. He varied the mixture quality from 0.1 to 100%. He varied the mass flux from 0.25×10^6 to 3×10^6 $\text{lb}_m/\text{ft}^2\cdot\text{hr}$. He showed that the reciprocal of the property index was $(dp/dz)_{f,go} / (dp/dz)_{f,lo}$ [i.e. ϕ_{lo}^2/ϕ_{go}^2], or the ratio of the frictional pressure drop if the total flow assumed gas in the pipe to the frictional pressure drop if the total flow assumed liquid in the pipe when each phase flowing alone at the total rate flow was turbulent. He compared the correlation with additional data for water-air, steam, sodium potassium-nitrogen, kerosene-air, diesel oil-air, and potassium. The comparison showed good agreement. This correlation had the disadvantage of being graphic in nature.

Turner [29] developed the separate-cylinder model by assuming that the two-phase flow, without interaction, in two horizontal separate cylinders and that the areas of the cross sections of these cylinders added up to the cross-sectional area of the actual pipe. The liquid and gas phases flow at the same flow rate through separate cylinders. The pressure gradient in each of the imagined cylinders was assumed to be equal, and its value was taken to be equal to the two-phase frictional pressure gradient in the actual flow. For this reason, the separate-cylinder model was not valid for gas-liquid slug flow, which gave rise to large pressure fluctuations. The pressure gradient was due to frictional effects only, and was calculated from single-phase flow theory. The separate-cylinder model resembled Lockhart and Martinelli correlation [16] but had the advantage that it could be pursued to an analytical conclusion. The results of his analysis were

$$\left(\frac{1}{\phi_l^2}\right)^{1/n} + \left(\frac{1}{\phi_g^2}\right)^{1/n} = 1 \quad (2.7)$$

The values of n were dependent on whether the liquid and gas phases were laminar or turbulent flow. The different values of n are given in Table 2.3.

Table 2.3 Values of Exponent (n) for Different Flow Types

Flow Type	n
Laminar Flow	2
Turbulent Flow (analyzed on a basis of friction factor)	2.375-2.5
Turbulent Flows (calculated on a mixing-length basis)	2.5-3.5
Turbulent-Turbulent Regime	4
All Flow Regimes	3.5

Chisholm [30] developed equations in terms of the Lockhart-Martinelli correlating groups for the friction pressure drop during the flow of gas-liquid or vapor-liquid mixtures in pipes. His theoretical development was different from previous treatments in the method of allowing for the interfacial shear force between the phases. Also, he avoided some of the anomalies occurring in previous “lumped flow”. He gave simplified equations for use in engineering design. His equations were

$$\phi_l^2 = 1 + \frac{C}{X} + \frac{1}{X^2} \quad (2.8)$$

$$\phi_g^2 = 1 + CX + X^2 \quad (2.9)$$

The values of C were dependent on whether the liquid and gas phases were laminar or turbulent flow. The values of C were restricted to mixtures with gas-liquid density ratios corresponding to air-water mixtures at atmospheric pressure. The different values of C are given in Table 2.4.

Table 2.4 Values of Chisholm Constant (C) for Different Flow Types

Liquid	Gas	C
Turbulent	Turbulent	20
Laminar	Turbulent	12
Turbulent	Laminar	10
Laminar	Laminar	5

He compared his predicted values using these values of C and his equation with the Lockhart-Martinelli values. He obtained good agreement with the Lockhart-Martinelli empirical curves.

Chisholm [31] studied the influence of mass flux on friction pressure drop during the flow of steam-water mixtures in rough and smooth tubes. He obtained the data at pressures between 3 MN/m^2 (435 psia) and 17.5 MN/m^2 (2 540 psia). He obtained the data at mass fluxes between 280 and 20 000 $\text{kg/m}^2\cdot\text{s}$. He obtained the experimental data at mass fluxes below $800 \text{ kg/m}^2\cdot\text{s}$ with 48 mm bore tubes. He obtained the experimental data at mass fluxes between 800 and 2 000 $\text{kg/m}^2\cdot\text{s}$ with 8 mm tubes. He obtained the experimental data at mass fluxes above 2 000 $\text{kg/m}^2\cdot\text{s}$ with 1-2.6 mm tubes. Data obtained at $800 \text{ kg/m}^2\cdot\text{s}$ with both the 48 mm and 8 mm tubes did not indicate a significant effect of diameter. From analysis of data, he developed equations for friction pressure drop. His equations allowed for the influence of the 'mass flux effect', not previously allowed for in accepted correlations. He put these equations in a form making them applicable at the critical point. His equations were

For mixture mass flux $G \leq G_m$,

$$\phi_l^2 = 1 + \frac{C}{X} + \frac{1}{X^2} \quad (2.10)$$

$$C = \left\{ \lambda + \left(\frac{G}{G_m} - \lambda \right) \left(\frac{\rho_l - \rho_g}{\rho_l} \right)^{0.5} \right\} \left\{ \left(\frac{\rho_l}{\rho_g} \right)^{0.5} + \left(\frac{\rho_g}{\rho_l} \right)^{0.5} \right\} \quad (2.11)$$

For rough tubes,

$G_m = 1\,500 \text{ kg/m}^2 \cdot \text{s}$, $n = 0$, and $\lambda = 1$.

For smooth tubes,

$G_m = 2\,000 \text{ kg/m}^2 \cdot \text{s}$, $n = 0.2$, and $\lambda = 0.5(2^{2-n} - 2) = 0.5(2^{1.8} - 2) = 0.74$.

For mixture mass flux $G > G_m$,

$$\phi_l^2 = \left[1 + \left\{ \left(\frac{\rho_l}{\rho_g} \right)^{0.5} + \left(\frac{\rho_g}{\rho_l} \right)^{0.5} \right\} \frac{1}{X} + \frac{1}{X^2} \right] \psi \quad (2.12)$$

$$\psi = \frac{1 + \frac{C}{M} + \frac{1}{M^2}}{1 + \left\{ \left(\frac{\rho_l}{\rho_g} \right)^{0.5} + \left(\frac{\rho_g}{\rho_l} \right)^{0.5} \right\} \frac{1}{M} + \frac{1}{M^2}} \quad (2.13)$$

For rough tubes, the parameter (M) in Eq. (2.13) could be defined as follows:

$$M = \left(\frac{x}{1-x} \right) \left(\frac{\rho_g}{\rho_l} \right)^{0.5} \quad (2.14)$$

For smooth tubes, the parameter (M) in Eq. (2.13) could be defined as follows:

$$M = \left(\frac{x}{1-x} \right)^{(2-n)/2} \left(\frac{\mu_l}{\mu_g} \right)^{n/2} \left(\frac{\rho_g}{\rho_l} \right)^{1/2} \quad (2.15)$$

Chisholm [32] defined a physical property coefficient (Γ):

$$\Gamma = \left(\frac{(dp/dz)_{f,go}}{(dp/dz)_{f,lo}} \right)^{0.5} \quad (2.16)$$

The Lockhart-Martinelli parameter was related to the physical property coefficient for turbulent flow in smooth tubes as

$$X = \left(\frac{1-x}{x} \right)^{(2-n)/2} / \Gamma \quad (2.17)$$

Chisholm [33] showed that his previous equation for predicting the friction pressure drop during two-phase flow, [Eq. (2.8)], was an unsatisfactory form for use with evaporating flows as $(dp/dz)_{f,l}$, in that case, varied along the flow path. That equation could be transformed with sufficient accuracy for engineering purposes to

$$\phi_{lo}^2 = 1 + (\Gamma^2 - 1) \{ Bx^{(2-n)/2} (1-x)^{(2-n)/2} + x^{2-n} \} \quad (2.18)$$

Also, the above equation could be used to transform the graphical procedure of Baroczy [28]. The values of B corresponding to Baroczy's correlation were approximated by the following equations:

$$B = \frac{55}{G^{1/2}} \quad 0 < \Gamma < 9.5 \quad (2.19)$$

$$B = \frac{520}{\Gamma G^{1/2}} \quad 9.5 < \Gamma < 28 \quad (2.20)$$

$$B = \frac{15000}{\Gamma^2 G^{1/2}} \quad \Gamma > 28 \quad (2.21)$$

There was evidence that the Baroczy's correlation might underestimate the prediction of friction in certain situations, and for this reason, the values of B in Table 2.5 were recommended (also depending on the mass flux (G)).

Table 2.5 Values of Coefficient (B) for Smooth Tubes

Γ	G (kg/m ² .s)	B
$0 < \Gamma \leq 9.5$	$G \leq 500$	4.8
	$500 < G < 1900$	$2400/G$
	$G \geq 1900$	$55/G^{1/2}$
$9.5 < \Gamma < 28$	$G \leq 600$	$520/\Gamma G^{1/2}$
	$G > 600$	$21/\Gamma$
$\Gamma \geq 28$		$15000/\Gamma^2 G^{1/2}$

Chisholm [34] studied the influence of pipe surface roughness on friction pressure drop during two-phase flow. He developed an equation that allowed his smooth pipe correlation to be extrapolated to rough pipe conditions. His equation was

$$\frac{B_R}{B_S} = \left[0.5 \left\{ 1 + \left(\frac{\mu_g}{\mu_l} \right)^2 + 10^{-600\varepsilon/d} \right\} \right]^{\frac{0.25-n}{0.25}} \quad (2.22)$$

In his equation, he made the exponent of the viscosity ratio term (μ_g/μ_l) large enough so that this term would be small for the data used in his analysis.

Johannessen [35] presented a theoretical method of predicting the pressure drop and hold up in stratified and wavy two-phase flow. He based his theory on the flow model of Lockhart and Martinelli [16]. The range of validity for his theory was bounded on one extreme by the turbulent flow requirement, and on the other extreme by the onset of slug, plug, or breaking wave flow. He made a comparison between pressure drop predicted by his theoretical analysis, the Lockhart and Martinelli method, and measurements made in the stratified and wavy two-phase flow region from previous works. These measurements employed pipe diameters of 52.5 mm, 140 mm, and 197 mm and the flow systems consisted of water/air, oil/air, and oil/natural gas. Compared with these measurements, he found that the theoretical solution agreed better than the generalized empirical solution developed by Lockhart and Martinelli. For $0.3 < X < 2$, the data points were relatively evenly distributed about the theoretical curve. For low values of X , i.e. large mass flow rates of gas, the theoretical curve was somewhat low. However, some deviation in this region was to be expected for many reasons. First, wave development because of high gas velocities was fairly intense in this region, requiring large energy transfer from the gas to the wave system. This energy transfer produced a gas phase pressure drop that was not considered in the theory. Second, the liquid phase received a thrust from the gas phase that was also not considered in the theory since the liquid was assumed to be flowing in an open channel. Thus, the computed liquid phase pressure drop was too large. This could only be reduced by increasing the liquid flow area that, in turn, would increase gas phase pressure drop. Third, some of these data points were probably measured in flow systems with breaking waves, since many authors

did not distinguish between this and wave flow. In the case of breaking waves, liquid droplets would be accelerated by the flowing gas, representing an additional gas phase energy loss. At the end of the paper, he presented a detailed calculation procedure for the theoretically developed pressure drop analysis.

For turbulent-turbulent flow, Serizawa and Michiyoshi [36] obtained a mathematical expression for the Lockhart-Martinelli correlation using the tabled values of ϕ_l . Their correlation was

$$\log \phi_l = \frac{-z + \sqrt{z^2 + 9.2}}{4} \quad (2.23)$$

$$z = 2 \log X_u + 0.176 X_u + 0.382 \quad (2.24)$$

$$X_u = \left(\frac{1-x}{x} \right)^{0.9} \left(\frac{\rho_g}{\rho_l} \right)^{0.5} \left(\frac{\mu_l}{\mu_g} \right)^{0.1} \quad (2.25)$$

After that, Serizawa and Michiyoshi [36] presented a new correlation for predicting a two-phase frictional pressure drop multiplier (ϕ_{lo}) that predicted satisfactorily the frictional pressure drop not only for liquid metals but also for ordinary fluid two-phase flow in a wide range of flow parameters. In their correlation, they took into account the effect of pressure level and the effect of mass flux by means of the property index (ξ) and the product of Reynolds and Froude numbers ($ReFr$). Their correlation was

$$\log \phi_{lo} = \frac{-z + \sqrt{z^2 + 9.2}}{4} \quad (2.26)$$

$$z = 2 \log X_u + \frac{f(A)}{X_u + f(C)} + f(B)X_u + 7.75\xi^{0.536} \quad (2.27)$$

$$X_u = \left(\frac{1-x}{x} \right)^{0.9} \left(\frac{\rho_g}{\rho_l} \right)^{0.5} \left(\frac{\mu_l}{\mu_g} \right)^{0.1} \quad (2.28)$$

$$f(B) = 10^m (Re Fr)^n \quad (2.29)$$

$$\xi = \left(\frac{\rho_g}{\rho_l} \right) \left(\frac{\mu_l}{\mu_g} \right)^{0.2} \quad (2.30)$$

They presented $f(A)$, m and n exponents in $f(B)$ and $f(C)$ in a graphical manner. They plotted $f(A)$ as a function of the product of Reynolds and Froude numbers ($ReFr$). They plotted $f(B)$ as a function of the property index (ξ). They plotted $f(C)$ as a function of the product of Reynolds and Froude numbers ($ReFr$) with the property index (ξ) as a parameter.

Russell, et al. [37] developed a mathematical model and an iterative procedure to calculate pressure drop and holdup for horizontal gas liquid pipelines in which the liquid was in laminar flow and the gas was in turbulent flow. The flow regime was stratified flow. In the theoretical analysis, they solved the equations of motion for the liquid phase by including the interfacial stress caused by the turbulent gas interacting at the interface. They carried out the experimental work to verify the theoretical analysis. They carried out the experimental work with both air-water and air-glycerine solutions in 14 m pipelines of diameter 0.0254, 0.0381, and 0.0508 m respectively. They used the range of fluid rates to produce laminar liquid and turbulent gas flows. They measured the pressure drop with recording transducers. They determined the holdup using in-line conductivity

probes instead of the standard double valve trapping procedure. They found that the predictions of the model agreed well with the experimental data points. Also, they presented a design procedure using the verified model that one could use with some confidence outside the range of pipe sizes and fluid properties used in this experimental work because no empirical fitting had been done to develop the models.

Chen and Spedding [38] extended the Lockhart-Martinelli model to which analytical and empirical methods were applied which resulted in solutions for pressure drop and holdup for the case of separated flow. They used air-water as a working fluid in their experiments. They measured pressure drop and other two-phase flow parameters in a rig consisting of a 4.55 cm inside diameter, 6 m long Perspex pipe in the horizontal position. For the case of stratified flow, they found that the analytical solution gave close agreement with pressure drop data and with the results of Johannessen's [35] and Taitel and Dukler's [39] analysis. For the annular flow case, they found that the analytical solution gave close agreement with pressure drop data for large diameter pipes where liquid surface effects were negligible. Using a further theoretical extension of the Lockhart-Martinelli approach, they developed a general pressure drop correlation for annular flow in which the effect of geometry was included. Lack of systemic data for large diameter pipes, particularly for the steam-water case hampered the application of the derivation. In spite of this draw-back, the correlation was developed and was useful in predicting frictional pressure drop in steam-water systems. The correlation was

$$\phi_g^2 = 4050 Re_g^{-0.91} Re_l^{0.44} \quad (2.31)$$

Asali et al. [40] presented new measurements for film height and pressure drop for vertical downward gas-liquid annular flows. They proposed correlations for the dimensionless liquid film thickness (δ_g^+) and the interfacial friction factor ratio (f_i/f_g). They defined the dimensionless liquid film thickness (δ_g^+) as follows:

$$\delta_g^+ = \delta \frac{(\tau_i / \rho_g)^{1/2}}{\nu_g} \quad (2.32)$$

For the case of annular flow with no liquid entrainment, Eq. (2.32) could be simplified as:

$$\delta_g^+ = 0.34 Re_l^{0.6} \left(\frac{\mu_l}{\mu_g} \right) \left(\frac{\rho_g}{\rho_l} \right)^{0.5} \quad (2.33)$$

They defined the interfacial friction factor ratio (f_i/f_g) for downward flow with no entrainment as follows:

$$\frac{f_i}{f_g} = 1 + 0.045(\delta_g^+ - 5.9) \quad (2.34)$$

For $\delta_g^+ < 5.9$, they took the interfacial friction factor ratio (f_i/f_g) as 1.

The above proposed correlations for the dimensionless liquid film thickness (δ_g^+) and the interfacial friction factor ratio (f_i/f_g) were sufficient to predict the two-phase frictional pressure gradient, $(dp/dz)_f$. Based on the momentum balance on the vapor core, they expressed the liquid film thickness (δ) as:

$$\delta = \frac{\delta_g^+ v_g}{(f_i/2)^{1/2} u_g} \quad (2.35)$$

Also, they expressed the vapor velocity (u_g) using the continuity equation as:

$$u_g = \frac{mx}{\rho_g \frac{\pi}{4} (d - 2\delta)^2} \quad (2.36)$$

They solved Eqs. (2.35) and (2.36) simultaneously to determine the liquid film thickness (δ) and the vapor velocity (u_g). Finally, they predicted the two-phase frictional pressure gradient, $(dp/dz)_f$ from

$$\left(\frac{dp}{dz}\right)_f = \frac{2f_i \rho_g u_g^2}{d - 2\delta} \quad (2.37)$$

Crowley and Izenson [41] developed a frictional pressure gradient correlation for annular flow based on a momentum balance of the two phases. They expressed the two-phase frictional multiplier (ϕ_g^2) directly as a function of the local void fraction (α) and the friction factor ratio (f_i/f_g).

$$\phi_g^2 = \frac{1}{\alpha^{2.5}} \frac{f_i}{f_g} \quad (2.38)$$

The momentum balance for the two phases gave a relationship between the Lockhart-Martinelli parameter (X), the local void fraction (α) and the friction factor ratio (f_i/f_g).

$$X^2 = \frac{1-\alpha^2}{\alpha^{2.5}} \frac{f_i}{f_g} \quad (2.39)$$

In order to complete their pressure drop correlation, they chose an extension of Wallis's interfacial friction factor correlation [18].

$$\frac{f_i}{f_g} = 1 + 75(1-\alpha) \quad (2.40)$$

They solved Eqs. (2.39) and (2.40) simultaneously to determine the local void fraction (α) and the interfacial friction factor ratio (f_i/f_g). Then, they substituted these values into Eq. (2.38) to obtain the two-phase frictional multiplier (ϕ_g^2). Finally, they used Eq. (2.4) to obtain the two-phase frictional pressure gradient, $(dp/dz)_f$, where they calculated the two-phase frictional pressure gradient if the vapor were flowing alone, $(dp/dz)_{f,g}$ as:

$$\left(\frac{dp}{dz}\right)_{f,g} = \frac{2f_g \rho_g U_g^2}{d} = \frac{2f_g G^2 x^2}{d\rho_g} \quad (2.41)$$

Crowley and Izenon method was valid only for annular flow. To define the limit of applicability for their method, they cited Barnea's work [42]. They found that the annular flow existed for $\alpha > 0.76$ where gravity was not a factor. As a result, the prediction in this method was considered to be valid only for $\alpha > 0.76$.

The smooth annular method is another method to predict the two-phase frictional pressure gradient, $(dp/dz)_f$ in annular flow regime. In this method, the friction factor ratio (f_l/f_g) is assumed to equal 1.

$$\frac{f_l}{f_g} = 1 \quad (2.42)$$

Equation (2.42) is used in with Eq. (2.39) to calculate the void fraction (α). Then, the result is used in Eq. (2.38) to obtain the two-phase frictional multiplier (ϕ_g^2). At the end, Eqs. (2.4) and (2.42) are used to obtain the two-phase frictional pressure gradient, $(dp/dz)_f$.

The smooth annular method is considered to be valid only for $\alpha > 0.76$ like Crowley and Izenon method [41].

Based on conservation principles and empirical correlations, Manzano-Ruiz [43] proposed a simple model to predict the frictional pressure-drop of two-phase, one-component (steam/water) or two-components (air/water), flow of gas/liquid mixtures through large pipe diameters. This proposed model could be applicable to annular-mist flow patterns that was the most common type of flow regime encountered in many industrial applications such as district heating, nuclear facilities, steam distribution for enhanced oil recovery, etc. He compared his model against steam/water flow data through pipes of 97 mm diameter. Also, he compared his model against air/water flow data through pipes of 23 mm diameter. He found that the agreement obtained with the experimental data was of the order of 12.5% for the steam/water data and of 32.5% for

the air/water data. This agreement could be improved significantly when entrainment data were available.

The Lockhart-Martinelli correlation [16] in its present form cannot be used to study a large set of data because it requires the use of charts and hence cannot be simulated numerically. As a result, Hemeida and Sumait [44] developed a correlation between Lockhart and Martinelli parameters ϕ and X for a two-phase pressure drop in pipelines using the Statistical Analysis System (SAS). To calculate the parameter ϕ as a function of X using SAS software, their equation was

$$\phi = \exp \left[2.303a + b \ln(X) + \frac{c}{2.30} (\ln X)^2 \right] \quad (2.43)$$

Where a , b , and c were constants. They selected the values of the constants a , b , and c according to the type of fluid and flow mechanisms (Table 2.6).

Table 2.6 Values of a , b , and c for Different Flow Mechanisms

Parameter	a	b	c
$\phi_{g,ll}$	0.4625	0.5058	0.1551
$\phi_{g,lt}$	0.5673	0.4874	0.1312
$\phi_{g,tl}$	0.5694	0.4982	0.1255
$\phi_{g,tt}$	0.6354	0.4810	0.1135
$\phi_{l,ll}$	0.4048	0.4269	0.1841
$\phi_{l,lt}$	0.5532	-0.4754	0.1481
$\phi_{l,tl}$	0.5665	-0.4586	0.1413
$\phi_{l,tt}$	0.6162	-0.5063	0.124

The above equation enabled the development of a computer program for the analysis of data using the Lockhart-Martinelli correlation [16]. Using this program, they analyzed field data from Saudi flow lines. The results showed that the improved Lockhart-Martinelli correlation predicted accurately the downstream pressure in flow lines with an average percent difference of 5.1 and standard deviation of 9.6%.

2.2.2 The Homogeneous Model

McAdams, et al. [45] defined the viscosity of two-phase gas-liquid flow (μ_m) as follows:

$$\mu_m = \left(\frac{x}{\mu_g} + \frac{1-x}{\mu_l} \right)^{-1} \quad (2.44)$$

They used the total mass flux (G), the pipe diameter (d) and the viscosity of the mixture (μ_m) to calculate the Reynolds number of the mixture (Re_m) as follows:

$$Re_m = \frac{Gd}{\mu_m} \quad (2.45)$$

They used the Reynolds number of the mixture (Re_m) to calculate the Fanning friction factor of the mixture (f_m) using single-phase flow equations but modified to use the homogeneous properties.

$$f_m = \begin{cases} 16 Re_m^{-1} & \text{laminar} \\ 0.046 Re_m^{-0.2} & \text{turbulent} \end{cases} \quad (2.46)$$

Finally, using the homogeneous model, they could calculate the frictional pressure gradient, $(dp/dz)_f$, by assuming a constant friction coefficient (f_m) between the inlet and outlet sections of the pipe as follows:

$$\left(\frac{dp}{dz}\right)_f = \frac{2f_m G^2}{d\rho_m} \quad (2.47)$$

$$\rho_m = \left(\frac{x}{\rho_g} + \frac{1-x}{\rho_l}\right)^{-1} \quad (2.48)$$

Cicchitti, et al. [46] attained preliminary studies of pressure drops, heat transfer coefficients, and burnout heat fluxes with wet steam at high pressures in upward vertical tube. They carried out their studies at experimental facility built for this purpose in the (Emilia) thermal power station at Piacenza, Italy. They obtained the pressure drop data for both zero power experiments (adiabatic) and experiments with power supply (non-adiabatic). The test section consisted of 0.51/0.6 cm, 304 stainless steel tube. They focused their attention on two-phase mixtures, in that the liquid phase was fully dispersed in the gas phase (fog flow, or spray flow, or dispersed flow). They achieved this flow pattern when the linear velocity of both liquid and gas phases was sufficiently high. For adiabatic experiments, they varied the useful tube length from 53 to 111 cm. The range of inlet pressure was from 20 to 80 kg/cm². The mass flux range was from 1 500 to 5 000 kg/m².s. The range of inlet steam quality was from 15 to 80%. Expressed with dimensionless groups, the results covered the range of Reynolds number from 0.9x10⁵ to 5x10⁵. For non-adiabatic experiments, the power supplied was about 90-95% of the

burnout heat flux. The heated section was 40 cm long. The range of inlet pressure was from 35 to 55 kg/cm². The mass flux range was from 2 000 to 4 000 kg/m².s. The range of inlet steam quality was from 20 to 70%. They based the pressure drop calculation on the homogeneous flow model. They defined the viscosity of two-phase gas-liquid flow (μ_m) as follows:

$$\mu_m = x\mu_g + (1-x)\mu_l \quad (2.49)$$

They used the above definition of μ_m instead of the definition of μ_m made by McAdams, et al. [45]. The only reason for doing this, in addition to simplicity, was a reasonable agreement with experimental data. They obtained a correlation for the pressure drop calculation. Their correlation was:

$$\left(\frac{dp}{dz}\right)_f = 0.092 \frac{G^{1.8} \mu_m^{0.2} v_m}{d^{1.2}} \quad (2.50)$$

Dukler et al. [13] calculated the two-phase frictional pressure gradient, $(dp/dz)_f$, on the basis of the homogeneous (no-slip) model as follows:

$$\left(\frac{dp}{dz}\right)_f = \frac{2G^2 f_0 \alpha(\lambda) B}{d\rho_m} \quad (2.51)$$

$$f_0 = 0.00140 + \frac{0.125}{Re^{0.32}} \quad (2.52)$$

$$\alpha(\lambda) = \frac{f}{f_0} = 1 - \frac{(\ln \lambda)}{[1.281 + 0.478 \ln \lambda + 0.444(\ln \lambda)^2 + 0.094(\ln \lambda)^3 + 0.00843(\ln \lambda)^4]} \quad (2.53)$$

$$B = \frac{\rho_l}{\rho_m} \frac{\lambda^2}{(1-\alpha)} + \frac{\rho_g}{\rho_m} \frac{(1-\lambda)^2}{\alpha} \quad (2.54)$$

$$\rho_m = \rho_l \lambda + \rho_g (1-\lambda) \quad (2.55)$$

$$\mu_m = \mu_l \lambda + \mu_g (1-\lambda) \quad (2.56)$$

$$\lambda = \frac{Q_l}{Q} = \frac{Q_l}{Q_l + Q_g} = \frac{1}{1 + \left(\frac{x}{1-x}\right) \left(\frac{\rho_g}{\rho_l}\right)} \quad (2.57)$$

Bo Pierre [47] studied the flow resistance that occurred with boiling mediums in evaporators. He included in his study both straight horizontal tubes and return bends, all of ordinary copper tubing. He used R-12, and R-22 as the flow mediums. To study the effect of oil on the pressure drop, he measured the experimental values partly with an oil-free medium (oil less than 0.5 vol. % of liquid), and partly with the presence of oil (for R-12, with oil between 6 and 12 vol. % of liquid). The test equipment used in the experiments consisted of 5 different evaporators, all of the double tube heat exchanger type. They used tube diameters of 12 and 18 mm. The used tube length was 4.08, 4.78, 6.50, 8.72, and 9.50 m. The mass flow rate of the refrigerant was in the range of 15-140 kg/hr. The heat flux was in the range of 1 000-26 000 kcal/m².hr. The evaporation temperature range was from -20 to 10°C. The average quality range was from 49 to 81%. For straight horizontal tubes, the flow resistance was separated into a friction pressure

drop and an acceleration pressure drop. He presented the flow resistance due to friction in the form of a dimensionless friction factor. He correlated this friction factor in terms of the Reynolds number (Re) and a boiling number (K_f). Thus, he obtained a general function for the friction factor for this complex type of two-phase flow. He gave equations for the calculation of the friction factor for both the oil-free medium and the oil-present medium. For the oil-free medium, the friction factor could be expressed as follows:

$$f_{av} = 0.0185 K_f^{0.25} Re^{-0.25} \quad (2.58)$$

The above equation was valid only if $(Re/K_f) > 1$.

For the oil-present medium, the friction factor could be expressed as follows:

$$f_{av} = 0.053 K_f^{0.25} Re^{-0.25} \quad (2.59)$$

The above equation was valid only if $(Re/K_f) > 2$.

In the above two equations, it should be noted that the boiling number (K_f) was not dimensionless, but had units of N/kg. The boiling number (K_f) was defined as follows:

$$K_f = \frac{J(x_o - x_i)h_{fg}}{L} \quad (2.60)$$

From Eqs. (2.58) and (2.59), it could be seen that oil significantly increased the friction factor, and, therefore, the pressure drop.

Based on the measured pressure drop data with R-12 and R-22 flowing inside 12 and 18 mm diameter tubes, he developed a correlation for the pressure drop. His correlation was:

$$\Delta p_{BP} = \left[f_{av} + \frac{(x_o - x_i)d}{x_{av}L} \right] \frac{G^2 L}{d\rho_{av}} \quad (2.61)$$

$$x_{av} = \left(\frac{x_i + x_o}{2} \right) \quad (2.62)$$

The above equation was valid only if $(Re/K_f) > 1$. The expression for the average density (ρ_{av}) was similar to that of the homogeneous density (ρ_m), but it was calculated at x_{av} . The average density (ρ_{av}) was defined as follows:

$$\rho_{av} = \left(\frac{x_{av}}{\rho_g} + \frac{1 - x_{av}}{\rho_l} \right)^{-1} \quad (2.63)$$

Although Bo Pierre's semi-empirical correlation was one of the best-accepted pressure drop correlations based on the homogeneous model, it was not applicable when heat flux was high with a small mass flux and hence the mass quality change between inlet and outlet (Δx) was relatively large. Because of this limitation ($(Re/K_f) > 1$), care should be exercised in the use of Bo Pierre's correlation.

Also, he arranged a calculation diagram for the determination of the pressure drop in conventional evaporators. He made comparison between this diagram and test data for

different types of evaporators. He obtained good overall agreement between this diagram and test data.

Powley [48] tried to predict Martinelli's correlation from the homogeneous theory. He obtained the expressions of ϕ_l and ϕ_g in terms of the Lockhart-Martinelli parameter (X) similar to Chisholm's expressions [30], but C was defined as

$$C = \left[\left(\frac{\rho_l}{\rho_g} \right)^{0.5} + \left(\frac{\rho_g}{\rho_l} \right)^{0.5} \right] \quad (2.64)$$

Wallis [18] assumed turbulent flow in a smooth pipe ($Re > 2000$). He represented the friction factor empirically by the Blasius equation with $n = 0.25$. He used the homogeneous model to calculate both the density and the viscosity. His correlation was:

$$\phi_{lo}^2 = \left(1 + x \frac{\rho_l - \rho_g}{\rho_g} \right) \left(1 + x \frac{\mu_l - \mu_g}{\mu_g} \right)^{-1/4} \quad (2.65)$$

The above multiplier could be evaluated for any x , temperature, and pressure condition for that density and viscosity data are available. He presented some calculated values for steam-water flows in a table. His table showed that ϕ_{lo}^2 decreased with increasing pressure at a given x and had a value of 1 at the critical point. He found that his method worked quite well for dispersed phase flows (bubbly flows) but tended to underpredict the pressure drop for separated flows. The Martinelli-Nelson correlation tended to be better for separated flows. This was perhaps to be expected since the Wallis

correlation based on the homogeneous model assumed a fully dispersed flow while the Martinelli-Nelson correlation was based on a separated (annular) flow concept.

Lombardi and Pedrocchi [49] carried out research programs on two-phase flow pressure drop at CISE. They obtained a new general correlation to predict pressure drops in two-phase flow on the basis of the CISE experimental data by rearranging and extending previous correlations. The CISE experimental data represented different geometries. The geometric configuration included tube, annulus, and rod cluster. The CISE experimental data represented different working fluid mixtures. The working fluid mixtures were steam-water, argon-water, nitrogen-water, and argon-ethyl alcohol. The CISE experimental data represented both adiabatic and heat transfer conditions. The working fluid mixtures for heat transfer conditions were steam-water only. In addition, they varied their correlation with samples of experimental data from other laboratories. The proposed correlation was all the conditions for which dispersed or annular dispersed flow was obtained over most of the duct length. They did not take into account the flow patterns for which the two-phases were macroscopically separated like plug-flow and stratified flow. They based the correlation on known parameters (i.e. no correlated quantities were needed like the gas volume fraction). They varied their correlation only in vertical upflow. They referred to an energy balance for subdividing the overall pressure drop into the usual head, acceleration and friction terms. The correlation was

$$\left(\frac{dp}{dz}\right)_f = C \frac{G^n v_m^{0.86} \sigma_l^{0.4}}{d_e^{1.2}} \quad (2.66)$$

Table 2.7 gives a set of suggested values of C and n .

Table 2.7 A Set of Suggested Values of C and n

Geometric Configuration	C	n
round tube	0.83 (*)	1.4
annulus, and rod cluster	0.213 (*)	1.6

(*) If CGS units are adopted in Eq. (2.66), the values of C are 0.087 and 0.0354 respectively.

It was obvious that the viscosity of neither phase did not affect the frictional pressure drop and a new controlling parameter appeared to be the liquid surface tension. The correlation could be applied directly in adiabatic conditions over the whole duct length using the average values of the properties between the inlet and the outlet sections of the duct. In heat transfer conditions; the integration of the correlation over the length of a heated channel was used to calculate the frictional pressure drop. They varied the correlation against 1 381 experimental data points obtained on 7 different loops for a wide range of different parameters. The experimental data had the mass flux range of 500-5 000 kg/m².s. The experimental data had the equivalent diameter range of 5-25 mm. The experimental data had the channel length range of 0.1-4 m. The experimental data had gas to liquid specific volume ratio range of 15-100 (this interval corresponded approximately to the pressure between 20 and 90 bar for steam-water mixtures). The experimental data had the surface tension range of 0.02-0.08 N/m. The experimental data had the quality range from 1% to 98%. As a result, they found that 87% of all experimental data were between $\pm 15\%$ of the predicted values. The correlation could

easily be adapted to better represent particular conditions, by slightly readjusting the constant and the exponents of the above equation. Moreover, they checked separately the influence of the various known parameters. To link between single-phase and two-phase correlations, they found a discrepancy with single-phase correlations appeared in correspondence with $x = 1$. This was a direct consequence of the experimental trend of two-phase pressure showed a rapid change in the vicinity of $x = 1$. The same kind of discrepancy could not be attributed to the present correlation in correspondence with $x = 0$ because the very flow patterns were no longer dispersed or annular dispersed in the vicinity of $x = 0$. In addition, they stated that acceleration and friction terms might not be singly correct but they were self-compensating so that their sum was correctly predicted anyway.

Beggs and Brill [50] studied two-phase air-water flow in inclined pipes of 1 and 1.5 in. (25.4 and 38.1 mm) diameter to determine the effect of pipe inclination angle (θ) on pressure loss and liquid holdup (1-void fraction). They developed correlations for friction factor and liquid holdup for predicting frictional pressure gradient for two-phase flow in pipes at all angles for many flow conditions. To predict the two-phase frictional pressure gradient, $(dp/dz)_f$, they calculated first the no-slip friction factor (f_m). They obtained the no-slip friction factor (f_m) from a Moody diagram [51] or, for smooth pipe, from

$$f_m = \left[4 \log \left(\frac{Re_m}{4.5223 \log Re_m - 3.8215} \right) \right]^{-2} \quad (2.67)$$

$$Re_m = \frac{Gd}{\mu_l \lambda + \mu_g (1 - \lambda)} \quad (2.68)$$

$$\lambda = \frac{Q_l}{Q} = \frac{Q_l}{Q_l + Q_g} = \frac{I}{1 + \left(\frac{x}{1-x} \right) \left(\frac{\rho_l}{\rho_g} \right)} \quad (2.69)$$

After that, they found that the normalized friction factor (f/f_m) to be a function of input liquid content (λ) and liquid holdup $H_l(\theta)$. Using regression analysis with normalized friction factor (f/f_m) as the dependent variable and input liquid content (λ) and liquid holdup $H_l(\theta)$ as the dependent variables, they obtained a relationship of the type

$$\frac{f}{f_m} = e^s \quad (2.70)$$

$$s = \frac{\ln(y)}{[-0.0523 + 3.182 \ln y - 0.8725(\ln y)^2 + 0.01853(\ln y)^4]} \quad (2.71)$$

$$y = \frac{\lambda}{[H_l(\theta)]^2} \quad (2.72)$$

Equation (2.71) became unbounded at a point in the interval $1 < y < 1.2$. For y in this interval, they calculated the function s from

$$s = \ln(2.2y - 1.2) \quad (2.73)$$

They found that as the flow approached all gas, input liquid content (λ) approached 0, s approached 0, both the friction factor (f) and the no-slip friction factor (f_m) approached the friction factor for gas (f_g). On the other hand, as the flow approached

all liquid, y approached 1, s approached 0, both the friction factor (f) and the no-slip friction factor (f_m) approached the friction factor for liquid (f_l). Using Eqs. (2.70)-(2.73), They plotted the normalized friction factor (f/f_m) versus input liquid content (λ) with liquid holdup H_l as a parameter. Equations for predicting liquid holdup H_l will be given in details in the section of void fraction models.

Finally, they obtained the two-phase frictional pressure gradient, $(dp/dz)_f$, on the basis of the homogeneous model using the Dukler et al. definition [13] of two-phase density (ρ_m)

$$\left(\frac{dp}{dz}\right)_f = \frac{2fG^2}{d\rho_m} \quad (2.74)$$

$$\rho_m = \rho_l\lambda + \rho_g(1-\lambda) \quad (2.75)$$

Lombardi and Ceresa [52] presented a new correlation (DIF-2) developed at CISE for predicting two-phase pressure drops. This correlation was a generalization of a previous correlation (DIF-1) [49]. CISE-DIF-2 correlation envisaged the usual breakdown of total pressure drops according to the energy balance; only the friction term was empirically correlated by a general expression. They grouped the relevant parameters into two dimensionless numbers. To have a smooth transition between single-phase and two-phase conditions as found experimentally, they used suitable weight functions with taking also into account the single-phase friction coefficients. CISE-DIF-2 correlation was

$$\left(\frac{dp}{dz}\right)_f = \frac{2G^2}{d\rho_m} \left\{ f_g x^{40} + f_l (1-x)^{100} + f_m [1-x^{40} - (1-x)^{100}] \right\} \quad (2.76)$$

$$f_g = \begin{cases} 0.046 Re_g^{-0.2} & Re_g > 2400 \\ 16 Re_g^{-1} & Re_g \leq 2400 \end{cases} \quad (2.77)$$

$$Re_g = \frac{G d}{\mu_g} \quad (2.78)$$

$$f_l = \begin{cases} 0.046 Re_l^{-0.2} & Re_l > 2400 \\ 16 Re_l^{-1} & Re_l \leq 2400 \end{cases} \quad (2.79)$$

$$Re_l = \frac{G d}{\mu_l} \quad (2.80)$$

$$f_m = \begin{cases} 0.046 Lo^{-0.25} & Lo \geq L\bar{o} \\ 0.046 Lo^{-1} L\bar{o}^{0.75} & Lo < L\bar{o} \end{cases} \quad (2.81)$$

$$Lo = \frac{G^2 d}{\rho_m \sigma} \left(\frac{\mu_g}{\mu_l} \right)^{0.5} \quad (2.82)$$

$$L\bar{o} = 1.65 \times 10^6 \frac{d^2}{\sigma^{0.5}} \left(\frac{\mu_g}{\mu_l} \right) \quad (2.83)$$

CISE-DIF-2 correlation was valid in a wide range of parameters, including very low flowrates. Also, it had a satisfactory reliability in predicting experimental data. In addition, a remarkable analogy with single-phase correlations was evident if the Reynolds number (Re) was substituted by the Lo number.

Bonfanti et al. [53] measured pressure drops of a water-nitrogen mixture flowing upward in two different tubular test sections. They obtained the data in the low specific mass flowrate region for the whole mass quality. They found that pressure drops, in

general, turned out to decrease by increasing specific mass flowrate or mass quality. These effects were just the opposite of those normally displayed. Also, total pressure drops might present a steep decrease in vicinity of pure gas conditions, strongly dependent on specific mass flowrate. In addition, friction pressure drops might present a steeper decrease in vicinity of pure liquid conditions, strongly dependent on specific mass flowrate. The data analysis suggested slight modifications both in the correlation structure and the relevant empirical constant values of previous CISE-DIF-2 correlation [52]. For round tubes, CISE-DIF-3 correlation was

$$\left(\frac{dp}{dz}\right)_f = \frac{2G^2}{d\rho_m} \left\{ f_g x^g + f_l (1-x)^{100} + f_m [1-x^g - (1-x)^{100}] \right\} \quad (2.84)$$

$$f_g = \begin{cases} 0.046 Re_g^{-0.2} & Re_g > 2400 \\ 16 Re_g^{-1} & Re_g \leq 2400 \end{cases} \quad (2.85)$$

$$Re_g = \frac{G d}{\mu_g} \quad (2.86)$$

$$g = \begin{cases} 20 & G < 100 \\ 7 & G \geq 100 \end{cases} \quad (2.87)$$

$$f_l = \begin{cases} 0.046 Re_l^{-0.2} & Re_l > 2400 \\ 16 Re_l^{-1} & Re_l \leq 2400 \end{cases} \quad (2.88)$$

$$Re_l = \frac{G d}{\mu_l} \quad (2.89)$$

$$f_m = \begin{cases} 0.046 Lo^{-0.25} & Lo \geq L\bar{o} \\ 0.046 Lo^{-1.25} L\bar{o} & Lo < L\bar{o} \end{cases} \quad (2.90)$$

$$L_o = \frac{G^2 d}{\rho_m \sigma} \left(\frac{\mu_g}{\mu_l} \right)^{0.5} \quad (2.91)$$

$$L_{\bar{o}} = 1.25 \times 10^6 \frac{d^2}{\sigma^{0.5}} \left(\frac{\mu_g}{\mu_l} \right) \quad (2.92)$$

CISE-DIF-3 correlation was relevant to pressure drops of two-phase mixtures flowing upflow in vertical ducts, both in adiabatic and diabatic conditions.

Bonfanti et al. [54] obtained density and pressure drop data in a 77.9 mm duct for three different flow inclinations: vertical upflow, horizontal flow and vertical downflow. They used water-nitrogen mixture as a working fluid. They performed their experiments at adiabatic conditions at room temperature of 18°C, at the pressure of 2.16 MPa and at low flow rates within a wide range of mass quality. In vertical upflow, pressure drops showed a trend opposite to that normally found. They decreased with mass quality and flow rate. In horizontal flow, pressure drops had a more regular trend, even if quantitatively unconventional. In vertical downflow, pressure drops decreased with flow rate at lower mass quality. The mixture density was not too different in vertical upflow and horizontal flow, whereas, except for higher flow rate, it was substantially different in vertical downflow. They found that CISE-DIF-3 correlation [53] predicted well pressure drops in vertical upflow.

Beattie and Whalley [55] presented a simple two-phase pressure drop calculation method. They adapted a theoretically based flow pattern dependent calculation method to yield a simple predictive method in which flow pattern influences were partially for in an implicit method and hence need not to be explicitly taken into account when using the

method. For both bubble flow and annular flow, they proposed that the average two-phase viscosity (μ_m) was replaced by a hybrid definition

$$\mu_m = \mu_l(1 - \alpha_m)(1 + 2.5\alpha_m) + \mu_g\alpha_m = \mu_l - 2.5\mu_l \left(\frac{x\rho_l}{x\rho_l + (1-x)\rho_g} \right)^2 + \left(\frac{x\rho_l(1.5\mu_l + \mu_g)}{x\rho_l + (1-x)\rho_g} \right) \quad (2.93)$$

The frictional pressure gradient in two-phase flow $(dp/dz)_f$ was calculated using the Fanning equation for single-phase flow, but modified to use the homogeneous properties. Thus

$$\left(\frac{dp}{dz} \right)_f = \frac{2f_m G^2}{d\rho_m} \quad (2.94)$$

$$f_m = \begin{cases} 0.079 Re_m^{-0.25} & \text{turbulent} \\ 16 Re_m^{-1} & \text{laminar} \end{cases} \quad (2.95)$$

$$Re_m = \frac{Gd}{\mu_m} \quad (2.96)$$

They compared the results of their method with an extensive adiabatic round tube data bank. The comparison showed that the method was as good as most alternative, more complex methods. Errors in the present method were due mainly to the neglect of effects like entrance effects rather than the neglect of mass flux effects. So, methods that more correctly allow for mass flow effects did not necessarily result in more reliable predictions. Excluding condensing flows, this method should also yield reasonable pressure drop calculation for non-adiabatic and/or complex geometry flows.

Lombardi and Ceresa [56] checked CISE-DIF-3 correlation [53] against 10 971 experimental data. Although the check was satisfactory, but it suggested some improvements to define a new version named CESNEF-2. CESNEF-2 correlation was fully dimensionless and improved the predictions at very low rates, pressures and diameters. It was reliable within wide parameter ranges and it could also be used to predict mixture density at very low specific mass flow rates. CESNEF-2 correlation was

$$\left(\frac{dp}{dz}\right)_f = \frac{2G^2}{d\rho_m} \left\{ f_g x^{600(\rho_g/\rho_l)} + f_l (1-x)^{2(\rho_l/\rho_g)} + f_m [1 - x^{600(\rho_g/\rho_l)} - (1-x)^{2(\rho_l/\rho_g)}] \right\} \quad (2.97)$$

The friction factors of both phases (f_g and f_l) were calculated as if the mixture mass flux densities were all gas or all liquid and taking into account the actual flow regime (turbulent or laminar) and the true duct roughness. In the case of turbulent flow, they used the Colebrook-White correlation, as modified by Selander [57] to render it explicit.

$$f_g = \begin{cases} \left[3.8 \log \left(\frac{10}{Re_g} + 0.2 \frac{\varepsilon}{d} \right) \right]^{-2} & Re_g > 2400 \\ 16 Re_g^{-1} & Re_g \leq 2400 \end{cases} \quad (2.98)$$

$$Re_g = \frac{G d}{\mu_g} \quad (2.99)$$

$$f_l = \begin{cases} \left[3.8 \log \left(\frac{10}{Re_l} + 0.2 \frac{\varepsilon}{d} \right) \right]^{-2} & Re_l > 2400 \\ 16 Re_l^{-1} & Re_l \leq 2400 \end{cases} \quad (2.100)$$

$$Re_l = \frac{G d}{\mu_l} \quad (2.101)$$

$$f_m = \begin{cases} 0.046 Lo^{-0.25} & Lo \geq 30Ce \\ 0.046 Lo^{-1.25} (30Ce) & Lo < 30Ce \end{cases} \quad (2.102)$$

$$Lo = \frac{G^2 d}{\rho_m \sigma} \left(\frac{\mu_g}{\mu_l} \right)^{0.5} \quad (2.103)$$

$$Ce = \begin{cases} \rho_l g \frac{(d - 0.001)^2}{\sigma} \left(\frac{\mu_g}{\mu_l} \right) & d > 0.001 \\ 0 & d \leq 0.001 \end{cases} \quad (2.104)$$

Reddy et al. [58] developed an accurate two-phase friction multiplier in round tubes for vertical upflow for use with the homogeneous model in nuclear core analysis. They employed a data base of 1 533 adiabatic and 864 diabatic two-phase pressure drop measurements on single tubes. The experimental data covered the ranges of $300 < p < 1300$ psia, $0.33 < G < 3.3$ lb_m/ft².hr, $0 < x < 100\%$, $0.2 < d < 0.6$ in., and $5 < L < 100$ in. They developed the two-phase friction multiplier as a function of pressure, mass quality and mass flux. Their correlation was

$$\phi_{lo}^2 = 1 + x \left(\frac{\rho_l - \rho_g}{\rho_g} \right) C \quad (2.105)$$

$$C = \begin{cases} 0.357(1 + p_r) x^{-0.175} G^{-0.45} & 300 < p < 600 \\ 1.02 x^{-0.175} G^{-0.45} & p > 600 \end{cases} \quad (2.106)$$

They established the adequacy of the correlation at the high pressure range (2 000 to 2 200 psia) of interest to PWRs by comparing the correlation with the Sher and Green [59] friction multiplier table, the Thom correlation [26] and the homogeneous model.

Awad and Muzychka [60] presented a simple two-phase frictional multiplier calculation method. They took into account the effect of the mass flux on ϕ_{lo}^2 . This was a modification of the Wallis method [18]. It overcame the main disadvantage in the Wallis method that ϕ_{lo}^2 was independent on the mass flux (i.e. both small and large mass fluxes gave the same results). The Wallis method made a discrepancy with many investigators who had found that ϕ_{lo}^2 was indeed a function of mass flux, among other things. In addition, comparison with other existing correlations for calculating ϕ_{lo}^2 such as the Wallis correlation based on the homogeneous model without mass effect on ϕ_{lo}^2 was presented. Comparison with results from other experimental test facilities for calculating ϕ_{lo}^2 was also presented.

2.2.2.1 The Homogeneous Model with Correction for Two-Dimensional Effects

Bankoff [61] presented a variable density single-fluid model for two-phase flow. This model was an extension of the homogeneous model with correction for two-dimensional effects. In his model, he proposed that the mixture flowed as a suspension of bubbles in the liquid, where radial gradients existed in the concentration of bubbles. The bubble concentration had a maximum value at the center of the pipe, decreased monotonically in a radial direction, and reached zero at the pipe wall. He assumed that the gas and liquid had the same velocity at any radial position. The relative velocity of

the bubbles with respect to the surrounding liquid was considered to be negligible compared to the stream velocity. The average velocity of the gaseous phase was greater than that of the liquid phase only because the gas concentration was in the regions of higher velocity. The mixture might be considered to be a single fluid whose density was a function of radial position because the slippage at any point was considered to be negligible. He expressed two-phase frictional pressure gradient $(dp/dz)_f$ as:

$$(dp/dz)_f = (dp/dz)_{f,l} \phi_{Bf}^{\frac{7}{4}} \quad (2.107)$$

His two-phase frictional multiplier (ϕ_{Bf}) was:

$$\phi_{Bf} = \frac{1}{1-x} \left[1 - \gamma \left(1 - \frac{\rho_g}{\rho_l} \right) \right]^{\frac{3}{7}} \left[1 + x \left(\frac{\rho_l}{\rho_g} - 1 \right) \right] \quad (2.108)$$

$$\gamma = \frac{0.71 + 2.35 \left(\frac{\rho_g}{\rho_l} \right)}{1 + \left(\frac{1-x}{x} \right) \left(\frac{\rho_g}{\rho_l} \right)} \quad (2.109)$$

His method was applicable to mass qualities from $0 < x < 1$.

2.2.3 Other Correlations

Wisman [62] proposed a new correlation for two-phase wall friction in vertical fluid flow. He derived his correlation from analytical considerations based upon an annular flow model. This new correlation was consistent for all flow patterns in vertical

two-phase flow although it was based upon an annular flow model. This new correlation yielded a smooth transition from two-phase flow to single-phase liquid flow, mainly because it incorporated the friction factor of the Moody diagram [51] for single-phase flow. The new correlation was

$$\left(\frac{dp}{dz}\right)_f = \frac{f}{1-0.5\alpha f} \frac{1}{d} \frac{1}{2} (1-\alpha) \rho_l u_l^2 \left[1 + \frac{\alpha}{1-\alpha} \frac{\rho_g}{\rho_l} \left(\frac{u_g}{u_l}\right)^2 + \alpha \frac{\rho_l - \rho_g}{\rho_l} \frac{gd}{u_l^2} \right] \quad (2.110)$$

$$f = 0.00560 + \frac{0.500}{Re^{0.32}} \quad (2.111)$$

$$Re = \frac{\rho_l u_l d}{\mu_l} (1-\alpha)(1-\sqrt{\alpha}) \left[1 + \frac{\alpha}{1-\alpha} \frac{\rho_g}{\rho_l} \left(\frac{u_g}{u_l}\right)^2 \right] \quad (2.112)$$

From the above equations, it is obvious that for the case of vanishing void fraction ($\alpha = 0$), the definitions of two-phase frictional pressure gradient and Reynolds number changed into the normal definitions for single-phase liquid flow. He checked the new correlation against 236 measurements from different sources. The standard deviation of these 236 measurements was 27.8%, with 68% having a relative error of less than 28.2%.

He also considered a simplification of the present correlation. For this simplification, he assumed that

$$0.5\alpha f \ll 1 \quad (2.113)$$

$$\frac{\alpha}{1-\alpha} \frac{\rho_g}{\rho_l} \left(\frac{u_g}{u_l}\right)^2 \ll 1 \quad (2.114)$$

$$\alpha \frac{\rho_l - \rho_g}{\rho_l} \frac{gd}{u_i^2} \ll 1 \quad (2.115)$$

These assumptions were valid for a wide range of two-phase flow conditions, including many practical engineering applications. The omission of these terms gave very simple formulae.

$$\left(\frac{dp}{dz} \right)_f = \frac{f}{d} \frac{1}{2} (1-\alpha) \rho_l u_i^2 \quad (2.116)$$

$$Re = \frac{\rho_l u_i d}{\mu_l} (1-\alpha)(1-\sqrt{\alpha}) \quad (2.117)$$

These simplifications gave increased deviations. For all 236 measurements together, these simplifications resulted in a mean deviation of -15.9% and a scatter band of 22.5%, i.e. a spread of 38.4% that justified the use of this simplified correlation for many practical engineering applications.

Friedel [63] proposed a method in terms of the multiplier (ϕ_{lo}^2). He developed his correlation and fit it with 25 000 data points. The smallest pipe diameter in the Friedel database was 4 mm. His correlation included both the gravity effect by Froude number (Fr), and the effect of surface tension and the total mass flux by Weber number (We). His correlation was

$$\phi_{lo}^2 = E + \frac{3.24FH}{Fr^{0.045} We^{0.035}} \quad (2.118)$$

$$E = (1-x)^2 + x^2 \left(\frac{\rho_l f_{go}}{\rho_g f_{lo}} \right) \quad (2.119)$$

$$F = x^{0.78} (1-x)^{0.224} \quad (2.120)$$

$$H = \left(\frac{\rho_l}{\rho_g} \right)^{0.91} \left(\frac{\mu_g}{\mu_l} \right)^{0.19} \left(1 - \frac{\mu_g}{\mu_l} \right)^{0.7} \quad (2.121)$$

$$Fr = \frac{G^2}{gd\rho_m^2} \quad (2.122)$$

$$We = \frac{G^2 d}{\rho_m \sigma} \quad (2.123)$$

$$\rho_m = \left(\frac{x}{\rho_g} + \frac{1-x}{\rho_l} \right)^{-1} \quad (2.124)$$

His correlation was for vertical upward flow and horizontal flow. He made comparisons between the bank data and the predictions of his correlation. The Friedel correlation had shown very good results in predicting two-phase frictional multiplier (ϕ_{lo}^2) for smooth pipes with $d > 7$ mm. The standard deviation was around 30% for single component flows, and about 40-50% for two-component flows.

Whalley [64] made evaluations based on heat transfer and fluid flow service proprietary data bank. He recommended with respect to the previous published correlations that the Friedel correlation should be used for $\mu_l/\mu_g < 1000$.

Friedel [65] presented a dimensionless power correlation for the calculation of two-phase frictional pressure drop in unheated straight pipes during vertical co current downward flow. It contained all the independent primary parameters of frictional

pressure drop in a physically correct relationship. Also, it included the physical limits of single-phase liquid and gas/vapor flow, as well as critical pressure conditions in single component systems. He based his correlation on a large number of published measurements. His correlation was

$$\phi_{io}^2 = (1-x)^2 + x^2 \left(\frac{\rho_l f_g}{\rho_g f_l} \right) + 5.7x^{0.7} (1-x)^{0.14} \left(\frac{\rho_l}{\rho_g} \right)^{0.85} \left(\frac{\mu_g}{\mu_l} \right)^{0.36} \left(1 - \frac{\mu_g}{\mu_l} \right)^{0.2} / (Fr^{0.09} We^{0.007}) \quad (2.125)$$

$$f_g = \begin{cases} 0.25 \{ 0.86859 \ln [Re_g / (1.964 \ln Re_g - 3.8215)] \}^{-2} & Re_g > 1055 \\ 16 Re_g^{-1} & Re_g \leq 1055 \end{cases} \quad (2.126)$$

$$Re_g = \frac{G d}{\mu_g} \quad (2.127)$$

$$f_l = \begin{cases} 0.25 \{ 0.86859 \ln [Re_l / (1.964 \ln Re_l - 3.8215)] \}^{-2} & Re_l > 1055 \\ 16 Re_l^{-1} & Re_l \leq 1055 \end{cases} \quad (2.128)$$

$$Re_l = \frac{G d}{\mu_l} \quad (2.129)$$

His correlation permitted an accurate reproduction of measured data sufficient for use in industrial design within all the individual parameter ranges. It should permit qualitatively correct predictions outside of the parameter ranges covered by measurements.

Olujic [66] presented a general correlation to predict frictional pressure gradient for gas-liquid flow in horizontal pipes. His correlation could be applied to all flow patterns except dispersed flow. In his model, he attempted to divide the flow regimes into

two regions based on the Froude number (Fr) and phase volume flow ratio (Q_l/Q_g). The first region was the β -region while the second region was α -region. The β -region corresponded to the range of low mass quality (bubble and plug flow), where the average liquid velocity (u_l) was approximately equal to the average gas velocity (u_g). The α -region corresponded to all other flow regimes such as wavy, slug and annular dispersed flow where the average gas velocity (u_g) was much greater than the average liquid velocity (u_l). He used different models in the two different regions. For the β -region, his model was

$$\left(\frac{dp}{dz}\right)_f = \left(\frac{2fG^2}{d\rho_l}\right) \left[1+x\left(\left(\frac{\rho_l}{\rho_g}\right)-1\right)\right] \left[1-x\left(\left(\frac{\rho_l}{\rho_g}\right)-1\right)(K_2-1)\right] \quad (2.130)$$

He estimated the Fanning friction factor (f) in the beta model for smooth and rough pipes from [67]

$$f = \left\{ -0.5 \log \left[\frac{\varepsilon}{3.7} - \frac{5.02}{Re} \log \left(\frac{\varepsilon}{3.7} + \frac{14.5}{Re} \right) \right] \right\} \quad (2.131)$$

$$Re = \frac{Gd}{\mu_l \left[1-x \left(1-\frac{\mu_l}{\mu_g} \right) \right]^{-1}} \quad (2.132)$$

He defined the parameter (K_2) in the beta model to be

$$K_2 = 1.2 \left[\frac{(7+8n)(7+15n)}{(7+9n)(7+16n)} \right] \quad (2.133)$$

$$n = \left(\frac{0.671}{Q_l / Q_g} \right) \left[1 + \left(1 + 0.907 \frac{Q_l}{Q_g} \right)^{1/2} \right] \quad (2.134)$$

For the α -region, his model was

$$\left(\frac{dp}{dz} \right)_f = \left(\frac{2fG^2 x^2}{d\rho_g} \right) \left[1 + \frac{\rho_g(1-x)}{\rho_l x \varepsilon_0} \right]^{19/8} \quad (2.135)$$

$$f = \frac{0.079}{Re_g^{0.25}} \quad (2.136)$$

$$Re_g = \frac{Gxd}{\mu_g} \quad (2.137)$$

The only unknown in Eq. (2.135) was the two-phase flow parameter (ε_0) that was a function of different independent variables like mass flux (G), mass quality (x) and pipe diameter (d). He defined the two-phase flow parameter (ε_0) as:

$$\varepsilon_0 = (\varepsilon_1^{-3} + \varepsilon_2^{-3})^{-1/3} \quad (2.138)$$

$$\varepsilon_1 = 0.77 \left(\frac{\rho_l}{\rho_g} \right)^{-0.55} \Gamma_0^{n_1} \quad (2.139)$$

$$\varepsilon_2 = 2.19 \left(\frac{\rho_l}{\rho_g} \right)^{-0.61} \Gamma_0^{n_2} \quad (2.140)$$

$$\Gamma_0 = \left(\frac{1-x}{x} \right) \left[\frac{G^2(1-x)^2}{\rho_l^2 g d} \right]^{-1/4} \left(\frac{\rho_l}{\rho_g} \right)^{-1/2} \left(\frac{\mu_l}{\mu_g} \right)^{-1/8} \quad (2.141)$$

$$n_1 = 0.266 \left(\frac{\rho_l}{\rho_g} \right)^{0.067} \quad (2.142)$$

$$n_2 = 1.78 \left(\frac{\rho_l}{\rho_g} \right)^{-0.078} \quad (2.143)$$

He compared the results of the proposed method with Lockhart-Martinelli predictions. The predictions of the proposed method were almost higher than those of Lockhart-Martinelli method, particularly for rough pipe data. He gave the comparison as the percentage of observed points reproduced within an accuracy of $\pm 30\%$.

Müller-Steinhagen and Heck [68] suggested a new correlation for the prediction of frictional pressure drop in two-phase flow $(dp/dz)_f$ in pipes. Their correlation had an advantage that was simple and more convenient to use than other methods. They developed an equation for the roughly linear increase of the pressure drop with increasing quality (for $x < 0.7$) as:

$$J = \left(\frac{dp}{dz} \right)_{f,lo} + 2 \left[\left(\frac{dp}{dz} \right)_{f,go} - \left(\frac{dp}{dz} \right)_{f,lo} \right] x \quad (2.144)$$

In order to cover the full range of flow quality ($0 < x < 1$), they used the method of superposition (at $x = 1$, $(dp/dz)_f = (dp/dz)_{f,go}$). Their correlation was

$$\left(\frac{dp}{dz} \right)_f = J(1-x)^{1/3} + \left(\frac{dp}{dz} \right)_{f,go} x^3 \quad (2.145)$$

It was obvious that their correlation related the frictional pressure gradient in two-phase flow $(dp/dz)_f$ to the frictional pressure gradient if the total flow assumed liquid in the pipe $(dp/dz)_{f,lo}$, the frictional pressure gradient if the total flow assumed gas in the pipe $(dp/dz)_{f,go}$, and the mass quality (x). To determine their reliabilities, they checked their correlation and another 14 correlations against a data bank containing 9 313 measurements of frictional pressure drop for different fluids, different tube diameters (between 4 and 352 mm), and different flow conditions (horizontal flow, vertical upwards flow, and vertical downwards flow). The data bank contained only measurements with the frictional pressure gradient $(dp/dz)_f$ was greater than 20 Pa/m to avoid uncertainties due to the scatter of data. They claimed that the best agreement between predicted and measured values was obtained using the correlation suggested by Bandel [12].

Xiao et al. [69] developed a comprehensive mechanistic model for gas-liquid two-phase flow in horizontal and near horizontal pipelines. In their model, they detected first the existing flow pattern. After that, they predicted the flow characteristics, primarily pressure drop and liquid holdup, for the stratified, intermittent, annular, or dispersed bubble flow patterns. They established a pipeline data bank that included large diameter field data collected from the A. G. A. database [70], and laboratory data published in the literature. The data bank included both black oil and compositional fluid systems. They evaluated the comprehensive mechanistic model against the data bank. In addition, they compared their model with the performance of some of the most commonly used correlations for two-phase flow in pipelines. Based on the comparison between the predicted and the measured pressure drops, the evaluation demonstrated that the overall

performance of the proposed model was better than that of any of the correlations for the wide variety of data contained in the data base, with the least absolute average percent error and the least standard deviation. In addition, they found that all individual flow pattern models gave better results than any of the empirical correlations.

Gomez et al. [71] presented a unified mechanistic model for the prediction of flow pattern, liquid holdup and pressure drop in wellbores and pipelines. Their model consisted of a unified flow pattern prediction model and unified individual models for stratified, slug, bubble, annular and dispersed bubble flow, applicable to the entire range of inclination angles, from horizontal ($\theta = 0^\circ$) to upward vertical flow ($\theta = 90^\circ$). This model could be applied to vertical wellbores, directional wells, horizontal wells, and pipelines, under normal production operation or artificial lift. The proposed model implemented new criteria to eliminate discontinuity problems and provide smooth transitions between the different flow patterns. Initially, they validated the new model against existing, various, elaborated, laboratory and field databases. After that, they tested the model against a new set of field data, from the North Sea and Prudhoe Bay, Alaska that included 86 cases. Also, they compared the proposed model with other 6 most commonly used models and correlations. They claimed that the proposed model showed an outstanding performance for pressure drop prediction, with -1.3% average error, 5.5% absolute average error and 6.2 standard deviation.

Osman and Aggour [21] presented an artificial neural network (ANN) model for accurate prediction of pressure drop for multiphase flow in horizontal and near horizontal pipes that could be used for a more effective and economical design of flow lines and

pipng networks. They developed and tested this model using field data covering a wide range of variables. They used a total of 225 field data sets for training and 113 sets data for cross-validation of the model. Also, they used another 112 sets of data to test the prediction accuracy of the model and compared its performance against existing correlations and mechanistic models. They claimed that the present model significantly out-performed all other methods and provided predictions with accuracy that had never been possible. They also conducted a trend analysis and showed that the present model provided the expected effects of the different physical parameters on pressure drop.

García et al. [72] took data from 2 435 gas-liquid flow experiments in horizontal pipelines, including new data for heavy oil. They compiled and processed data for power law and composite power law friction factor correlations. Their database included the widest range of operational conditions and fluid properties for two-phase friction factor correlations. They obtained separate power laws for laminar and turbulent flows for all flows in the database and also for flows sorted by flow pattern. They obtained composite analytical expressions for the friction factor covering both laminar and turbulent flows by fitting the transition region between laminar and turbulent flow with logistic dose curves. Logistic dose curves led to rational fractions of power laws that reduced to the power laws for laminar flow when the Reynolds number was low and to turbulent flow when the Reynolds number was large. The Reynolds number appropriate for gas-liquid flows in horizontal pipes was based on the mixture velocity and the liquid kinematic viscosity because the frictional resistance of the mixture was due mainly to the liquid. The definition of the Fanning friction factor for gas-liquid flow used in this study is based on

the mixture velocity and density. Their universal (independent of flow type) composite (for all Reynolds number) correlation for gas-liquid Fanning friction factor (FFUC) was

$$f_m = 0.0925 Re_m^{-0.2534} + \frac{13.98 Re_m^{-0.9501} - 0.0925 Re_m^{-0.2534}}{\left(1 + \left(\frac{Re_m}{293}\right)^{4.864}\right)^{0.1972}} \quad (2.146)$$

$$Re_m = \frac{U_m d}{\nu_l} \quad (2.147)$$

$$U_m = U_l + U_g \quad (2.148)$$

The standard deviation of the correlated friction factor from the measured value was estimated to be 29.05% of the measured value. They claimed that the above correlation was a best guess for the pressure gradient when the flow type was unknown or different flow types were encountered in one line.

Also, they obtained friction factor correlations for each flow type including slug flow, dispersed bubble flow, stratified flow, and annular flow. They presented error estimates for the predicted vs. measured friction factor together with standard deviation for each correlation. They compared the correlations in this study with previous correlations, homogeneous models and mechanistic models most commonly used for gas-liquid flow in pipelines. They presented comparisons of the predicted pressure drop for each and every data point in the database because different authors used different definitions for friction factors and Reynolds numbers. They claimed that their correlations predicted the pressure drop with much greater accuracy than those presented by previous authors.

It should be noted that García et al. [72] definition of the mixture Reynolds number is not suitable at high values of the dryness fraction. For example, for single-phase gas flow of air-water mixture at atmospheric conditions, García et al. [72] definition gives $Re_m = 14.9Re_g$ while other well-known expressions of two-phase viscosity such as McAdams et al. [45] expression gives $Re_m = Re_g$.

Bendiksen et al. [73] used the dynamic two-fluid model: OLGA in the simulation of two-phase oil and gas flow in pipelines. In this paper, they presented their model, in detail, stressing the basic equations and the two-fluid models applied. They applied separate continuity equations for gas, liquid bulk, and liquid droplets. These equations could be coupled through interphasial mass transfer. For conservation of momentum, they used only two equations. The first equation was a combined equation for the gas phase and for liquid droplets by canceling out the drag force on the gas/droplet. The second equation was for the liquid film at the wall. Also, they applied a mixture conservation energy equation. The formulation of the problem gave a set of coupled first-order, nonlinear, partial differential equations with rather complex coefficients. They solved these equations numerically. For the flow regime description, they applied two basic flow regime classes: distributed and separated. The distributed class included bubble and slug flow. The separated class included stratified and annular-mist flow. They compared predictions of steady-state pressure drop, liquid hold-up, and flow-regime transitions with data from the SINTEF Two-Phase Flow Laboratory and from the literature over a substantial range in geometrical scale (diameters (d) from 2.5 to 20 cm, some at 76 cm, pipeline length/diameter ratios (L/d) up to 5 000, and pipe inclination (θ)

of -15° to 90°), pressures from 100 kPa to 10 MPa, and a variety of different fluids. They claimed that the model gave reasonable results compared with transient data in most cases. The predicted flow maps and the frequencies of terrain slugging agreed well with experiments as they claimed. Also, they presented comparisons with evaluated field data.

2.2.4 Experimental Study

Hoogendoorn [74] made an investigation of gas-liquid flow in horizontal smooth and rough pipes under adiabatic conditions. He used air-water, air-gas oil and air-spindle oil mixtures as the working fluid. For smooth pipes, the range of inner diameter was from 24 to 140 mm. For rough pipes, the inner diameter was 50 mm with roughness (ϵ/d) values of 0.030, 0.019, 0.0030, and 0.0012. During his experiments, the observed flow patterns were stratified flow, wave flow, plug flow, slug flow, mist-annular flow, and froth flow. The flow patterns occurring with gas-oil flow could be predicted from one diagram, the effect of pipe diameter and liquid viscosity was small. The same diagram could be used for gas-water flow with an enlarged wave flow region. For the pressure drop, he found that the Lockhart-Martinelli correlation was valid only for plug, slug, and froth flow at atmospheric pressure. He discovered that the Lockhart-Martinelli correlation could not be used for plug, slug, and froth flow, if gas densities were different from that of air at atmospheric pressure. Also, he found that it was inadequate for stratified, wave, and mist-annular flow under any conditions. As a result, he gave separate new correlations for these cases that the Lockhart-Martinelli correlation was not suitable. For the case of plug, slug, and froth flow, he gave a new correlation in the form:

$$\Delta p_f = \Delta p_{f,lo} \left[1 + 230 \left(\frac{G_g}{G_l} \right)^{0.84} \right] \left[0.00138 \left(\frac{\rho_l}{\rho_g} \right) \right]^n \quad \text{for} \left(\frac{G_g}{G_l} \right) < 0.05; Re_{lo} > 3000 \quad (2.149)$$

$$n = 9.5 \left(\frac{G_g}{G_l} \right)^{0.5} - 62.6 \left(\frac{G_g}{G_l} \right)^{1.3} \quad \text{for} \left(\frac{G_g}{G_l} \right) < 0.03 \quad (2.150)$$

$$n = 1 \quad \text{for} \left(\frac{G_g}{G_l} \right) \geq 0.03 \quad (2.151)$$

For the case of wave flow, he gave a new correlation that included the effect of pipe diameter and pipe roughness. His correlation was

$$\Delta p_f = C \left(\frac{G_g}{G_l} \right)^{1.45} \left(\frac{1}{2} \frac{L G_l^2}{d \rho_g} \right) \quad \text{for} \left(\frac{G_g}{G_l} \right) < 0.8 \quad (2.152)$$

Table 2.8 shows the effects of pipe diameter and liquid viscosity on C .

Table 2.8 Effects of Pipe Diameter and Liquid Viscosity on C

d (m)	C (air-gas oil)	C (air-spindle oil)
0.050	0.026	0.028
0.091	0.022	
0.140	0.021	0.022

Table 2.9 shows the effect of pipe roughness on C , for air-gas oil in 50 mm pipes.

Table 2.9 Effect of Pipe Roughness on C , for Air-Gas Oil in 50 mm Pipes

Pipe Roughness (ε/d)	C
0.0012	0.026
0.0030	0.032
0.019	0.045
0.030	0.052

For the case of mist-annular flow, he found that Δp_f was independent of liquid mass flux if this was greater than $30 \text{ kg/m}^2\cdot\text{s}$. For air-gas oil flow, he gave a new correlation in the form:

$$\Delta p_f = 0.12(G_g)^{-0.25} \left(\frac{1}{2} \frac{L}{d} \frac{G_g^2}{\rho_g} \right) \text{ for } 30 < G_l < 200 \text{ kg/m}^2\cdot\text{s} \quad (2.153)$$

For rough 50 mm pipes with air-gas oil flow, he found that in the case of not too great roughness ($\varepsilon/d = 0.0012$, and 0.0030 , or $\varepsilon = 0.06$, and 0.15 mm), the pressure drop was nearly equal to that for mist-annular flow in smooth pipes. For great roughness ($\varepsilon/d = 0.019$, and 0.03 , or $\varepsilon = 0.95$, and 1.5 mm), the pressure drop was about 1.1 of that for air flowing alone. Also, he developed a capacitive method enabling accurate measurements of liquid holdup to be made. He correlated the results of liquid holdup measurements empirically with the slip velocity between the phases.

Isbin et al. [75] studied frictional pressure drop of steam-water mixtures for adiabatic flow in horizontal pipes of 0.484 and 1.062 in. diameter respectively. The range of pressure was from 25 to 1 415 psia. They carried out the low pressure experiments (25

to 100 psia) in 1.062 in. diameter. The range of the intermediate pressure was from 400 to 800 psig). They carried out the high pressure experiments (1 000 to 1 415 psia) in 0.484 in. diameter. The total mass flow rate range was from 454 to 4 350 lb_m/hr. In their experiments, they used 3 ranges of inlet steam flow rates; low (330 to 434 lb_m/hr), medium (800 to 900), and high (1 250 to 1 350). They varied the mass quality from about 8 to 98%. They calculated the mass quality in the test section from an energy balance. They synthesized the steam-water mixtures by mixing steam and water. They took considerable care to ensure that the method of mixing did not affect the pressure drop results and that the pressure measurements were made far from the inlet and outlet sections of the pipe. They compared the data to standard correlations. They suggested a new restricted correlation that took into account the pressure and flow rate dependencies.

Chawla [76] determined the local heat transfer coefficient and the pressure drop in horizontal evaporator tubes experimentally as a function of the quality, the heat flux intensity, the mass flow rate of refrigerant, and the saturation temperature. He used R-11 as a working fluid. He used copper tubes of 6, 14, and 25 mm internal diameter for his experiments. He found that in the region of low intensity heat fluxes, the local heat transfer coefficient was essentially a function of the mass flow rate and independent on the heat flux intensity. On the other hand, in the case of high heat flux intensities, he found that the local heat transfer coefficient was primarily dependent on the heat flux intensity. The graphs for local heat transfer coefficient and pressure drop indicated a maximum value at a definite quality. He correlated the experimental values for the local heat transfer coefficient and the pressure drop with good accuracy by means of

dimensionless equations. He suggested his correlation based on the velocity ratio between the vapor and liquid phases. Based on gas frictional pressure gradient $(dp/dz)_{f,g}$, Chawla suggested the following method:

$$(dp/dz)_f = (dp/dz)_{f,g} \phi_{Chawla} \quad (2.154)$$

His two-phase frictional multiplier (ϕ_{Chawla}) was:

$$\phi_{Chawla} = x^{1.75} \left[1 + S \left(\frac{1-x}{x} \right) \left(\frac{\rho_g}{\rho_l} \right) \right]^{2.375} \quad (2.155)$$

$$S = \frac{1}{9.1 \left[\left(\frac{1}{Re_g Fr_m} \right)^{0.167} \left(\frac{1-x}{x} \right) \left(\frac{\rho_g}{\rho_l} \right)^{0.9} \left(\frac{\mu_g}{\mu_l} \right)^{0.5} \right]} \quad (2.156)$$

$$Re_g = \frac{Gd}{\mu_g} \quad (2.157)$$

$$Fr = \frac{G^2}{gd\rho_m^2} \quad (2.158)$$

$$\rho_m = \left(\frac{x}{\rho_g} + \frac{1-x}{\rho_l} \right)^{-1} \quad (2.159)$$

His method was applicable to mass qualities from $0 < x < 1$.

Grønnerud [77] investigated two-phase flow resistance that occurred with boiling refrigerants in circulation type evaporators. He used R-12, and R-717 (NH₃) as the refrigerants. Most of the data used were supplied from extensive tests on a coil-type

evaporator. The coil was constructed from 26.2/33 mm steel pipe. He supplied the heat load by electric heating cables. He measured wall and refrigerant temperatures by a large number of fine thermocouples. He used 13 pressure taps to find the development of pressure during the passage of the heat transfer zone. He observed the actual flow pattern through short glass sections installed at equal distances along the tube. He varied the heat flux up to $2\ 600\ \text{W/m}^2$ for tests with R-717, and somewhat less for R-12. The range of evaporation temperature was from -45 to 5°C . The mass flux range was from 20 to $1\ 600\ \text{kg/m}^2\cdot\text{s}$. Expressed with dimensionless groups, the results covered the range $Re_{lo} = 2 \times 10^3$ to 2×10^5 , $Fr_{lo} = 0.004$ to 20, boiling number (B_{gd}) up to 2.2×10^{-4} , and density ratio (ρ_l/ρ_g) = 70 to 1 100. The experimental data included about 400 measurements of two-phase pressure drop with R-12, and about 600 measurements with R-717. He carried out the test series with R-12 with high thermal stability, while R-717 tests were somewhat less satisfactory in this respect. The observed flow patterns included all the main flow patterns described as bubbly, plug, stratified, wavy, slug, crescent, annular, and spray. He compared the experimental data from R-12 tests with Lockhart-Martinelli, Chawla, and Bo Pierre correlations. The pressure drop predicted by Lockhart-Martinelli correlation was much higher than the measured one. The scatter was far beyond what could be expected. The pressure drop predicted by Chawla correlation agreed with the measured one within $\pm 30\%$. For $x < 0.1$, the calculated values dropped too much below the measured values, and the scatter was high. The predicted values by Bo Pierre correlation partly agreed with the measured values for lower pressure drop. At higher pressure drop, the predicted values were much too low. The scatter was unreasonably great, and similar

to that of Lockhart-Martinelli correlation. Also, he compared the experimental data from R-717 tests with Lockhart-Martinelli correlation. The Lockhart-Martinelli correlation gave calculated values between 50% and 200% higher than the measured ones. The scatter in this comparison was greater than for the R-12 data due to the stability problem connected with R-717 tests. From the comparison of the measurements with the commonly used pressure drop correlations, it could be seen that the calculations did not give the precision required for optimizing evaporators. So, he developed a general formula that could assure better accuracy of pressure drop calculations. His correlation was

$$\Delta p_f = \phi_{gd} \Delta p_{f,l} \quad (2.160)$$

His two-phase frictional multiplier (ϕ_{gd}) could be defined as follows:

$$\phi_{gd} = 1 + f_{Fr} \left[x + 4(x^{1.8} - x^{10} f_{Fr}^{0.5}) \right] \left[\frac{\left(\frac{\rho_l}{\rho_g} \right)}{\left(\frac{\mu_l}{\mu_g} \right)^{0.25}} - 1 \right] \quad (2.161)$$

If the Froude number when the total flow assumed liquid in the pipe (Fr_{lo}) was greater than or equal to 1, then the friction factor (f_{Fr}) had a value of 1.0. If Fr_{lo} was less than 1, then:

$$f_{Fr} = Fr_{lo}^{0.3} + 0.0055 \left(\ln \frac{1}{Fr_{lo}} \right)^2 \quad (2.162)$$

His correlation was applicable to $0 \leq x < 1$. His equations correlated 98% of R-12 data within the limits of $\pm 30\%$ deviation and 95% of the data within $\pm 20\%$. His equations correlated 87% of R-717 data within the limits of $\pm 30\%$. Although the scatter of these results was greater, the experimental data verified the general applications of his equations. Also, the analysis included about 250 measurements of total pressure drop of adiabatic R-12 two-phase flow in a horizontal tube with inside diameter of 20.8 mm. The data obtained from these tests could also be correlated with his equations within the limits of $\pm 20\%$. He claimed that the pressure drop predicted by his correlation agreed reasonably well, both for R-12 and R-717, in spite of the great differences in physical properties. The scatter that appeared in the comparison diagrams between the measured and calculated values was relatively small taking into consideration the fluctuations normally occurring in large industrial evaporators.

Rashid and Edward [78] used a horizontal boiling water loop to obtain pressure drop and heat transfer data for two-phase steam-water flow for pressures of up to 825 kPa. They used the data to examine the predictions of the separated flow model using the Lockhart-Martinelli method of estimating the two-phase friction multiplier. The influence of mass flux on the two-phase friction multiplier has been reported for high pressure systems by many workers. Their work confirmed the existence of the influence of mass flux on the two-phase friction multiplier at low pressures. Also, they found that the system pressure had an effect on the two-phase friction multiplier. They presented a

correlation for the two-phase friction multiplier, incorporating the effects of mass flux and pressure. They expressed the Chisholm parameter, C , as

$$C = 3.218(2000/G)^{0.3602} (v_g/v_l)^{0.262} \quad (2.163)$$

They tested the correlation against data from two independent sources. They found the predictions to be in very good agreement with the data.

Hashizume [79] performed experiments to obtain data on flow pattern, void fraction, and pressure drop of refrigerant two-phase flow in a horizontal pipe. He used R-12 and R-22 as refrigerants. He changed the saturation pressure from 5.7 bar (corresponding to a saturation temperature of 20°C for R-12) to 19.6 bar (corresponding to a saturation temperature of 50°C for R-22). He used a natural circulation loop. The inner diameter of the measurement section was 10 ± 0.05 mm. The measurement section included the entrance region, the pressure drop measurement section, the void fraction measurement section, the flow pattern observation section, and the exit region. Their lengths were 1 000, 2 000, 100, 200, and 400 mm, respectively. To minimize the heat leakage to or from the environment, he thermally insulated all piping and components of the loop, except for some parts of the void fraction measurement section, and the flow pattern observation section with 50 mm glass wool. Further, he located the loop, except for the condenser, in a room with an air conditioner, and the room temperature was held at a constant value that was below 5-10 K than the saturation temperature in the measurement section. He observed 5 types of flow pattern. They were stratified flow, wavy flow, slug flow, semi-annular flow, and annular flow. Semi-annular flow was a

transient flow pattern to annular flow. In semi-annular flow, a continuous liquid film flow could be observed, but the liquid film at the top of the pipe was too thinner than at the bottom to be determined as annular flow. He performed void fraction measurement by the shut-off method. He used a differential transducer with lineariser and amplifier for the pressure drop measurement. To protect the transducer, he closed a pressure-balancing valve between capillary tubes only during the pressure drop measurement. He found that systematically produced experimental data, especially on void fraction, had not been published previously in this range, though they would be useful in practical applications. In addition, the experimental data would be helpful to clarify the applicability of the available correlations and their accuracy, and to develop theoretical models of two-phase flow.

Hashizume et al. [80] analyzed two-phase flow in horizontal pipe using simplified models for annular and stratified flow. They described the velocity profiles for the liquid and gas phase for the turbulent flow with the Prandtl mixing length. They modeled the stratified flow as flow between parallel plates. From these models, they calculated the frictional pressure drop for each flow pattern region (annular and stratified flow). They covered the intermediate region (wavy flow) between annular and stratified flow using linear interpolation on a log-log plot between the two extremes according to the proposal by Bandel [12], and Bandel and Schlünder [81,82]. They determined the flow pattern transitions using the modified Baker map, whereas Bandel determined the flow pattern transitions empirically from the comparison of their pressure drop calculation method with experimental data. They compared the calculation method for frictional pressure

drop based on this analysis with the flow pattern transition according to the modified Baker map with refrigerant data presented by Hashizume [79], Chawla [76], and Bandel [12]. They claimed that comparison of their analysis with existing experimental data of refrigerants showed good agreement.

Jung and Radermacher [83] made an experimental study on pressure drop of pure and mixed refrigerants during horizontal annular flow boiling under uniform heat flux. The objective of the study was investigating mixture effects (if there were any) on pressure drop as well as developing of a simple correlation for design engineers. They used R22, R114, R12, and R152a as the working fluid. The primary experimental parameters were overall composition, mass flow rate, heat flux, and quality. The overall compositions for R22/ R114, and R12/R152a mixtures were 0, 23, 48, 77, and 100 mole % R22, and 0, 21, 60 (azeotrope, R500), 89, and 100 mole % R12, respectively. The range of mass flow rate was 16-46 g/s (equivalent to 250-720 kg/m².s). The range of heat flux was 10-45 kW/m². The quality ranged up to 95%. They made the test section of two identical 4 m long, 9.1 mm i.d., type 304 stainless steel tubes (specification ASTM A 269/213) with a nominal thickness of 0.25 mm. The test section was very long to eliminate entry length effects. Due to space limitation, they connected these test sections by a 180° U-turn bend, made of copper tube with the same inside diameter. They heated the test section using DC power supply (60 V, 300 A). There were three bus connections to the DC power supply on the first 4 m section and five on the second 4 m section. These bus connections effectively created a variable length test section. They used four pressure transducers and one differential pressure transducer in conjunction with two-5 way valves

for the pressure measurements at 8 bus connections. For most of the tests, they kept the pressure at the outlet of the test section at a reduced pressure of 0.08. To determine the effect of pressure, they performed several tests at reduced pressures of 0.12 and 0.16. They determined the reduced pressures for mixtures from the critical pressures calculated by a linear mole fraction weighting (ideal mixing rule) of the pure components' critical pressure values. They took more than 600 pressure drop data of R22/R114, and R12/R152a mixtures. For single-phase pressure drops, they compared the results of five tests for pure refrigerants and eight for mixtures with the Blasius type correlation suggested by McAdmas [84]. The correlation predicted the present results with a mean deviation of 8%. In addition, they compared the results against well-known correlations. Bo Pierre's correlation based on the homogeneous model failed to correlate half of the present data. Care should be taken in its use especially when mass flow rate was low with a high heat flux. Martinelli and Nelson correlation based on the separate model overpredicted the present data by 20%. However, pressure drops with both pure and mixed refrigerants were well correlated by Lockhart-Martinelli parameter for the turbulent liquid-turbulent gas flow type (X_{tt}). Furthermore, no composition dependence of pressure drop was found with mixtures. They developed a new correlation by modifying Martinelli and Nelson correlation. They applied the thermodynamic corresponding states principles to correlate the property group commonly encountered in two-phase flow by using a reduced pressure. They provided a chart to facilitate the estimation of pressure drop during flow boiling. The correlation was

$$\phi_p^2 = 12.82 X_u^{-1.47} (1-x)^{1.8} = 30.78 x^{1.323} (1-x)^{0.477} p_r^{-0.7232} \quad (2.164)$$

The correlation predicted the present data for both pure and mixed refrigerants with a mean deviation of 8.4%.

Souza et al. [85] conducted an experimental study to provide the local pressure drop during two-phase flow of pure refrigerants and refrigerant-oil mixtures in horizontal smooth copper tubes. Examples of pure refrigerants were R-12 and R-134a (ozone-safe refrigerant). For refrigerant-oil mixtures, they investigated the influence of oil on the pressure drop with oil concentrations up to 5% by weight. They added PAG (Polyalkylene Glycol) and ester oils to R-134a and mineral oils to R-12. They made the test section of 8.0 ft (2.44 m) long, 0.43 in. (10.9 mm) i.d. smooth copper tube. They conducted adiabatic and uniform heat flux applied to test section (non-adiabatic) tests in the application range of residential and automobile air conditioning evaporators. They applied a uniform heat flux to the test section using electrical resistance strip heaters that were wrapped along the tube. They soldered sixteen thermocouples inside grooves along the external surface of the tube to measure surface temperature at various axial locations. They soldered pressure taps at the inlet and outlet of the test section onto the tube. They measured the pressure drop directly from the differential pressure transducer through the data acquisition system. They determined the inlet quality to the test section from an energy balance on the preheater. They observed the flow patterns through the sight glasses at the inlet and outlet of the horizontal test section. For most of the tests, the predominant flow pattern was annular flow. For lower mass fluxes and qualities, they

also observed wavy-stratified and semi-annular flow. For higher mass fluxes and qualities, they also observed misty-annular flow. They developed a new correlation for two-phase frictional pressure drop of pure refrigerants inside horizontal straight smooth tubes using the separated flow model, the Lockhart-Martinelli parameter for the turbulent liquid-turbulent gas flow type (X_{tt}), and the liquid Froude number (Fr_l). They included the liquid Froude number (Fr_l) in their correlation because when body forces and inertia forces were significant in the flow, i.e. for stratified or wavy flow regimes, the liquid Froude number played an important role in the correlation. The correlation was

$$\phi_{to}^2 = (1.376 + c_1 X_{tt}^{-c_2}) (1-x)^{1.75} \quad (2.165)$$

For $0 < Fr_l \leq 0.7$

$$\begin{aligned} c_1 &= 4.172 + 5.480 Fr_l - 1.564 Fr_l^2 \\ c_2 &= 1.773 - 0.169 Fr_l \end{aligned} \quad (2.166)$$

For $Fr_l > 0.7$

$$\begin{aligned} c_1 &= 7.242 \\ c_2 &= 1.655 \end{aligned} \quad (2.167)$$

In their correlation, when the liquid Froude number (Fr_l) was greater than 0.7, the flow was predominantly annular, the gravitational force was negligible, and the two-phase flow frictional multiplier could be well correlated based on the Lockhart-Martinelli

parameter alone. Therefore, when the liquid Froude number (Fr_l) was greater than 0.7, the liquid Froude number (Fr_l) dependence of coefficients in Eq. (2.165) was dropped. They found that their correlation predicted the frictional pressure drop for both R-134a and R-12 data within $\pm 10\%$ with a mean deviation of 4.6%. To determine the acceleration pressure drop, they used a model for which the void fraction was determined by the correlation of Zivi [17] using the concept of minimum entropy production. The total pressure drop for two-phase flow, i.e. frictional and acceleration, could be obtained by adding the resulted numerical integration of the frictional local pressure drop correlation over the length of the tube (i.e. over the evaporator quality change) with the acceleration pressure drop. They found that they predicted the total pressure drop for both R-134a and R-12 data within $\pm 20\%$ with a mean deviation of 6.2%. For refrigerant-oil mixtures, they found that the pressure drop increased as oil concentration increased. They developed a functional dependence between the ratio of the pressure drop with and without oil and the oil concentration. The correlation could be expressed as follows for oil concentrations between 0 and 5% only:

$$\Delta p_{oil} = \Delta p_{pure} (1 + 12.4\omega - 110.8\omega^2) \quad (2.168)$$

The above correlation predicted the average pressure drop for both R-134a and R-12 data within $\pm 7.5\%$ with a mean deviation of 3.3%.

Souza and Pimenta [86] designed and developed a single tube evaporator test facility to measure pressure drop and heat transfer coefficients during two-phase flow of pure and mixed refrigerants inside horizontal straight copper tubes. For both adiabatic

and non-adiabatic (uniform heat flux) tests, they conducted tests in the application range of automobile and domestic refrigeration. They used R-12 and R-22 as an example of pure refrigerants. They used R-134a, MP-39 (zeotropic which had different saturation temperatures for same evaporator pressure, a mixture of 52 wt% R-22, 33% R-124, and 15 wt% R-152a) and R-32/125 (azeotropic which had the same saturation temperatures for same evaporator pressure, a mixture of 60 wt% R-32, and 40 wt% R-125) as an example of mixed refrigerants. They varied the inside tube diameter from 7.747 to 10.92 mm. They varied the tube length from 1.27 to 1.2954 m. They varied the test section inlet quality from 0 to 100%. They varied the mass flux from 50 to 600 kg/m².s. They varied the heat flux from 5 to 30 kW/m². They varied the saturation temperature from -20 to +15°C. They measured the pressure drop directly from the differential pressure transducer through the data acquisition system. They determined the inlet quality to the test section from an energy balance on the preheater. For both adiabatic and non-adiabatic (uniform heat flux) tests, they observed the flow patterns through the sight glasses at the inlet and outlet of the horizontal test section. The observed flow patterns were stratified, stratified-wavy, wavy, slug, wavy-annular, annular, and spray. For most of the tests, the predominant flow pattern was annular flow. For high mass fluxes, the observed flow pattern was predominantly annular while the observed flow pattern was predominantly stratified-wavy for low mass fluxes. They developed a new correlation for two-phase frictional pressure drop of pure and mixed refrigerants inside horizontal straight tubes using the separated flow model, the Lockhart-Martinelli parameter for the turbulent

liquid-turbulent gas flow type (X_{tt}), and an adequate physical property index (Γ). The correlation was

$$\phi_{lo}^2 = 1 + (\Gamma^2 - 1)x^{1.75} (1 + 0.9524\Gamma X_{tt}^{0.4126}) \quad (2.169)$$

$$\Gamma = \left(\frac{\rho_l}{\rho_g} \right)^{0.5} \left(\frac{\mu_g}{\mu_l} \right)^{0.125} \quad (2.170)$$

When compared the obtained results with this semi-empirical correlation to the obtained experimental data, they found that the mean absolute error was 0.276 kPa and the mean relative error or mean deviation was 8.2%. They claimed that comparisons with other correlations (Martinelli-Nelson [8], Baroczy [28], Chisholm [33], and Jung-Radermacher [83]) were adequate and consistent. They also claimed that comparisons with results from other experimental test facilities (Anderson et al. [87], Chaddock and Noerager [88]) showed good results. Thus, the obtained results with this semi-empirical correlation were good and sufficient accurate for engineering purposes. To determine the acceleration pressure drop, they used a model for which the void fraction was determined by the correlation of Zivi [17] using the concept of minimum entropy production. The total pressure drop for two-phase flow, i.e. frictional and acceleration, could be obtained by adding the resulted numerical integration of the frictional local pressure drop correlation over the length of the tube (i.e. over the evaporator quality change) with the acceleration pressure drop. They found that the calculated total pressure drop predicted the data well within the range of variation of the parameters considered in this study.

Ungar and Cornwell [89] presented data for an adiabatic two-phase pressure drop of ammonia in small diameter horizontal tubes. They performed their tests at NASA/Johnson Space Center, Houston, TX, U. S. A. in October 1991. Their data had direct application to the sizing of the flow through radiator tubes in the Space Station Freedom heat rejection system. They operated the insulated system at or near ambient temperature to minimize the heat leakage to or from the environment. They enclosed the entire test apparatus in an ammonia test enclosure that incorporated a vent system because ammonia was a hazardous material. They compared their data to existing correlations for pressure drop. They found that their data were significantly lower than the most commonly used correlations. So, two-phase pressure drop of ammonia in small diameter tubes could not predict with acceptable accuracy using the methods normally used for large diameter tubes. On the other hand, several of the less commonly used correlations (McAdams et al. [45], for homogeneous prediction and Asali et al. [40], for annular flow prediction) predicted the data accurately. Because of ease of calculation, McAdams et al. [45] correlation used for homogeneous pressure drop prediction had been recommended for use in sizing the Space Station Freedom Active Thermal Control System (SSF ATCS) flow through radiator tubes to yield an acceptable pressure drop.

Huang and Van Sciver [90] reported pressure drop and void fraction of two-phase helium flowing in horizontal tubes. They used a single stroke bellows pump to drive the horizontal flow loop. They changed the mass flow rate (m) from 0.5 to 2.0 g/s. They changed the system pressure from 0.65 to 1.2 atm. They used an in-line capacitance probe to obtain void fraction data. Then, they deduced from void fraction data using the

slip ratio relation. They found that the slip ratio was always greater than unity and decreased towards unity with increasing mass flow rate and increasing system pressure. They analyzed their results for the two-phase pressure drop measurements in terms of the conventional two-phase pressure drop multiplier (ϕ_{lo}^2) that was found to depend on system pressure and vapor quality. They found that the mass flow rate did not appear to have an effect on the two-phase frictional multiplier. In addition, they found that the tube size had a slight effect on the two-phase pressure drop multiplier at 1.2 atm. However, the tube size effect quickly diminished as the system pressure reduced. In general, for the range of parameters studied, the homogeneous model gave a much better prediction of the two-phase friction multiplier than did the Lockhart-Martinelli correlation.

Wang et al. [91] studied two-phase flow heat transfer and pressure drop characteristics of both pure refrigerants and mixtures in a smooth horizontal tube with a nominal diameter of 9.52 mm. The used refrigerants were R-22 and R-407C (a mixture of 23 wt% R-32, 25 wt% R-125, and 52 wt% R-134a). They used two different evaporation pressures of 600 kPa, and 680 kPa. The used mass flux (G) was between 100 to 300 kg/m².s. The used heat flux (q) was between 6 000 to 14 000 W/m². They presented experimental data in the form of quasi-local (locally averaged) heat transfer coefficients by controlling the inlet quality of the test tube using the preheater and frictional pressure drop. In addition, they reported the effects of heat flux, mass flux, and evaporation pressure on the heat transfer coefficients in their investigation. They found that the heat transfer coefficient increased with heat flux, mass flux, and evaporation pressure for R-22. On the other hand, the effect of evaporation pressure on the heat transfer coefficients

for R-407C was assumed negligible. The reduction of heat transfer coefficients for R-407C was approximately 50% to 70% as compared to R-22. The pressure drop of R-407C was similar to that of R-22 at low mass flux ($G = 100 \text{ kg/m}^2\cdot\text{s}$). The reduction of pressure drop for R-407C was approximately 45% as compared to R-22 at higher mass flux ($G = 300 \text{ kg/m}^2\cdot\text{s}$). The reduction in both of the heat transfer coefficients and frictional pressure drop might be attributed to the difference in flow pattern for the pure refrigerant and the mixture.

Yang and Webb [92] measured single-phase liquid, and two-phase flow pressure drop of R-12 in small hydraulic diameter extruded aluminum horizontal tubes with and without micro-fins under adiabatic conditions. They used two different tubes in this study. The first tube was a rectangular plain tube with a hydraulic diameter of 2.64 mm. The second tube was a rectangular micro-fin tube with a hydraulic diameter of 1.56 mm. For single-phase liquid flow, the data spanned Reynolds number based on hydraulic diameter between 2 500 and 23 000. For two-phase flow, the data spanned mass flux between 400 and 1 400 $\text{kg/m}^2\cdot\text{s}$, and vapor quality between 0.1 and 0.9. For single-phase liquid flow, they claimed that the friction factors for the plain and micro-fin tubes were uniformly 14% and 36% higher, respectively, than that predicted by the Blasius equation. For two-phase flow, they found that the pressure drop increased with increasing mass flux and vapor quality. The pressure drop of the micro-fin tube was higher than that of the plain tube at same mass flux and vapor quality. Also, they developed predictive methods for the single-phase liquid and two-phase friction factor. These data were not well correlated by the Chisholm correlation that used the Lockhart-Martinelli two-phase

multiplier. However, the equivalent mass flux concept proposed by Akers et al. [93], provided a very good correlation of the present data. Both the plain and micro-fin tube data were correlated within $\pm 20\%$ by a single curve. They found that the ratio of the two-phase and single-phase liquid friction factors for both the plain and micro-fin tubes were well correlated by a single curve, for all mass fluxes and vapor qualities tested. Since vapor shear was the only force that contributed to the frictional pressure drop in the plain tube, it was also the only significant force operative in the micro-fin tube. Thus, surface tension force played no significant role in affecting the frictional pressure drop in the micro-fin tube.

Zhang and Webb [94] measured single-phase, and two-phase flow pressure drop of refrigerants in small-diameter horizontal tubes under adiabatic conditions. They used R-134a, R-22, and R-404A as refrigerants. They used three different tubes in this study. The first tube was a multi-port, flat extruded aluminum tube with a hydraulic diameter of 2.13 mm. The other two tubes were copper tubes with inside diameters of 6.25 and 3.25 mm, respectively. The used range of mass flux (G) was from 200 to 1 000 kg/m².s. The used range of vapor quality (x) was from 20 to 89%. The used range of saturation temperature was from 20 to 65°C. They found that the single-phase friction factor data agreed with the Blasius equation ($f = 0.079Re^{-0.25}$) within $\pm 10\%$. The Friedel correlation did not predict the friction two-phase pressure drops in small diameter tubes accurately, especially for high-reduced pressure ($p_r = p/p_c$). This was due to the Friedel correlation gave good results in predicting two-phase frictional multiplier (ϕ_{lo}^2) for smooth tubes with $d > 7$ mm. They developed a new correlation for two-phase friction pressure drop in

small diameter tubes by modifying the Friedel correlation using the data taken in the present and in a previous study. The new correlation was

$$\phi_{lo}^2 = (1-x)^2 + 2.87x^2 p_r^{-1} + 1.68x^{0.8} (1-x)^{0.25} p_r^{-1.64} \quad (2.171)$$

The new correlation predicted 119 data points with a mean deviation of 11.5%.

Chen et al. [95] measured two-phase pressure drop in small horizontal smooth round copper tubes of diameters of 1.02, 3.17, 5.05, and 7.02 mm respectively. The corresponding lengths for the pressure drop measurements were 150, 995, 995, and 995 mm respectively. They used air-water as a working fluid. They compared their experimental data with homogeneous, slug, and annular flow models, as well as the commonly used empirical correlations. They compared all the measured pressure data with the predictions of empirically correlations of Troniewski-Ulbrich [96], Friedel [63], and Chisholm [33]. Their deviations were 276.35%, 156.94%, and 84.82%, respectively. Thus, their tested results indicated that the empirical correlations available in the literature were failed to predict the data. They found that the slug flow and annular flow model gave fair predictions to their corresponding flow regime data. Also, the homogeneous model showed the best prediction as compared to other empirical correlations. However, they observed over-predictions for homogeneous and annular models at higher mass flux and higher quality region for 1.02, and 3.17 mm data. Since surface tension had a strong effect on the smooth liquid-vapor interface in smaller tubes. So, they developed empirical correlation based on the homogeneous model by introducing the Bond (Bo) and Weber (We) numbers. The modified correlation was:

$$\left(\frac{dp}{dz}\right)_f = \Omega_m \left(\frac{dp}{dz}\right)_{f,m} \quad (2.172)$$

$$\Omega_m = \begin{cases} 1 + (0.2 - e^{-Bo}) & Bo < 2.5 \\ 1 + \left(\frac{We^{0.2}}{e^{Bo^{0.3}}}\right) - e^{-Bo} & Bo > 2.5 \end{cases} \quad (2.173)$$

$$Bo = \frac{g(\rho_l - \rho_g)(d/2)^2}{\sigma} \quad (2.174)$$

$$We = \frac{G^2 d}{\rho_m \sigma} \quad (2.175)$$

They compared between the modified homogeneous predications and their experimental data. The new correlation gave a mean deviation of 23.98%. Also, They modified the Friedel correlation. The modified Friedel correlation was:

$$\left(\frac{dp}{dz}\right)_f = \Omega_{Friedel} \left(\frac{dp}{dz}\right)_{f,Friedel} \quad (2.176)$$

$$\Omega_{Friedel} = \begin{cases} \frac{0.0333 Re_{lo}^{0.45}}{Re_g^{0.09} (1 + 0.4e^{-Bo})} & Bo < 2.5 \\ \frac{We^{0.2}}{2.5 + 0.06 Bo} & Bo > 2.5 \end{cases} \quad (2.177)$$

$$Bo = \frac{g(\rho_l - \rho_g)(d/2)^2}{\sigma} \quad (2.178)$$

$$We = \frac{G^2 d}{\rho_m \sigma} \quad (2.179)$$

They compared between the modified Friedel correlation predications and their experimental data. The new correlation gave a mean deviation of 23.76%. The modified homogeneous model and the modified Friedel correlation were applicable for tube diameters less 10 mm. In order to check the capabilities of the proposed correlations, they compared the modified homogeneous model and the modified Friedel correlation with four refrigerants data sets of R-12, R-22, R-134, and R-410A from other investigators. They observed that there were fairly good agreements of data and predictions.

Chen et al. [97] developed an empirical correlation to predict the two-phase pressure drop in small diameter tubes ($d < 10$ mm). In order to collect two-phase pressure drop data in small diameter tubes, they performed experiments and updated data from the literature. Data from the literature contained 8 refrigerants (ammonia, R-12, R-22, R-125, R-134a, R-404, R-407C, and R-410A) and 3 air-water data sets. The total number of data points was 1 484. They made comparisons between commonly used correlations and the collected data. They found that the Chisholm correlation showed poor predictive ability to the referred data having smaller diameter tubes. The Chisholm correlation gave a mean deviation of 95.1%. The Friedel correlation and the Souza and Pimenta correlation gave fair predictions for the refrigerant data, but failed to predict the air–water data because of the surface tension effect. The Friedel correlation gave a mean deviation of 80.4%. The Souza and Pimenta's correlation gave a mean deviation of 66.9%. They concluded that the homogeneous model gave good predictions for the refrigerant and air–water data sets. The homogeneous model gave a mean deviation of 34.7%. In this regard, they developed an empirical correlation based on the homogeneous model since they noticed that it

showed a better predictive ability than the other empirical correlations. They modified the homogeneous model by introducing the Bond (Bo) and Weber (We) numbers and other related dimensionless parameters in order to develop a general correlation for practical applications. They gave the proposed modified homogeneous model as:

$$\left(\frac{dp}{dz}\right)_f = \Omega_m \left(\frac{dp}{dz}\right)_{f,m} \quad (2.180)$$

$$\Omega_m = \frac{0.85 - 0.082Bo^{-0.5}}{0.57 + 0.004Re_g^{0.5} + 0.04Fr^{-1}} + \frac{80We^{-1.6} + 1.76Fr^{0.068} + \ln(Re_g) - 3.34}{1 + e^{(8.5 - 1000\rho_g/\rho_l)}} \quad (2.181)$$

$$\left(\frac{dp}{dz}\right)_{f,m} = \frac{2f_m G^2}{d\rho_m} \quad (2.182)$$

$$f_m = \begin{cases} 16 Re_m^{-1} & \text{laminar} \\ 0.079 Re_m^{-0.25} & \text{turbulent} \end{cases} \quad (2.183)$$

They claimed that the new correlation gave a mean deviation of 19.1%.

Ould Didi et al. [98] obtained two-phase pressure drop data for evaporation of refrigerants in horizontal tubes. They used two different horizontal test sections of 10.92 and 12.00 mm diameter. They used five different refrigerants (R-134a, R-123, R-402A, R-404A and R-502). They changed the mass flux (G) from 100 to 500 kg/m².s. They changed the vapor quality (x) from 0.04 to 1.0. They compared their data against seven two-phase frictional pressure drop prediction methods. Overall, the method by Müller-Steinhagen and Heck [68], and that by Grönnerud [77] were concluded to provide the most accurate predictions. The widely quoted method of Friedel [63] gave the third best results. In addition, the data were classified by two-phase flow pattern using the Kattan-

Thome-Favrat [99-101] flow pattern map. For annular flow, they concluded that the best available method was that of Müller-Steinhagen and Heck [68]. For intermittent flow and stratified-wavy flow, they concluded that the best available method in both cases was that of Grønnerud [77]. The statistical deviations of the best methods still remained completely large with respect to the accuracy desired for reliable thermal design of evaporators and condensers. They observed that the peak in the experimental two-phase frictional pressure drop at high vapor qualities coincided with the onset of dryout in the annular flow regime, like the equivalent peak in the flow boiling heat transfer coefficient.

Yoon et al. [102] studied the evaporation heat transfer and pressure drop of carbon dioxide in a horizontal smooth tube made of a seamless stainless steel tube with d_i of 7.53 mm, and L of 5 m. They conducted their experiments at saturation temperatures of -4 to 20°C , heat fluxes of 12 to 20 kW/m^2 and mass fluxes of 200 to $530 \text{ kg/m}^2\cdot\text{s}$. To obtain a frictional pressure drop correlation for CO_2 , they modified the Chisholm correlation [48] with setting the exponent in the Blasius relation for friction factor to 0.25 by including the Weber number, with We based here in the mean flow velocity instead of the vapor superficial velocity. Their correlation was

$$\phi_{lo}^2 = 1 + a(\Gamma^2 - 1) \left[\frac{B}{We} x^{0.875} (1-x)^{0.875} + x^{1.75} \right] \quad (2.184)$$

$$\Gamma = \left(\frac{(dp/dz)_{f,go}}{(dp/dz)_{f,lo}} \right)^{0.5} = \left(\frac{\rho_l}{\rho_g} \right)^{0.5} \left(\frac{\mu_g}{\mu_l} \right)^{0.125} \quad (2.185)$$

$$We = \frac{\rho_g u_m^2 d}{\sigma} \quad (2.186)$$

They evaluated the constant a to be 4.2 by a least square fitting. They determined the B value according to the criteria given in Table 2.5. The resulting correlation presented an absolute deviation relative to the original database of 16.2%.

2.2.5 Computer Study

Soliman [103] presented a computer program for quick calculation of two-phase and single-phase flow pressure drops per 100 feet of pipe. He wrote the program in the BASIC language. He calculated the friction factor (f) based on Churchill model [104]. The pipe roughness factor (ϵ) used in the program was for old steel pipe and equal 0.00015 ft. For two-phase flow, he used the Baker and Lockhart-Martinelli correlations as outlined by Kern [105]. The program determined the flow region using a simplified Baker graph. To simplify the program, he grouped the seven conventional flow regions (dispersed, annular, bubble, stratified, wave, slug and plug flow) into only four regions (dispersed, annular, bubble, and plug flow). The reason was the wave and stratified regions were rare and only occurred in long horizontal pipes; otherwise the flow was annular. Thus, the program assumed the flow region was annular. Also, the plug flow was rare and thus, omitted from the program. He used the dispersed flow correlation for all the flow regions for pipes smaller than 2.5 inches. He used the annular and bubble flow correlations for pipes greater than 3 inches. He used the value of pipe inside diameter as 10 inches in the annular flow correlation for pipes equal or greater than 12 inches. Slug flow should be avoided in process piping because of different operational problems such as pressure fluctuations that could upset the process conditions and cause inconsistent

instrument reading and recording. The program gave the total summary of all inputs and the results of the calculation. For comparison, the examples considered here were the same examples of Kern [105]. The results from the program were very close to the graphical solutions of Kern [105]. Thus, the program was accurate and would save the user valuable time. The accuracy was still reasonable even if the flow regime calculated by the program was different than the Baker flow regime since the Baker flow regime boundaries were approximated. Single-phase pressure drop was accurate unless the equation limitation was exceeded. In this case, the line should be broken to smaller segments.

Parlikar et al. [106] presented a computer program to determine the flow pressure drop. They wrote the program in BASIC language. The program considered FPS system of units that could be easily converted to other units. They assumed that the two-phase flow was isothermal and turbulent in both the liquid and vapor phases. The pipe roughness factor (ϵ) used in the program was 0.00015 ft. The program could handle different types of flow patterns like dispersed, annular, bubble, stratified, wave, slug and plug flow. They used the dispersed flow correlations for all the flow regions for pipes smaller than 2.5 inches. The program followed the Baker flow regime boundaries truly without any approximation for all flow patterns. They fitted Baker flow regime boundaries with equations. The program used these equations to determine the flow region. If the calculated point fell exactly on the flow region curve (i.e. curve separating stratified and wave flow region) then the program calculated two-phase flow pressure drop for each type and considered the higher value. Whenever slug flow existed, the

program suggested different methods to avoid it. One of the methods was gas injection. The program made use of this method in calculating the additional gas flow to come out of the slug flow region. This was highly repetitive process that made almost manual calculation impossible. At the end, the program gave the total summary of all inputs and the results of the calculation. For comparison, the examples considered here were the same examples of Kern [105]. The results from the program were very close to the graphical solutions of Kern [105].

2.3 Comparison of Selected Two-Phase Frictional Pressure Gradient Flow Models

Figure 2.1 presents a comparison of several two-phase frictional pressure gradient models for steam flow at $x = 0.5$ and $p_s = 5\,000$ kPa in a smooth horizontal pipe at $d = 5.1$ mm. Figure 2.2 presents a comparison of several two-phase frictional pressure gradient models for R 12 flow at $x = 0.5$ and $T_s = 50^\circ\text{C}$ in a smooth horizontal pipe at $d = 10$ mm. Figure 2.3 presents a comparison of several two-phase frictional pressure gradient models for R 22 flow at $x = 0.5$ and $T_s = 50^\circ\text{C}$ in a smooth horizontal pipe at $d = 10$ mm. Figure 2.4 presents a comparison of several two-phase frictional pressure gradient models for Argon flow at $x = 0.4$ and $p_r = 0.188$ in a smooth horizontal pipe at $d = 14$ mm. The frictional pressure gradient is calculated using their definition of ϕ_l^2 and Eq. (2.3) or using their definition of ϕ_{lo}^2 and Eq. (2.1) if it is not given directly such as the Müller-Steinhagen and Heck correlation. It is clear from Figs. 2.1-2.4 that no two frictional pressure gradient models provide the same results. The abrupt change in the Chisholm [33] model in Figs. 2.2-2.4 is due to its piece wise construction. Since all two-phase

frictional pressure gradient models were developed in conjunction with experimental data, which are prone to measurement error, it is reasonable to expect that any prediction is also subject to similar error.

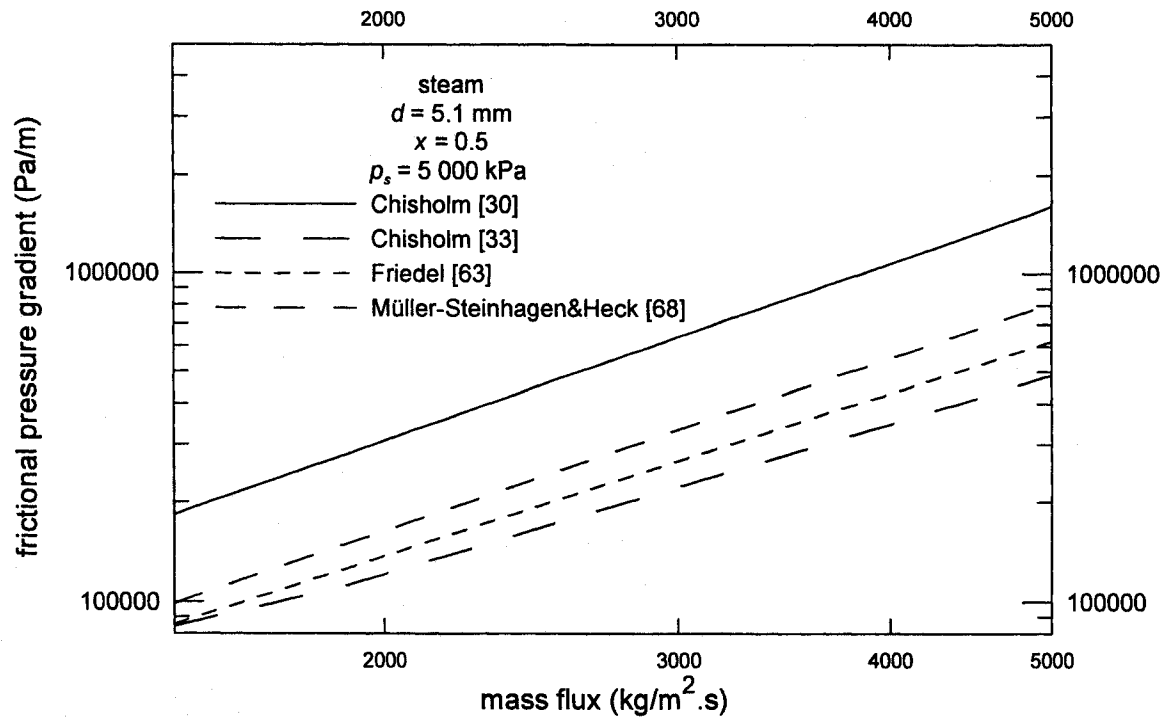


Figure 2.1 Comparison of Two-Phase Frictional Pressure Gradient Flow Models

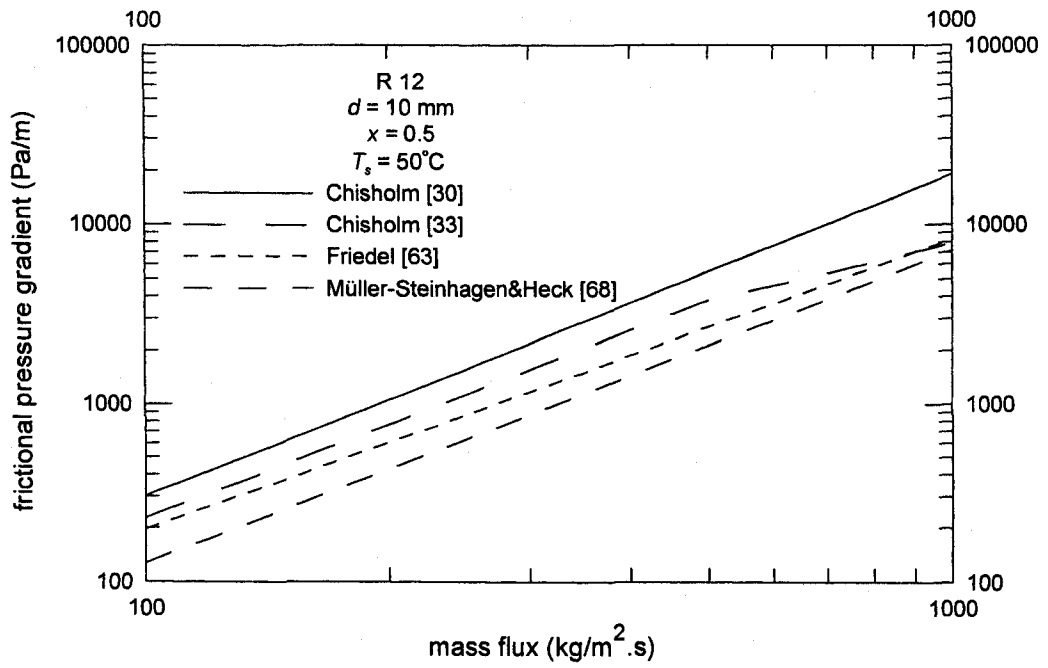


Figure 2.2 Comparison of Two-Phase Frictional Pressure Gradient Flow Models

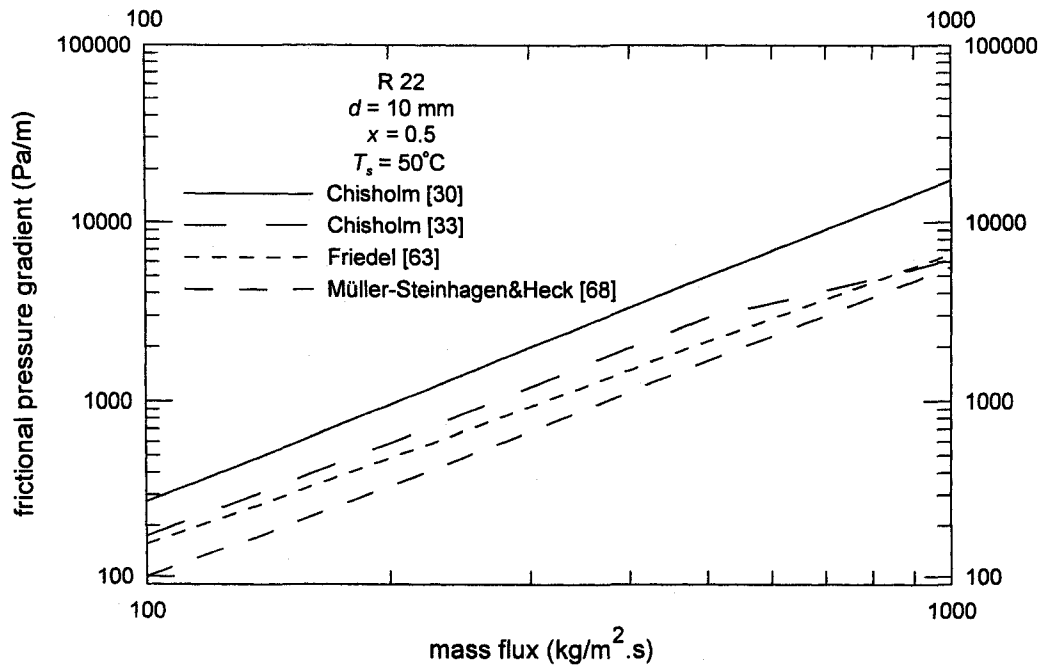


Figure 2.3 Comparison of Two-Phase Frictional Pressure Gradient Flow Models

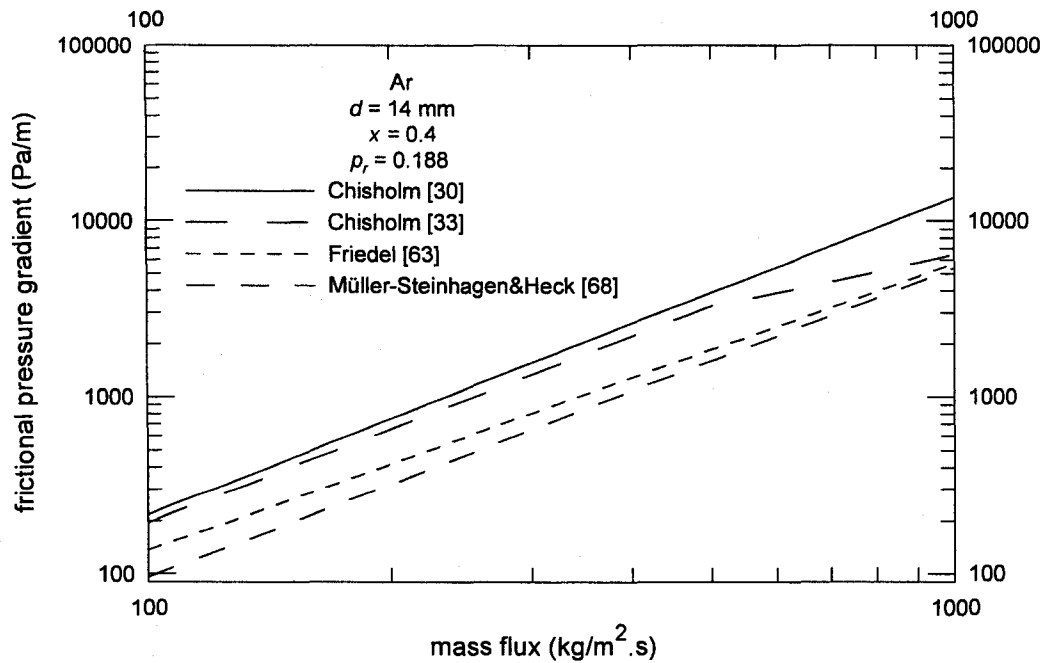


Figure 2.4 Comparison of Two-Phase Frictional Pressure Gradient Flow Models

2.4 Summary

The extensive literature review is presented in Chapter 2 to find most if not all of the two-phase frictional pressure gradient models and correlations that are available in the open literature. Comparison of several two-phase flow frictional pressure gradient models and correlations shows that no two frictional pressure gradient models provide the same result. In Chapters 4-6, the development of models of two-phase frictional pressure gradient in circular pipes is presented along with comparisons with the data and models reviewed in this chapter. At the end of this chapter, Table 2.10 presents a summary of pressure drop studies.

Table 2.10 Summary of Pressure Drop Studies

Author	d	Fluids	Orientation/ Conditions	Range/ Applicability	Techniques, Basis, Observations
Martinelli and Nelson [8]		Steam	Horizontal	6.89 < p < 221.2 bar Turbulent- Turbulent flow regime Better suited to annular flow	Graphical correlation in terms of two- phase frictional multiplier ϕ_{lo}^2
Lockhart and Martinelli [16]	0.0586 -1.017 in	Air and benzene, kerosene, water, and different oils	Adiabatic	1.013 < p < 3.445 bar	Graphical correlation in terms of two- phase frictional multiplier ϕ_l^2 and ϕ_g^2
Chenoweth and Martin [25]	1.5, 3 in.			3.445 < p < 6.89 bar	Graphical correlation in terms of two- phase frictional multiplier ϕ_{lo}^2
Thom [26]		Steam- water	Vertical		Graphical correlation in terms of two- phase frictional multiplier ϕ_{lo}^2
Baroczy [28]		Steam, water-air and mercury- nitrogen			Generalized correlation in a graphical manner $\phi_{lo}^2 = f$ $((\mu_l/\mu_g)^{0.2}/(\rho_l/\rho_g))$
Turner [29]			Horizontal		ϕ_l^2 and $\phi_g^2 = f$ (X)
Chisholm [30]					Equations for Lockhart and Martinelli [16] correlation as ϕ_l^2 and $\phi_g^2 = f(C, X)$

Chisholm [31]	1-2.6, 8 and 48 mm	Steam-water			$30 < p < 175$ bar $280 < G < 2000$ kg/m ² .s	Equations with mass flux effect on ϕ_i^2 for smooth and rough tubes
Chisholm [32]						$\Gamma = f((dp/dz)_{f,go}/dp/dz)_{f,lo}$
Chisholm [33]		Steam				Based on Baroczy [28] graphical correlation to develop ϕ_{lo}^2 correlation
Chisholm [34]						Includes pipe surface roughness effects on ϕ_{lo}^2
Johannessen [35]			Horizontal			Theoretical solution of Lockhart and Martinelli [16] model Stratified and wavy flow
Serizawa and Michiyoshi [36]						New correlation for ϕ_{lo} $\phi_{lo} = f(z)$
Russell, et al. [37]	0.0254, 0.0381, 0.0508 m	Air-water and air-glycerine	Horizontal		Laminar liquid-turbulent gas Stratified flow	Mathematical model/experimental
Chen and Spedding [38]	0.0455 m	Air-water	Horizontal			Extension of the Lockhart-Martinelli model
Asali et al. [40]			Vertical downward			Annular flow with no liquid entrainment
Crowley and Izenon [41]					$\alpha > 0.76$	Annular flow
Manzano-Ruiz [43]	97 mm	Steam-water	Horizontal		$20 < p < 100$ bar $110 < G < 450$ kg/m ² .s $0.5 < x < 0.95$	Annular-mist flow

	23 mm	Air-water			$p = 1-3$ bar $70 < G < 450$ $\text{kg/m}^2 \cdot \text{s}$ $0.57 < x <$ 0.97	
Hemeida and Sumait [44]						Equations for Lockhart and Martinelli [16] correlation as ϕ_l and $\phi_g = f(a, b, c, X)$ using SAS
McAdams, et al. [45]		Benzene and lubricating oil	Horizontal			Homogeneous Series model for μ_m
Cicchitti, et al. [46]	0.51 cm	Steam	Vertical upward/ Adiabatic		$20 < p < 80$ kg/cm^2 $1\ 500 < G < 5$ $000 \text{ kg/m}^2 \cdot \text{s}$ $0.15 < x < 0.8$ $0.9 \times 10^5 < Re <$ 5×10^5	Homogeneous Parallel model for μ_m
			Non-adiabatic		$35 < p < 55$ kg/cm^2 $2\ 000 < G < 4$ $000 \text{ kg/m}^2 \cdot \text{s}$ $0.2 < x < 0.7$	
Dukler et al. [13]			Horizontal			Homogeneous Parallel model for ν_m
Bo Pierre [47]	12 and 18 mm	R-12 and R-22	Horizontal		$15 < m < 140$ kg/hr $1\ 000 < q <$ $26\ 000$ $\text{kcal/m}^2 \cdot \text{hr}$ $T_s = -20-10^\circ\text{C}$ $0.49 < x <$ 0.81 $(Re/K_f) > 1$	Semi-empirical correlation based on the homogeneous model
Powley [48]						Homogeneous theory

Wallis [18]				$Re > 2000$	$C = f(\rho_b, \rho_g)$ Homogeneous $\phi_{lo}^2 = f(x, \rho_b, \rho_g, \mu_b, \mu_g)$
Lombardi and Pedrocchi [49]	5-25 mm	Steam-water, argon-water, nitrogen-water, and argon-ethyl alcohol	Adiabatic Non-adiabatic with steam-water only	$500 < G < 5000$ kg/m ² .s $\rho_l/\rho_g = 15-100$ $0.02 < \sigma < 0.08$ N/m $0.01 < x < 0.98$	CISE-DIF-1 correlation
Beggs and Brill [50]	25.4 and 38.1 mm	Air-water	Horizontal, up flow, down flow, inclined		Homogeneous
Lombardi and Ceresa [52]					CISE-DIF-2 correlation based on suitable weight functions
Bonfanti et al. [53]		Water-nitrogen	Vertical upward		CISE-DIF-3 correlation based on suitable weight functions
Bonfanti et al. [54]	77.9 mm	Water-nitrogen	Vertical upflow, horizontal and vertical downflow/ Adiabatic	$T = 18^\circ\text{C}$ $p = 2.16$ MPa	CISE-DIF-3 correlation [53] predicted well pressure drops in vertical upflow
Beattie and Whalley [55]					Homogeneous Hybrid definition for μ_m
Lombardi and Ceresa [56]					CESNEF-2 correlation
Reddy et al. [58]	0.2-0.6 in	Steam	Vertical upflow	$300 < p < 1300$ psia $0.33 < G < 3.3$ lb _m /ft ² .hr $0 < x < 1$	$\phi_{lo}^2 = f(x, \rho_b, \rho_g, p_r, G)$

Bankoff [61]			$0 < x < 1$	Homogeneous model with correction for two-dimensional effects
Wisman [62]		Vertical		Based upon an annular flow model Consistent for all flow patterns
Friedel [63]		Vertical upward and horizontal/Adiabatic	$\mu_l/\mu_g < 1\ 000$	Developed ϕ_{lo}^2 correlation from database of 25 000 points Includes surface tension effects
Friedel [65]		Vertical downward/Adiabatic		Developed ϕ_{lo}^2 correlation Includes surface tension effects
Olujic [66]		Horizontal		Not applied to dispersed flow
Müller-Steinhagen and Heck [68]			$0 < x < 1$	$(dp/dz)_f = f(x, (dp/dz)_{f,lo}, (dp/dz)_{f,go})$
Xiao et al. [69]		Horizontal and near horizontal		Comprehensive mechanistic model
Gomez et al. [71]			$\theta = 0^\circ-90^\circ$	Unified mechanistic model
Osman and Aggour [21]		Horizontal and near horizontal		ANN model
García et al. [72]				Composite power law friction factor correlation $\nu_m = \nu_l$
Bendlksen et al. [73]	Oil and gas			Dynamic two-fluid model: OLGA
Hoogendoorn	0.024- Air-	Horizontal/		Δp_f expressions

n [74]	0.14 m	water, air-gas oil and air-spindle oil mixtures	adiabatic		for plug, slug, froth, wave and mist-annular flow
Isbin et al. [75]	0.484 and 1.062 in.	Steam-water	Horizontal/adiabatic	$25 < p < 1415$ psia $454 < m < 4350$ lb _m /hr $0.08 < x < 0.98$	ϕ_{lo}^2 correlation
Chawla [76]	6, 14, and 25 mm	R-11	Horizontal	$0 < x < 1$	Correlation based on the velocity ratio between the vapor and liquid phases
Grønnerud [77]	26.2 mm	R-12, and R-717	Horizontal	$T_s = -45-5^\circ\text{C}$ $20 < G < 1600$ kg/m ² .s $0.004 < Fr_{lo} < 20$ $\rho_l/\rho_g = 70$ to 100	His two-phase frictional multiplier (ϕ_{gd}) is a function of Fr_{lo}
Rashid and Edward [78]		Steam-water	Horizontal		$C = f(G, v_g, v_b)$
Hashizume et al. [79]	10 mm	R-12, R-22	Horizontal/Condensation	$5.7 < p < 19.6$ bar	Stratified flow, wavy flow, slug flow, semi-annular flow, and annular flow
Hashizume et al. [80]	10 mm	R-12, R-22	Horizontal/Condensation	$5.7 < p < 19.6$ bar	Δp_f expressions for annular and stratified flow Liquid and gas phase velocity in terms of Prandtl mixing length Stratified flow modeled as flow between parallel plates

Jung and Radermacher [83]	9.1 mm	R22, R114, R12, R152a, R22/R114, and R12/R152a	Horizontal/ Non-adiabatic	$G = 250-720$ $\text{kg/m}^2.\text{s}$ $q = 10-45$ kW/m^2	$\phi_p^2 = f(X_{tt}, x, p_r)$
Souza et al. [85]	10.9 mm	R-12 R-134a	Horizontal	$p_r = 0.07-0.12$ $200 < G < 600$ $\text{kg/m}^2.\text{s}$	New correlation for ϕ_{lo}^2 Investigated effect of oil in refrigerant on pressure drop
Souza and Pimenta [86]		R-12, R-22, R-134a, MP-39, and R-32/125	Horizontal/ Adiabatic and non-adiabatic		$\phi_{lo}^2 = f(X_{tt}, \Gamma)$
Ungar and Cornwell [89]	0.0575, 0.0701, 0.1017, 0.1240 in.	Ammonia	Horizontal/ Adiabatic		McAdams et al. [45] for homogeneous prediction and Asali et al. [40] for annular flow prediction predicted the data accurately
Huang and Van Sciver [90]	4.57, 5.33 mm	Helium	Horizontal	$m = 0.5$ to 2.0 g/s $p_s = 0.65-1.2$ atm	ϕ_{lo}^2 was dependent on p_s and x m did not appear to have an effect on ϕ_{lo}^2
Wang et al. [91]	9.52 mm	R-22 and R-407C		$p_s = 600$ and 680 kPa $100 < G < 300$ $\text{kg/m}^2.\text{s}$ $6\ 000 < q < 14\ 000$ W/m^2	
Yang and Webb [92]	Rectangular	R-12	Horizontal/ Adiabatic	$400 < G < 1\ 400$ $\text{kg/m}^2.\text{s}$	Δp_f in micro-fin tube higher than

	plain: $d_h =$ 2.64 mm Micro- fin: d_h $= 1.56$ mm			$0.1 < x < 0.9$	plain tube Equivalent Re- based model for Δp_f Concluded surface tension does not affect Δp_f
Zhang and Webb [94]	6.25 and 3.25 mm Multi- port, extrude d Al $d_h =$ 2.13 mm	R-134a, R-22, and R-404A	Horizontal/ Adiabatic	$200 < G < 1$ $000 \text{ kg/m}^2 \cdot \text{s}$ $0.2 < x < 0.89$ $T_s = 20\text{-}65^\circ\text{C}$	Friedel correlation did not predict data accurately Δp_f function of reduced pressure rather than density or viscosity ratio New correlation for ϕ_{lo}^2
Chen et al. [95]	1.02, 3.17, 5.05, and 7.02 mm	Air-water	Horizontal	Room temperature $50 < G < 3$ $000 \text{ kg/m}^2 \cdot \text{s}$ $0.001 < x <$ 0.9	Accounted for increased σ influence, decreased g influence Poor agreement with Chisholm [33], Friedel [63], and homogeneous flow models
Chen et al. [97]	< 10 mm	Ammonia , R-12, R-22, R-125, R-134a, R-404, R-407C, R-410A, and 3 air- water	Horizontal		Modified homogeneous model to include Bo and We to account for effect of σ and G
Ould Didi et al. [98]	10.92 and 12.00	R-134a, R-123, R-402A,	Horizontal	$100 < G <$ $500 \text{ kg/m}^2 \cdot \text{s}$ $0.04 < x < 1.0$	

	mm	R-404A and R-502		
Yoon et al. [102]	7.53 mm	CO ₂	Horizontal	$T_s = -4$ to 20°C $12 < q < 20$ kW/m^2 $200 < G <$ $530 \text{ kg/m}^2 \cdot \text{s}$

CHAPTER 3

LITERATURE REVIEW OF VOID FRACTION

3.1 Introduction

The research on void fraction in two-phase flow began in the 1940's. Since then, void fraction data have been collected for horizontal, vertical, and inclined gas-liquid systems. From the void fraction data, many attempts have been made to develop general procedures for predicting it. The void fraction is an important parameter for predicting flow pattern transitions, heat transfer, and pressure drops in two-phase flow models. For this reason, a comprehensive review of analytical and empirical void fraction models is presented in this chapter.

3.2 Review of Two-Phase Void Fractions Models and their Limitations

Armand [107] correlated data for the void fraction for the air-water flow in a horizontal pipe of 26 mm diameter at 1 bar by plotting α versus β . He observed that for $\alpha < 0.72$ ($\beta < 0.9$), the relationship between α and β was linear and could be represented by the following equation:

$$\alpha = C_A \beta \quad (3.1)$$

Where $C_A = 0.833$.

The empirical equation of Armand, Eq. (3.1), could be expressed in terms of $\alpha/(1-\alpha)$ and $\beta/(1-\beta)$ as follows:

$$\frac{\alpha}{1-\alpha} = \frac{1}{[0.2 + 1.2/(\beta/(1-\beta))]} \quad (3.2)$$

In terms of the mass quality (x), Armand equation was

$$\frac{1-\alpha}{\alpha} = 1.2 \left(\frac{1-x}{x} \right) \left(\frac{\rho_g}{\rho_l} \right) + 0.2 \quad (3.3)$$

For $\beta > 0.9$, Massena [108] suggested the following approximate equation:

$$\alpha = [C_A + (1 - C_A) x] \beta \quad (3.4)$$

Martinelli and Nelson [8] presented an empirical correlation for the void fraction in a graphic manner on semi-log plot. In their study, they assumed that the flow regime would always be 'turbulent-turbulent' since any normal forced circulation boiler design for all practical purposes would involve this flow mechanism only. On the horizontal axis, the independent parameter was the mass quality (x). On the vertical axis, the dependent parameter was the void fraction (α). On the grid, they plotted a family of curves for pressures from atmospheric pressure to the critical pressure. They derived their correlation in the following method: at the critical pressure, when $\rho_l = \rho_g$ and $\mu_l = \mu_g$, the relationships that $\alpha = x$ and $X_{tt} = ((1-x)/x)$ were valid. So, the relationship between the void fraction and X_{tt} at critical pressure could be calculated easily. Also, the relationship

between the void fraction and X_H could be known from the curve at atmospheric pressure. Using these two known curves of void fraction versus X_H for both critical and atmospheric pressures, curves at intermediate pressures were interpolated. They replaced X_H by x , with pressure as a parameter. However, this method was based upon a meager amount of data. So, further experimental verification was required, particularly at the higher pressures, before this method could be considered valid.

Lockhart and Martinelli [16] correlated the percent of pipe filled with liquid under any flow conditions for all four-flow types (turbulent-turbulent, turbulent-laminar, laminar-turbulent, and laminar-laminar) by means of the Lockhart-Martinelli parameter (X).

Baker [3] gave an empirical equation to allow for the effect of mass flux on the void fraction in vertical upward flow. His equation was:

$$x = \frac{\alpha^2(Y^{1/3} - 1) + \alpha}{Y - \alpha(Y - Y^{1/3})} \quad (3.5)$$

$$Y = 0.021 \left(\frac{\rho_l}{\rho_g} \right) G^{0.686} \quad (3.6)$$

Equations (3.5) and (3.6) were valid over the range $7.5 < Y < 300$ and $G < 950$ kg/m².s.

Based in field data acquired on a pipe with an inner diameter of 16 in, Flanigan [109] developed a holdup correlation as a function of the superficial liquid velocity. His liquid holdup correlation was

$$H_l = \frac{1}{1 + 0.3264U_l^{1.006}} \quad (3.7)$$

Hoogendoorn [74] derived an implicit equation to calculate the void fraction in horizontal pipes. His correlation was

$$\frac{H_g}{H_l} = 0.60 \left[U_g \left(1 - \frac{H_g}{1 - H_g} \frac{U_l}{U_g} \right) \right]^{0.85} \quad (3.8)$$

Levy [110] derived theoretical equations governing slip effects in forced circulation of boiling water. His equations indicated that steam slip was dependent upon inlet water velocity, channel geometry and rate of heat addition. He based a simplified momentum model on the assumption of equal friction and head losses for the liquid and vapor phases. He gave the following expression for the void fraction:

$$x = \frac{\alpha (1 - 2\alpha) + \alpha \sqrt{(1 - 2\alpha)^2 + \alpha \left[2 \left(\frac{\rho_l}{\rho_g} \right) (1 - \alpha)^2 + \alpha (1 - 2\alpha) \right]}}{2 \left(\frac{\rho_l}{\rho_g} \right) (1 - \alpha)^2 + \alpha (1 - 2\alpha)} \quad (3.9)$$

His correlation satisfied the important boundary conditions namely: (i) at $\beta = 0$, $\alpha = 1$, and (ii) at $p/p_c = 1$ ($\rho_l = \rho_g$), $\alpha = x$. His model gave good agreement with available experimental results in horizontal and vertical test sections with and without heat addition

at pressures from 12 to 2 000 psia. He discussed his model in terms of non-quasi steady state unbalances of friction and heat losses of the liquid and vapor phases to explain experimental deviations from the predictions and the previously noted effects of inlet water velocity. He also gave trends for the effects of channel geometry and rate of heat addition. He included application of his simplified model to calculate two-phase pressure drop.

Also, he found that if the Martinelli-Nelson correlation and the turbulent Lockhart-Martinelli correlation were replotted as ϕ_l versus $(1-\alpha)$, the following correlation was valid:

$$\phi_l = \frac{1}{1-\alpha} \quad (3.10)$$

Bankoff [61] assumed in his model a power law distribution for both the velocity and the void fraction.

$$u = u_{max} \left(\frac{2y}{d} \right)^{\frac{1}{k}} \quad (3.11)$$

$$\alpha = \alpha_{max} \left(\frac{2y}{d} \right)^{\frac{1}{n}} \quad (3.12)$$

Integration and manipulation of the above two equations lead directly to the result that the average void fraction (α_{av}), was related to the average volumetric quality (β_{av}), through the following relationship

$$\alpha_{av} = C_A \beta_{av} \quad (3.13)$$

Where C_A was a function of k and n as follows:

$$C_A = \frac{2(k+n+kn)(k+n+2kn)}{(n+1)(2n+1)(k+1)(2k+1)} \quad (3.14)$$

The symmetry of the above equation in k and n was noteworthy. For $k = 2-7$, and $n = 0.1-5$, C_A had an effective range of 0.5-1. Bankoff compared the prediction of average void fraction versus mass quality in steam-water flow with the Martinelli-Nelson correlation [8] using a constant average value of 0.89 for C_A . He found that the agreement with the Martinelli-Nelson correlation was good over a range of pressures from 100 to 2 500 psia and a range of average void fractions from 0 to 0.85. He concluded that a reasonable fit to the void fraction data for steam-water mixture flows could be achieved using

$$C_A = 0.71 + 15p \quad (3.15)$$

Jones [111] represented the pressure dependency of C_A by noting at the critical pressure that $\alpha = C_A = 1$. Also, at $x = 1$, $C_A = 1$. The resulting form for C_A was

$$C_A = a + (1-a)\alpha^{-b} \quad (3.16)$$

$$a = 0.71 + 13p \quad (3.17)$$

$$b = 3.53125 - 27.19p + 12330p^2 \quad (3.18)$$

Hughmark [112] presented a void fraction correlation based on the Bankoff correlation [61],

$$\frac{1}{x} = 1 - \frac{\rho_l}{\rho_g} \left(1 - \frac{C_A}{\alpha} \right) \quad (3.19)$$

or

$$C_A = \frac{\alpha}{\beta} \quad (3.20)$$

He related C_A to a parameter Z in a non-linear function in his correlation. He defined Z as follows:

$$Z = Re^{1/6} Fr^{1/8} [1 - \beta]^{-1/4} \quad (3.21)$$

$$Re = \frac{G d}{(1 - \alpha) \mu_l + \alpha \mu_g} \quad (3.22)$$

$$Fr = \frac{U_m^2}{g d} \quad (3.23)$$

$$U_m = U_l + U_g \quad (3.24)$$

$$\beta = \frac{Q_g}{Q} = \frac{Q_g}{Q_l + Q_g} = \frac{1}{1 + \left(\frac{1-x}{x} \right) \left(\frac{\rho_g}{\rho_l} \right)} \quad (3.25)$$

Table 3.1 gives values of C_A as a function of Z .

Table 3.1 Values of C_A as a function of Z

Z	1.3	1.5	2	3	4	5	6
C_A	0.185	0.225	0.325	0.49	0.605	0.675	0.72
Z	8	10	15	20	40	70	130
C_A	0.767	0.78	0.808	0.83	0.88	0.93	0.98

This correlation required an iterative procedure to obtain the void fraction (α). Although Hughmark correlation was also developed for vertical flow, it was widely used for horizontal flow applications [113].

Later, García et al. [114] found that the dimensionless flow parameter (C_A) could be adjusted by a fifth order logarithmic equation as a function of Z . This equation was

$$C_A = 0.1746 - 0.1301 \ln Z + 0.7508 (\ln Z)^2 - 0.4308 (\ln Z)^3 + 0.09553 (\ln Z)^4 - 0.007452 (\ln Z)^5 \quad (3.26)$$

Using the curve fitting tools available in the grapher software [115], the fifth order logarithmic equation must be

$$C_A = 0.1542 - 0.02247 \ln Z + 0.6071 (\ln Z)^2 - 0.3545 (\ln Z)^3 + 0.07749 (\ln Z)^4 - 0.005878 (\ln Z)^5 \quad (3.27)$$

The current equation has a root mean square error of 0.92% while García et al. [114] equation had a root mean square error of 2.27%.

Hewitt et al. [116] linearized Lockhart-Martinelli's data because Lockhart-Martinelli empirical correlation for void fraction was presented between liquid void fraction, $(1-\alpha)$, and Lockhart-Martinelli parameter (X) on log-log scale. They fitted Lockhart-Martinelli's empirical correlation for void fraction using a six-term equation. Their equation was:

$$\begin{aligned} \ln(1-\alpha) = & -1.482 + 4.915 \ln X - 5.955(\ln X)^2 + 2.675(\ln X)^3 \\ & + 6.399(\ln X)^4 - 8.768(\ln X)^5 \end{aligned} \quad (3.28)$$

Nishino and Yamazaki [117] introduced a new parameter to predict the steam volume fractions and the slip ratios of upward vertical steam-water mixtures in boiling systems. They defined new parameter, K , as the ratio of the velocity difference between steam and water to the superficial steam velocity. For the case of the new parameter, K , was equal to the inverse of the volumetric mass quality $(1/\beta)$, they obtained a simple correlation related the void fraction (α) to the mass quality (x) , the liquid density (ρ_l) and the gas density (ρ_g) . Their correlation was

$$\alpha = 1 - \left(\frac{(1-x)\rho_g}{x\rho_l + (1-x)\rho_g} \right)^{0.5} \quad (3.29)$$

Their correlation satisfied the following conditions: (i) at $x = 0$, $\alpha = 0$ and (ii) at $x = 1$, $\alpha = 1$.

Kowalczewski [118] developed an alternative void fraction correlation. He started with an analysis of the variables that significantly had an effect on the void fraction in vertical upflow. He obtained the following correlation

$$\alpha = \beta - 0.71(1 - \beta)^{0.5} Fr_1^{-0.045} \left(1 - \frac{p}{p_c}\right) \quad (3.30)$$

$$Fr_1 = \frac{G^2}{\rho_l^2 g d} \quad (3.31)$$

His correlation satisfied the important boundary conditions namely: (i) at $\beta = 0$, $\alpha = 0$, (ii) at $\beta = 1$, $\alpha = 1$, and (iii) at $p/p_c = 1$, $\alpha = \beta$. He based the coefficient and exponents values in his correlation, Eq. (3.30), upon water and R12 data. For the case of R12, the coefficient value was equal to 0.8 instead of 0.71.

By comparison with extensive steam water data in the range of $0.1 < Fr_1 < 1000$ and $p/p_c \leq 0.65$, Kütükçüoğlu and Njo [119] modified the coefficient and exponents values in Kowalczewski correlation [118] as follows:

$$\alpha = \beta - (1 - \beta)^{0.5} Fr_1^{-0.2} \left(1 - \frac{p}{p_c}\right)^2 \quad (3.32)$$

$$Fr_1 = \frac{G^2}{\rho_l^2 g d} \quad (3.33)$$

From the new values of coefficient and exponents, it is clear that the effect of Froude number and pressure on the void fraction is more strongly accentuated.

Löscher and Reingardt [120] suggested a void fraction correlation similar to Kowalczewski correlation [118] with replacing the constant coefficient in Kowalczewski correlation [118] by an additional critical pressure ratio raised to a negative power. Their correlation was

$$\alpha = \beta - \left(\frac{p}{p_c}\right)^{-0.22} \beta^{1.39} (1 - \beta)^{0.8} Fr_l^{-0.25} \left(1 - \frac{p}{p_c}\right)^{3.4} \quad (3.34)$$

$$Fr_l = \frac{G^2}{\rho_l^2 g d} \quad (3.35)$$

Their correlation fitted R11, R12 and water data in the ranges of $0.01 \leq p/p_c \leq 0.36$, $15 \leq \rho_l/\rho_g \leq 900$ and $4 \leq \mu_l/\mu_g \leq 32$, respectively.

Friedel [121] fitted the Kowalczewski correlation [118] to R12 data in the vertical upflow. He modified the coefficient and exponents values in Kowalczewski correlation [118] as follows:

$$\alpha = \beta - 0.539(1 - \beta)^{0.5} Fr_l^{-0.321} \left(1 - \frac{p}{p_c}\right)^{1.016} \quad (3.36)$$

$$Fr_l = \frac{G^2}{\rho_l^2 g d} \quad (3.37)$$

The new values of coefficient and exponents further augmented the effect of Froude number but significantly reduced the effect of pressure on the void fraction back to that originally proposed by Kowalczewski. His correlation was limited by the ranges of $0.12 \leq p/p_c \leq 0.57$ and $1 \leq Fr_l \leq 88$ respectively.

Zivi [17] developed a correlation to determine the void fraction using the concept of minimum entropy production. His correlation was

$$\alpha = \frac{1}{1 + \left(\frac{1-x}{x}\right) \left(\frac{\rho_g}{\rho_l}\right)^{\frac{2}{3}}} \quad (3.38)$$

He found that the slip ratio (S) in an idealized two-phase flow with zero wall friction and zero entrainment was equal to $(\rho_l/\rho_g)^{1/3}$. Therefore, the slip ratio (S) was dependent only on the phase density ratio. Also, he noted that the slip ratio (S) should decrease as the pressure increased which agreed with experimental data [122]. This model proved particular successful in predicting pressure drop [123] and heat transfer [124] during condensation. Also, this model was used to calculate the acceleration pressure drop during two-phase flow [85,86].

Also, Zivi [17] derived a void fraction model for annular flow accounting for liquid entrainment in the vapor core with a fraction e of the liquid entrained as droplets because entrainment was an important factor in the dynamics of two-phase flow. He assumed that the liquid entrained in the vapor traveled at the same velocity as the vapor. Starting with a summation of the kinetic energies of the vapor, the liquid in the annular film, and the liquid entrained in the vapor, he obtained his second void fraction expression as

$$\alpha = \frac{1}{1 + e \left(\frac{1-x}{x} \right) \left(\frac{\rho_g}{\rho_l} \right) + (1-e) \left(\frac{1-x}{x} \right) \left(\frac{\rho_g}{\rho_l} \right)^{\frac{2}{3}} \left[\frac{1 + e \left(\frac{1-x}{x} \right) \left(\frac{\rho_g}{\rho_l} \right)}{1 + e \left(\frac{1-x}{x} \right)} \right]^{\frac{1}{3}}} \quad (3.39)$$

Zivi did not present a method for the prediction of the actual value of e . However, the limits on feasible values of e were as follows:

1. For $e = 0$ (no liquid entrainment), Eq. (3.39) reduces to Eq. (3.38).
2. For $e = 1$, Eq. (3.39) reduces to the homogeneous void fraction (α_m).

Thom [26] correlated steam-water void fraction data in terms of slip factor, which was a unique function of pressure and mass quality. His equation was given by:

$$\alpha = \frac{S x}{1 + x (S - 1)} \quad (3.40)$$

Baroczy [125] presented a generalized correlation in a graphical manner for the liquid fraction in two-phase flow. He proposed his correlation for use with all fluids, including liquid metals. The correlation was based on isothermal, two-phase, two-component liquid fraction data for liquid mercury-nitrogen, and water-air. His correlation was for liquid void fraction data as a function of the Lockhart-Martinelli parameter (X) and the property index, $((\mu_l/\mu_g)^{0.2}/(\rho_l/\rho_g))$. The property index had the advantage of not requiring knowledge of the critical pressure and temperature in order to establish the property ratios at the critical point, where they had a value of 1. By similar reasoning, it

could be used to establish the analogous condition for two-phase, two-component flow, that was, equal viscosity and density for each phase. Thus, the physical properties of single and two-component, two-phase fluids could be described on a common basis. He claimed that there was a good agreement between the liquid fraction predicted by his correlation and the Martinelli-Nelson correlation for steam, experimental data for steam, and experimental data for Santowax R, an organic coolant. He also showed the prediction of liquid fraction by this method for sodium, potassium, rubidium, and mercury. He demonstrated the application of this method to boiling mercury, for a range of temperatures and exit mass qualities.

Turner [29] developed the separate-cylinders model of two-phase flow. The results of his analysis gave:

$$\alpha = \frac{1}{1 + X^{2/n}} \quad (3.41)$$

The values of n were dependent on whether the liquid and gas phases were laminar or turbulent flow. The different values of n were given in Table 2.3.

However, it should be noted that this model was not a particularly good representation of experimental data because no function of the form of Eq. (3.41) would predict Lockhart-Martinelli data. For all values of n , Eq. (3.41) would predict $\alpha = 0.5$ at $X = 1$ instead of the correct value of 0.77. Also, it was noted that the Lockhart-Martinelli empirical correlation for void fraction could be represented well by the equation

$$\alpha = \left(\frac{1}{1 + X^{0.8}} \right)^{1/2.65} \quad (3.42)$$

Which is easier to use compared to Eq. (3.28).

Later, Domanski and Didion [126] modified the above correlation for a range of $X_{tt} > 10$ as follows:

$$\alpha = 0.823 - 0.157 X_{tt} \quad (3.43)$$

Zuber and Findlay [127] developed a method that defined a structure for correlating the void fraction (α). In their correlation, they took into account the effect of a non-uniform distribution of the two-phases and the effect of the local slip ratio. The Zuber-Findlay correlation was

$$\alpha = \frac{x}{C_o \left[x + \frac{\rho_g}{\rho_l} (1-x) \right] + \frac{\rho_g u_{gj}}{G}} \quad (3.44)$$

Where C_o and u_{gj} were two empirical constants. C_o represented the effect of the non-uniform distribution of the void fraction (α) and velocities ($C_o = 1$ in the case of uniform distribution). u_{gj} represented the effect of the local slip ratio ($u_{gj} = 0$ in the case of two phases with the same velocity through the whole duct cross-section).

Zuber et al. [128] studied the effect of mass flux on the void fraction for the evaporation of R22 in a vertical 1 cm heated pipe. For non-equilibrium nature of the flow at 11.5 bar, the effects of mass flux on the void fraction were clearly visible at low void

fractions. For $x > 0$ at 11.5 bar, the void fraction increased with increased mass flux at a given value of x . They also showed on the same graph that the void fractions predicted from the Martinelli-Nelson correlation for the steam-water system at the same value of (ρ_l/ρ_g) might be expected to correspond to mass fluxes near 1 000 kg/m.s². In addition, the void fractions predicted from the homogeneous model were higher than the void fractions predicted from the Martinelli-Nelson correlation and might be expected to correspond to mass fluxes $> 2\ 000$ kg/m.s².

Guzhov et al. [129] derived a void fraction correlation for transportation in gas-liquid systems. Their correlation related the gas holdup and no-slip gas holdup ($H_g/H_{g,m}$) to the Froude number (Fr) for all angles from 0° to 9°. Their correlation was

$$\frac{H_g}{H_{g,m}} = 0.81 \left(1 - \exp(-2.2\sqrt{Fr}) \right) \quad (3.45)$$

$$H_{g,m} = \beta = \frac{Q_g}{Q} = \frac{Q_g}{Q_l + Q_g} = \frac{1}{1 + \left(\frac{1-x}{x} \right) \left(\frac{\rho_g}{\rho_l} \right)} \quad (3.46)$$

$$Fr = \frac{U_m^2}{gd} \quad (3.47)$$

$$U_m = U_l + U_g \quad (3.48)$$

Eaton et al. [130] developed a correlation to evaluate the liquid holdup in horizontal pipes. They showed the liquid holdup graphically. They correlated the liquid holdup (H_l) as a vertical axis with the following dimensionless group

$\frac{1.84 N_{Ul}^{0.575}}{N_{Ug} N_d^{0.0277}} \left(\frac{p}{p_{atm}} \right)^{0.05} N_l^{0.1}$ as a horizontal axis, based in the liquid velocity influence number (N_{Ul}), the gas velocity influence number (N_{Ug}), the pipe diameter influence number (N_d), the system pressure (p), the reference atmospheric pressure (p_{atm}) and the liquid viscosity influence number (N_l) defined by Ros [131].

Later, García et al. [114] found that the Eaton et al. correlation [130] could be expressed in terms of the parameter Z used in the Hughmark correlation [112] as follows:

$$H_l = \frac{Z}{0.2578 + 0.9555Z + 0.1397Z^{0.5}} \quad (3.49)$$

Wallis [132] proposed a simple theory for annular two-phase flow in terms of equations for interfacial and wall shear stress. He based his equations on two simplified conditions. The first condition was there was no liquid entrainment. The second condition was the liquid film velocity was low compared with the velocity of the gas core. He proposed separate correlations for vertical and horizontal annular flow. He gave criteria for the minimum pressure drop, zero wall shear stress, and flow regime transition in vertical flow. He compared his results with numerous data and alternative theories from the literature.

After that, Wallis [133] modified his simple theory to develop a more accurate, but more complex, theoretical structure. He considered that the liquid film, the gas core, and the interface were separated. He took into account the effects of liquid entrainment, compressibility, liquid and gas Reynolds number, shear-stress distribution, the relative

velocity between liquid film and gas core, and the different types of interfacial waves. However, he found that the effects of these modifications to be secondary.

Rouhani and Axelsson [19] divided the complex problem of void calculation in the different regions of flow boiling in two parts. In the first part, they included only the description of the mechanisms and the calculation of the rates of heat transfer for vapor and liquid. They assumed that heat was removed by vapor generation, heating of the liquid that replaced the detached bubbles, and in some parts, by single-phase heat transfer. By considering the rate of vapor condensation in liquid, they obtained an equation for the differential changes in the true steam mass quality throughout the boiling regions. Integration of this equation gave the vapor weight fraction at any position. In the second part of the problem, they were concerned with the determination of the void fractions corresponding to the calculated steam mass qualities. For this purpose, they used the derivations of Zuber and Findlay [127]. This model was a type of drift flux model, and yielded the following equation for vertical flows:

$$\alpha = \frac{x}{\rho_g} \left[\left((1 + 0.2(1-x)) \left(\frac{gd\rho_l^2}{G^2} \right)^{0.25} \right) \left(\frac{x}{\rho_g} + \frac{1-x}{\rho_l} \right) + \frac{1.18(1-x)[g\sigma(\rho_l - \rho_g)]^{0.25}}{G\rho_l^{0.5}} \right]^{-1} \quad (3.50)$$

Equation (3.50) provided a method for calculating void fractions including the effects of mass flux and surface tension. Rouhani and Axelsson [19] compared this model with data from different geometries including small rectangular channels and large rod bundles. The data covered pressures from 19 to 138 bars, heat fluxes from 18 to 120

W/cm^2 with many different subcoolings and mass fluxes. They found that the agreement between the model and data was generally very good.

Premoli et al. [134] presented an empirical correlation of void fraction. This correlation is usually known as the CISE correlation. They covered a wide range of data in their correlation and took into account the effect of mass flux on the void fraction. They expressed their correlation in terms of slip ratio (S). The slip ratio (S) was defined as:

$$S = 1 + E_1 \left(\frac{z}{1+z} - z E_2 \right)^{0.5} \quad (3.51)$$

$$z = \frac{\beta}{1-\beta} \quad (3.52)$$

$$E_1 = 1.578 Re^{-0.19} \left(\frac{\rho_l}{\rho_g} \right)^{0.22} \quad (3.53)$$

$$E_2 = 0.0273 We Re^{-0.51} \left(\frac{\rho_l}{\rho_g} \right)^{-0.08} \quad (3.54)$$

$$Re = \frac{Gd}{\mu_l} \quad (3.55)$$

$$We = \frac{G^2 d}{\rho_l \sigma} \quad (3.56)$$

The CISE correlation was the most accurate generally applicable correlation to calculate the mean density ($\bar{\rho}$). The mean density ($\bar{\rho}$) was defined as:

$$\bar{\rho} = (1 - \alpha) \rho_l + \alpha \rho_g \quad (3.57)$$

The standard deviation of the mean density calculated by the CISE correlation was approximately 40%, although it was a little less in the case of steam-water flow.

Smith [135] assumed a separated flow consisting of a liquid phase and a gas phase with a fraction e of the liquid entrained as droplets. He obtained the following expression in terms of slip ratio (S) assuming that the momentum fluxes of the two separated phases were equal:

$$S = e + (1 - e) \left(\frac{\rho_l / \rho_g + e (1/x - 1)}{1 + e (1/x - 1)} \right)^{0.5} \quad (3.58)$$

A value of $e = 0.4$ gave the best fit to the data.

Bonnecaze et al. [136] developed a model for two-phase slug flow that took into account the pipeline inclination and gravity forces acting on the liquid slug. Their model related the slug translational velocity, mixture velocity and holdup to the buoyancy force acting in the alternating gas bubbles. Their correlation was

$$H_l = 1 - \frac{\beta}{1.2 + 0.35(1 - \rho_g / \rho_l) \delta \sqrt{Fr}} \quad (3.59)$$

$$Fr = \frac{U_m^2}{gd} \quad (3.60)$$

$$U_m = U_l + U_g \quad (3.61)$$

Where $\delta = 0$ for horizontal flow, $\delta = 1$ for uphill flow and $\delta = -1$ for downhill flow. They claimed that the test results showed that this model had successfully predicted the holdup in inclined slug flow.

Chisholm [137] presented a particularly simple correlation of void fraction, in terms of slip ratio (S):

$$S = \left[1 - x \left(1 - \frac{\rho_l}{\rho_g} \right) \right]^{0.5} \quad (3.62)$$

It was clear that as (ρ_l/ρ_g) approached 1 (i.e. approaching the critical point), the slip ratio (S) approached 1 as the flow became homogeneous in character. Chisholm claimed that although his correlation was very simple, but it provided a reasonably accurate result.

Serizawa and Michiyoshi [36] compared published data of void fraction for liquid metal two-phase flow with their correlation of the form

$$\alpha = 1 - \sqrt{\frac{(1-x)^3}{1+Kx}} \quad (3.63)$$

$$K = c \left(\frac{\rho_l}{\rho_g} \right) U_l^{0.5} \quad (3.64)$$

Where $c = 1.3$ for bubble flow and $c = 1.0$ for slug and annular flow. They claimed that their correlation represented well the mass flux effect.

To predict the liquid holdup, Beggs and Brill [50] developed first a method to predict the different types of flow regime in horizontal two-phase flow. In this method, they plotted the Froude number (Fr) versus input liquid content (λ) on the log-log scale. They determined the flow pattern empirically as follows:

1. If $Fr < L_1$, the flow pattern was segregated (stratified, wavy and annular).
2. If $Fr > L_1$ and $> L_2$, the flow pattern was distributed (bubbly and mist).
3. If $L_1 < Fr < L_2$, the flow pattern was intermittent (plug and slug).

They defined L_1 and L_2 as follows:

$$L_1 = \exp[-4.62 - 3.757 \ln \lambda - 0.481(\ln \lambda)^2 - 0.0207(\ln \lambda)^3] \quad (3.65)$$

$$L_2 = \exp[1.061 - 4.602 \ln \lambda - 1.609(\ln \lambda)^2 - 0.179(\ln \lambda)^3 + 635 \times 10^{-8} (\ln \lambda)^5] \quad (3.66)$$

Then, they developed equations to predict the liquid holdup in two-phase flow for all conditions as follows:

$$H_l(0) = \frac{C_{B1} \lambda^{C_{B2}}}{Fr^{C_{B3}}} \quad (3.67)$$

$$Fr = \frac{U_m^2}{gd} \quad (3.68)$$

$$U_m = U_l + U_g \quad (3.69)$$

Table 3.2 gives the values of the constants for Beggs and Brill equation for predicting liquid holdup.

Table 3.2 Constants for Beggs and Brill Equation for Predicting Liquid Holdup

Constant	Segregated	Distributed	Intermittent
C_{B1}	0.98	1.065	0.845
C_{B2}	0.4846	0.5824	0.5351
C_{B3}	0.0868	0.0609	0.0172
C_{B4} (up flow)	Eq. (3.70)	0	Eq. (3.72)
C_{B4} (down flow)	Eq. (3.71)	Eq. (3.71)	Eq. (3.71)

With

$$C_{B4} = (1 - \lambda) \ln \left[\frac{0.011 N_{Ul}^{3.539}}{\lambda^{3.768} Fr^{1.614}} \right] \quad (3.70)$$

$$C_{B4} = (1 - \lambda) \ln \left[\frac{4.7 N_{Ul}^{0.1244}}{\lambda^{0.3692} Fr^{0.5056}} \right] \quad (3.71)$$

$$C_{B4} = (1 - \lambda) \ln \left[\frac{2.96 \lambda^{0.305} N_{Ul}^{0.0978}}{Fr^{0.4472}} \right] \quad (3.72)$$

$$N_{Ul} = U_l \left(\frac{\rho_l}{g\sigma} \right)^{0.25} \quad (3.73)$$

Finally, after they determined the values for $H_l(0)$ and C_{B4} , they calculated the liquid holdup at any angle from

$$H_l(\theta) = H_l(0) \left\{ 1 + C_{B4} \left[\sin(1.8\theta) - 0.333 \sin^3(1.8\theta) \right] \right\} \quad (3.74)$$

The restrictions in Eq. (3.74) were $H_l(0) \geq \lambda$ and $0 \leq H_l(\theta) \leq 1$. From Eq. (3.74), It could be seen that the liquid holdup reached a maximum value of $+50^\circ$ for up flow and a minimum value of -50° for down flow.

Mattar and Gregory [138] performed experiments with the co-current flow of two-phase mixtures of air and a light oil in a transparent 1-inch-diameter pipe at angles of inclination varying from 0° to 10° above the horizontal. They obtained visual observations and numerical data for in-situ liquid volume fractions, slug velocities, and bubble rise velocity in stagnant oil. They used these data were to generate expressions for the liquid holdup a function of the superficial liquid velocity and the superficial gas velocity. Their liquid holdup correlation was:

$$H_l = 1 - \frac{U_g}{1.3(U_g + U_l) + 0.7} \quad (3.75)$$

Madsen [139] correlated semiempirically void-fraction data from three sources, obtained by three experimental methods. He derived his equation based on the assumption of a continuous transition from bubbly to separate flow, expressing void fraction point from bubbly to churn or slug flow. The equation was

$$\alpha = \frac{1}{1 + \left(\frac{\rho_l}{\rho_g}\right)^{0.5} \left(\frac{x}{1-x}\right)^{-m}} \quad (3.76)$$

$$m = \frac{0.5 \log(\rho_l / \rho_g) - \log[(\alpha_0 / 1 - \alpha_0)]}{\log(\rho_l / \rho_g) - \log[(\alpha_0 / 1 - \alpha_0)]} \quad (3.77)$$

The value of void fraction (α_0) was 0.302 with a variance of 0.00178 for all the data. This equation applied to water-air adiabatic and to water-steam diabatic systems inside round tubes, at pressures from atmospheric to 144.80 bar, and mass qualities from 0.1% to 50%.

Moussalli and Chawla [140] proposed the following correlation for the void fraction

$$\alpha = C_A \beta \quad (3.78)$$

$$C_A = 1 - \frac{30.4 \left(\frac{x}{1-x} \right) \left(\frac{\rho_l}{\rho_g} \right) + 11}{60 \left[1 + 1.6 \left(\frac{x}{1-x} \right) \left(\frac{\rho_l}{\rho_g} \right) \right] \left[1 + 3.2 \left(\frac{x}{1-x} \right) \left(\frac{\rho_l}{\rho_g} \right) \right]} \quad (3.79)$$

In their correlation, they successfully reproduced available data even in the case where the void fraction tended towards 1. This range was not covered accurately by the original Hughmark correlation [112].

Butterworth [141] presented a short note about a comparison of some void fraction relationships for co-current gas-liquid flow. His comparison was among six different models and correlations. The models and correlations considered by Butterworth were: the homogeneous model, Eq. (1.19) with $S = 1$, Zivi model, separate-cylinders model, Eq. (3.41) with $n = 2.5$, Lockhart-Martinelli correlation, Thom correlation, and Baroczy correlation. He suggested that the following equation could be used as the basis for a new void fraction correlation:

$$\alpha = \frac{I}{1 + c \left(\frac{1-x}{x} \right)^q \left(\frac{\rho_g}{\rho_l} \right)^r \left(\frac{\mu_l}{\mu_g} \right)^s} \quad (3.80)$$

The values of c , q , r , and s for the different models and correlations were given in Table 3.3.

Table 3.3 Values of c , q , r , and s for Different Models and Correlations

Model or Correlation	c	q	r	s
Homogeneous Model	1	1	1	0
Zivi [17]	1	1	0.67	0
Separate-Cylinders [29]	1	0.72	0.40	0.08
Lockhart-Martinelli [16]	0.28	0.64	0.36	0.07
Thom [26]	1	1	0.89	0.18
Baroczy [125]	1	0.74	0.65	0.13

The values of c , q , r , and s could be determined by fitting Eq. (3.80) to experimental data. However, two of these constants might be removed on physical grounds. For example, at the critical state, when $\rho_l = \rho_g$ and $\mu_l = \mu_g$, the relationship that $\alpha = x$ was valid. So, both c and q had a value of 1.

Taitel and Dukler [14] presented a theoretical model for determining flow regime transitions in two-phase gas-liquid flow. Their model predicted the relationship between the following variables at which the flow regime transitions took place: gas and liquid mass flow rates, properties of the fluids, pipe diameter, and angle of inclination of the pipe to the horizontal. The regimes considered in their model were intermittent (slug and

plug), stratified smooth, stratified wavy, dispersed bubble, and annular-annular dispersed liquid flow. They based the mechanisms for transition on physical concepts. These mechanisms were fully predictive in that no flow regime transition were used in their development. They presented a generalized flow regime map based on this theory. Two-phase flow patterns could be predicted using this mechanistic approach rather than correlated using experimental data. Also, they developed a method to predict the liquid height in stratified flows for their flow pattern map. This flow pattern map could be used to obtain the void fraction.

Nabizadeh [142] modified Zuber and Findlay equation [127]:

$$\alpha = \frac{x}{\rho_g} \left[C_o \left(\frac{x}{\rho_g} + \frac{1-x}{\rho_l} \right) + \frac{1.18 [g\sigma(\rho_l - \rho_g)]^{0.25}}{G\rho_l^{0.5}} \right]^{-1} \quad (3.81)$$

Using a large number of his own measurements, Nabizadeh developed an empirical correlation for the C_o factor in the equation of Zuber and Findlay [127] of the form:

$$C_o = \left(1 + \frac{1-x}{x} \frac{\rho_g}{\rho_l} \right)^{-1} \left[1 + \frac{1}{n} Fr^{-0.1} \left(\frac{\rho_g}{\rho_l} \right)^n \left(\frac{1-x}{x} \right)^{\frac{11n}{9}} \right] \quad (3.82)$$

$$Fr = \frac{G^2}{gd\rho_l^2} \quad (3.83)$$

$$n = \sqrt{0.6 \frac{\rho_l - \rho_g}{\rho_l}} \quad (3.84)$$

Applying the extended and improved Zuber-Findlay equation, he obtained good agreement between correlated and measured data for water, R12, and R113.

Yamazaki and Yamaguchi [143] proposed a generalized void fraction correlation for boiling and non-boiling vertical two-phase flows in tube. Their correlation was:

$$\frac{\alpha}{(1-\alpha)(1-K\alpha)} = \frac{\beta}{1-\beta} = \left(\frac{x}{1-x}\right) \left(\frac{\rho_l}{\rho_g}\right) \quad (3.85)$$

$$K = \frac{u_g - u_l}{U_g} \quad (3.86)$$

They established a criterion with a dimensionless group (Eo/La) that determined the K value as:

$$K = \begin{cases} 1 & Eo/La \geq 2 \times 10^{-6} \\ 0.57 & Eo/La < 2 \times 10^{-6} \end{cases} \quad (3.87)$$

$$Eo = \frac{gd^2(\rho_l - \rho_g)}{\sigma} \quad (3.88)$$

$$La = \frac{\rho_l d \sigma}{\mu_l^2} \quad (3.89)$$

A comparison between the predicted values of their method and experimental values showed that their correlation was adequate within $\pm 15\%$ of deviation.

Trimble and Turner [144] mentioned that Beattie obtained a void fraction correlation by integrating his local voidage and velocity profiles for bubble flow over the duct cross section. His correlation should only be used for $\alpha < 0.6$. His correlation was

$$\alpha = \frac{1}{1 + \left(\frac{1-x}{x}\right) \left(\frac{\rho_g}{\rho_l}\right) C_o} \quad (3.90)$$

$$C_o = 1 + 2.65\sqrt{f} \quad (3.91)$$

He evaluated the fanning friction factor (f) using Beattie's small bubble friction factor model [145] with absolute roughness 5 μm and an equivalent diameter of 10 mm. At $f=0$, $C_o = 1$ and his model reduced to homogeneous flow.

Ishii [146] developed a one-dimensional drift-flux model in different two-phase flow regimes. In his model, he developed flow regime dependent expressions for C_o and u_{gj} taking into account the interfacial geometry, the body-force field, shear stresses and the interfacial momentum transfer. Based on the relative velocity between the phases, he developed transition criteria between different flow regimes. For churn turbulent flow, the transition criteria was:

$$|U_g| \leq \sqrt{\frac{gd(\rho_l - \rho_g)}{\rho_g} \left(\frac{1}{C_o} - 1\right)} \quad (3.92)$$

For churn turbulent flow, the expressions of C_o and u_{gj} were:

$$C_o = \left(1.2 - 0.2\sqrt{\frac{\rho_g}{\rho_l}}(1 - \exp(-18\alpha))\right) \quad (3.93)$$

$$u_{gj} = (C_o - 1) U + \sqrt{2} \left(\frac{g\sigma(\rho_l - \rho_g)}{\rho_l^2}\right)^{0.25} \quad (3.94)$$

For annular flow, the expressions of C_o and u_{gj} were:

$$C_o = 1 + \frac{1 - \alpha}{\alpha + \left[\left(\frac{1 + 75(1 - \alpha)}{\sqrt{\alpha}} \right) \left(\frac{\rho_g}{\rho_l} \right) \right]^{0.5}} \quad (3.95)$$

$$u_{gj} = (C_o - 1) \left(U + \frac{gd(\rho_l - \rho_g)(1 - \alpha)}{0.015\rho_l} \right) \quad (3.96)$$

Gregory et al. [147] reported experimental data for gas holdup in liquid slugs are for two different pipe sizes of 2.58 cm and 5.12 cm diameter. They developed a simple empirical correlation to evaluate the liquid volume fraction in the slug for horizontal gas-liquid slug flow. Their correlation was

$$H_l = \frac{1}{1 + \left(\frac{U_m}{8.66} \right)^{1.39}} \quad (3.97)$$

$$U_m = U_l + U_g \quad (3.98)$$

They concluded that their correlation to be a significant improvement over the only other published correlation proposed by Hubbard [148]. The results of this investigation were important for the development of a mechanistic model for the prediction of pressure drop and holdup for slug flow in pipes.

Gardner [149] examined data from a large number of German, American and Russian sources regarding the induced separation of steam from water in boilers. It was clear that there were differences between the experimental results obtained by different

groups of researchers for the voidage when bubbling vapor through a stagnant liquid pool. He found that data could be correlated in general by

$$\frac{\alpha}{(1-\alpha)^2} = K \left[\left(\frac{\rho_l^2 U_g^4}{g\sigma(\rho_l - \rho_g)} \right)^{0.25} \left(\frac{\rho_g v_l^2 (g(\rho_l - \rho_g))^{0.5}}{\sigma^{1.5}} \right)^m \right]^n \quad (3.99)$$

With $K = 1.70$ given by the first group of researchers, $K = 11.2$ given by the second group of researchers and $K = 2.13$ given by the third group of researchers. The value of exponent m was either 0.16 or 0.3 depending chiefly upon the method of measurement of the voidage. The exponent n varied from $2/3$ to 0.79, depending upon the sources of the data. The most probable value for n was $2/3$.

Based on the Lockhart–Martinelli parameter (X), Chen and Spedding [38] developed a correlation to determine the holdup for stratified and annular flow. For stratified flow, they recommended to use the following correlation:

$$H_l = \frac{X^{2/3}}{1 + X^{2/3}} \quad (3.100)$$

For annular flow, they proposed to include an experimental adjustment factor, k_i , to give good agreement with experimental data. Their correlation was

$$H_l = \frac{X^{2/3}}{k_i + X^{2/3}} \quad (3.101)$$

Where $k_i = 2.5$ for large diameter pipes ($d \geq 0.2$ m), $k_i = 6$ for small diameter pipes ($d \leq 0.045$ m), while $k_i = 1$ for diameter pipes between 0.045 m and 0.2 m.

Chen and Spedding [150] justified the Butterworth form of correlation [141] for holdup in two-phase gas-liquid flow theoretically for certain conditions. For turbulent-turbulent and laminar-laminar ideal stratified flow, they expressed the Butterworth correlation [141] in terms of the volumetric flow rate (Q) instead of the mass quality (x) as follows:

$$\frac{H_g}{H_l} = K \left(\frac{Q_g}{Q_l} \right)^a \left(\frac{\rho_g}{\rho_l} \right)^b \left(\frac{\mu_g}{\mu_l} \right)^c \quad (3.102)$$

Where K , a , b and c were dependent constants of flow regimes and the H_g/H_l range. Table 3.4 gives values of K , a , b and c for ideal stratified flow.

Table 3.4 Values of K , a , b and c for Ideal Stratified Flow

Flow Type	H_g/H_l Range	K	a	b	c
Turbulent-Turbulent	$2.5 \times 10^{-6} - 3 \times 10^{-4}$	1.02	0.69	0.31	0.08
Turbulent-Turbulent	$3 \times 10^{-4} - 2.1 \times 10^{-2}$	1.14	0.70	0.31	0.08
Turbulent-Turbulent	$2.1 \times 10^{-2} - 2.5 \times 10^{-1}$	1.31	0.72	0.32	0.08
Turbulent-Turbulent	$2.5 \times 10^{-1} - 1.3$	1.48	0.77	0.34	0.09
Turbulent-Turbulent	1.3-8.0	1.49	0.83	0.37	0.09
Turbulent-Turbulent	8.0- 1.4×10^2	1.28	0.90	0.40	0.10
Turbulent-Turbulent	$1.4 \times 10^2 - 10^5$	1.09	0.93	0.41	0.10
Laminar-Laminar	$10^{-3} - 0.2$	1.46	0.45	0.00	0.45
Laminar-Laminar	0.2-3.0	1.95	0.50	0.00	0.50
Laminar-Laminar	3.0- 10^3	1.83	0.57	0.00	0.57

For gas-liquid, turbulent-laminar ideal stratified flow, they derived the following correlation:

$$\frac{H_g}{H_l} = \left(W_1 \frac{\rho_g Q_g^{1.8} v_g^{0.2}}{\rho_l Q_l v_l d^{0.8}} \right)^{1/\omega_1} \quad (3.103)$$

Where W_1 and ω_1 are dependent constants of H_g/H_l . Table 3.5 gives values of W_1 and ω_1 for gas-liquid, turbulent-laminar ideal stratified flow.

Table 3.5 Values of W_1 and ω_1 for Gas-Liquid, Turbulent-Laminar Ideal Stratified Flow

H_g/H_l Range	W_1	ω_1
0.1-0.7	0.01383	2.25
0.7-3.5	0.01516	2.00
3.5-20.0	0.01200	1.83
20.0-200.0	0.00826	1.70

For gas-liquid, laminar-turbulent ideal stratified flow, they proposed the following correlation:

$$\frac{H_g}{H_l} = \left(W_2 \frac{\rho_g Q_g v_g}{\rho_l Q_l^{1.8} v_l^{0.2} d^{0.8}} \right)^{1/\omega_2} \quad (3.104)$$

Where W_2 and ω_2 are dependent constants of H_g/H_l . Table 3.6 gives values of W_2 and ω_2 for gas-liquid, laminar-turbulent ideal stratified flow.

Table 3.6 Values of W_2 and ω_2 for Gas-Liquid, Laminar-Turbulent Ideal Stratified Flow

H_g/H_l Range	W_2	ω_2
0.04-0.2	538.69	2.25
0.2-6.0	630.44	2.15
6.0-150.0	474.14	2.00

For gas-liquid, turbulent-turbulent and laminar-laminar ideal annular flow, they also obtained the form of Eq. (3.102) but with the values of K , a , b and c as given in Table. 3.7.

Table 3.7 Values of K , a , b and c for Ideal Annular Flow

Flow Type	H_g/H_l	K	a	b	c
Turbulent-Turbulent	-	1.0	0.9	0.4	0.1
Laminar-Laminar	-	1.0	0.5	0.0	0.5

Spedding and Chen [151] analyzed a wide range of experimental holdup data on the basis of the general correlations of Chen and Spedding [150]. For slug and plug flow, they gave the holdup by the Armand type of equation (Eq. (3.2)). For stratified flow, they gave the holdup by the theoretical equations that were derived. For annular flow with values of $H_g/H_l \geq 4$, they satisfactorily represented the data by a semi-empirical correlation as:

$$\frac{H_g}{H_l} = 0.45 \left(\frac{Q_g}{Q_l} \right)^{0.65} \quad (3.105)$$

Tandon et al. [152] developed an analytical model for predicting void fraction in two-phase annular flow. In their analysis, they used the Lockhart-Martinelli method to calculate two-phase frictional pressure drop. They used von Karman's universal velocity profile to represent the velocity distribution in the annular liquid film. Their model was

$$\alpha = \begin{cases} 1 - 1.928 Re_l^{-0.315} [F(X_u)]^{-1} + 0.9293 Re_l^{-0.63} [F(X_u)]^{-2} & 50 < Re_l < 1125 \\ 1 - 0.38 Re_l^{-0.088} [F(X_u)]^{-1} + 0.0361 Re_l^{-0.176} [F(X_u)]^{-2} & Re_l > 1125 \end{cases} \quad (3.106)$$

$$F(X_u) = 0.15 [X_u^{-1} + 2.85 X_u^{-0.476}] \quad (3.107)$$

They claimed that void fractions predicted by the proposed model were generally in good agreement with available experimental data. Their model appeared to be as good as Smith correlation [135] and better than Wallis correlation [132] and Zivi correlation [17] for computing void fraction.

Liao et al. [153] developed a drift-flux model. They based their model primarily on the Ishii model [145] with the addition of a separate expression for the drift velocity in the bubbly flow regime. The transition criteria and the expressions for C_o and u_{gj} for different flow regime were as follows:

For bubbly flow:

$$U_l > 2.34 - 1.07 \left(\frac{g\sigma(\rho_l - \rho_g)}{\rho_l^2} \right)^{0.25} \quad (3.108)$$

$$C_o = 1 \quad (3.109)$$

$$u_{gj} = 1.53 (\alpha - 1)^2 \left(\frac{g\sigma(\rho_l - \rho_g)}{\rho_l^2} \right)^{0.25} \quad (3.110)$$

For churn turbulent flow:

$$C_o = \left(1.2 - 0.2 \sqrt{\frac{\rho_g}{\rho_l}} (1 - \exp(-18\alpha)) \right) \quad (3.111)$$

$$u_{gj} = 0.33 \left(\frac{g\sigma(\rho_l - \rho_g)}{\rho_g^2} \right)^{0.25} \quad (3.112)$$

For annular flow:

$$|U_g| > \sqrt{\frac{gd(\rho_l - \rho_g)}{\rho_g}} \left(\frac{1}{C_o} - 1 \right) \quad (3.113)$$

$$C_o = 1 + \frac{1 - \alpha}{\alpha + 4 \left(\frac{\rho_g}{\rho_l} \right)^{0.5}} \quad (3.114)$$

$$u_{gj} = (C_o - 1) \sqrt{\frac{gd(\rho_l - \rho_g)(1 - \alpha)}{0.015\rho_l}} \quad (3.115)$$

The above modifications led to smaller scatter of the data points.

Regarding Armand coefficient (C_A), Spedding and Chen [154] proposed another C_A correlation depending on the ratio of gas to liquid superficial velocities, U_g/U_l :

$$C_A = \begin{cases} 1.2 & U_g/U_l < 31 \\ \beta + 2.22 \left(\frac{\beta}{1-\beta} \right)^{-0.65} & 31 \leq U_g/U_l < 1.5 \times 10^4 \end{cases} \quad (3.116)$$

Minami and Brill [155] conducted an experimental study of two-phase flow to investigate liquid holdup in wet-gas pipelines. They obtained the liquid-holdup data by passing spheres through a 1 333 ft (406.3 m) long, 3.068 in. (77.93 mm) inside diameter horizontal pipe and measuring the liquid volumes removed. They used three different two-phase mixtures. They compared the holdup data with predicted holdup values. They used the holdup data to evaluate a mechanistic model for stratified flow. They concluded that none of the methods could accurately predict liquid holdup in this low-holdup region. They proposed two new empirical liquid holdup correlations for horizontal flow. The first correlation was strictly for wet-gas pipelines ($0 < H_l < 0.35$) while the second correlation was general and could be applied for any horizontal pipeline ($0 < H_l < 1.0$). The general correlation was:

$$H_l = 1 - \exp \left[- \left(\frac{\ln Z + 9.21}{8.7115} \right)^{4.3374} \right] \quad (3.117)$$

Where Z is the Eaton et al. [130] abscissa.

Using a force balance under steady-state conditions, Hart et al. [156] derived for small liquid void fraction ($(1-\alpha) \leq 0.06$) the following equation for the liquid void fraction in the stratified, wavy and annular flow regimes:

$$\frac{1-\alpha}{\alpha} = \frac{U_l}{U_g} \left\{ 1 + \left[10.4 Re_l^{-0.363} \left(\frac{\rho_l}{\rho_g} \right)^{1/2} \right] \right\} \quad (3.118)$$

They claimed that good agreement between the experimentally determined values of the liquid void fraction and the values calculated with Eq. (3.118) for the air-water and four different air-water+ethylene glycol systems was obtained.

Huq [157] presented an analytical two-phase flow void fraction prediction method. His void fraction model was:

$$\alpha = 1 - \frac{2(1-x)^2}{1-2x + [1+4x(1-x)(\rho_l/\rho_g - 1)]^{0.5}} \quad (3.119)$$

Schmidt [158] mentioned that Huq void fraction model [157] was one of the few models that were not based on experimental data. As a result, it was not a priori constraint to a specific parameter range. A consideration of reasonable boundary limits for the slip ratio (S) was the aim to a straightforward development of the equation. Also, Schmidt and Friedel [159] recommended Huq void fraction model [157] except for high viscosity fluid flow or mass fluxes than 50 kg/m².s.

Chexal et al. [160] presented an empirical void fraction correlation based on the drift flux model that eliminated the need to know the flow regime before predicting the

void fraction. The correlation, referred as the Chexal-Lellouche correlation, was developed originally to provide a continuous void fraction model for use in the light water reactor industry. The Chexal-Lellouche correlation covered the full range of pressures (high and low), flows (high and low), void fractions for cocurrent or countercurrent vertical flow conditions, and fluid types (steam-water, air-water, hydrocarbons, and oxygen). They qualified their correlation against many sets of steady-state two-phase/two-component flow test data that covered a wide range of thermodynamic conditions and geometries typical of PWR and BWR fuel assemblies as well as for pipes up to $d = 450$ mm. The Chexal-Lellouche correlation was available as a source code module for inclusion into any thermal-hydraulic computer program, and as an interactive personal computer program.

Takeuchi et al. [161] generalized Wallis' flooding correlation [18] for both small and large pipes by the use of the critical Kutateladze number. Then, they obtained a drift flux correlation that was tangential to the generalized flooding curve. Their correlation was as follows:

$$C_o = 1.11775 + 0.45881\alpha - 0.57656\alpha^2 \quad (3.120)$$

$$u_{gj} = \sqrt{\frac{K_{d^*}^2}{d^*} \frac{C_o(1-C_o\alpha)}{1.367^2 + C_o\alpha(\sqrt{\rho_g/\rho_l} - 1.367^2)}} \sqrt{\frac{gd(\rho_l - \rho_g)}{\rho_l}} \quad (3.121)$$

$$K_{d^*} = \sqrt{d^* \cdot \min\left(\frac{1}{2.4}, \frac{10.24}{d^*}\right)} \quad (3.122)$$

$$d^* = d \sqrt{\frac{g(\rho_l - \rho_g)}{\sigma}} \quad (3.123)$$

They claimed that their simple function of void fraction for the correlation parameter was sufficient to provide good agreement with steam generator test data, without using flow regime maps. After they determined the drift flux correlation with the large-pipe test, they implemented the drift flux correlation in the TRAC-PD2 computer code to be tested against the flooding curve for a small-diameter pipe. Also, they applied the Chexal-Lellouche formulas [160] to the data analysis, and compared the results with the present correlations.

Steiner [162] modified the Rouhani-Axelsson [19] void fraction model for application to horizontal flows. His equation was:

$$\alpha = \frac{x}{\rho_g} \left[(1 + 0.12(1-x)) \left(\frac{x}{\rho_g} + \frac{1-x}{\rho_l} \right) + \frac{1.18(1-x)[g\sigma(\rho_l - \rho_g)]^{0.25}}{G\rho_l^{0.5}} \right]^{-1} \quad (3.124)$$

He did not provide a comparison of Eq. (3.124) to void fraction data but only noted that he found it to work for R-12 and R-22. Kattan et al. [101] used Steiner expression in their two-phase flow heat transfer model. Also, Steiner expression was used in the new condensation heat transfer model and flow pattern map of Thome and coworkers [163,164].

Abdul-Majeed [165] simplified and improved the mechanistic model developed by Taitel and Dukler [14] for estimating the holdup in horizontal two-phase flow. First, he conducted an experimental study to develop a data bank used for evaluation and improvement. He obtained the holdup data using an air-kerosene mixture flowed through a test section consisting of a horizontal pipe 2-in (50.8 mm) in diameter and 118 ft (36 m)

long. The liquid holdup ranged from 0.009 to 0.61 and the flow patterns observed were stratified, slug and annular. Based on the measured data, he concluded that Taitel-Dukler model tended to overestimate liquid holdup for stratified wavy, slug, and annular flow patterns, whereas it tended to underestimate the liquid holdup for stratified smooth flow. Therefore, he proposed an empirical modification that resulted in a significant improvement in predictions compared to experimental data. His single explicit equations were as follows:

For turbulent flow:

$$H_l = \exp(-0.9304919 + 0.5285852 \ln X - 9.219634 \times 10^{-2} (\ln X)^2 + 9.02418 \times 10^{-4} (\ln X)^4) \quad (3.125)$$

For laminar flow:

$$H_l = \exp(-1.099924 + 0.6788495 \ln X - 0.1232191 \times 10^{-2} (\ln X)^2 - 1.778653 \times 10^{-3} (\ln X)^3 + 1.626819 \times 10^{-3} (\ln X)^4) \quad (3.126)$$

$$X^2 = \left[\frac{U_g \rho_g \mu_l}{U_l \rho_l \mu_g} \right]^m \frac{\rho_l U_l^2}{\rho_g U_g^2} \quad (3.127)$$

For turbulent flow, $m = 0.2$, whereas for laminar flow, $m = 1.0$.

Based on statistical results, he observed that the proposed model gave excellent results and clearly outperformed the original model and all the existing correlations when tested against his own data (89 points) and against data from the literature.

Spedding et al. [166] presented data on horizontal and slightly inclined flows at +5 and -5° for a 0.058 m inner diameter pipe with the co-current air-water system. Holdup

prediction proved to be flow regime dependent. For $U_g \geq 6$ m/s, they proposed a new relation between the liquid holdup (H_l), the ratio of the liquid volumetric flow rate to the total volumetric flow rate ($Q_l/(Q_l+Q_g)$) and the pipe diameter (d) as follows:

$$H_l = (3.5 + d) \left(\frac{Q_l}{Q_l + Q_g} \right)^{0.7} \quad (3.128)$$

Equation (3.128) could not predict the smooth stratified, stratified inertia wave, stratified blown-through-slug, bubble, slug and plug regime.

Graham et al. [167] performed experiments on smooth horizontal tubes using R134a and R410A as working fluids during evaporation and condensation. They expressed the void fraction in terms of the Lockhart-Martinelli parameter for turbulent-turbulent flow (X_{tt}) and the Froude rate (Ft) as follows:

$$\alpha = \left(1 + X_{tt} + \frac{1}{Ft} \right)^{-0.321} \quad (3.129)$$

$$Ft = \left(\frac{x^3 G^2}{\rho_g^2 g d (1-x)} \right)^{0.5} \quad (3.130)$$

The Froude rate (Ft) was a parameter derived by Hulburt and Newell [168]. It was the ratio of the vapor kinetic energy to the energy required to lift the liquid phase around the tube.

Gomez et al. [169] used data from six different slug flow studies for the development of the liquid holdup correlation. The data showed that the liquid holdup in

the slug flow varied with the inclination angle. It had a maximum value at horizontal flow conditions, decreasing as the upward inclination increased, and it had a minimum value for upward vertical flow. The data also revealed that the liquid holdup was also a function of the mixture velocity and the liquid phase viscosity. Their correlation was

$$H_l = \text{Exp}(-0.45\theta - 2.48 \cdot 10^{-6} \text{Re}_l) \quad 0 \leq \theta \leq 1.57 \quad (3.131)$$

$$\text{Re}_l = \frac{\rho_l U_m d}{\mu_l} \quad (3.132)$$

$$U_m = U_l + U_g \quad (3.133)$$

Based on the data for vertical flows in circular pipes of 5 to 50 mm in diameter using air-water and air-viscous liquid as working fluids, Sakaguchi et al. [170] derived the following empirical correlation as a function of seven non-dimensional parameters:

$$\alpha = 2.20 \left(\frac{U_g}{U_l + U_g} \right)^{0.866} \left(\frac{U_l}{U_l + U_g} \right)^{-0.0574} \left(\frac{\mu_g}{\mu_l} \right)^{0.0190} \left(\frac{\rho_g}{\rho_l} \right)^{0.148} \left[\frac{U_l + U_g}{(gd)^{0.5}} \right]^{-0.0701} \left[\frac{\rho_l d (U_l + U_g)}{\mu_l} \right]^{-0.0213} \left[\frac{\rho_l d (U_l + U_g)^2}{\sigma} \right]^{0.0359} - 0.00925 \quad (3.134)$$

Osman [22] presented two artificial neural network (ANN) models to identify the flow regime and calculate the liquid holdup in horizontal multiphase flow. He developed these models with 199 experimental data sets and with three-layer back-propagation neural networks (BPNs). He used superficial liquid and gas velocities (U_l and U_g), pressure (p), temperature (T), and fluid properties (density and viscosity) as inputs to the

model. He divided data into three portions: training, cross validation, and testing. He concluded that the developed models provided better predictions and higher accuracy than the empirical correlations developed specifically for these data groups. The developed flow-regime model predicted correctly for more than 97% of the data points. The liquid-holdup model outperformed the published models. It provided holdup predictions with an average absolute error of 9.407%, a standard deviation of 8.544%, and a correlation coefficient of 0.9896.

Shippen and Scott [23] presented a neural network model for prediction of liquid holdup in two-phase horizontal flow. They used data from five independent studies to develop a neural network for predicting liquid holdup in two-phase horizontal flow. They used pipe diameter (d), superficial gas velocity (U_g), superficial liquid velocity (U_l), liquid velocity (σ_l), liquid density (ρ_l), liquid viscosity (μ_l), and log value of no slip liquid holdup ($\log(1-\alpha)$) as inputs to the model. The output of the model was log value of no slip liquid holdup. For this data set, a detailed comparison with existing empirical correlations and mechanistic models revealed that the neural network model showed an improvement in overall accuracy and performed more consistently across the range of liquid-holdup and flow patterns.

Yun-Long et al. [171] derived the mathematical model of void fraction of gas-liquid two-phase annular flow in vertical tubes using the theorem of pressure energy consumption minimum. The basic principle in this model was that there was a quite steady flow state of annular flow in the flow pattern of gas-liquid two-phase flow. According to the principle of the fluid mechanics, any system tends towards to a

minimum steady state of energy. As a result, the energy in steady flow of annular flow should be minimum. They proposed the mathematical model of pressure energy consumption to calculate void fraction. They claimed that their calculated results agreed well with the experimental data.

García et al. [114] analyzed a wide range of experimental holdup data from different sources based on a theoretical model proposed in their work to evaluate the liquid holdup in horizontal pipes. They included 2 276 gas-liquid flow experiments in horizontal pipelines with a wide range of operational conditions and fluid properties in the database. Their theoretical model related the liquid holdup and no-slip liquid holdup ($H_l/H_{l,m}$) to the gas-liquid volumetric flow rates relation (Q_g/Q_l) for different mixture Reynolds numbers ranges. To classify the experimental data for gas-liquid flows in horizontal pipes, they based the Reynolds number on the mixture velocity (U_m) and the liquid kinematic viscosity (ν). They obtained composite analytical expressions by fitting the data with logistic dose curves. Their particular composite power laws equation was:

$$\frac{H_l}{H_{l,m}} = a \text{Re}^b + \frac{(1 - a \text{Re}^b)}{\left(1 + \left(\frac{1}{t} \left(\frac{Q_g}{Q_l}\right)\right)^c\right)^d} \quad (3.135)$$

$$H_{l,m} = \frac{Q_l}{Q} = \frac{Q_l}{Q_l + Q_g} = \frac{1}{1 + \left(\frac{x}{1-x}\right) \left(\frac{\rho_l}{\rho_g}\right)} \quad (3.136)$$

$$\text{Re} = \frac{U_m d}{\nu_l} \quad (3.137)$$

$$U_m = U_l + U_g \quad (3.138)$$

The parameters a , b , c , d and t for the universal composite correlations for holdup are presented in Table 3.8.

Table 3.8 Parameters of the Universal Composite Correlations for Holdup

Range	a	b	c	d	t
$Re < 2\,000$	85.5969	0.4503	0.4240	0.0781	432.0226
$2\,000 \leq Re < 5\,000$	73.9792	0.2936	0.6536	0.2634	429.8162
$5\,000 \leq Re < 10\,000$	74.1824	0.0001	0.9458	1.5020	430.7731
$10\,000 \leq Re < 20\,000$	70.5777	0.1238	1.04086	0.3322	107.5723
$20\,000 \leq Re < 40\,000$	70.5791	0.04267	1.0423	0.3410	107.5740
$40\,000 \leq Re < 100\,000$	17.5825	0.1077	0.8963	0.9592	151.007
$100\,000 \leq Re < 300\,000$	2.5383	0.3001	0.8655	3.5587	100.0044
$300\,000 \leq Re < 2\,670\,000$	1.4976	0.3820	0.9985	2.5626	99.9486

They claimed that the universal (all flow patterns) composite holdup correlations (UCHC) had an average error of -4.1% and an average absolute error of 21.0% . 73.9% of the points (1 682 experimental points) were in the band between $\pm 30\%$. They claimed that they obtained the best agreements for slug and dispersed bubble flow data, with an average absolute error of 13.1% and 1.9% , respectively. They claimed that they obtained the worst agreements for annular and stratified flow data, with an average absolute error of 34.9% and 31.3% , respectively.

Also, they obtained composite power law holdup correlations for flows sorted by flow pattern (FPHC). They presented error estimates for the predicted versus measured holdup correlations together with standard deviation for each correlation. They compared

the accuracy of the correlations developed in their study with the accuracy of 26 previous correlations and models in the literature. They claimed that their correlations predicted the liquid holdup in horizontal pipes with much greater accuracy than those presented by previous authors.

It should be noted that García et al. [114] universal (all flow patterns) composite holdup correlations (UHC) give impossible results. For example, assuming the no-slip liquid holdup $(H_{l,m}) = 0.8$. Thus, $Q_g/Q_l = (1/0.8) - 1 = 0.25$. Assuming the Reynolds number $(Re) = 3125$. From Table 3.8, at $Re = 3125$, $a = 73.9792$, $b = 0.2936$, $c = 0.6536$, $d = 0.2634$ and $t = 429.8162$. Using Eq. (3.134), we obtain $H_l/H_{l,m} = 2.5796$. As a result, $H_l = 0.8 \times 2.5796 = 2.0367 > 1$ which is an impossible result and $H_g = 1 - H_l = -1.0367 < 0$ which is an impossible result. Values of liquid holdup and gas holdup cannot be greater than one or negative (i.e. $0 \leq H_l \leq 1$ and $0 \leq H_g \leq 1$).

In addition, there are impossible results using composite power law holdup correlations for flows sorted by flow pattern (FPHC). For example, García et al. [114] gave parameters of the holdup correlations for slug flow for $Re \leq 139$ and $0.33 \leq Q_g/Q_l \leq 48.8$ as $a = 85.8992$, $b = 0.3717$, $c = 0.7275$, $d = 0.3116$ and $t = 115.1512$. Assuming $Q_g/Q_l = 0.33$. Thus, the no-slip liquid holdup $(H_{l,m}) = 1/(1+0.33) = 0.75$. Assuming the Reynolds number $(Re) = 139$. Using Eq. (3.134), we obtain $H_l/H_{l,m} = 3.3585$. As a result, $H_l = 0.75 \times 3.3585 = 2.5188 > 1$ which is an impossible result and $H_g = 1 - H_l = -1.5188 < 0$ which is an impossible result. Values of liquid holdup and gas holdup cannot be greater than one or negative (i.e. $0 \leq H_l \leq 1$ and $0 \leq H_g \leq 1$).

3.3 Comparison of Selected Two-Phase Flow Void Fraction Models

Figure 3.1 presents a comparison of several two-phase flow void fraction models for steam flow at $p_s = 1\,000$ psia (6 894.74 kPa) in a smooth horizontal pipe. Figure 3.2 presents a comparison of several two-phase flow void fraction models for R 12 flow at $T_s = 50^\circ\text{C}$ in a smooth horizontal pipe at $d = 10$ mm. Figure 3.3 presents a comparison of several two-phase flow void fraction models for R 22 flow at $T_s = 50^\circ\text{C}$ in a smooth horizontal pipe at $d = 10$ mm. Figure 3.4 presents a comparison of several two-phase flow void fraction models for R 410A flow at $T_s = 5^\circ\text{C}$ in a smooth horizontal pipe at $d = 5/8$ in. (15.875 mm). It is clear from Figs. 3.1-3.4 that no two void fraction models provide the same result. Since all two-phase flow void fraction models were developed in conjunction with experimental data, which are prone to measurement error, it is reasonable to expect that any prediction is also subject to similar error.

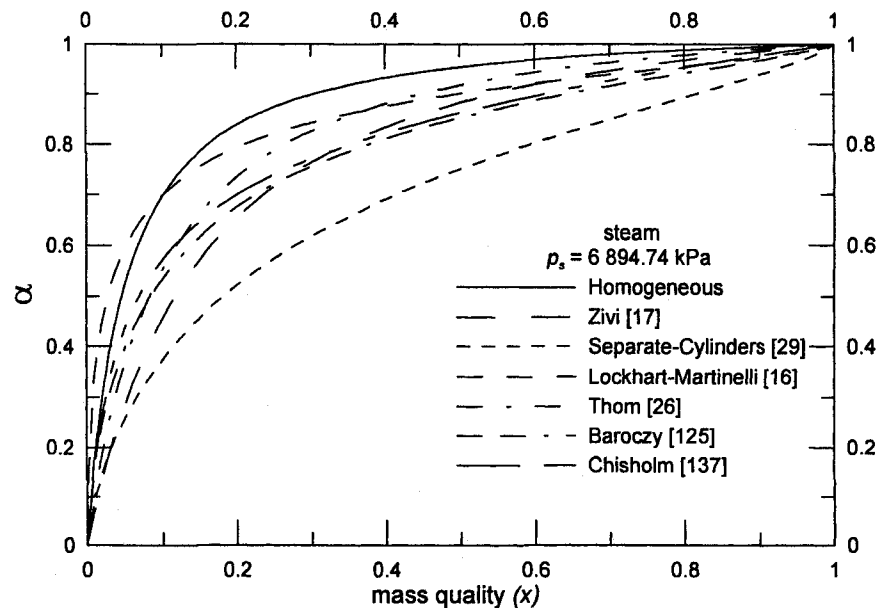


Figure 3.1 Comparison of Selected Two-Phase Flow Void Fraction Models

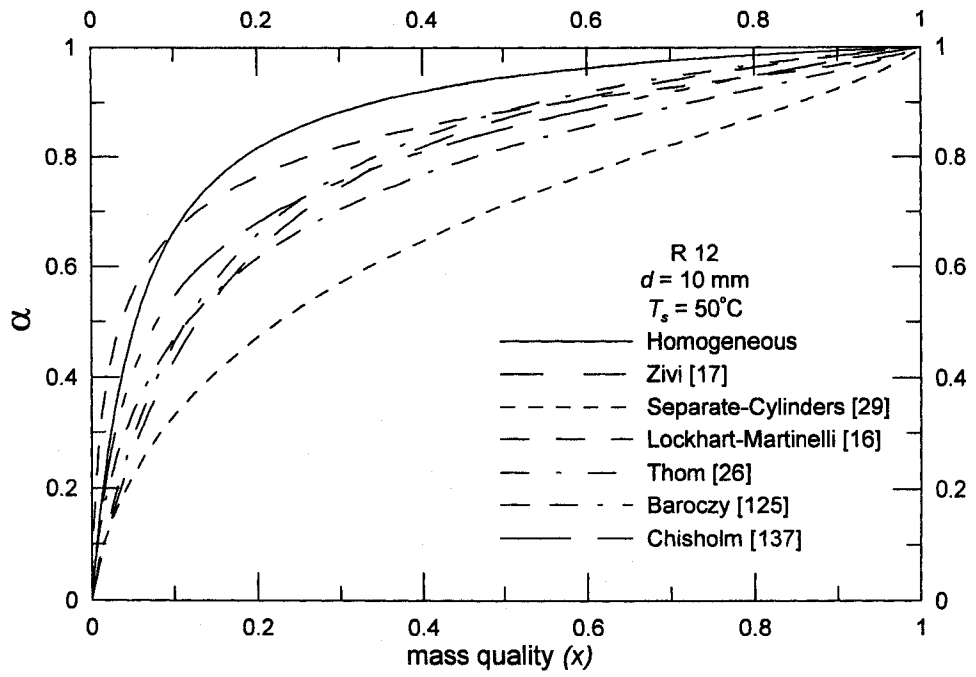


Figure 3.2 Comparison of Selected Two-Phase Flow Void Fraction Models

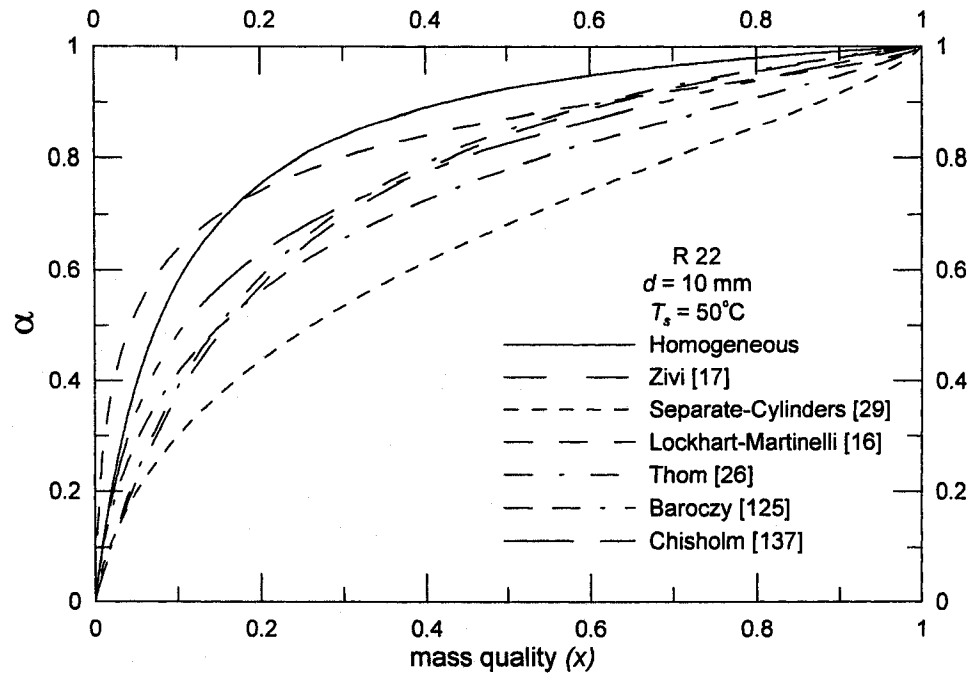


Figure 3.3 Comparison of Selected Two-Phase Flow Void Fraction Models

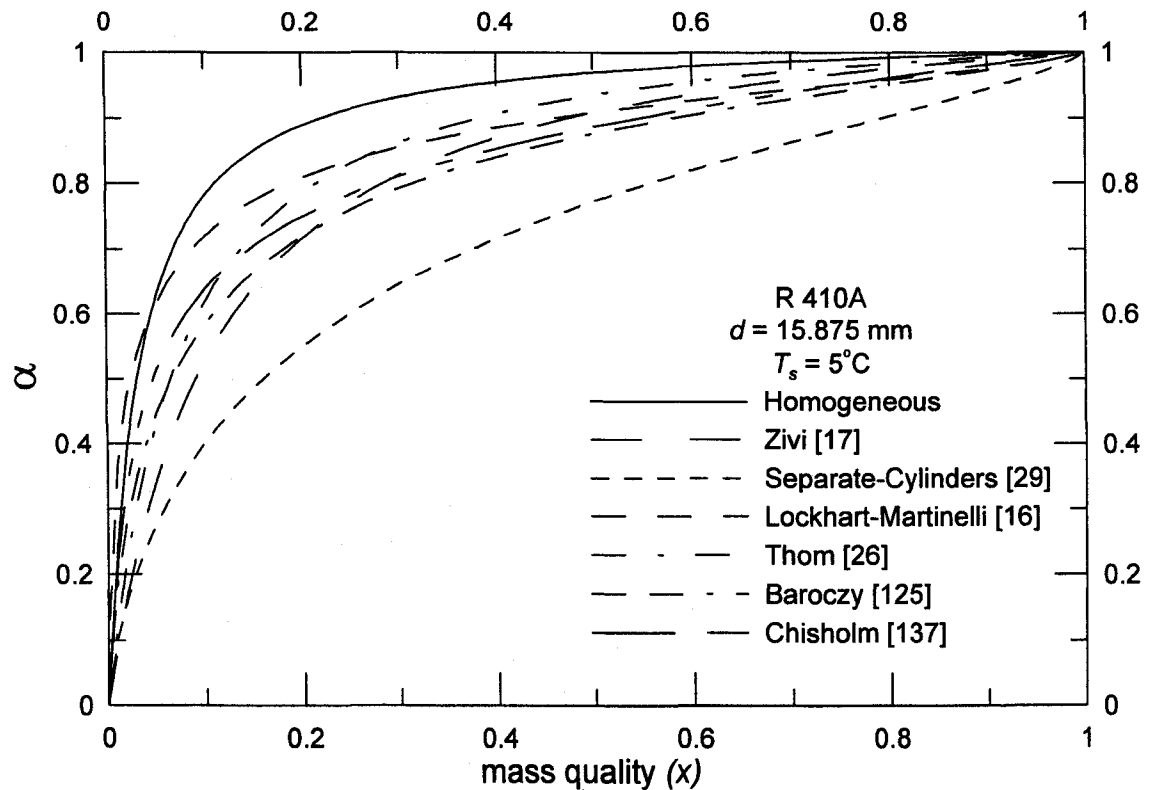


Figure 3.4 Comparison of Selected Two-Phase Flow Void Fraction Models

3.4 Summary

The extensive literature review is presented in Chapter 3 to find most if not all of the void fraction correlations that are available in the open literature. Comparison of several two-phase flow void fraction models and correlations shows that no two void fraction models provide the same result. In Chapter 6, the development of models of two-phase flow void fraction in circular pipes is presented along with comparisons with the data and models reviewed in this chapter. At the end of this chapter, Table 3.9 presents a summary of void fraction studies.

Table 3.9 Summary of Void Fraction Studies

Author	d	Fluids	Orientation/ Conditions	Range/ Applicability	Techniques, Basis, Observations
Armand [107]	26 mm	Air-water	Horizontal	$\beta < 0.9$ Atmospheric pressure	Empirical correlation
Massena [108]				$\beta > 0.9$	Empirical correlation
Martinelli and Nelson [8]		Steam	Horizontal	$6.89 < p < 221.2$ bar Turbulent- Turbulent flow regime Better suited to annular flow	Empirical correlation in a graphic manner on semi-log plot
Lockhart and Martinelli [16]	0.0586 -1.017 in	Air and benzene, kerosene, water, and different oils	Adiabatic	$1.013 < p < 3.445$ bar	Graphical correlation in terms of $1-\alpha$ and α versus X
Baker [3]			Vertical upward	$7.5 < Y < 300$ $G < 950$ $\text{kg/m}^2 \cdot \text{s}$	Empirical equation to allow for the effect of G on α
Flanigan [109]	16 in	Natural gas- condensat e			$H_l = f(U_l)$
Hoogendoorn [74]	0.024- 0.14 m	Air- water, air- gas oil and air- spindle oil mixtures	Horizontal/ adiabatic		Implicit
Levy [110]		Steam			$x = f(\alpha, \rho_v, \rho_g)$
Bankoff					Power law

[61]					distribution for both u and α C_A correlation
Jones [111]					C_A correlation as a function of p
Hughmark [112]					C_A correlation as a function of Z
Nishino and Yamazaki [117]		Steam-water	Vertical upward		$\alpha = f(x, \rho_l, \rho_g)$ at $K = 1/\beta$
Kowalczewski [118]		Water and R12	Vertical upflow		$\alpha = f(\beta, Fr_b, p/p_c)$
Küttükçüoğlu and Njo [119]		Steam-water		$0.1 < Fr_l < 1000$ $p/p_c \leq 0.65$	$\alpha = f(\beta, Fr_b, p/p_c)$
Löscher and Reingardt [120]		R11, R12 and water		$0.01 \leq p/p_c \leq 0.36$ $15 \leq \rho_l/\rho_g \leq 900$ $4 \leq \mu_l/\mu_g \leq 32$	$\alpha = f(\beta, Fr_b, p/p_c)$
Friedel [121]		R12	Vertical upward	$0.12 \leq p/p_c \leq 0.57$ $1 \leq Fr_l \leq 88$	$\alpha = f(\beta, Fr_b, p/p_c)$
Zivi [17]	Several	Steam-water	Horizontal/ Vertical		Analytical model (annular flow assumption), minimization of energy dissipation rate 3 models: (i) without liquid entrainment and wall friction, (ii) with wall friction, and (iii) with liquid entrainment Wall friction effect is much lower than liquid entrainment effect As p increases, α approaches α_m

					Model (i) widely used, does not depend on data
Thom [26]		Steam-water	Vertical		$\alpha = f(S, x)$
Baroczy [125]		Liquid mercury-nitrogen, and water-air			Generalized correlation in a graphical manner $1 - \alpha = f(X, (\mu_l/\mu_g)^{0.2}/(\rho_l/\rho_g))$
Turner [29]			Horizontal		$\alpha = f(X)$
Zuber and Findlay [127]					Drift flux correlation
Zuber et al. [128]	0.01 m	R22	Vertical		G had an effect on α
Guzhov et al. [129]				$\theta = 0^\circ - 9^\circ$	$H_g = f(\beta, Fr)$
Eaton et al. [130]	2, 4 and 17 in.	Water-natural gas, crude-natural gas and distillate-natural gas	Horizontal		Graphical correlation as H_l versus $\frac{1.84 N_{ul}^{0.575}}{N_{ug} N_d^{0.0277}} \left(\frac{p}{p_{atm}} \right)^{0.05} N_l^c$
Rouhani and Axelsson [19]					Drift flux correlation Includes the effects of G and σ
Premoli et al. [134]					Slip ratio correlation
Smith [135]	6 mm 38 mm	Boiling heavy water Boiling water	Vertical Horizontal, vertical	$7 < p < 59$ bar $0 < x < 0.38$ $650 < G < 2050$ kg/m ² .s $380 < q < 1200$ kW/m ² $17.25 < p < 145$ bar $0.003 < x < 0.38$	Semi-empirical model for stratified annular flow (liquid phase) with liquid entrainment in gas phase States that the model is independent of

	11 mm	Air-water	Vertical	0.17 $750 < G < 1$ $950 \text{ kg/m}^2 \cdot \text{s}$ $20 < q < 140$ kW/m^2 Atmospheric pressure $0.005 < x <$ 0.525 $50 < G < 1$ $330 \text{ kg/m}^2 \cdot \text{s}$	flow regime, p , G , x ; applicable to horizontal and vertical flow For $e = 0.4$, applicability assumed only for circular pipes Not recommended for $x < 0.01$ in boiling flow (due to thermal inequilibrium)
Bonnecaze et al. [136]			Horizontal, uphill, downhill	$\theta = -10^\circ$ - $+10^\circ$	Slug flow model
Chisholm [137]					Slip ratio correlation
Serizawa and Michiyoshi [36]					$\alpha = f(x, \rho_b, \rho_g, U_j)$
Beggs and Brill [50]	25.4 and 38.1 mm	Air-water	Horizontal, up flow, down flow, inclined		Determines the flow pattern by comparing Fr with L_1 and L_2
Mattar and Gregory [138]	1 in	Air-light oil		$\theta = 0^\circ$ - 10°	$H_l = f(U_l, U_g)$
Madsen [139]		Water-air Water- steam	Adiabatic Diabatic	$1.013 < p <$ 144.80 bar $0.1 < x < 0.5$	Semi empirical correlation
Moussalli and Chawla [140]					C_A correlation
Nabizadeh [142]	10 mm	Water, R12, and R113	Vertical upward		C_A correlation
Yamazaki and Yamaguchi [143]			Vertical/ boiling and non-boiling		General correlation

Ishii [146]						Drift-flux model Churn turbulent flow, annular flow
Gregory et al. [147]	25.8 and 51.2 mm	Oil-air	Horizontal		$0.03 \leq U_l \leq 2.316 \text{ m/s}$ $0.088 \leq U_g \leq 15.376 \text{ m/s}$	Slug flow model $H_l = f(U_l, U_g)$
Gardner [149]		Steam-water				General correlation
Chen and Spedding [38]	0.0455 m	Air-water	Horizontal			Extension of the Lockhart-Martinelli model
Tandon et al. [152]	6.1 mm 22 mm	Boiling heavy water Steam-water	Vertical		$7 < p < 60 \text{ bar}$ $x < 0.41$ $650 < G < 2050 \text{ kg/m}^2 \cdot \text{s}$ $380 < q < 1200 \text{ kW/m}^2$ $0.24 < \alpha < 0.92$ Atmospheric pressure $x < 0.04$	Semi empirical model Assumed annular flow without liquid entrainment in gas phase and turbulent flow in both phases As good as Smith correlation [135] and better than Wallis correlation [132] and Zivi correlation [17]
Liao et al. [153]						Drift-flux model Bubbly flow, churn turbulent flow, annular flow
Spedding and Chen [154]						C_A correlation depends on U_g/U_l
Minami and Brill [155]	77.93 mm	Kerosene-air, water-air, water plus surfactant-air	Horizontal			Stratified flow model $H_l = f(Z)$
Hart et al.	51 mm	Air-water	Horizontal		$(1-\alpha) \leq 0.06$	Apparent rough

[156]		and air-water + ethyleneglycol		$0.038 < \sigma < 0.072 \text{ N/m}$	surface (ARS) model Stratified, wavy and annular flow
Huq [157]					Analytical method $\alpha = f(x, \rho_b, \rho_g)$
Chexal et al. [160]		Steam-water, air-water, hydrocarbons, and oxygen	Cocurrent or countercurrent vertical		Drift-flux model
Takeuchi et al. [161]					Drift-flux model
Steiner [162]			Horizontal		Drift-flux model
Abdul-Majeed [165]	50.8 mm	Air-kerosene	Horizontal	$0.009 < H_l < 0.61$	$H_l = f(X)$ for turbulent flow and laminar flow
Spedding et al. [166]	0.058 m	Air-water	Horizontal/ slightly inclined,	$\theta = +5$ and -5° $U_g \geq 6 \text{ m/s}$	$H_l = f(d, Q_l, Q_g)$
Graham et al. [167]		R134a and R410A	Horizontal		$\alpha = f(X_u, Ft)$
Gomez et al. [169]				$0 \leq \theta \leq 1.57$	Slug flow model
Sakaguchi et al. [170]	5-50 mm	Air-water and air-viscous liquid	Vertical		Empirical correlation
Osman [22]			Horizontal		ANN model for H_l
Shippen and Scott [23]			Horizontal		Neural network model for H_l
Yun-Long et al. [171]			Vertical		Annular flow
García et al. [114]			Horizontal		UCHC for H_l FPHC for H_l

CHAPTER 4

HOMOGENEOUS TWO-PHASE FLOW PROPERTIES

4.1 Introduction

In this chapter, three new definitions for two-phase viscosity will be introduced using the analogy between thermal conductivity in porous media and viscosity in two-phase flow. These new definitions for two-phase viscosity are satisfying the following two conditions: namely (i) the two-phase viscosity is equal to the liquid viscosity at the mass quality = 0%, and (ii) the two-phase viscosity is equal to the gas viscosity at the mass quality = 100%. These new definitions of two-phase viscosity can be used to compute the two-phase frictional pressure gradient in circular pipes using the homogeneous model. Expressing the published data of two-phase frictional pressure gradient in a dimensionless form as Fanning friction factor (f_m) versus Reynolds number (Re_m) can also be done.

Before we go to the section of proposed methodology in this chapter to introduce the new definitions of two-phase viscosity, we present first the different definitions of homogeneous two-phase flow properties such as density and viscosity available in the literature.

The void fraction based on the homogeneous model (α_m) can be expressed as follows:

$$\alpha_m = \frac{1}{1 + \left(\frac{1-x}{x}\right) \left(\frac{\rho_g}{\rho_l}\right)} \quad (4.1)$$

When (ρ_l/ρ_g) is large, the void fraction based on the homogeneous model (α_m) increases very rapidly once the mass quality (x) increases even slightly above zero. The prediction of the void fraction using the homogeneous model is reasonably accurate only for bubble and mist flows since the entrained phase travels at nearly the same velocity as the continuous phase. Also, when (ρ_l/ρ_g) approaches 1 (i. e. near the critical state), the void fraction based on the homogeneous model (α_m) approaches the mass quality (x) and the homogeneous model is applicable at this case.

For the homogeneous model, the density of two-phase gas-liquid flow (ρ_m) can be expressed as follows:

$$\rho_m = \left(\frac{x}{\rho_g} + \frac{1-x}{\rho_l} \right)^{-1} \quad (4.2)$$

Equation (4.2) can be derived knowing that the density is equal to the reciprocal of the specific volume and using thermodynamics relationship for the specific volume

$$v_m = (1-x)v_l + xv_g \quad (4.3)$$

Equation (4.2) can also be obtained based on the volumetric averaged value as follows:

$$\rho_m = x\alpha_m + (1-x)\alpha_m = \left(\frac{x}{\rho_g} + \frac{1-x}{\rho_l} \right)^{-1} \quad (4.4)$$

Equation (4.2) satisfies the following limiting conditions between (ρ_m) and mass quality (x) :

$$\text{at } x = 0, \rho_m = \rho_l; \quad \text{at } x = 1, \rho_m = \rho_g; \quad (4.5)$$

The Reynolds number based on the homogeneous model (Re_m) can be expressed as follows:

$$Re_m = \frac{Gd}{\mu_m} \quad (4.6)$$

In the homogeneous model, there are some common expressions for the viscosity of two-phase gas-liquid flow (μ_m) . The expressions available for the two-phase liquid-gas viscosity are mostly of an empirical nature as a function of mass quality (x) . The liquid and gas are presumed to be uniformly mixed due to the homogeneous flow. The possible definitions for the viscosity of two-phase gas-liquid flow (μ_m) can be divided into two groups. In the first group, the form of the expression between (μ_m) and mass quality (x) satisfies the following limiting conditions:

$$\text{at } x = 0, \mu_m = \mu_l; \quad \text{at } x = 1, \mu_m = \mu_g; \quad (4.7)$$

For example, McAdams, et al. [45], introduced the definition of two-phase viscosity (μ_m) based on the mass averaged value of reciprocals as follows:

$$\mu_m = \left(\frac{x}{\mu_g} + \frac{1-x}{\mu_l} \right)^{-1} \quad (4.8)$$

They proposed their viscosity expression by analogy to the expression for the homogeneous density (ρ_m). Equation (4.8) leads to the homogeneous Reynolds number (Re_m) is equal to the sum of the liquid Reynolds number (Re_l) and the gas Reynolds number (Re_g).

Also, Cicchitti, et al. [46], introduced the definition of two-phase viscosity (μ_m) based on the mass averaged value as follows:

$$\mu_m = x\mu_g + (1-x)\mu_l \quad (4.9)$$

In addition, Dukler et al. [13], introduced the definition of two-phase viscosity (μ_m) based on the volumetric averaged value as follows:

$$\mu_m = \rho_m [xv_g\mu_g + (1-x)v_l\mu_l] \quad (4.10)$$

Equation (4.10) can be rewritten in terms of kinematic viscosity as follows:

$$v_m = xv_g + (1-x)v_l \quad (4.11)$$

Moreover, Beattie and Whalley [55], introduced the definition of two-phase viscosity (μ_m) as follows:

$$\mu_m = \mu_l(1-\alpha_m)(1+2.5\alpha_m) + \mu_g\alpha_m = \mu_l - 2.5\mu_l \left(\frac{x\rho_l}{x\rho_l + (1-x)\rho_g} \right)^2 + \left(\frac{x\rho_l(1.5\mu_l + \mu_g)}{x\rho_l + (1-x)\rho_g} \right) \quad (4.12)$$

Lin et al. [172] introduced the definition of two-phase viscosity as follows:

$$\mu_m = \frac{\mu_l \mu_g}{\mu_g + x^{1.4} (\mu_l - \mu_g)} \quad (4.13)$$

In their study, the range of x appearing in the capillary tubes was $0 < x < 0.25$. For the best fit to their experimental data, they took the value of the exponent in Eq. (4.13) as 1.4.

Finally, Fourar and Bories [173] presented an unusual expression of the two-phase viscosity as follows:

$$\mu_m = \rho_m (x v_g \mu_g + (1-x) v_l \mu_l + 2 \sqrt{x(1-x) v_g \mu_g v_l \mu_l}) = \rho_m (\sqrt{x v_g \mu_g} + \sqrt{(1-x) v_l \mu_l})^2 \quad (4.14)$$

Equation (4.14) can be rewritten in terms of kinematic viscosity as follows:

$$\nu_m = (\sqrt{x \nu_g} + \sqrt{(1-x) \nu_l})^2 \quad (4.15)$$

It should be noted that Fourar and Bories [173] definition of two-phase viscosity is similar of Dukler et al. [13] definition of two-phase viscosity with adding an extra term.

In the second group, the form of the expression between (μ_m) and mass quality (x) does not satisfy the following limiting conditions:

$$\text{at } x = 0, \mu_m = \mu_l; \quad \text{at } x = 1, \mu_m = \mu_g; \quad (4.16)$$

For example, Davidson, et al. [174], defined the viscosity of two-phase gas-liquid flow (μ_m) as follows:

$$\mu_m = \mu_l \left[1 + x \left(\frac{\rho_l}{\rho_g} - 1 \right) \right] \quad (4.17)$$

The reason for this definition is that when Davidson, et al., plotted the experimental two-phase friction factor (f_{tp}) of their high pressure steam-water pressure drop data against the Reynolds number for all-liquid flow (Re_{lo}), they observed that there were large discrepancies from the single-phase friction factor at $Re_{lo} < 2 \times 10^5$. They found that considerably better agreement with the normal single-phase flow relationship represented by the Blasius equation was obtained if they plotted the experimental two-phase friction factor against the Reynolds number for all-liquid flow multiplied by the ratio of the inlet to outlet mean specific volumes. It should be noted that the above definition of the viscosity of two-phase gas-liquid flow (μ_m), does not extrapolate to the gas viscosity (μ_g) as the mass quality (x) approaches 1.

Also, Owens [175] introduced the definition of two-phase viscosity based on the liquid viscosity as follows:

$$\mu_m = \mu_l \quad (4.18)$$

In addition, García et al. [114] defined the Reynolds number of two-phase gas-liquid flow using the kinematic viscosity of liquid flow (ν_l) instead of the kinematic viscosity of two-phase gas-liquid flow (ν_m). They used this definition because the

frictional resistance of the mixture was due mainly to the liquid. This was equivalent to define μ_m as

$$\mu_m = \mu_l \left(\frac{\rho_m}{\rho_l} \right) = \frac{\mu_l \rho_g}{x \rho_l + (1-x) \rho_g} \quad (4.19)$$

The main disadvantage for the forms of μ_m in the second group is that they are not accurate as the mass quality (x) approaches 1. For example, at $x = 1$, Davidson et al. definition [174], Owens definition [175] and García, et al. definition [114] give $\mu_m = \mu_l \rho_l / \rho_g$, μ_l and $\mu_l \rho_g / \rho_l$ respectively.

Collier and Thome [24] mentioned that the definition of μ_m made by McAdams et al. in Eq. (4.8) is the most common definition of μ_m . The reason for different definition of μ_m is that the friction factor depends very small on viscosity.

4.2 Proposed Methodology

Using the analogy between thermal conductivity in porous media [163] and viscosity in two-phase flow, three new definitions for two-phase viscosity will be introduced. These new definitions are generated by analogy as follows:

- i.* μ_m is analogous to k_e .
- ii.* μ_l is analogous to k_1 .
- iii.* μ_g is analogous to k_2 .
- iv.* x is analogous to v_2 .

These new definitions for two-phase viscosity are given in Table 4.1. Figures 4.1 and 4.2 show the analogy between thermal conductivity in porous media [176]

and viscosity in two-phase flow where Fig. 4.1 shows k_e/k_1 versus v_2 [176] while Fig. 4.2 shows μ_m/μ_l versus x for air-water system at atmospheric conditions.

Table 4.1 Analogy between Thermal Conductivity in Porous Media and Viscosity in Two-Phase Flow

System	Porous Media	Two-Phase Flow
Property	Thermal conductivity (k)	Viscosity (μ)
Def.1	$k_e = \left(\frac{1-v_2}{k_1} + \frac{v_2}{k_2} \right)^{-1}$ (Series model)	$\mu_m = \left(\frac{1-x}{\mu_l} + \frac{x}{\mu_g} \right)^{-1}$ (McAdams et al. [45])
Def.2	$k_e = (1-v_2)k_1 + v_2k_2$ (Parallel model)	$\mu_m = (1-x)\mu_l + x\mu_g$ (Cicchitti et al. [46])
Def.3	$k_e = k_1 \frac{2k_1 + k_2 - 2(k_1 - k_2)v_2}{2k_1 + k_2 + (k_1 - k_2)v_2}$ (Maxwell-Eucken 1 [177])	$\mu_m = \mu_l \frac{2\mu_l + \mu_g - 2(\mu_l - \mu_g)x}{2\mu_l + \mu_g + (\mu_l - \mu_g)x}$ (Generated by analogy)
Def.4	$k_e = k_2 \frac{2k_2 + k_1 - 2(k_2 - k_1)(1-v_2)}{2k_2 + k_1 + (k_2 - k_1)(1-v_2)}$ (Maxwell-Eucken 2 [177])	$\mu_m = \mu_g \frac{2\mu_g + \mu_l - 2(\mu_g - \mu_l)(1-x)}{2\mu_g + \mu_l + (\mu_g - \mu_l)(1-x)}$ (Generated by analogy)
Def.5	$(1-v_2) \frac{k_1 - k_e}{k_1 + 2k_e} + v_2 \frac{k_2 - k_e}{k_2 + 2k_e} = 0$ Effective Medium Theory (EMT [178,179])	$(1-x) \frac{\mu_l - \mu_m}{\mu_l + 2\mu_m} + x \frac{\mu_g - \mu_m}{\mu_g + 2\mu_m} = 0$ (Generated by analogy)
Comment	All definitions satisfy the following conditions: <ol style="list-style-type: none"> i. at $v_2 = 0$, $k_e = k_1$ ii. at $v_2 = 1$, $k_e = k_2$ 	All definitions satisfy the following conditions: <ol style="list-style-type: none"> i. at $x = 0$, $\mu_m = \mu_l$ ii. at $x = 1$, $\mu_m = \mu_g$

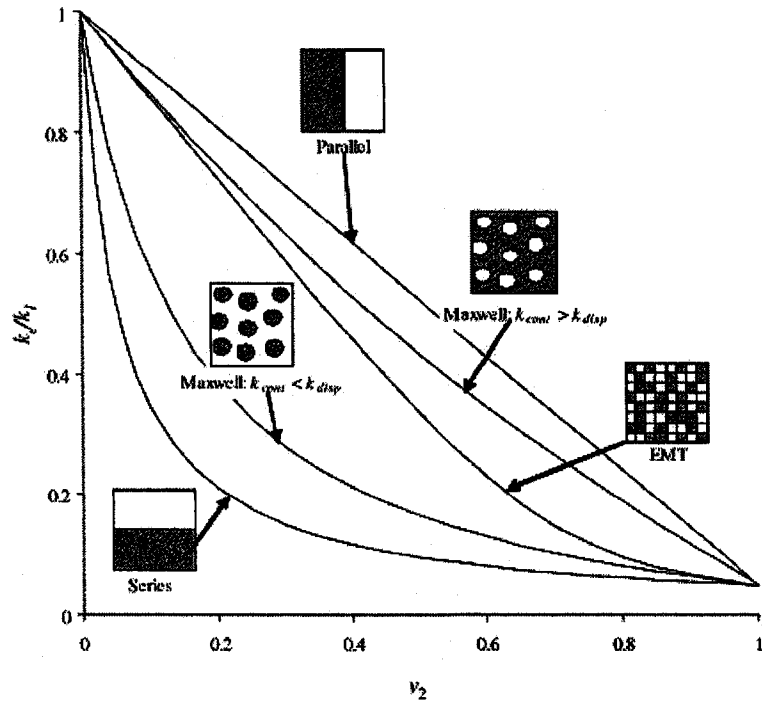


Figure 4.1 k_r/k_1 versus v_2 [176]

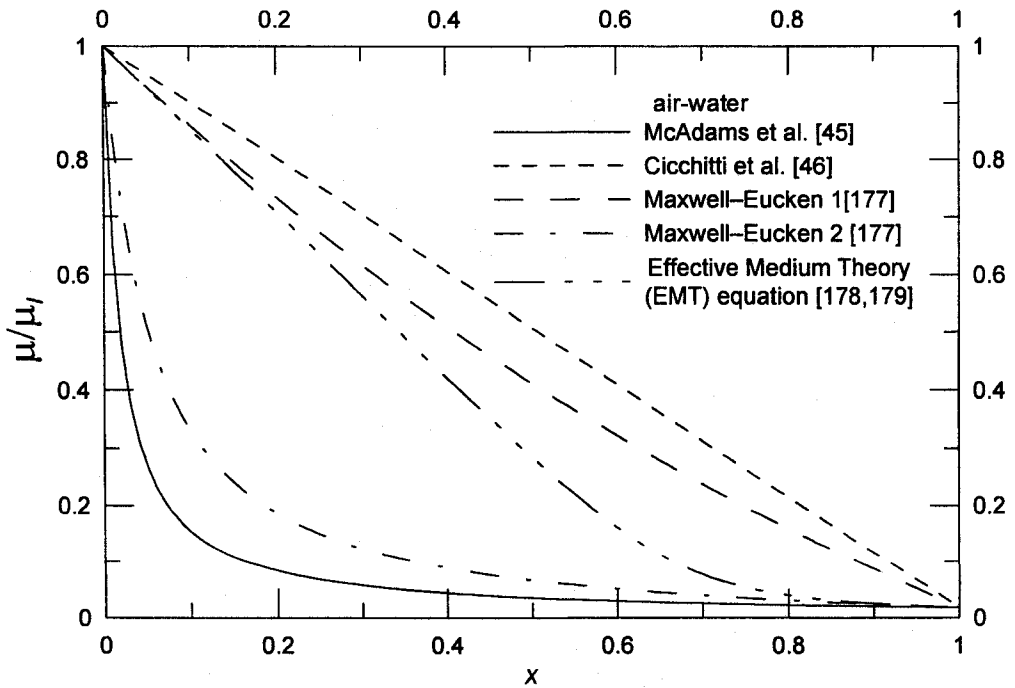


Figure 4.2 μ_r/μ_1 versus x

These new definitions overcome the disadvantages of some definitions of two-phase viscosity such as Davidson et al. definition [174], Owens definition [175] and García, et al. definition [114] that do not satisfy the condition at $x = 1$, $\mu_m = \mu_g$. These new definitions of two-phase viscosity can be used to compute the two-phase frictional pressure gradient in circular pipes using the homogeneous model. Often, it is desirable to express the two-phase frictional pressure gradient, $(dp/dz)_f$, versus the total mass flux (G) in a dimensionless form like the Fanning friction factor (f_m) versus the Reynolds number (Re_m) as follows:

$$f_m = \frac{d\rho_m (dp/dz)_f}{2G^2} \quad (4.20)$$

Equations (4.2) and (4.6) represent the two-phase density based on the homogeneous model (ρ_m) and Reynolds number based on the homogeneous model (Re_m).

To satisfy a good agreement between the experimental data and well-known friction factor models, selection of the best definition of two-phase viscosity among the different definitions (old and new) is based on the definition that corresponds to the minimum root mean square (RMS) error.

The fractional error (e) in applying the model to each available data point is defined as:

$$e = \left| \frac{Pr edicted - Available}{Available} \right| \quad (4.21)$$

For groups of data, the root mean square error, e_{RMS} , is defined as:

$$e_{RMS} = \left[\frac{1}{N} \sum_{K=1}^N e_K^2 \right]^{1/2} \quad (4.22)$$

For turbulent-turbulent flow, the Fanning friction factor (f_m) can be predicted using the Blasius equation [10] as follows:

$$f_m = \frac{0.079}{Re_m^{0.25}} \quad (4.23)$$

For the case of small diameter pipes, minichannels and microchannels, the friction factor is calculated using the Churchill model [104] that allows for prediction over the full range of laminar-transition-turbulent regions. The fanning friction factor (f_m) can be predicted using Churchill model [104] as follows:

$$f_m = 2 \left[\left(\frac{8}{Re_m} \right)^{12} + \frac{1}{(a_m + b_m)^{3/2}} \right]^{1/12} \quad (4.24)$$

$$a_m = \left[2.457 \ln \frac{1}{(7 / Re_m)^{0.9} + (0.27 \epsilon / d)} \right]^{16} \quad (4.25)$$

$$b_m = \left(\frac{37530}{Re_m} \right)^{16} \quad (4.26)$$

4.3 Results and Discussion

Examples of two-phase frictional pressure gradient versus mass flux from published experimental studies in circular pipes, minichannels and microchannels after expressing it in a dimensionless form as Fanning friction factor versus Reynolds number are presented. The published data include different working fluids such as R-12, R-22, Argon (R740), R717, R134a, R410A and Propane (R290) at different

diameters and different saturation temperatures.

4.3.1 Fanning friction factor (f_m) versus Reynolds number (Re_m) in Circular Pipes

Figures 4.3-4.7 show the Fanning friction factor (f_m) versus Reynolds number (Re_m) in circular pipes using the five different definitions of two-phase viscosity shown in Table 4.1. The sample of the published data includes Bandel's data [12] for R 12 flow at $x = 0.3$ and $T_s = 0^\circ\text{C}$ in a smooth horizontal pipe at $d = 14$ mm, Hashizume's data [79] in a smooth horizontal pipe at $d = 10$ mm for R 12 flow at $x = 0.5$ and $T_s = 39^\circ\text{C}$ and R 22 flow at $x = 0.5$ and $T_s = 20^\circ\text{C}$, and Müller-Steinhagen's data [180] for Argon (R740) flow at $x = 0.3$ and reduced pressure of 0.188 in a smooth horizontal pipe at $d = 14$ mm. Equation (4.18) represents the measured Fanning friction factor while Eq. (4.23) represents the predicted Fanning friction factor. From $e_{RMS}\%$ values based on measured Fanning friction factor and predicted Fanning friction factor using the five different definitions of two-phase viscosity for this sample of the published data, it can be seen that two-phase viscosity based on Maxwell-Eucken 2 [177] gives the best agreement between the published data and the Blasius equation [10] with the root mean square error (e_{RMS}) of 27.86%. If the lower point of Bandel's data [12] in Fig. 3.6 is excluded, the root mean square error (e_{RMS}) will be 18.36% instead 27.86%.

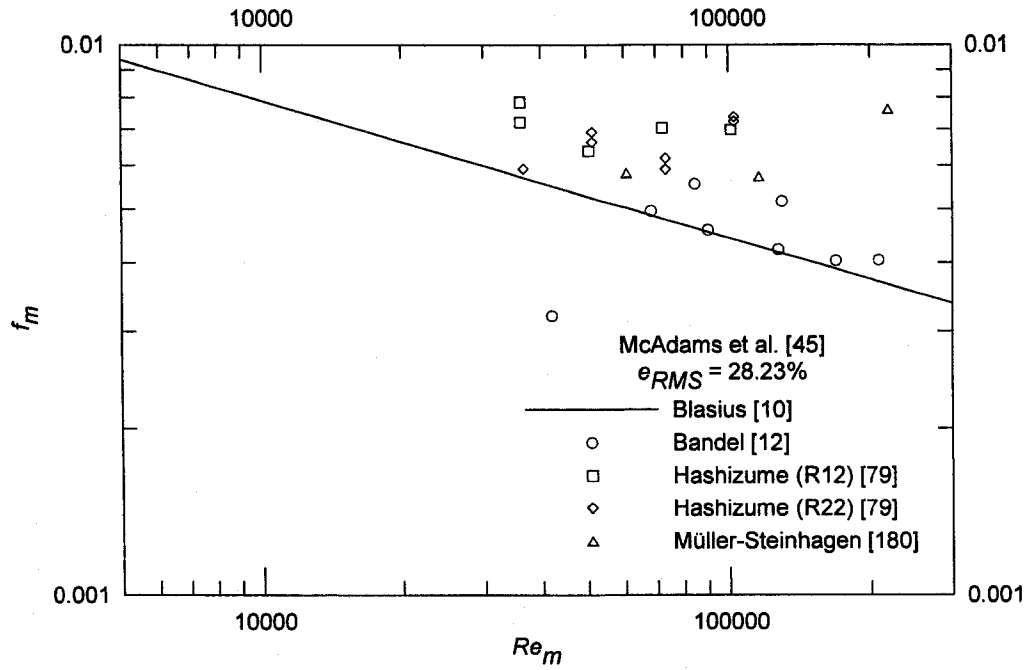


Figure 4.3 f_m versus Re_m in Circular Pipes Using Definition 1 of Two-Phase Viscosity

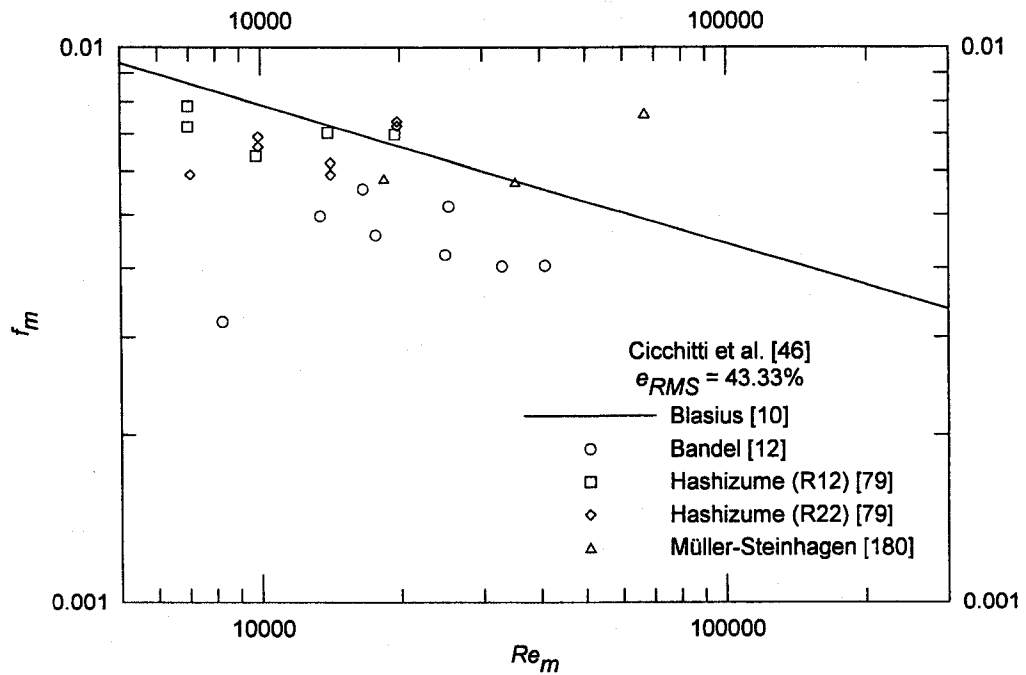


Figure 4.4 f_m versus Re_m in Circular Pipes Using Definition 2 of Two-Phase Viscosity

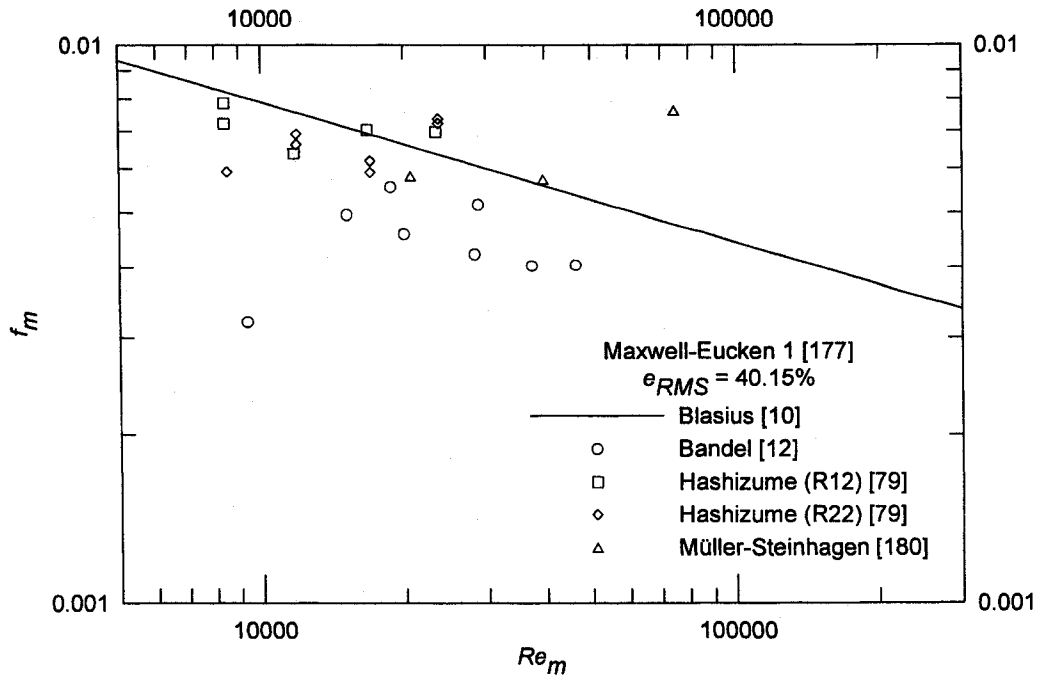


Figure 4.5 f_m versus Re_m in Circular Pipes Using Definition 3 of Two-Phase

Viscosity

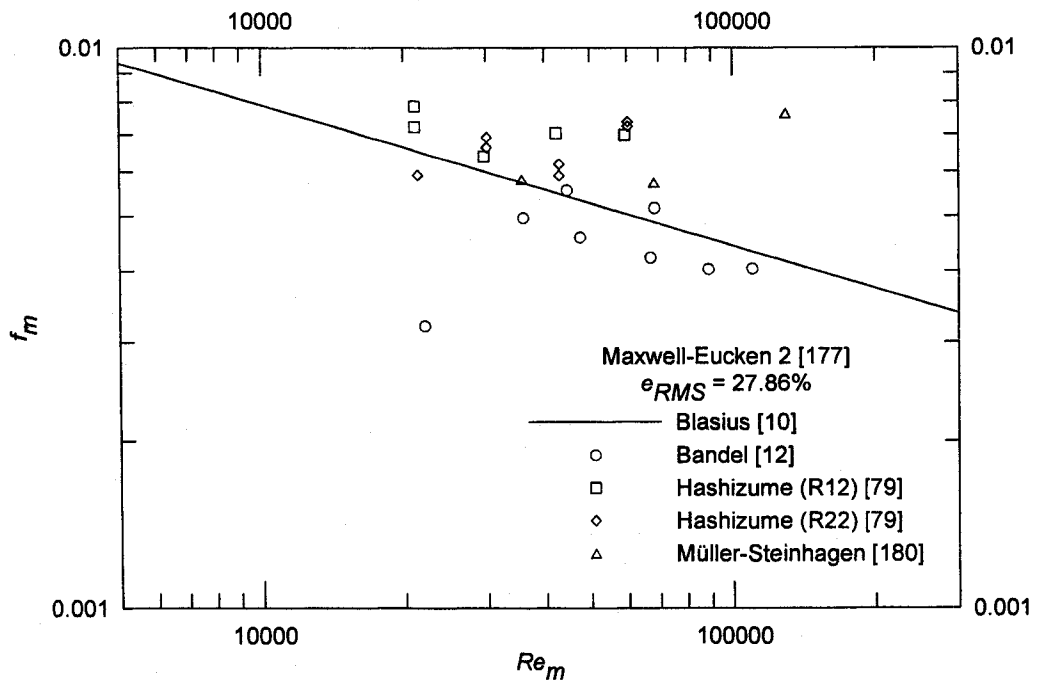


Figure 4.6 f_m versus Re_m in Circular Pipes Using Definition 4 of Two-Phase

Viscosity

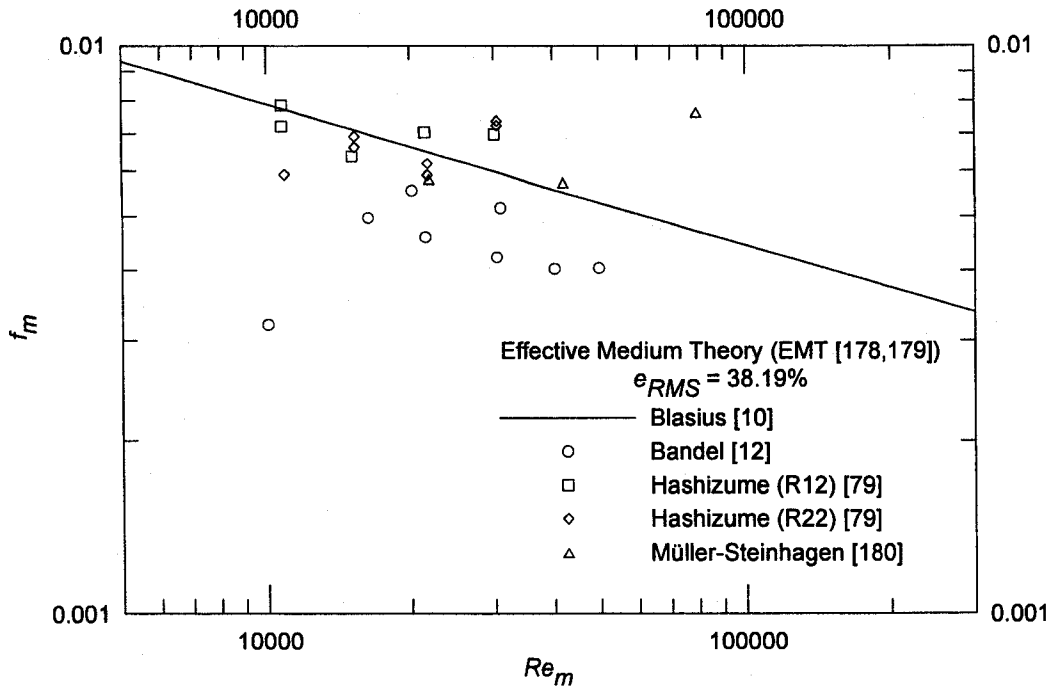


Figure 4.7 f_m versus Re_m in Circular Pipes Using Definition 5 of Two-Phase Viscosity

4.3.2 Fanning friction factor (f_m) versus Reynolds number (Re_m) in Minichannels and Microchannels

Figures 4.8-4.12 show the Fanning friction factor (f_m) versus Reynolds number (Re_m) in minichannels and microchannels using the five different definitions of two-phase viscosity shown in Table 4.1. The sample of the published data includes Ungar and Cornwell's data [89] for R 717 flow at $T_s \approx 74^\circ\text{F}$ (165.2°C) in a smooth horizontal tube at $d = 0.1017$ in. (2.583 mm), Tran et. al's data [181] for R 134a flow at $p_s = 365$ kPa and $x \approx 0.73$ in a smooth horizontal pipe at $d = 2.46$ mm, Cavallini et. al's data [182] for R 410A flow at $T_s = 40^\circ\text{C}$ and $x = 0.74$ in smooth multi-port minichannels at hydraulic diameter of 1.4 mm, and Field and Hrnjak data [183] for Propane (R 290)

flow at reduced pressure of 0.23 and $G \approx 330 \text{ kg/m}^2 \cdot \text{s}$ in a smooth horizontal pipe at hydraulic diameter of 0.148 mm. Equation (4.20) represents the measured Fanning friction factor while Eqs. (4.24)-(4.26) represent the predicted Fanning friction factor. From $e_{RMS}\%$ values based on measured Fanning friction factor and predicted Fanning friction factor using the five different definitions of two-phase viscosity for this sample of the published data, it can be seen that two-phase viscosity based on Maxwell-Eucken 2 [177] gives the best agreement between the published data and the Churchill model [104] with the root mean square error (e_{RMS}) of 16.47%.

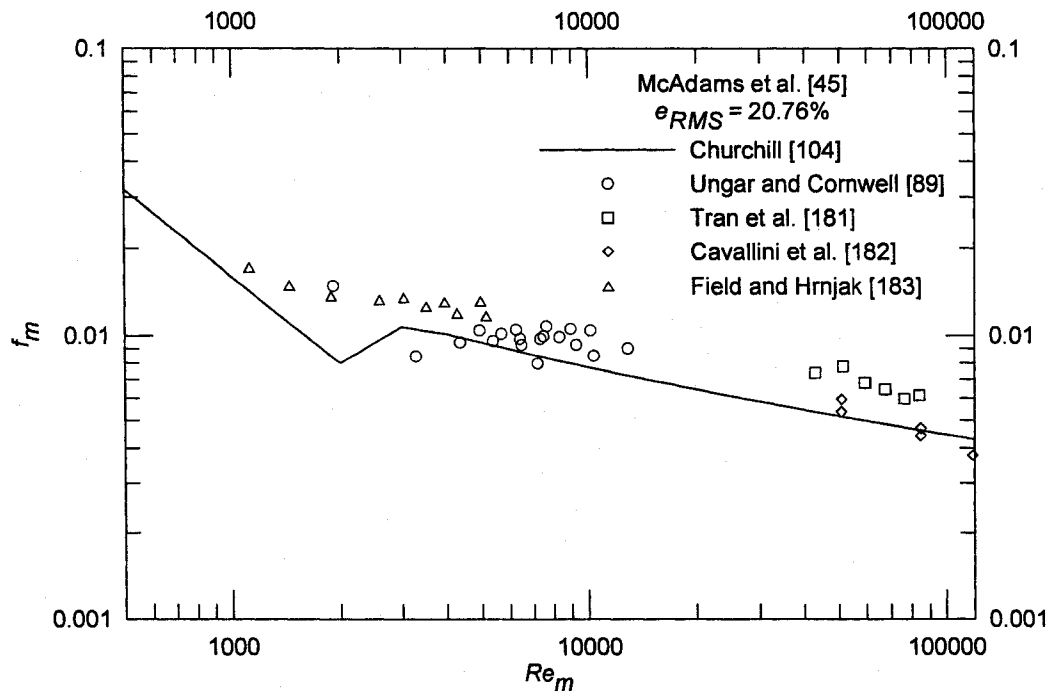


Figure 4.8 f_m versus Re_m in Minichannels and Microchannels Using Definition 1 of Two-Phase Viscosity

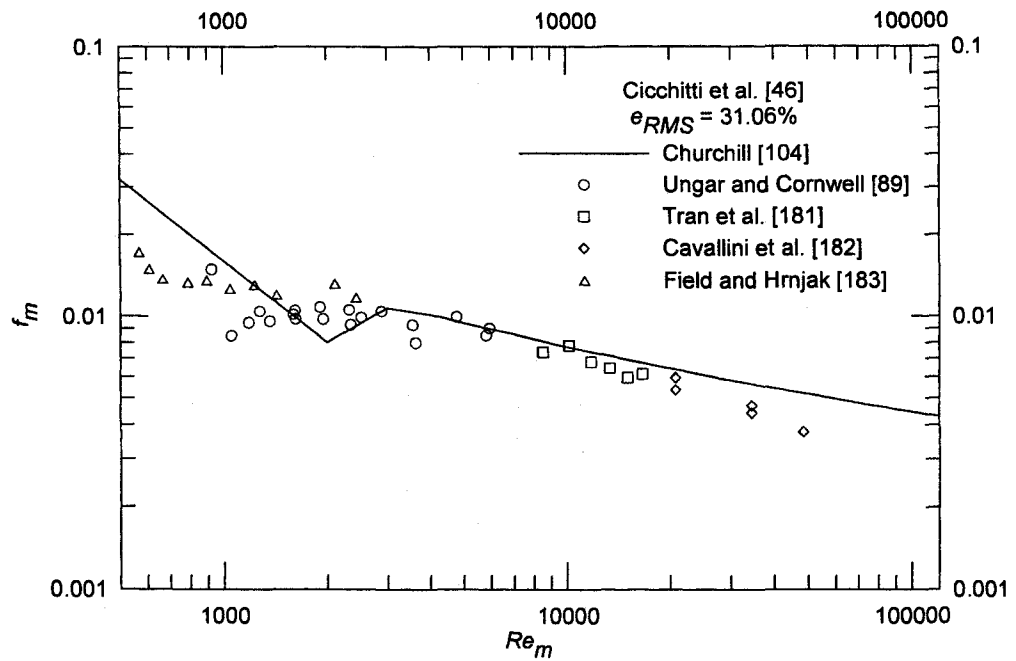


Figure 4.9 f_m versus Re_m in Minichannels and Microchannels Using Definition 2 of Two-Phase Viscosity

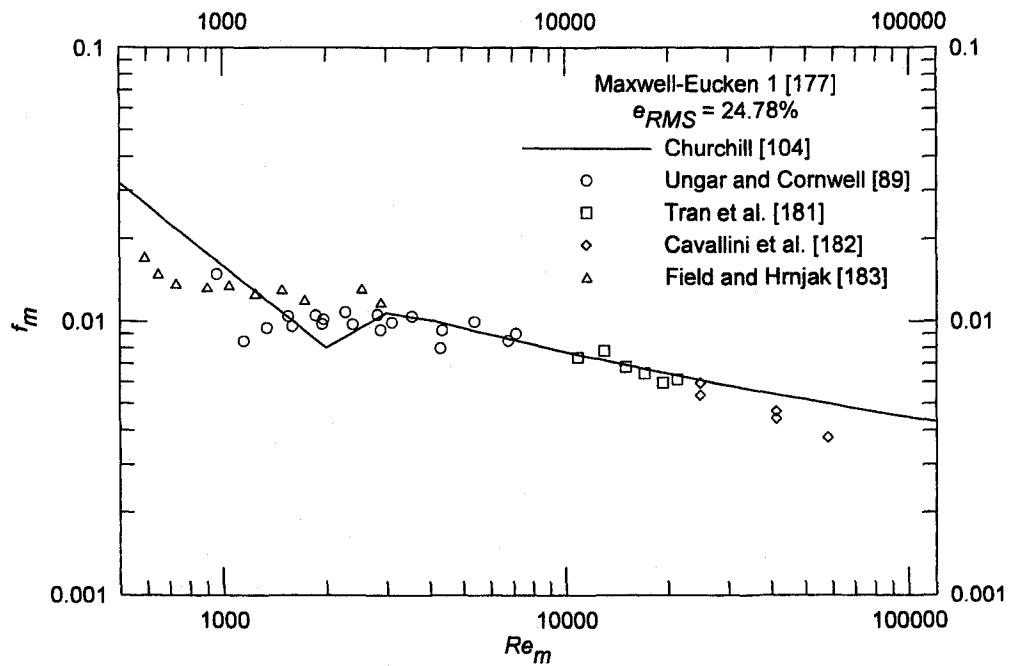


Figure 4.10 f_m versus Re_m in Minichannels and Microchannels Using Definition 3 of Two-Phase Viscosity

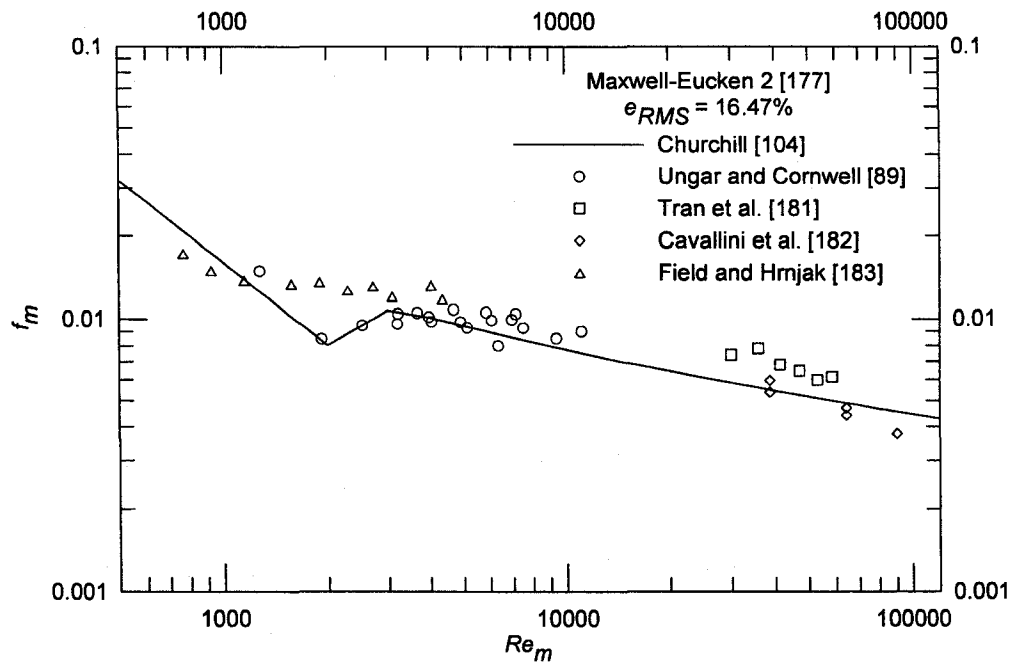


Figure 4.11 f_m versus Re_m in Minichannels and Microchannels Using Definition 4 of Two-Phase Viscosity

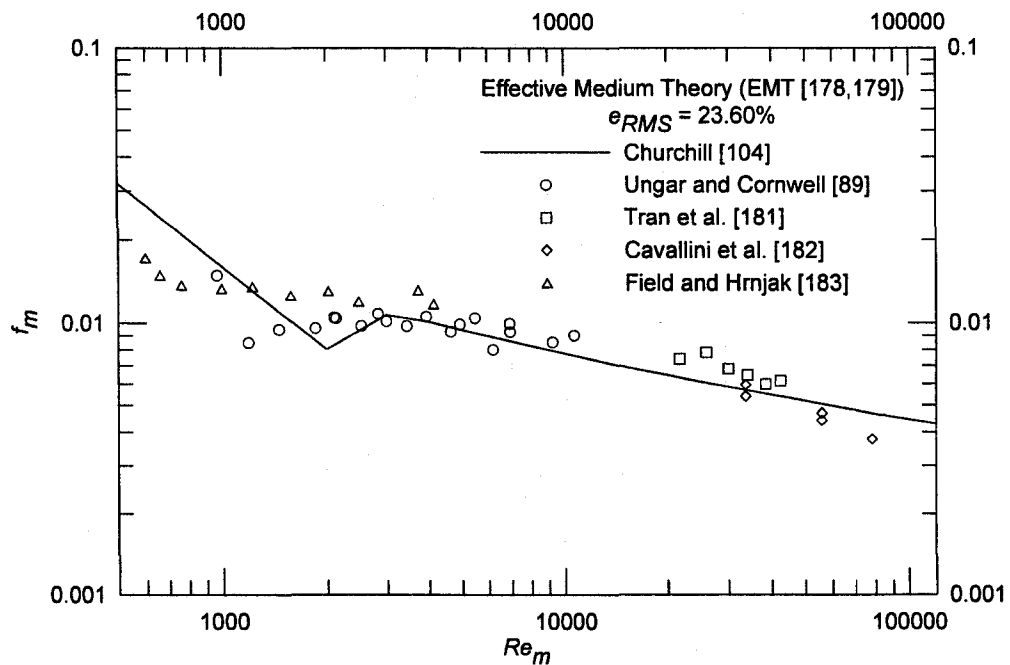


Figure 4.12 f_m versus Re_m in Minichannels and Microchannels Using Definition 5 of Two-Phase Viscosity

4.4 Summary

To compute the two-phase frictional pressure gradient using the homogeneous model, three new definitions for two-phase viscosity are introduced using the analogy between thermal conductivity in porous media and viscosity in two-phase flow. These new definitions for two-phase viscosity are

$$\mu_m = \mu_l \frac{2\mu_l + \mu_g - 2(\mu_l - \mu_g)x}{2\mu_l + \mu_g + (\mu_l - \mu_g)x} \quad (4.27)$$

$$\mu_m = \mu_g \frac{2\mu_g + \mu_l - 2(\mu_g - \mu_l)(1-x)}{2\mu_g + \mu_l + (\mu_g - \mu_l)(1-x)} \quad (4.28)$$

$$(1-x) \frac{\mu_l - \mu_m}{\mu_l + 2\mu_m} + x \frac{\mu_g - \mu_m}{\mu_g + 2\mu_m} = 0 \quad (4.29)$$

Equation (4.29) can be rewritten to be explicit for μ_m :

$$\mu_m = 1/4 \left((3x-1)\mu_g + [3(1-x)-1]\mu_l + \sqrt{[(3x-1)\mu_g + (3\{1-x\}-1)\mu_l]^2 + 8\mu_l\mu_g} \right) \quad (4.30)$$

It is obvious from the above equations that these new definitions for two-phase viscosity are satisfying the following two conditions: namely (i) $\mu_m = \mu_l$ at $x = 0$. and (ii) $\mu_m = \mu_g$ at $x = 1$. Expressing the published data of two-phase frictional pressure gradient in a dimensionless form as Fanning friction factor (f_m) versus Reynolds number (Re_m) can also be done as it is often desirable. Analysis of new properties of two-phase flow showed that the new definitions of two-phase viscosity could be used to analyze the experimental data of two-phase frictional pressure gradient in circular pipes.

CHAPTER 5

ASYMPTOTIC METHODS IN TWO-PHASE FLOW

5.1 Introduction

This chapter deals with the development of robust models for predicting two-phase frictional pressure gradient flow in horizontal pipes. A fresh view of two-phase flow modeling is proposed, based upon an asymptotic modeling method. Through consideration of liquid phase and gas phase limits, new models may be developed by combining the asymptotic behavior of the liquid phase and gas phase. This approach is direct, flexible and simple. This approach has led to great success in the modeling of complex heat transfer and fluid flow in single-phase flows.

5.2 The Separate Cylinders Model of Two-Phase Flow

We begin with a generalization of the separate cylinders model of two-phase flow. The separate cylinders model of two-phase flow was introduced first by Turner [29]. Then, it was appeared in other references such as [18] and [184]. In [29], [18] and [184], the separate cylinders model of two-phase flow was presented for the case of constant friction factor and when both liquid and gas were either turbulent or laminar. In the present study, a generalization of the separate cylinders model of two-phase flow will be presented to include laminar liquid-turbulent gas flow and turbulent liquid-laminar gas flow that were not presented in [29], [18] and [184]. In the separate cylinders model of two-phase flow, the liquid and gas phases are assumed

to flow independently of each other in two separate parallel circular cylinders of radii r_{le} and r_{ge} respectively. The radius of the actual pipe is r_o , and its area is the sum of the area of the separate cylinders.

The gas and liquid volumetric fractions are given as follows:

$$\alpha = \frac{A_{ge}}{A_o} = \frac{\pi r_{ge}^2}{\pi r_o^2} = \frac{r_{ge}^2}{r_o^2} \quad (5.1)$$

$$1 - \alpha = \frac{A_{le}}{A_o} = \frac{\pi r_{le}^2}{\pi r_o^2} = \frac{r_{le}^2}{r_o^2} \quad (5.2)$$

The pressure over any cross-section of the two-phase flow is assumed to be constant so that the two-phase pressure gradient is the same for each phase. Due to this assumption, the separate cylinders model of two-phase flow is not valid for gas-liquid slug flow that gives rise to large pressure fluctuations [29]. The pressure gradients in the imagined cylinders are therefore both equal to the two-phase frictional pressure gradient in the actual pipe.

The pressure gradient in the separate cylinder of radius r_{ge} carrying the gas phase is given by

$$\left(\frac{dp}{dz}\right) = \frac{2f_{ge}}{2r_{ge}} \left[\frac{(\pi r_o^2 G)^2 x^2 / (\pi r_{ge}^2)^2}{\rho_g} \right] = \frac{f_{ge} G^2 x^2}{\rho_g r_{ge} \alpha^2} \quad (5.3)$$

$$f_{ge} = c Re_{ge}^{-n} \quad (5.4)$$

$$Re_{ge} = \frac{(\pi r_o^2 G)x(2r_{ge}) / (\pi r_{ge}^2)}{\mu_g} = \frac{2r_{ge} Gx}{\mu_g \alpha} \quad (5.5)$$

For the gas flowing alone through the actual pipe of radius r_o , the frictional pressure gradient is given by

$$\left(\frac{dp}{dz}\right)_{f,g} = \frac{f_g G^2 x^2}{\rho_g r_o} \quad (5.6)$$

$$f_g = c Re_g^{-n} \quad (5.7)$$

$$Re_g = \frac{2r_o Gx}{\mu_g} \quad (5.8)$$

Using the assumption that the pressure gradient in the imagined cylinder of radius r_{ge} is equal to the two-phase frictional pressure gradient in the actual pipe of radius r_o and using the definition of ϕ_g^2 , we obtain

$$\phi_g^2 = \frac{(dp/dz)_f}{(dp/dz)_{f,g}} = \left(\frac{r_o}{r_{ge}}\right)^{5-n} = \frac{1}{\alpha^{(5-n)/2}} \quad (5.9)$$

The pressure gradient in the separate cylinder of radius r_{le} carrying the liquid phase is given by

$$\left(\frac{dp}{dz}\right) = \frac{2f_{le}}{2r_{le}} \left[\frac{(\pi r_o^2 G)^2 (1-x)^2 / (\pi r_{le}^2)^2}{\rho_l} \right] = \frac{f_{le} G^2 (1-x)^2}{\rho_l r_{le} (1-\alpha)^2} \quad (5.10)$$

$$f_{le} = b Re_{le}^{-m} \quad (5.11)$$

$$Re_{le} = \frac{(\pi r_o^2 G)(1-x)(2r_{le}) / (\pi r_{le}^2)}{\mu_l} = \frac{2r_{le} G(1-x)}{\mu_l (1-\alpha)} \quad (5.12)$$

For the liquid flowing alone through the actual pipe of radius r_o , the frictional pressure gradient is given by

$$\left(\frac{dp}{dz}\right)_{f,l} = \frac{f_l G^2 (1-x)^2}{\rho_l r_o} \quad (5.13)$$

$$f_l = b Re_l^{-m} \quad (5.14)$$

$$Re_l = \frac{2r_o G(1-x)}{\mu_l} \quad (5.15)$$

Using the assumption that the pressure gradient in the imagined cylinder of radius r_{le} is equal to the two-phase frictional pressure gradient in the actual pipe of radius r_o and using the definition of ϕ_l^2 , we obtain

$$\phi_l^2 = \frac{(dp/dz)_f}{(dp/dz)_{f,l}} = \left(\frac{r_o}{r_{le}}\right)^{5-m} = \frac{1}{(1-\alpha)^{(5-m)/2}} \quad (5.16)$$

Combining Eqs. (5.9) and (5.16) to eliminate α , we obtain

$$\frac{1}{\phi_l^{4/(5-m)}} + \frac{1}{\phi_g^{4/(5-n)}} = 1 \quad (5.17)$$

The definition of X^2 is given by

$$X^2 = \frac{(dp/dz)_{f,l}}{(dp/dz)_{f,g}} = \frac{\phi_g^2}{\phi_l^2} \quad (5.18)$$

Multiplying both sides of Eq. (5.17) by $\phi_l^{4/(5-m)}$ and using Eq. (5.18), we obtain

$$\phi_l^2 = \left[1 + (\phi_l^2)^{2(m-n)/((5-m)(5-n))} \left(\frac{1}{X^2} \right)^{2/(5-n)} \right]^{(5-m)/2} \quad (5.19)$$

Multiplying both sides of Eq. (5.17) by $\phi_g^{4/(5-n)}$ and using Eq. (5.18), we obtain

$$\phi_g^2 = \left[1 + (\phi_g^2)^{2(n-m)/((5-m)(5-n))} (X^2)^{2/(5-m)} \right]^{(5-n)/2} \quad (5.20)$$

Tables 5.1 and 5.2 show the expressions of ϕ_l^2 and ϕ_g^2 for different flow conditions respectively.

Table 5.1 Expressions of ϕ_l^2 for Different Flow Conditions

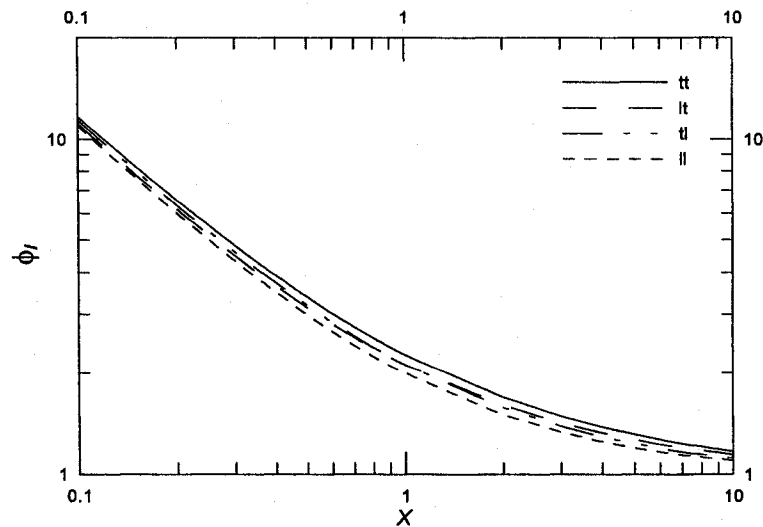
Liquid	Gas	ϕ_l^2
Turbulent $m = 0.25$	Turbulent $n = 0.25$	$\phi_l^2 = \left[1 + \left(\frac{1}{X^2} \right)^{1/2.375} \right]^{2.375}$
Laminar $m = 1$	Turbulent $n = 0.25$	$\phi_l^2 = \left[1 + (\phi_l^2)^{(3/38)} \left(\frac{1}{X^2} \right)^{1/2.375} \right]^2$
Turbulent $m = 0.25$	Laminar $n = 1$	$\phi_l^2 = \left[1 + (\phi_l^2)^{(-3/38)} \left(\frac{1}{X^2} \right)^{0.5} \right]^{2.375}$
Laminar $m = 1$	Laminar $n = 1$	$\phi_l^2 = \left[1 + \left(\frac{1}{X^2} \right)^{0.5} \right]^2$
$f = \text{constant}$ $m = n = 0$		$\phi_l^2 = \left[1 + \left(\frac{1}{X^2} \right)^{0.4} \right]^{2.5}$

Table 5.2 Expressions of ϕ_g^2 for Different Flow Conditions

Liquid	Gas	ϕ_g^2
Turbulent $m = 0.25$	Turbulent $n = 0.25$	$\phi_g^2 = \left[1 + (X^2)^{1/2.375} \right]^{2.375}$
Laminar $m = 1$	Turbulent $n = 0.25$	$\phi_g^2 = \left[1 + (\phi_g^2)^{(-3/38)} (X^2)^{0.5} \right]^{2.375}$
Turbulent $m = 0.25$	Laminar $n = 1$	$\phi_g^2 = \left[1 + (\phi_g^2)^{(3/38)} (X^2)^{(1/2.375)} \right]^2$
Laminar $m = 1$	Laminar $n = 1$	$\phi_g^2 = \left[1 + (X^2)^{0.5} \right]^2$
$f = \text{constant}$ $m = n = 0$		$\phi_g^2 = \left[1 + (X^2)^{0.4} \right]^{2.5}$

From Tables 5.1 and 5.2, it is clear that the expressions of ϕ_l^2 and ϕ_g^2 are implicit for liquid-gas laminar-turbulent flow and turbulent-laminar flow. These implicit expressions can be solved by means of computer algebra systems like Maple™ Release 9 software [185].

Figures 5.1 and 5.2 show ϕ_l and ϕ_g versus the Lockhart-Martinelli parameter (X) for different flow conditions.

**Figure 5.1 ϕ_l versus X for Different Flow Conditions**

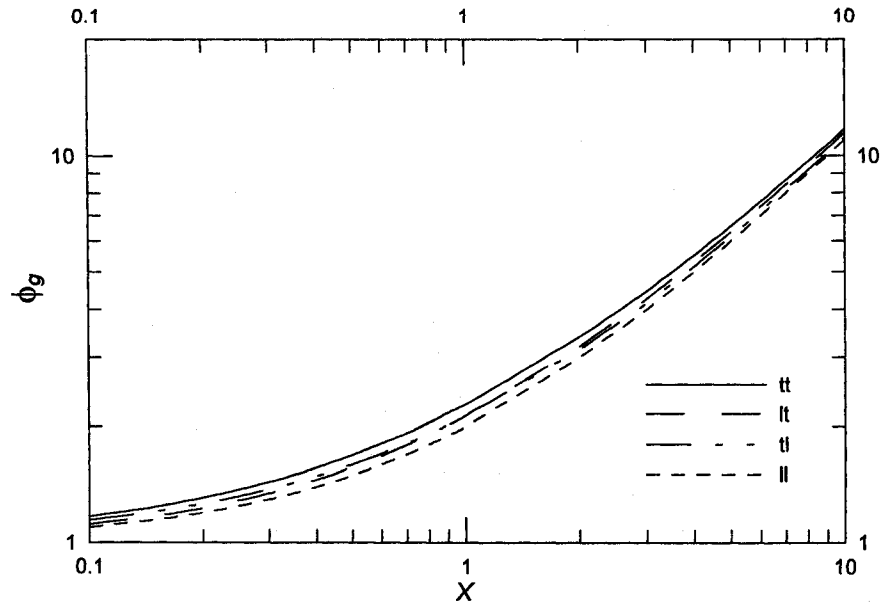


Figure 5.2 ϕ_g versus X for Different Flow Conditions

It is clear from Figs. 5.1 and 5.2 that $\phi_{l,lt} < \phi_{l,tl}$ for $X < 1$ and $\phi_{g,lt} < \phi_{g,tl}$ for $X < 1$, $\phi_{l,lt} = \phi_{l,tl}$ for $X = 1$ and $\phi_{g,lt} = \phi_{g,tl}$ for $X = 1$ while $\phi_{l,lt} > \phi_{l,tl}$ for $X > 1$ and $\phi_{g,lt} > \phi_{g,tl}$ for $X > 1$. On the other hand, when Chisholm [30] expressed the Lockhart-Martinelli correlation [16] in the mathematical form, he obtained that $\phi_{l,lt} > \phi_{l,tl}$ for all X and $\phi_{g,lt} > \phi_{g,tl}$ for all X because $C_{lt} = 12$ while $C_{tl} = 10$.

The separate cylinders model of two-phase flow can be also used to obtain the expressions of the void fraction (α) and the liquid holdup ($1-\alpha$) for different flow conditions.

Rearranging Eq. (5.9), we obtain

$$\alpha = \left(\frac{1}{\phi_g^2} \right)^{2/(5-n)} = (\phi_g^2)^{-2/(5-n)} \quad (5.21)$$

From Eqs. (5.20) and (5.21), we obtain the general form of the void fraction (α) in separate cylinders model of two-phase flow as

$$\alpha = \left[1 + \alpha^{(m-n)/(5-m)} X^{4/(5-m)} \right]^{-1} \quad (5.22)$$

The general form of the liquid holdup ($1-\alpha$) in separate cylinders model of two-phase flow can be obtained using two different methods. First, for any flow mechanism, sum of the void fraction and the liquid holdup is equal to 1 [16]. Thus, from Eq. (5.22), we obtain

$$1 - \alpha = 1 - \left[1 + \alpha^{(m-n)/(5-m)} X^{4/(5-m)} \right]^{-1} \quad (5.23)$$

Second, we can use the general form of the liquid holdup ($1-\alpha$) in separate cylinders model of two-phase flow by rearranging Eq. (5.16) as

$$1 - \alpha = \left(\frac{1}{\phi_1^2} \right)^{2/(5-m)} = (\phi_1^2)^{-2/(5-m)} \quad (5.24)$$

From Eqs. (5.19) and (5.24), we obtain the general form of ($1-\alpha$) in separate cylinders model of two-phase flow as

$$1 - \alpha = \left[1 + (1 - \alpha)^{(n-m)/(5-n)} X^{-4/(5-n)} \right]^{-1} \quad (5.25)$$

Tables 5.3 and 5.4 show the expressions of α and ($1-\alpha$) for different flow conditions.

Table 5.3 Expressions of α for Different Flow Conditions

Liquid	Gas	α
Turbulent $m = 0.25$	Turbulent $n = 0.25$	$\alpha = [1 + X^{1/1.1875}]^{-1}$
Laminar $m = 1$	Turbulent $n = 0.25$	$\alpha = [1 + \alpha^{0.1875} X]^{-1}$
Turbulent $m = 0.25$	Laminar $n = 1$	$\alpha = [1 + \alpha^{-3/19} X^{1/1.1875}]^{-1}$
Laminar $m = 1$	Laminar $n = 1$	$\alpha = [1 + X]^{-1}$
$f = \text{constant}$ $m = n = 0$		$\alpha = [1 + X^{0.8}]^{-1}$

Table 5.4 Expressions of $(1-\alpha)$ for Different Flow Conditions

Liquid	Gas	$(1-\alpha)$
Turbulent $m = 0.25$	Turbulent $n = 0.25$	$1-\alpha = [1 + X^{-1/1.1875}]^{-1}$
Laminar $m = 1$	Turbulent $n = 0.25$	$1-\alpha = [1 + (1-\alpha)^{-3/19} X^{-1/1.1875}]^{-1}$
Turbulent $m = 0.25$	Laminar $n = 1$	$1-\alpha = [1 + (1-\alpha)^{0.1875} X^{-1}]^{-1}$
Laminar $m = 1$	Laminar $n = 1$	$1-\alpha = [1 + X^{-1}]^{-1}$
$f = \text{constant}$ $m = n = 0$		$1-\alpha = [1 + X^{-0.8}]^{-1}$

From Tables 5.3 and 5.4, it is clear that the expressions of α and $(1-\alpha)$ are implicit for liquid-gas laminar-turbulent flow and turbulent-laminar flow. These implicit expressions can be solved by means of computer algebra systems like MapleTM Release 9 software [185].

Figures 5.3 and 5.4 show α and $(1-\alpha)$ versus the Lockhart-Martinelli parameter (X) for different flow conditions.

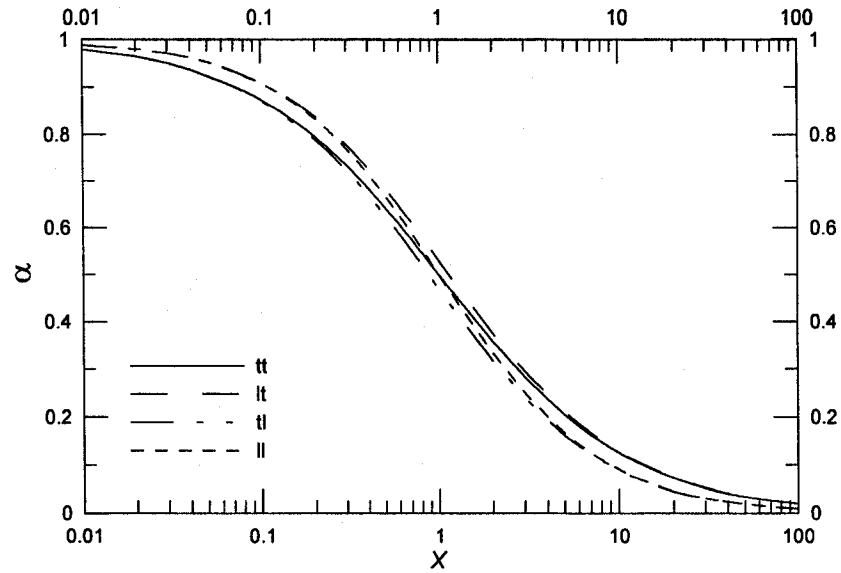


Figure 5.3 α versus X for Different Flow Conditions

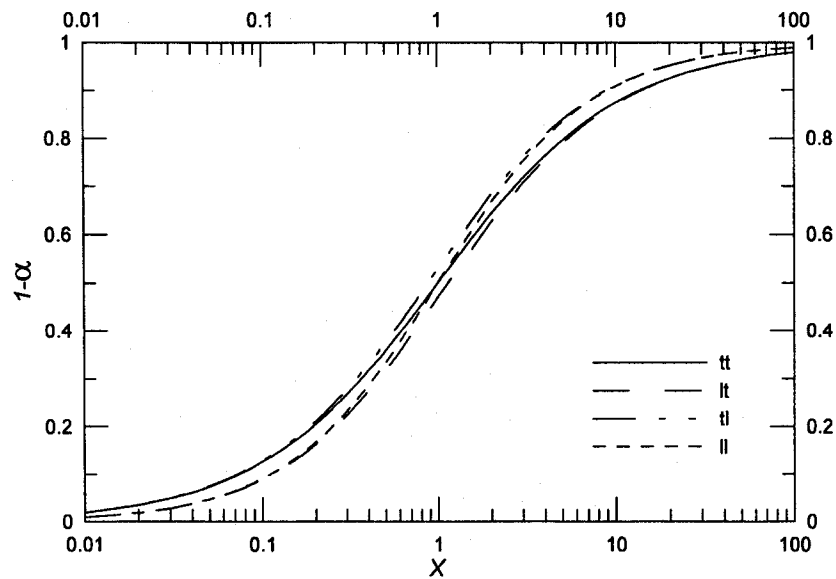


Figure 5.4 $(1-\alpha)$ versus X for Different Flow Conditions

It is clear from Figs. 5.3 and 5.4 that each flow condition (i.e. turbulent-turbulent, laminar-turbulent, turbulent-laminar, and laminar-laminar) has a different curve although there is not much difference in the values of α and $(1-\alpha)$ at the same value of the Lockhart-Martinelli parameter (X) for different flow conditions. On the

other hand, Lockhart and Martinelli [16] correlated the percent of pipe filled with liquid under any flow conditions for all four-flow types (turbulent-turbulent, laminar-turbulent, turbulent-laminar, and laminar-laminar) by means of the Lockhart-Martinelli parameter (X) with one curve instead of four curves.

The main disadvantage of the separate cylinders model for two-phase flow is not taking into account the important frictional interactions that occur at the interface between liquid and gas, and, needless to say, it would simply neglect the nature of two-phase flow because the liquid and gas phases are assumed to flow independently of each other in two separate parallel circular cylinders. Also, the values of the Reynolds number for the liquid and gas phases are important because these values determine the flow condition and hence the suitable expression for this flow condition. In addition, the obtained expressions are implicit for liquid-gas laminar-turbulent flow or turbulent-laminar flow. As a result, new two-phase flow modeling is proposed, based upon an asymptotic modeling method in the next section to overcome these disadvantages of the separate cylinders model of two-phase flow.

5.3 Asymptotic Analysis

5.3.1 Asymptotic Behavior

In the present study, asymptotes and simple compact model development for two-phase frictional pressure gradient in horizontal pipes are proposed. Two-phase frictional pressure gradient is expressed in terms of the asymptotic single-phase frictional pressure gradients for liquid and gas flowing alone. Asymptotes appear in many engineering problems such as steady and unsteady internal and external

conduction, free and forced internal and external convection, fluid flow, and mass transfer. Often, there exists a smooth transition between two asymptotic solutions [186-189]. This smooth transition indicates that there is no sudden change in slope and no discontinuity within the transition region.

The asymptotic analysis method was first introduced by Churchill and Usagi [186], in 1972. After this time, this method of combining asymptotic solutions proved quite successful in developing models in many applications like predicting forced convection from flat plates and in circular ducts for a wide range of Prandtl numbers [190,191], natural convection [192], transient conduction from isothermal convex bodies [193], pressure drop in channels containing periodic cuboid shaped obstructions [194], and fluid friction and heat transfer in low Reynolds number flow for singly and doubly connected cross section tubes, pipes and ducts [195-199].

In the asymptotic model, the dependent parameter y has two asymptotes. The first asymptote is y_0 , which corresponds to very small value of the independent parameter z . The second asymptote is y_∞ which corresponds to very large value of the independent parameter z . The two asymptotes y_0 and y_∞ can be expressed as follows [186-189]:

$$y_0 = c_0 z^i, z \rightarrow 0 \quad (5.26)$$

$$y_\infty = c_\infty z^j, z \rightarrow \infty \quad (5.27)$$

The two asymptotes y_0 and y_∞ are based on analytical solution. They consist of a constant, which has a positive real value. The two constants are called c_0 as $z \rightarrow 0$

and c_∞ as $z \rightarrow \infty$. The values of the two exponents i and j are often 0, 1, 1/2, 1/4, 1/3 [186-189].

From analytical, experimental, or numerical methods, it is known that y frequently transitions in a smooth manner between the two asymptotes y_0 and y_∞ .

For the case of two-phase frictional pressure gradient in horizontal pipes, the two asymptotes y_0 and y_∞ increase with increasing values of z , and the solution y is concave upwards. This trend is also found in the case of external free and forced convection from single isothermal convex bodies.

5.3.2 Superposition of Asymptotes

Since $y_0 > y_\infty$ as $z \rightarrow 0$, so the solution y is concave upwards, and the two asymptotes y_0 and y_∞ can be combined in the following method [186-189]:

$$y = [y_0^p + y_\infty^p]^{1/p} \quad (5.28)$$

The parameter p is a fitting or “blending” parameter whose value can be determined in a simple method. The effect of the parameter p in Eq. (5.28) is only important in the transition region. The results for small and large values of the independent parameter z , remain unchanged with changing the parameter p .

To determine a value of p , there are a number of methods as discussed by Churchill and Usagi [186]. For example, we can select an intermediate value of $z = z_{int}$ corresponding or near to the intersection of the two asymptotes for which $y(z_{int})$ is known from analytical, experimental, or numerical methods. Using Eqs. (5.26), (5.27), and (5.28), we can write for the intermediate value of $z = z_{int}$,

$$y(z_{int}) = \left[(c_0 z_{int}^i)^p + (c_\infty z_{int}^j)^p \right]^{1/p} \quad (5.29)$$

Although the fitting or “blending” parameter p is unknown, it can be calculated by numerical methods for solving a non-linear equation or by means of computer algebra systems like Maple™ Release 9 software [185].

In another method, p is chosen as the value, which minimizes the root mean square (RMS) error, e_{RMS} , between the model predictions and the available data. The fractional error (e) in applying the model to each available data point is defined as:

$$e = \left| \frac{\text{Predicted} - \text{Available}}{\text{Available}} \right| \quad (5.30)$$

For groups of data, the root mean square (RMS) error, e_{RMS} , is defined as:

$$e_{RMS} = \left[\frac{1}{N} \sum_{k=1}^N e_k^2 \right]^{1/2} \quad (5.31)$$

If p is a weak function of the mass flow rate, or mass flux of either the liquid phase or the gas phase, a single value may be chosen which best represents all of the available data for two-phase frictional pressure gradient.

The approximate solution y is often presented in a form, which is based on one of the two asymptotes y_0 and y_∞ . For example, if the approximate solution y is presented in terms of the asymptote y_0 , then the model can be expressed as follows [186-189]:

$$\frac{y}{y_0} = \left[1 + \left(\frac{y_\infty}{y_0} \right)^p \right]^{1/p} \quad (5.32)$$

On the other hand, if the approximate solution y is presented in terms of the asymptote y_∞ , then the model can be expressed as follows [186-189]:

$$\frac{y}{y_\infty} = \left[1 + \left(\frac{y_0}{y_\infty} \right)^p \right]^{1/p} \quad (5.33)$$

5.4 Asymptotic Methods in Two-Phase Flow

Using the asymptotic analysis method, two-phase frictional pressure gradient $(dp/dz)_f$ can be expressed in terms of single-phase frictional pressure gradient for liquid flowing alone $(dp/dz)_{f,l}$ and single-phase frictional pressure gradient for gas flowing alone $(dp/dz)_{f,g}$ as follows:

$$\left(\frac{dp}{dz} \right)_f = \left[\left(\frac{dp}{dz} \right)_{f,l}^p + \left(\frac{dp}{dz} \right)_{f,g}^p \right]^{1/p} \quad (5.34)$$

Equation (5.34) reduces to $(dp/dz)_{f,l}$ and $(dp/dz)_{f,g}$ as $x = 0$ and 1 respectively.

If the two-phase frictional pressure gradient $(dp/dz)_f$ is presented in terms of the single-phase frictional pressure gradient for liquid flowing alone $(dp/dz)_{f,l}$, then the model can be expressed using the Lockhart-Martinelli parameter (X) as follows:

$$\left(\frac{dp}{dz}\right)_f = \left(\frac{dp}{dz}\right)_{f,l} \left[1 + \left(\frac{l}{X^2}\right)^p\right]^{1/p} \quad (5.35)$$

Equation (5.35) can be expressed in terms of a two-phase frictional multiplier liquid flowing alone in the pipe (ϕ_l^2) as follows:

$$\phi_l^2 = \left[1 + \left(\frac{l}{X^2}\right)^p\right]^{1/p} \quad (5.36)$$

Equation (5.36) is similar to the separate cylinders model formulation [29] for constant friction factor ($1/p = 2.5$) or when both liquid and gas are either turbulent ($1/p = 2.375$) or laminar ($1/p = 2$) although the physical concept is different. Also, Eq. (5.36) is still explicit for liquid-gas laminar-turbulent flow and turbulent-laminar flow.

On the other hand, if the two-phase frictional pressure gradient $(dp/dz)_f$ is presented in terms of the single-phase frictional pressure gradient for gas flowing alone $(dp/dz)_{f,g}$, then the model can be expressed using the Lockhart-Martinelli parameter (X) as follows:

$$\left(\frac{dp}{dz}\right)_f = \left(\frac{dp}{dz}\right)_{f,g} \left[1 + (X^2)^p\right]^{1/p} \quad (5.37)$$

Equation (5.37) can be expressed in terms of a two-phase frictional multiplier for gas flowing alone in the pipe (ϕ_g^2) as follows:

$$\phi_g^2 = [1 + (X^2)^p]^{1/p} \quad (5.38)$$

Once again, Eq. (5.38) is similar to the separate cylinders model formulation [29] for constant friction factor ($1/p = 2.5$) or when both liquid and gas are either turbulent ($1/p = 2.375$) or laminar ($1/p = 2$). Also, Eq. (5.38) is still explicit for liquid-gas laminar-turbulent flow and turbulent-laminar flow.

5.4.1 Single-Phase Frictional Pressure Gradient Equations

The single-phase frictional pressure gradient can be related to the Fanning friction factor in terms of mass flow rate of both the liquid phase and the gas phase as follows:

$$\left(\frac{dp}{dz}\right)_{f,l} = \frac{32 f_l m_l^2}{\pi^2 d^5 \rho_l} \quad (5.39)$$

$$\left(\frac{dp}{dz}\right)_{f,g} = \frac{32 f_g m_g^2}{\pi^2 d^5 \rho_g} \quad (5.40)$$

Equations (5.39) and (5.40) can be written in terms of mass flux and mass quality as follows:

$$\left(\frac{dp}{dz}\right)_{f,l} = \frac{2 f_l G^2 (1-x)^2}{d \rho_l} \quad (5.41)$$

$$\left(\frac{dp}{dz}\right)_{f,g} = \frac{2 f_g G^2 x^2}{d \rho_g} \quad (5.42)$$

The model that was developed by Churchill [104] is introduced to define the Fanning friction factor. When a computer is used, the Churchill model equations [104] are more recommended than the Blasius equations [10] to define the Fanning friction factor [200]. The Churchill model was a correlation of the Moody chart [51]. Churchill's correlation spanned the entire range of laminar, transition, and turbulent flow in pipes. The Churchill model equations that define the Fanning friction factor are

$$f = 2 \left[\left(\frac{8}{Re} \right)^{12} + \frac{1}{(a+b)^{3/2}} \right]^{1/12} \quad (5.43)$$

$$a = \left[2.457 \ln \frac{1}{(7/Re)^{0.9} + (0.27\epsilon/d)} \right]^{16} \quad (5.44)$$

$$b = \left(\frac{37530}{Re} \right)^{16} \quad (5.45)$$

The Reynolds number equations can be expressed in terms of mass flow rate of both the liquid phase and the gas phase or mass flux and mass quality as follows:

$$Re_l = \frac{4m_l}{\pi d \mu_l} = \frac{G(1-x)d}{\mu_l} \quad (5.46)$$

$$Re_g = \frac{4m_g}{\pi d \mu_g} = \frac{Gxd}{\mu_g} \quad (5.47)$$

5.5 Results and Discussion

Examples of two-phase frictional pressure gradient in horizontal pipes for published data of different pipe diameters are presented to show features of the asymptotes, asymptotic analysis and the development of simple compact models. At the end of the chapter, the present asymptotic model is also extended to minichannels and microchannels.

5.5.1 Comparison of the Present Asymptotic Model with Data

Figure 5.5 shows comparison of the present asymptotic model [201] with Dukler's data [202] for air-water flow in a smooth horizontal pipe at $d = 2$ in. (50.8 mm). The frictional pressure gradient is represented as a function of the liquid mass flow rate on log-log scale for the gas mass flow rate values of 7.8, 23.3, 81.8, 381, and 1 103 lb_m/hr (3.54, 10.57, 37.1, 172.82, and 500.32 kg/s) respectively. For the same value of the gas mass flow rate, the frictional pressure gradient increases with increasing with the liquid mass flow rate. Also, the frictional pressure gradient increases with increasing with the gas mass flow rate at the same value of the liquid mass flow rate. Equation (5.34) represents the present asymptotic model [201]. It can be seen that the present model with fitting parameter, $p = 1/3.9$ represents Dukler's data in a successful manner. The root mean square (RMS) error, e_{RMS} , is equal to 12.11%. The worst agreement is obtained for data points with an absolute error (e) of 23.34%.

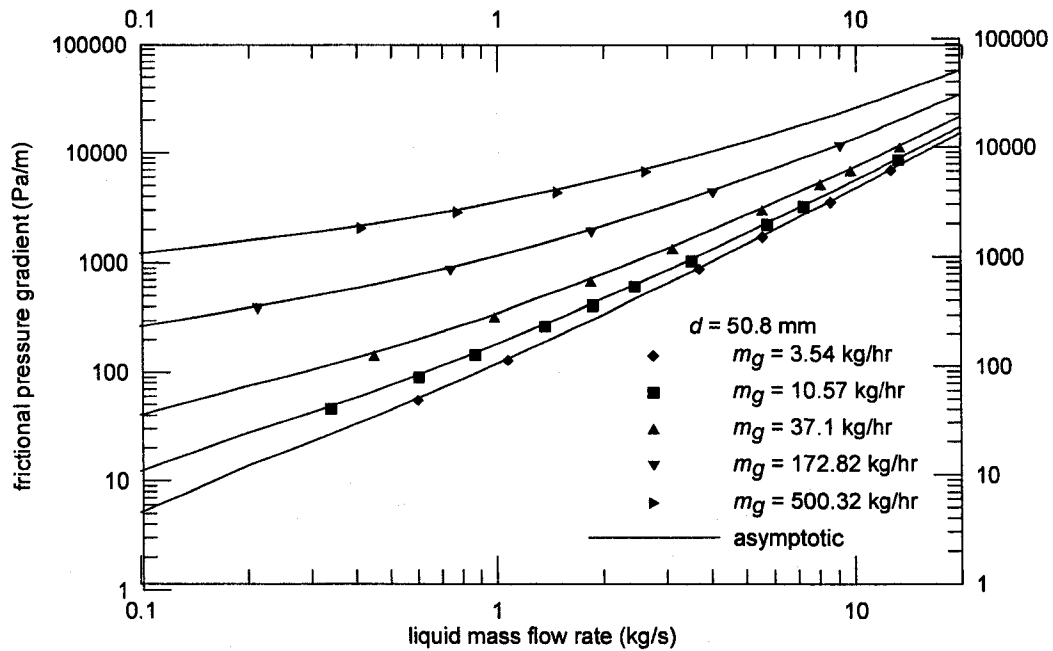


Figure 5.5 Comparison of the Asymptotic Model with Dukler's Data [202]

Comparison of different models such as Chisholm [30], Chisholm [33], Friedel [63], Müller-Steinhagen and Heck [68] as well as the present asymptotic model [201] with $p = 1/3.9$ with Dukler's data [202] is shown in Table 5.5.

Table 5.5 Comparison of Different Models with Dukler's Data [202]

Model	RMS (%)
Chisholm [30]	23.08
Chisholm [33]	63.13
Friedel [63]	83.32
Müller-Steinhagen and Heck [68]	36.20
Asymptotic [201]	12.11

Figure 5.6 shows comparison of the present asymptotic model [201] with Chisholm's data [200] for air-water flow in a smooth horizontal pipe at $d = 27$ mm

and mixture pressure ~ 1.3 bar. The frictional pressure gradient is represented as a function of the gas mass flux on log-log scale for the liquid mass flux values of 190, 581, 1 269, and 2 786 $\text{kg/m}^2\cdot\text{s}$ respectively. For the same value of the liquid mass flux, the frictional pressure gradient increases with increasing with the gas mass flux. Also, the frictional pressure gradient increases with increasing with the liquid mass flux at the same value of the gas mass flux. Equation (5.34) represents the present asymptotic model [201]. It can be seen that the present asymptotic model [201] with fitting parameter, $p = 1/4$ represents Chisholm's data in a successful manner. The root mean square (RMS) error, e_{RMS} , is equal to 16.73%. The worst two data points have an absolute error (e) of 49.48% and 39.2%, respectively (lie at the left hand side for $G_l = 190 \text{ kg/m}^2\cdot\text{s}$).

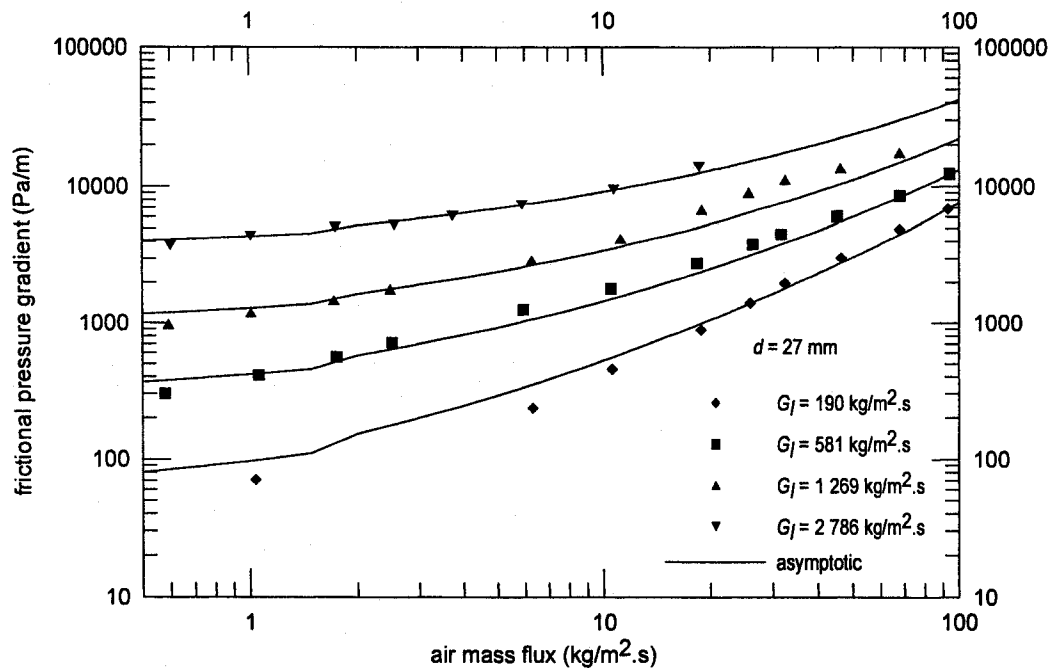


Figure 5.6 Comparison of the Asymptotic Model with Chisholm's Data [200]

Comparison of different models such as Chisholm [30], Chisholm [33], Friedel [63], Müller-Steinhagen and Heck [68] as well as the present asymptotic model [201] with fitting parameter, $p = 1/4$ with Chisholm's data [200] is shown in Table 5.6.

Table 5.6 Comparison of Different Models with Chisholm's Data [200]

Model	RMS (%)
Chisholm [30]	21.98
Chisholm [33]	70.29
Friedel [63]	79.88
Müller-Steinhagen and Heck [68]	38.83
Asymptotic [201]	16.73

5.5.2 Effect of Mass Flux on the Frictional Pressure Gradient

Figure 5.7 shows effect of mass flux on the frictional pressure gradient with air-water flow in a smooth horizontal pipe at $d = 2$ in. (50.8 mm) for the mass flux values of 500, 1 000 and 2 000 $\text{kg/m}^2 \cdot \text{s}$ respectively. It can be seen that the frictional pressure gradient increases with increasing mass flux at a given mass quality. For example, at a mass quality of 80%, increasing the mass flux from 500 to 1 000 $\text{kg/m}^2 \cdot \text{s}$ increases the frictional pressure gradient from 23 947.07 to 84 783.42 Pa/m. It is observed that the two-phase frictional pressure gradient for $x \cong 0$ is nearly identical to single-phase liquid frictional pressure gradient. Also, the two-phase frictional pressure gradient for $x \cong 1$ is nearly identical to single-phase gas frictional pressure gradient.

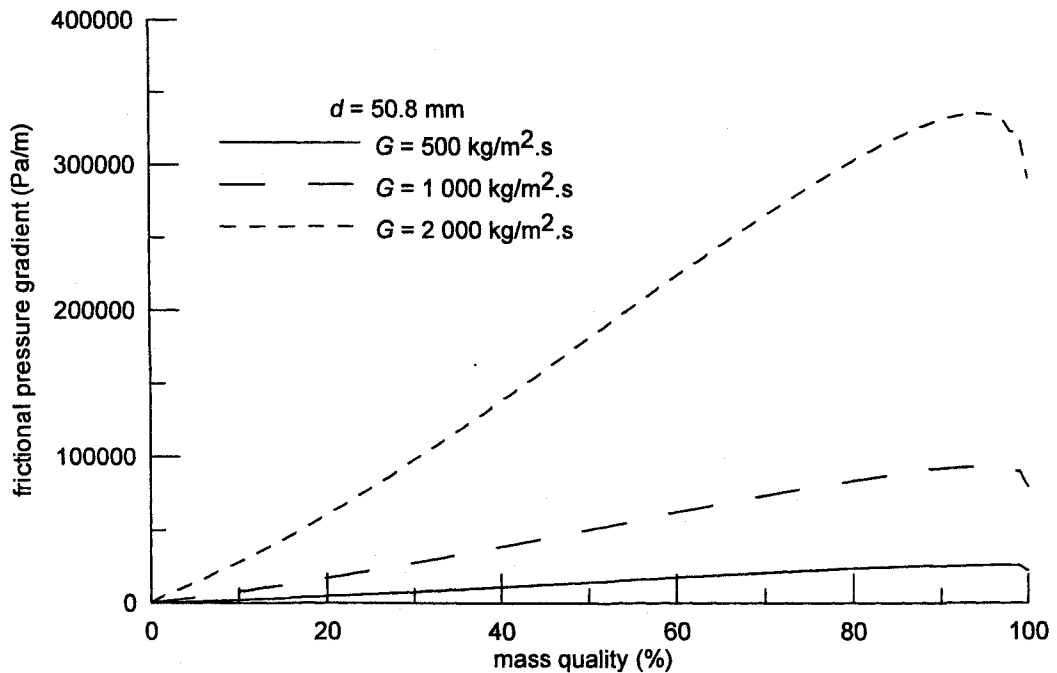


Figure 5.7 Effect of Mass Flux on the Frictional Pressure Gradient

5.5.3 Comparison of the Present Asymptotic Model with Other Correlations

Figure 5.8 shows comparison of the present asymptotic model [201] with other correlations such as the Wallis correlation, the Chisholm correlation, the Friedel correlation, and the Müller-Steinhagen and Heck correlation with air-water flow in a smooth horizontal pipe at $d = 2 \text{ in. (50.8 mm)}$ and $G = 2\,000 \text{ kg/m}^2\cdot\text{s}$. The Fanning friction factor is represented by the Blasius equation with $n = 0.25$ in the other correlations. The frictional pressure gradient is calculated in the other correlations using their definition of ϕ_o^2 and Eq. (2.1) if it is not given directly such as the Müller-Steinhagen and Heck correlation. The Müller-Steinhagen and Heck correlation shows better agreement with the present asymptotic model than the other correlations. Also,

all other correlations give the same values for single-phase liquid frictional pressure gradient and single-phase gas frictional pressure gradient.

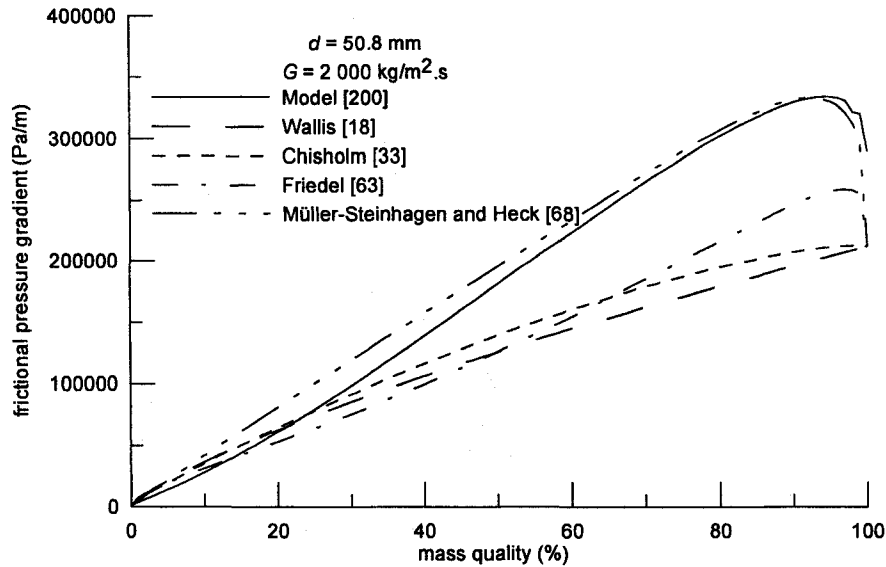


Figure 5.8 Comparison of the Present Asymptotic Model with Other Correlations at $d = 50.8$ mm

Figure 5.9 shows comparison of the present asymptotic model [201] with other correlations such as the Wallis correlation, the Chisholm correlation, the Friedel correlation, and the Müller-Steinhagen and Heck correlation with air-water flow in a smooth horizontal pipe at $d = 27$ mm and $G = 500$ kg/m².s for and mixture pressure ~ 1.3 bar. The Fanning friction factor is represented by the Blasius equation with $n = 0.25$ in the other correlations. The frictional pressure gradient is calculated in the other correlations using their definition of ϕ_o^2 and Eq. (2.1) if it is not given directly such as the Müller-Steinhagen and Heck correlation. The Friedel correlation shows better agreement with the present asymptotic model than the other correlations. Also, all other correlations give the same values for single-phase liquid frictional pressure gradient and single-phase gas frictional pressure gradient.

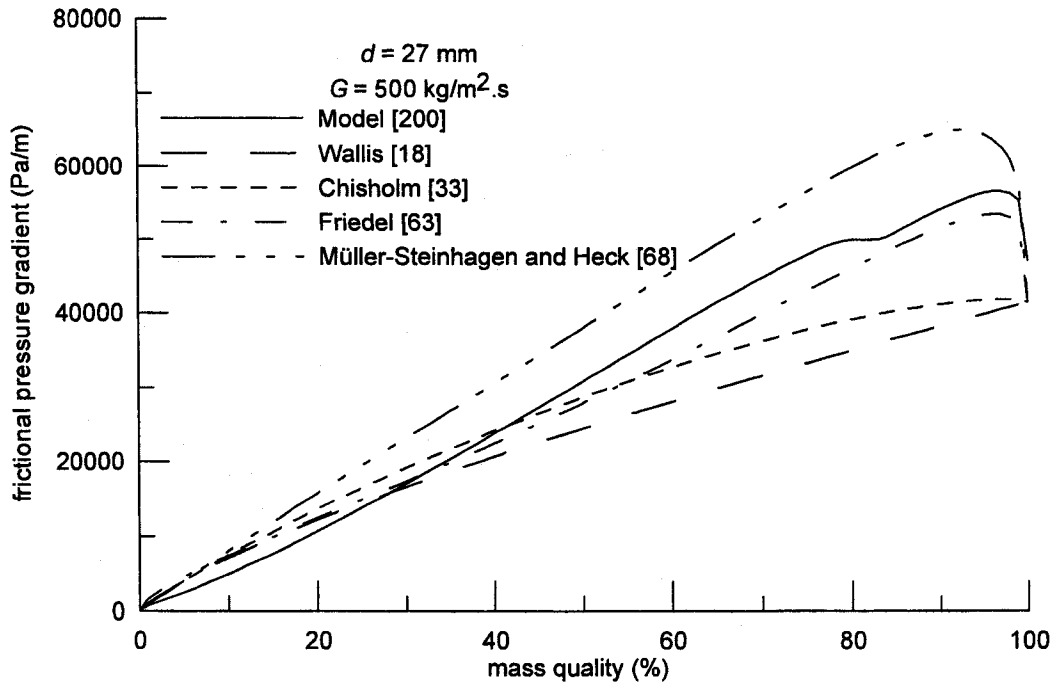


Figure 5.9 Comparison of the Present Asymptotic Model with Other Correlations at $d = 27$ mm

From Figs. 5.8 and 5.9, it is obvious that Müller-Steinhagen and Heck correlation has the maximum value of frictional pressure gradient among other correlations. Since the Fanning friction factor is represented by the Churchill model [104] in the present model while the Fanning friction factor is represented by the Blasius equation [10] with $n = 0.25$ in the other correlations. So, the Fanning friction factor in the present asymptotic model for a smooth pipe is greater than the Fanning friction factor in the other correlations at high Reynolds number. Since the frictional pressure gradient is a function of G^2 . So, with increasing the mass flux (i.e. at high mass flux), the Müller-Steinhagen and Heck correlation shows better agreement with the present asymptotic model than the other correlations.

5.5.4. ϕ_l and ϕ_g versus Lockhart-Martinelli Parameter (X) in Circular Pipes

Figures 5.10-5.15 show ϕ_l versus Lockhart-Martinelli parameter (X) for turbulent-turbulent flow for different working fluids in a smooth horizontal pipe of different diameters at different conditions using the present asymptotic model and the different data sets. Equation (5.36) represents the present model with different values of p as shown in Table 5.7.

Figures 5.16 and 5.17 show ϕ_g versus Lockhart-Martinelli parameter (X) for turbulent-turbulent flow for different working fluids in a smooth horizontal pipe of different diameters at different conditions using the present asymptotic model and the different data sets. Equation (5.38) represents the present model with different values of p as shown in Table 5.7.

It can be seen that there is a good agreement between the present asymptotic model and the different data sets in Figs. 5.10-5.17.

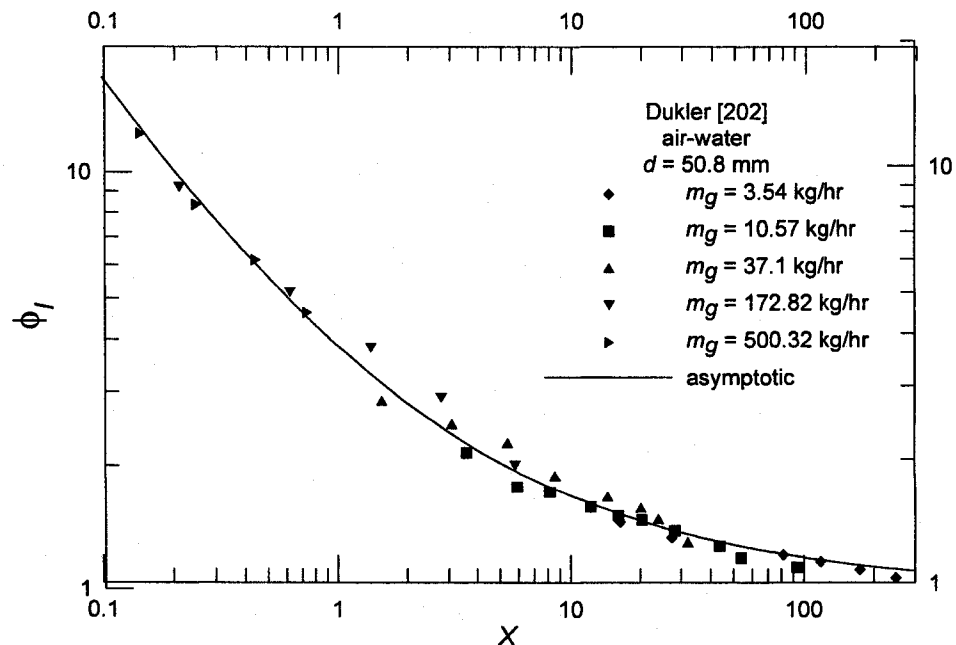


Figure 5.10 Comparison of the Asymptotic Model with Dukler's Data [202]

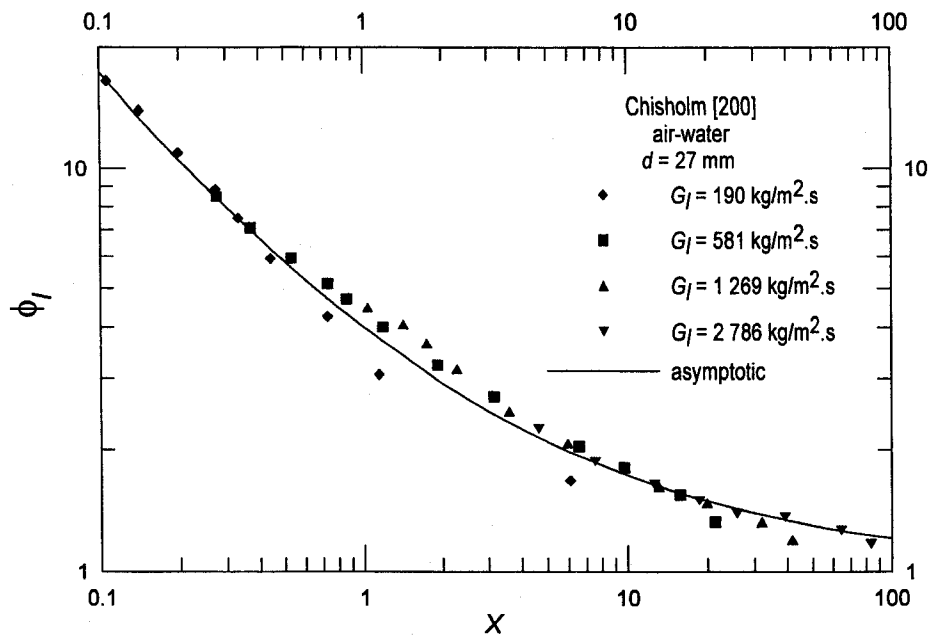


Figure 5.11 Comparison of the Asymptotic Model with Chisholm's Data [200]

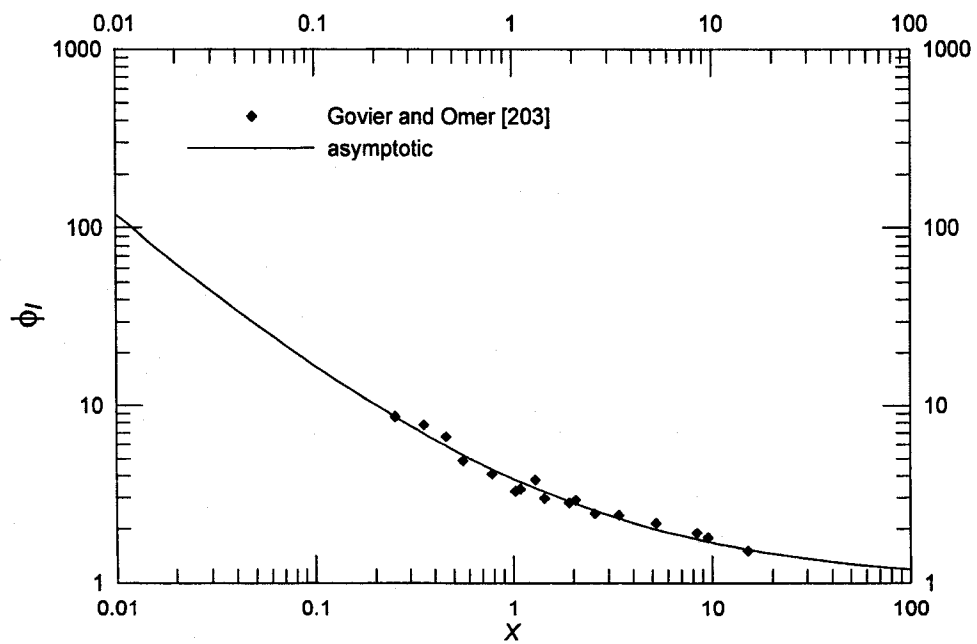


Figure 5.12 Comparison of the Present Asymptotic Model with Govier and Omer's Data [203]

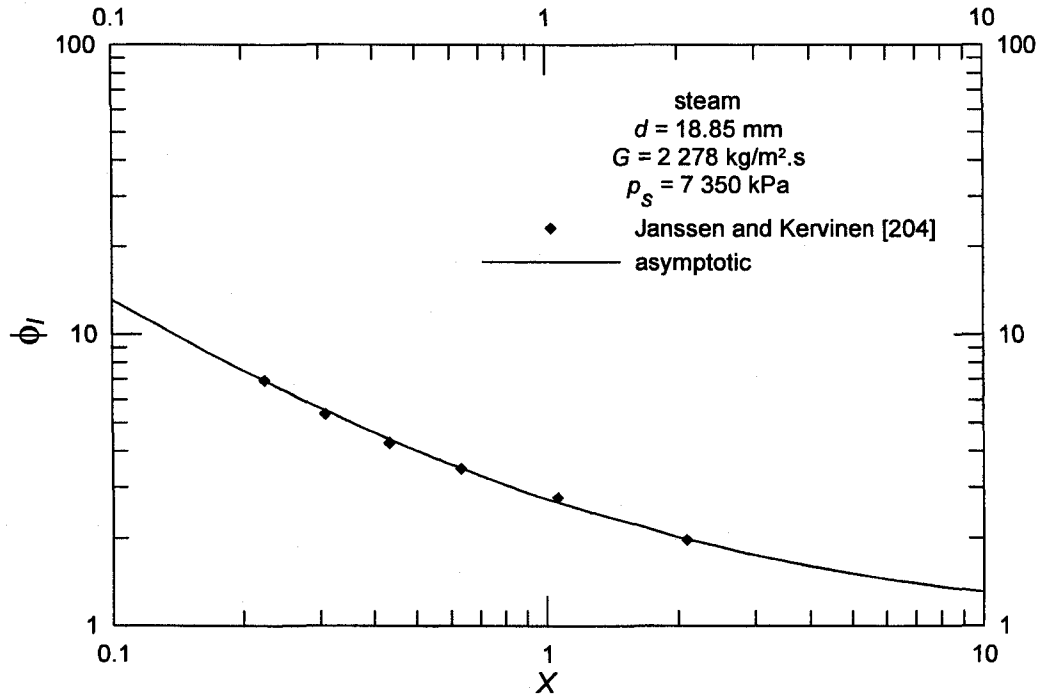


Figure 5.13 Comparison of the Present Asymptotic Model with Janssen and Kervinen's Data [204]

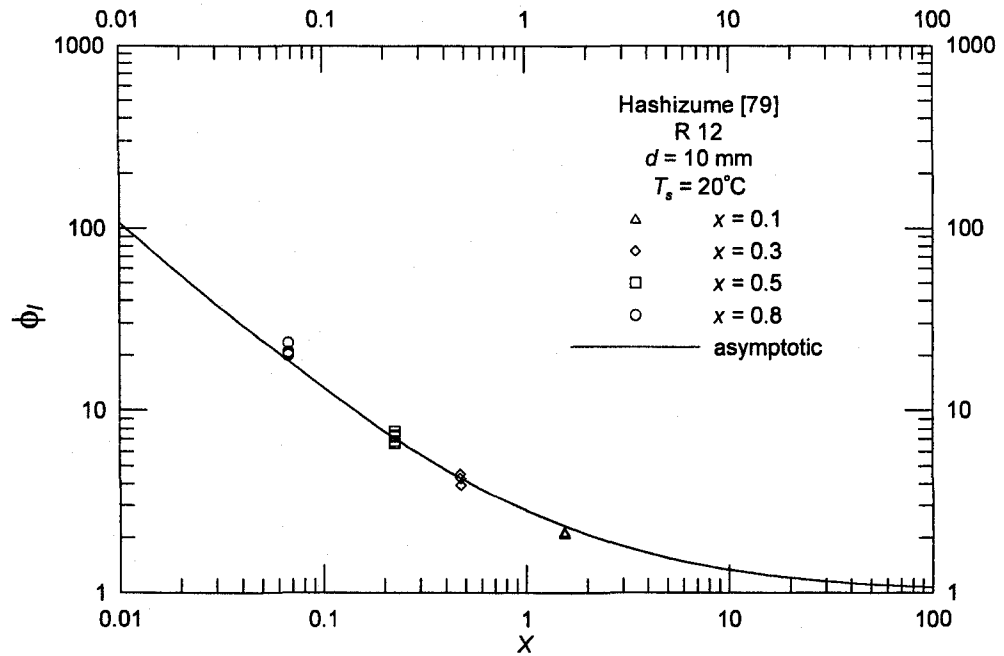


Figure 5.14 Comparison of the Asymptotic Model with Hashizume's Data [79]

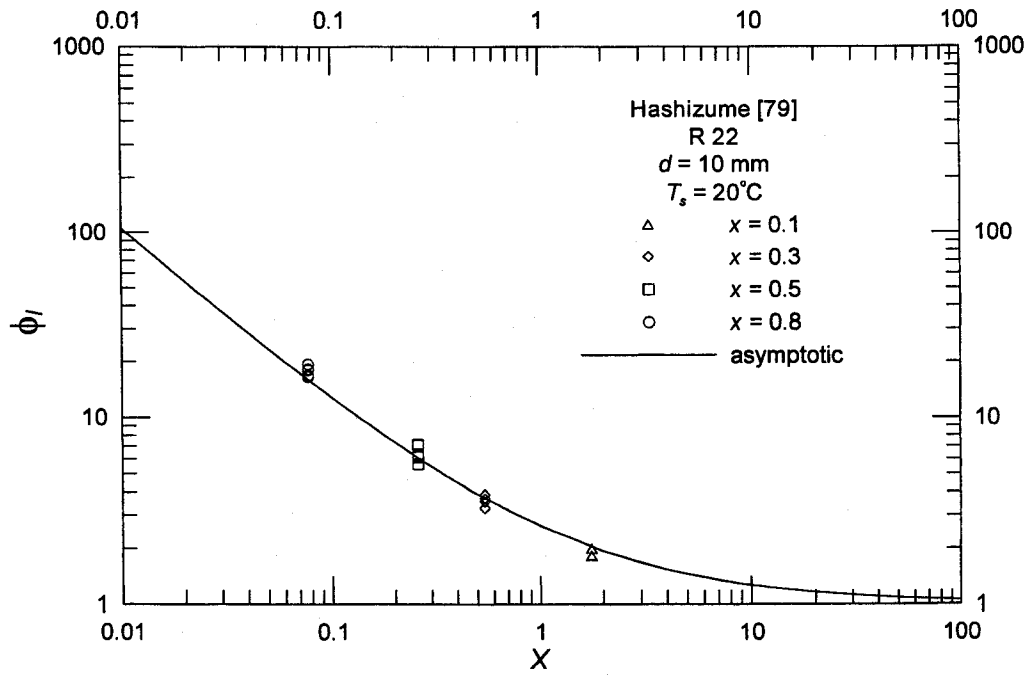


Figure 5.15 Comparison of the Asymptotic Model with Hashizume's Data [79]

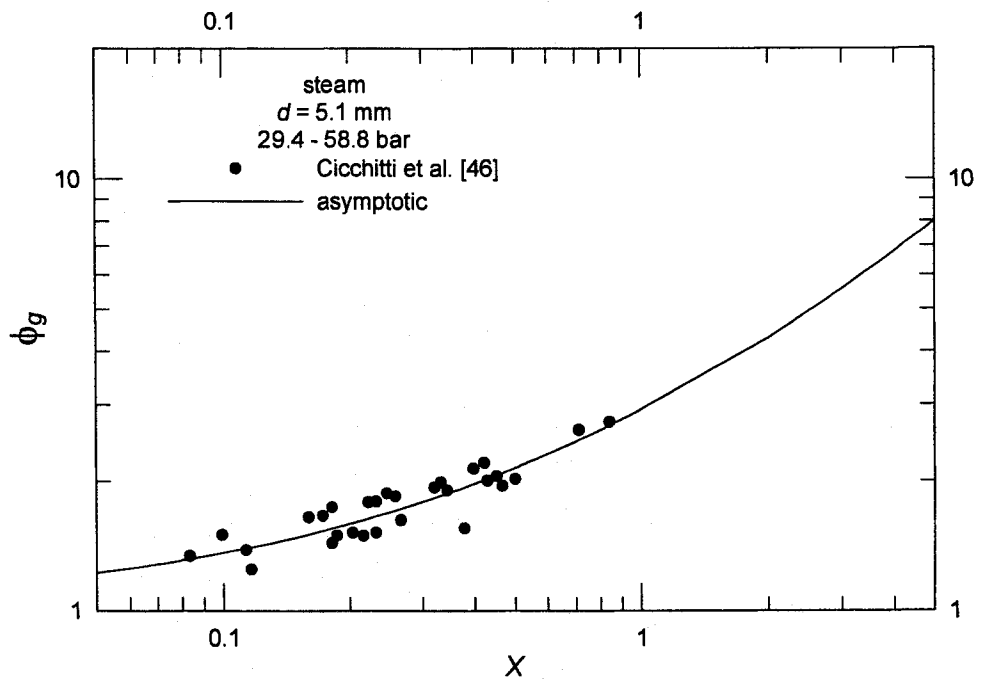


Figure 5.16 Comparison of the Present Asymptotic Model with Cicchitti et al.'s Data [46]

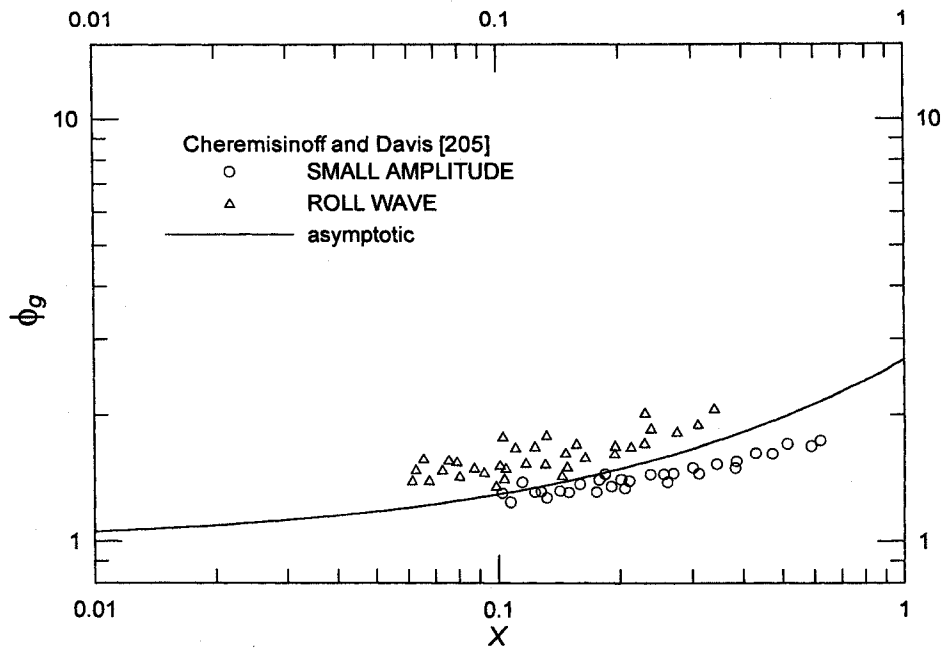


Figure 5.17 Comparison of the Present Asymptotic Model with Cheremisinoff and Davis's Data [205]

Table 5.7 Values of the Asymptotic Parameter (p) in Circular Pipes at Different Conditions

Author	d (mm)	Working Fluid	p	e_{RMS}	e_{RMS}^*
Dukler [202]	50.8	Air-Water	1/3.9	12.11%	29.43%
Chisholm [200]	27	Air-Water	1/4	16.73%	38.21%
Govier and Omer [203]	26.06	Air-Water	1/3.9	8.03%	19.87%
Janssen and Kervinen [204]	18.85	Steam	1/2.9	2.44%	12.90%
Hashizume [79]	10	R12	1/3	8.44%	10.80%
Hashizume [79]	10	R22	1/2.8	9.12%	16.68%
Cicchitti et al. [46]	5.1	Steam	1/3.1	8.29%	9.56%
Cheremisinoff and Davis [205]	63.5	Air-Water	1/2.85	14.21%	18.51%

*Calculated at $p = 1/3.25$.

To have a robust model, one value of the fitting parameter (p) is chosen as $p = 1/3.25$. When $p = 1/3.25$, the root mean square (RMS) error, $e_{RMS} = 23.80\%$. Figure

5.18 shows ϕ_l versus X for the first six data sets in Table 5.7 while Fig. 5.19 shows ϕ_g versus X for the last two data sets in Table 5.7 with $p = 1/3.25$.

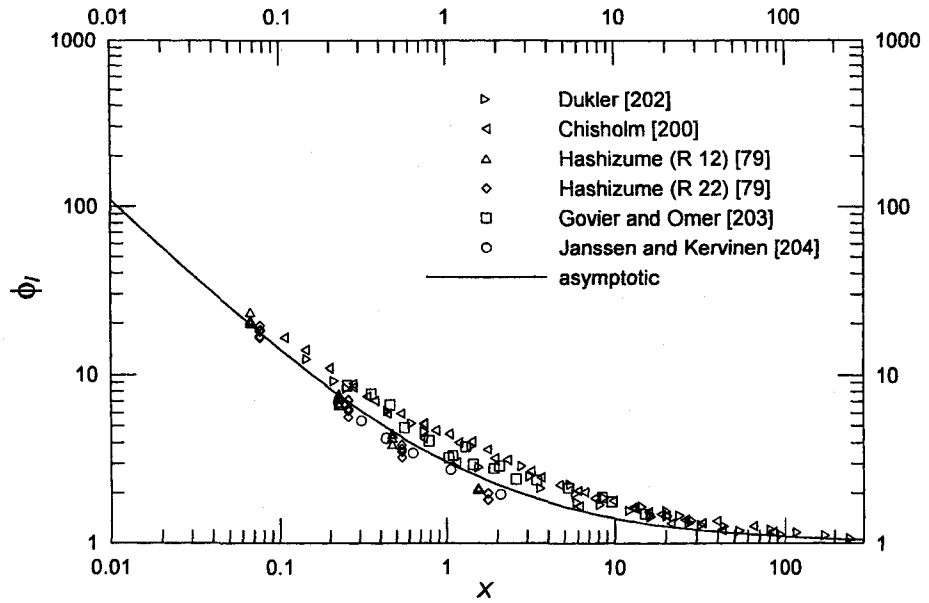


Figure 5.18 ϕ_l versus X for Different Sets of Data

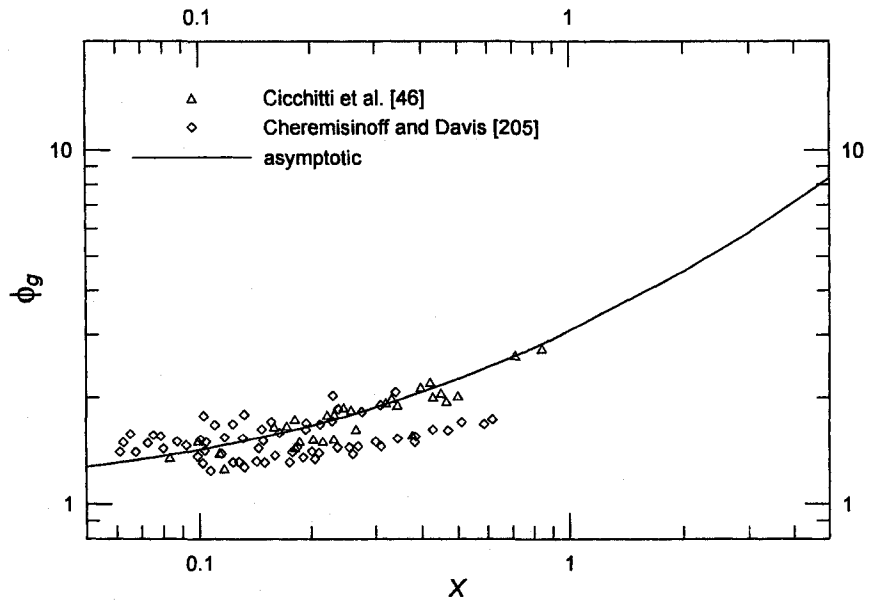


Figure 5.19 ϕ_g versus X for Different Sets of Data

5.5.5. ϕ_l and ϕ_g versus Lockhart-Martinelli Parameter (X) in Minichannels and Microchannels

Figures 5.20-5.22 show ϕ_l versus Lockhart-Martinelli parameter (X) for laminar-laminar flow for different working fluids in smooth minichannels and microchannels of different diameters at different conditions using the present asymptotic model and the different data sets. Equation (5.36) represents the present model with different values of p as shown in Table 5.8.

Figures 5.23 and 5.24 show ϕ_g versus Lockhart-Martinelli parameter (X) for laminar-laminar flow for different working fluids in smooth minichannels and microchannels at different conditions using the present asymptotic model and the different data sets. Equation (5.38) represents the present model with different values of p as shown in Table 5.8.

It can be seen that there is a good agreement between the present asymptotic model and the different data sets in Figs. 5.20-5.24.

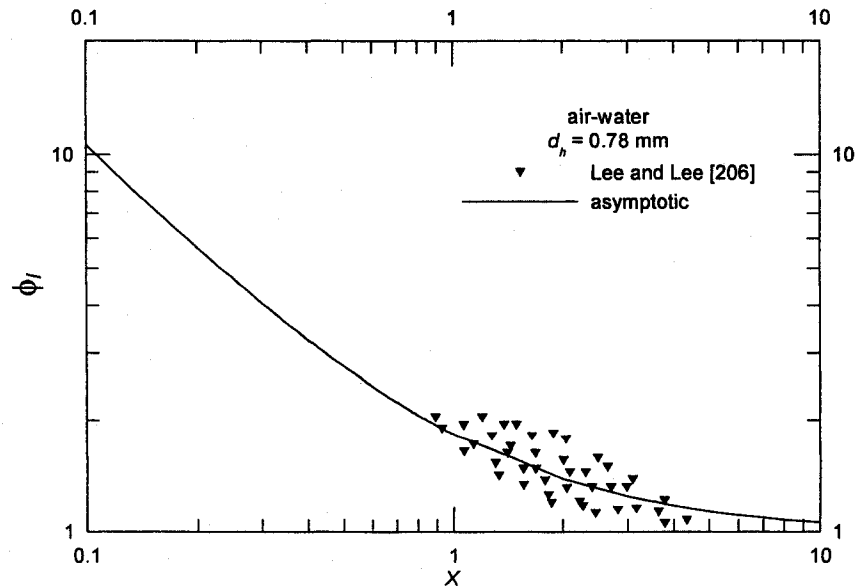


Figure 5.20 Comparison of the Asymptotic Model with Lee and Lee's Data [206]

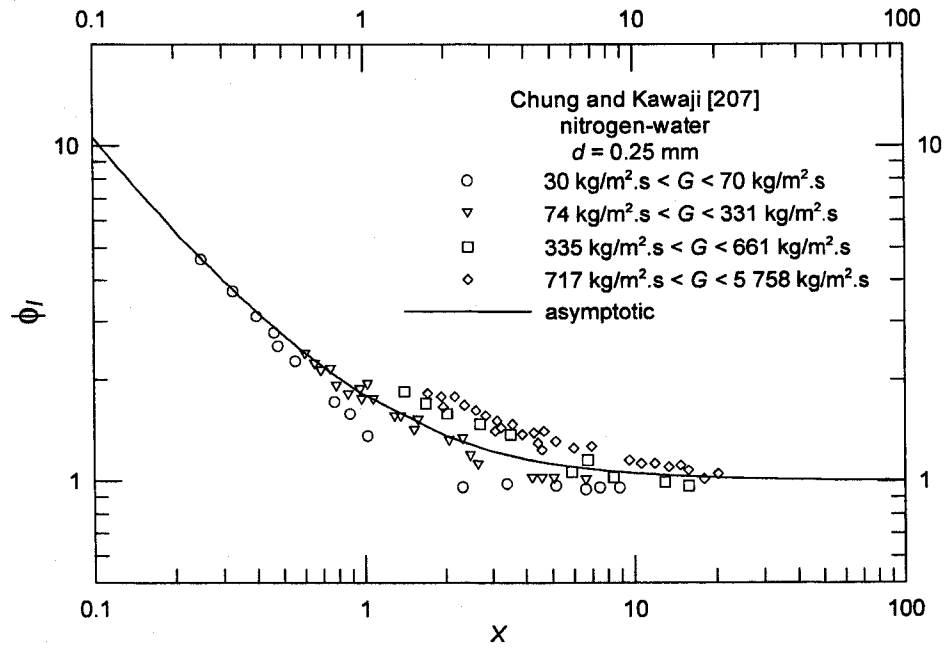


Figure 5.21 Comparison of the Present Asymptotic Model with Chung and Kawaji's Data [207]

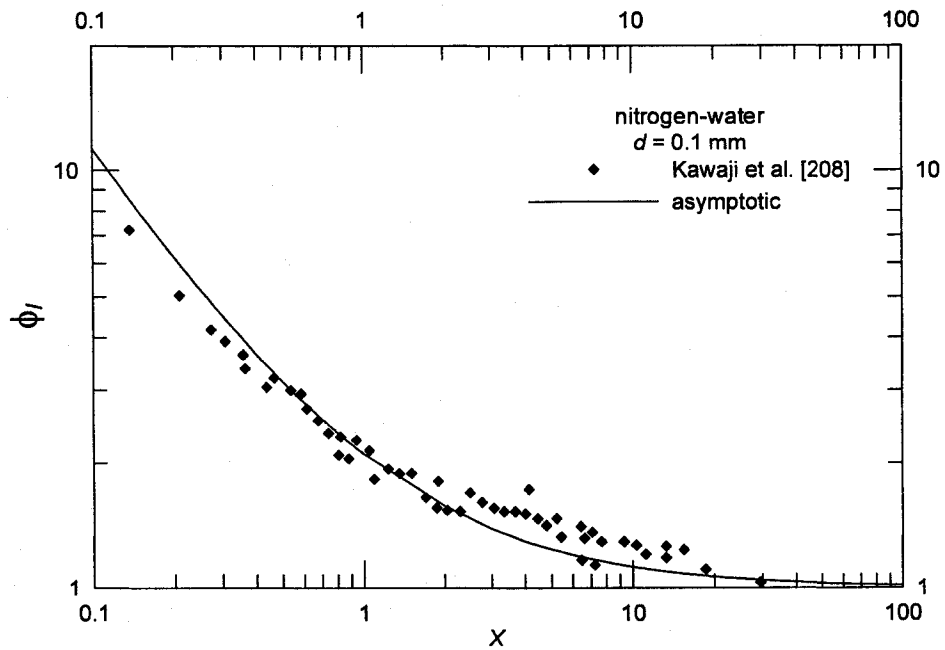


Figure 5.22 Comparison of the Present Asymptotic Model with Kawaji et al.'s Data [208] (Gas in the Main Channel and Liquid in the Branch)

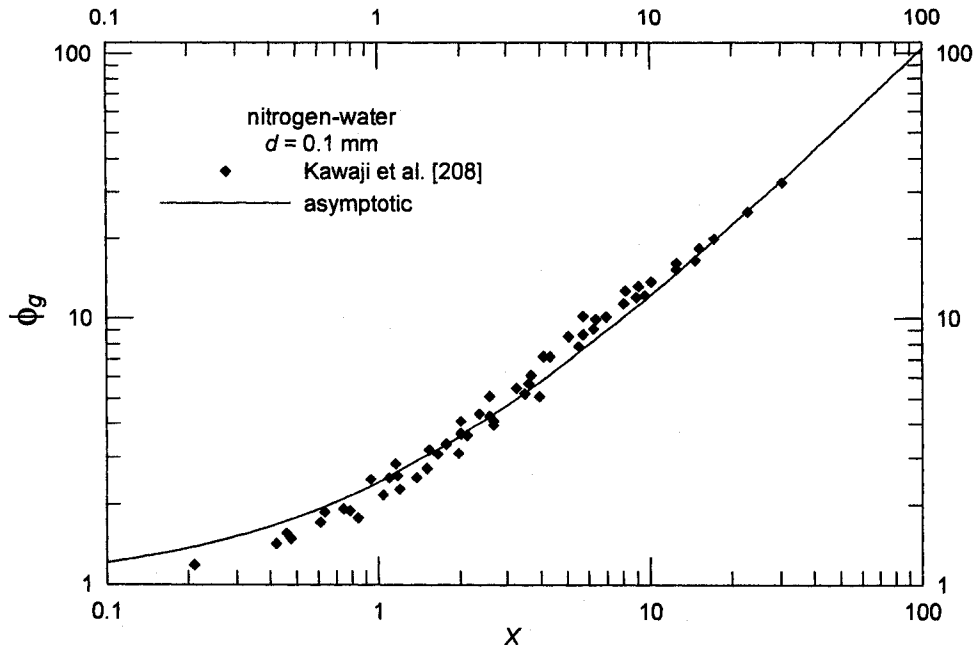


Figure 5.23 Comparison of the Present Asymptotic Model with Kawaji et al.'s Data [208] (Liquid in the Main Channel and Gas in the Branch)

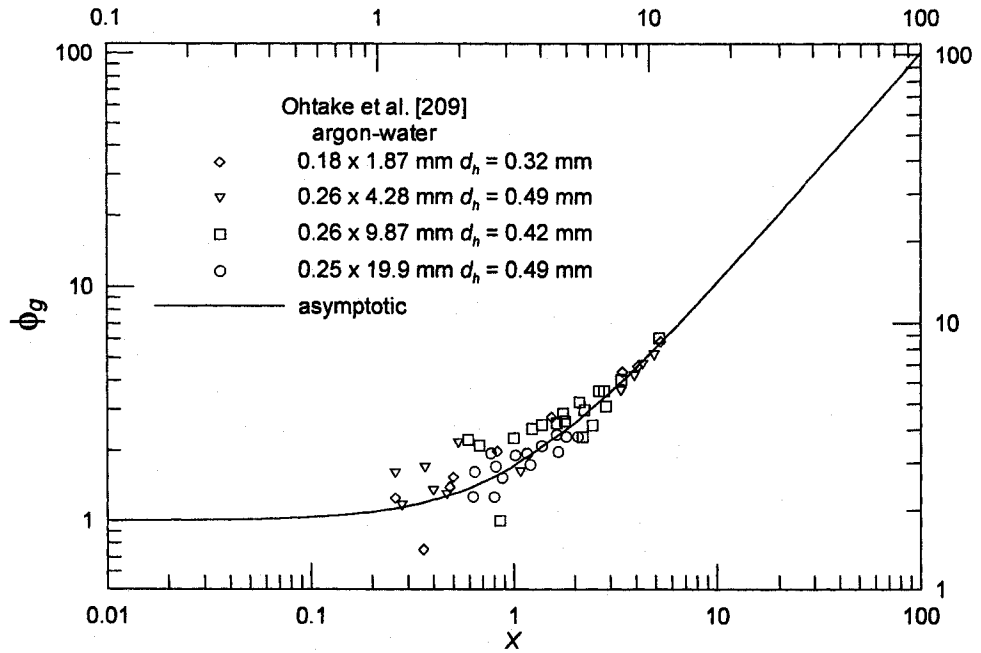


Figure 5.24 Comparison of the Present Asymptotic Model with Ohtake et al.'s Data [209]

Table 5.8 Values of the Asymptotic Parameter (p) in Minichannels and Microchannels at Different Conditions

Author	d (mm)	Working Fluid	p	e_{RMS}	e_{RMS} at $p = 1/2$
Lee and Lee [206]	0.78*	Air-Water	1/1.75	11.7%	14.07%
Chung and Kawaji [207]	0.1	Nitrogen-Water	1/1.7	13.44%	16.09%
Kawaji et al. [208]	0.1	Nitrogen-Water	1/2.15	10.39%	11.34%
Kawaji et al. [208]	0.1	Nitrogen-Water	1/2.55	11.65%	17.36%
Ohtake et al. [209]	0.32* 0.42* 0.49*	Argon-Water	1/1.55	19.56% 16.08%**	24.16% 18.24%**

*Hydraulic diameter. **The two lower points are not taken into account.

To have a robust model, one value of the fitting parameter (p) is chosen as $p = 1/2$. When $p = 1/2$, the root mean square (RMS) error, $e_{RMS} = 17.14\%$ or 15.69% if the two lower points of Ohtake et al. data [209] are not taken into account. Figure 5.25 shows ϕ_l versus X for the first three data sets in Table 5.8 while Fig. 5.26 shows ϕ_g versus X for the last two data sets in Table 5.8 with $p = 1/2$.

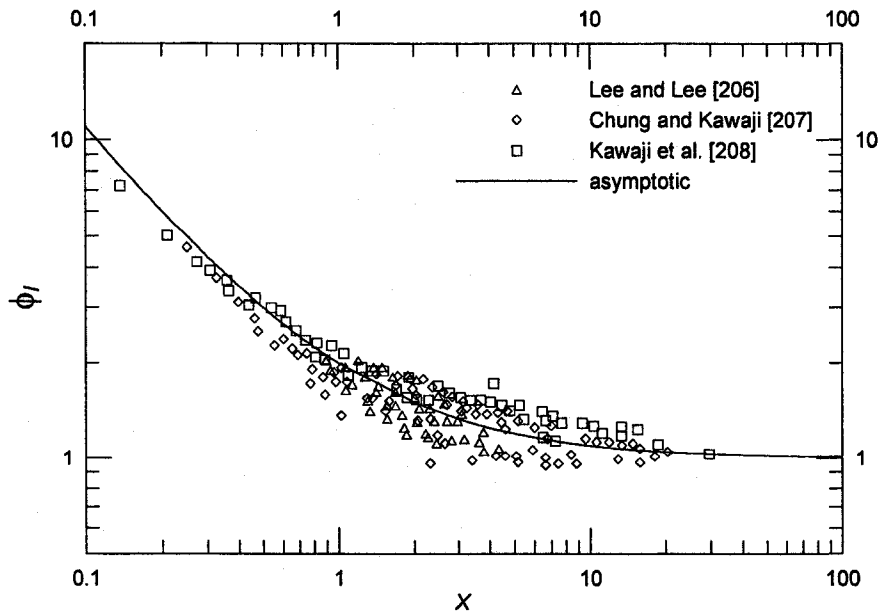


Figure 5.25 ϕ_l versus X for Different Sets of Data

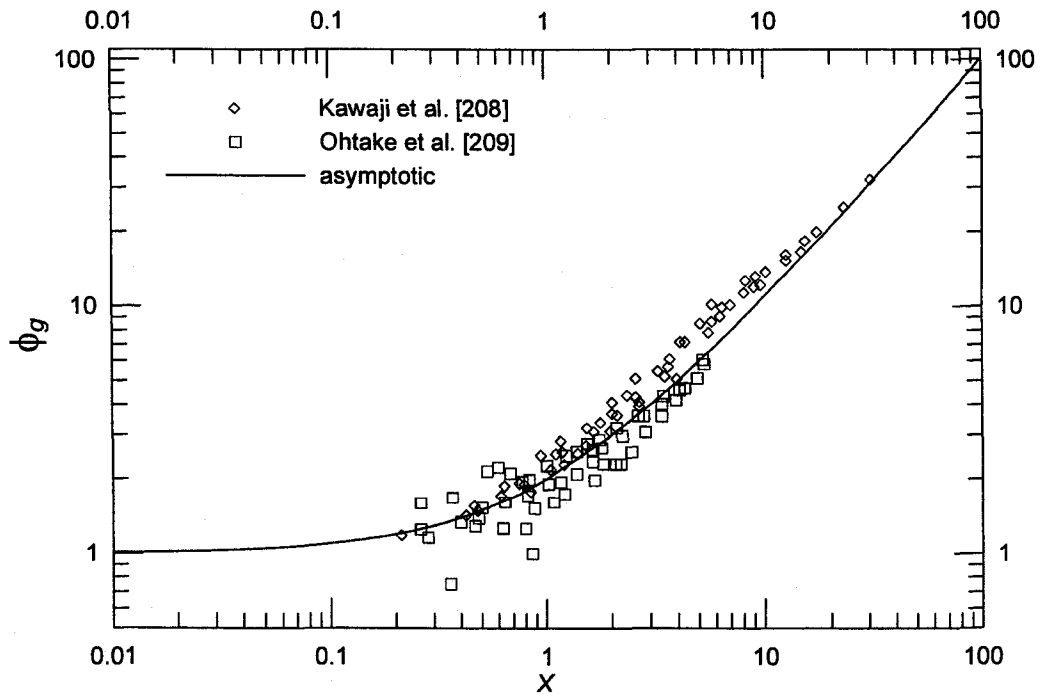


Figure 5.26 ϕ_g versus X for Different Sets of Data

5.6 Summary

New two-phase flow modeling is proposed, based upon an asymptotic modeling method. The main advantage of the asymptotic modeling method in two-phase flow is taking into account the important frictional interactions that occur at the interface between liquid and gas because the liquid and gas phases are assumed to flow dependently of each other in the same pipe. Also, the values of the Reynolds number for the liquid and gas phases are not important because the Churchill model [104] that spanned the entire range of laminar, transition, and turbulent flow in pipes is introduced to define the Fanning friction factor. In addition, the obtained expressions of ϕ_l^2 and ϕ_g^2 are explicit for all flow conditions. The only unknown parameter in the asymptotic modeling method in two-phase flow is the fitting

parameter (p). The value of the fitting parameter (p) corresponds to the minimum root mean square (RMS) error, e_{RMS} for any data set. To have a robust model, one value of the fitting parameter (p) is chosen as $p = 1/3.25$ for large diameter (macro scale) and $p = 1/2$ for small diameter (micro scale). The difference between the values of $p = 1/3.25$ for large diameter (macro scale) and $p = 1/2$ for small diameter (micro scale) can be due to the effect of diameter (d) on p .

CHAPTER 6

BOUNDS ON TWO-PHASE FLOW

6.1 Introduction

This chapter describes the development of lower and upper bounds for two-phase frictional pressure gradient and void fraction in circular pipes. This approach is very useful in design and analysis, as engineers can then use the resulting average and bounding values in predictions of system performance. The approach is also useful when conducting new experiments, since it provides a reasonable envelope for the data to fall within. The bounds are intended to provide the most realistic range of data not firm absolute limits. Statistically, this is unreasonable as the bounds would be far apart. The bounds are not fit to capture all data but rather a majority of data points, as some outlying points are due to experimental error. If a vast majority of data is within the bounds, then a reasonable expectation is realistically assured.

6.2 Development of Bounds on Two-Phase Frictional Pressure Gradient in Circular Pipes

In this section, rational bounds for two-phase frictional pressure gradient in circular pipes will be developed. These bounds may be used to determine the maximum and minimum values that may reasonably be expected in a two-phase flow. Further, by averaging these limiting values an acceptable prediction for the pressure gradient is obtained which is then bracketed by the bounding values:

$$\left(\frac{dp}{dz}\right)_{f,lower} \leq \left(\frac{dp}{dz}\right)_f \leq \left(\frac{dp}{dz}\right)_{f,upper} \quad (6.1)$$

The bounds model will be in the form of two-phase frictional pressure gradient versus mass flux at constant mass quality. The bounds model may also be presented in the form of two-phase frictional multiplier, which is often useful for calculation and comparison needs. For this reason, development of lower and upper bounds in terms of two-phase frictional multiplier (ϕ_l and ϕ_g) versus the Lockhart-Martinelli parameter (X) will also be presented.

6.2.1 Large Circular Pipes

For the case of large circular pipes, the bounds method is based on turbulent liquid-turbulent gas assumption [210,211]. This assumption is suitable because, in practice, both Re_l and Re_g are most often greater than 2 000 in large circular pipes.

Both the lower and upper bounds are based on the separate cylinders formulation. The reasons of choosing lower and upper bounds can be explained as follows:

From Table 2.3, it is obvious that the different values of n for turbulent-turbulent flow in separate-cylinders model can be:

- i. $n = 2.375$ ($f = 0.079/Re^{0.25}$).
- ii. $n = 2.4$ ($f = 0.046/Re^{0.2}$).
- iii. $n = 2.5$ ($f = \text{constant}$).
- iv. $n = 3.5$ (maximum value in mixing-length analysis).

- v. $n = 4$ (good empirical representation of the Lockhart-Martinelli correlation).

The present model is based on the minimum and maximum values of n for turbulent-turbulent flow, 2.375 and 4 respectively from the separate-cylinders formulation.

Also, although the data points are in turbulent-turbulent flow, they cover different flow patterns such as stratified, wavy, slug and annular. As the mass flow rate of the gas in two-phase flow increases, the flow pattern changes from stratified to wavy to slug to annular. As mentioned in the literature, the Lockhart-Martinelli correlation has a good accuracy for annular flow pattern but it has a poor accuracy (over prediction) for stratified and wavy flow pattern. This is why it is taken as an upper bound. Further $n = 4$ as a closure constant was arbitrarily chosen to fit the data and thus accounts for interfacial effects between phases making it an upper bound, where as $n = 2.375$ as a closure constant is obtained from the Blasius friction model and does not account for interfacial effects, and therefore represents a lower bound for the data. Faghri and Zhang [212] further commented that the advantage of the pressure drop correlations based on the separated-flow model is that it is applicable for all flow patterns. This flexibility is accompanied by low accuracy.

6.2.1.1 The Lower Bound

In chapter 5, the separate cylinders analysis [29] was utilized and introduced the Blasius equation [10] to represent the Fanning friction factor for turbulent-turbulent flow. From Tables 5.1 and 5.2, expressions of ϕ_l^2 and ϕ_g^2 for turbulent-turbulent flow are

$$\phi_l^2 = \left[1 + \left(\frac{1}{X^2} \right)^{1/2.375} \right]^{2.375} \quad (6.2)$$

$$\phi_g^2 = \left[1 + (X^2)^{1/2.375} \right]^{2.375} \quad (6.3)$$

For turbulent-turbulent flow, the Lockhart-Martinelli parameter (X) can be expressed as [86]:

$$X = \left(\frac{1-x}{x} \right)^{7/8} \left(\frac{\rho_g}{\rho_l} \right)^{1/2} \left(\frac{\mu_l}{\mu_g} \right)^{1/8} \quad (6.4)$$

The Lockhart-Martinelli expression for the two-phase frictional multiplier (ϕ_l^2) is given by:

$$\phi_l^2 = \frac{(dp/dz)_f}{(dp/dz)_{f,l}} \quad (6.5)$$

The single-phase liquid frictional pressure gradient can be related to the Fanning friction factor in terms of mass flux and mass quality for liquid flowing alone as follows:

$$\left(\frac{dp}{dz} \right)_{f,l} = \frac{2f_l G^2 (1-x)^2}{d\rho_l} \quad (6.6)$$

For turbulent-turbulent flow, the Fanning friction factor is defined using the Blasius equation [10] with $n = 0.25$ as:

$$f_l = \frac{0.079}{Re_l^{1/4}} \quad (6.7)$$

The Reynolds number equation can be expressed in terms of mass flux and mass quality for liquid flowing alone as:

$$Re_l = \frac{G(1-x)d}{\mu_l} \quad (6.8)$$

Using Eq. (6.2), and Eqs. (6.4)-(6.8), we obtain

$$\left(\frac{dp}{dz}\right)_{f,lower} = \frac{0.158G^{1.75}(1-x)^{1.75}\mu_l^{0.25}}{d^{1.25}\rho_l} \left[1 + \left(\frac{x}{1-x}\right)^{0.7368} \left(\frac{\rho_l}{\rho_g}\right)^{0.4211} \left(\frac{\mu_g}{\mu_l}\right)^{0.1053} \right]^{2.375} \quad (6.9)$$

6.2.1.2 The Upper Bound

The equation of the upper bound is similar for the lower bound case except for the definitions of ϕ_l^2 and ϕ_g^2 . The equation of the separate cylinders model [29] in Chapter 2 is

$$\left(\frac{1}{\phi_l^2}\right)^{1/n} + \left(\frac{1}{\phi_g^2}\right)^{1/n} = 1 \quad (6.10)$$

Introducing the Lockhart-Martinelli parameter (X) into Eq. (6.10), we obtain ϕ_l^2 and ϕ_g^2 for turbulent-turbulent flow ($n = 4$, Table 2.3) respectively as follows:

$$\phi_l^2 = \left[1 + \left(\frac{1}{X^2}\right)^{1/4} \right]^4 \quad (6.11)$$

$$\phi_g^2 = \left[1 + (X^2)^{1/4} \right]^4 \quad (6.12)$$

Equations (6.11) and (6.12) represent well the Lockhart-Martinelli correlation [16] for turbulent-turbulent flow. Using Eq. (6.11), and Eqs. (6.4)-(6.8), we obtain

$$\left(\frac{dp}{dz} \right)_{f,upper} = \frac{0.158G^{1.75} (1-x)^{1.75} \mu_l^{0.25}}{d^{1.25} \rho_l} \left[1 + \left(\frac{x}{1-x} \right)^{0.4375} \left(\frac{\rho_l}{\rho_g} \right)^{0.25} \left(\frac{\mu_g}{\mu_l} \right)^{0.0625} \right]^4 \quad (6.13)$$

6.2.1.3 Mean Model

A simple model may be developed by averaging the two bounds. This is defined as follows:

$$\phi_{l,av}^2 = \frac{1}{2} \left[\left[1 + \left(\frac{1}{X^2} \right)^{1/2.375} \right]^{2.375} + \left[1 + \left(\frac{1}{X^2} \right)^{1/4} \right]^4 \right] \quad (6.14)$$

or

$$\phi_{g,av}^2 = \frac{1}{2} \left[\left[1 + (X^2)^{1/2.375} \right]^{2.375} + \left[1 + (X^2)^{1/4} \right]^4 \right] \quad (6.15)$$

and

$$\left(\frac{dp}{dz}\right)_{f,av} = \frac{0.079G^{1.75}(1-x)^{1.75}\mu_l^{0.25}}{d^{1.25}\rho_l} \left[\begin{aligned} & \left[1 + \left(\frac{x}{1-x}\right)^{0.7368} \left(\frac{\rho_l}{\rho_g}\right)^{0.4211} \left(\frac{\mu_g}{\mu_l}\right)^{0.1053} \right]^{2.375} \\ & + \left[1 + \left(\frac{x}{1-x}\right)^{0.4375} \left(\frac{\rho_l}{\rho_g}\right)^{0.25} \left(\frac{\mu_g}{\mu_l}\right)^{0.0625} \right]^4 \end{aligned} \right] \quad (6.16)$$

Otherwise the more accurate asymptotic model from Chapter 5 should be used, Eq. (5.34) with $p = 1/3.25$.

6.2.2 Small Circular Pipes

For the case of small circular pipes, the bounds method is based on laminar liquid-laminar gas assumption [213]. This assumption is suitable because, in practice, both Re_l and Re_g are most often less than 2 000 in small circular pipes. This assumption is also suitable for the flow in minichannels and microchannels [213].

6.2.2.1 The Lower Bound

The lower bound is based on Ali et al. correlation [214]. This correlation is based on a modification of the simplified stratified flow model derived from the theoretical approach of Taitel and Dukler [14] for the case of two-phase flow in a narrow channel. The correlation is

$$\phi_l^2 = \left[1 + (X)^{2/(n-2)} \right]^{2-n} \quad (6.17)$$

Equation (6.17) can be obtained at the critical state using the relationship between ϕ_{lo}^2 and ϕ_l^2 as follows:

$$\phi_{lo}^2 = \phi_l^2 (1-x)^{(2-n)} \quad (6.18)$$

At the critical state, $\phi_{lo}^2 = 1$. So, Eq. (6.18) becomes

$$\phi_l^2 = (1-x)^{(n-2)} \quad (6.19)$$

The Lockhart-Martinelli parameter (X) can be expressed as [86]:

$$X = \left(\frac{1-x}{x} \right)^{(2-n)/2} \left(\frac{\rho_g}{\rho_l} \right)^{1/2} \left(\frac{\mu_l}{\mu_g} \right)^{n/2} \quad (6.20)$$

At the critical state, $\rho_l = \rho_g$ and $\mu_l = \mu_g$. So, Eq. (6.20) becomes

$$X = \left(\frac{1-x}{x} \right)^{(2-n)/2} \quad (6.21)$$

From Eqs. (6.19) and (6.21), we can obtain Eq. (6.17). It is well known that the homogeneous model is applicable at the critical state where the properties of the gas phase are equal to the properties of the liquid phase.

Returning to Eq. (6.17) for laminar-laminar flow ($n = 1$), we obtain

$$\phi_l^2 = 1 + \frac{1}{X^2} \quad (6.22)$$

$$\phi_g^2 = 1 + X^2 \quad (6.23)$$

In the context of the asymptotic model from chapter 5, Eqs. (6.22) and (6.23) are equivalent to Eqs. (5.36) and (5.38) with $p = 1$. In addition, Eqs. (6.22) and (6.23) are equivalent to the Chisholm correlation [30] with $C = 0$. The physical meaning of

the lower bound ($C = 0$) is that the two-phase frictional pressure gradient is the sum of the frictional pressure gradient of liquid phase alone and the frictional pressure gradient of gas phase alone:

$$\left(\frac{dp}{dz}\right)_f = \left(\frac{dp}{dz}\right)_{f,l} + \left(\frac{dp}{dz}\right)_{f,g} \quad (6.24)$$

This means there is no contribution to pressure gradient through phase interaction. The above result can also be obtained using the asymptotic model for two-phase frictional pressure gradient [201] with linear superposition (i.e. $p = 1$ in Eq. (5.34)). Also, using the homogeneous model with the Dukler et al. [13] definition of two-phase viscosity for laminar-laminar flow leads to the same result of Eq. (6.24). It is well known that the homogeneous model gives reasonably accurate prediction for flow pattern such as bubble flow where the slip ratio is close to 1. From the point of view of the phase interaction and prediction of bubble flow, this is why Eq. (6.22) is taken as a lower bound

For laminar-laminar flow ($n = 1$), the Lockhart-Martinelli parameter (X) can be expressed as [86]:

$$X = \left(\frac{1-x}{x}\right)^{1/2} \left(\frac{\rho_g}{\rho_l}\right)^{1/2} \left(\frac{\mu_l}{\mu_g}\right)^{1/2} \quad (6.25)$$

For laminar-laminar flow, the Fanning friction factor is defined using the Hagen-Poiseuille flow [215]:

$$f_l = \frac{16}{Re_l} \quad (6.26)$$

Using Eq. (6.22), Eq. (6.25), Eqs. (6.5)-(6.6), Eq. (6.26), and Eq. (6.8), we obtain

$$\left(\frac{dp}{dz}\right)_{f,lower} = \frac{32G(1-x)\mu_l}{d^2\rho_l} \left[1 + \left(\frac{x}{1-x}\right) \left(\frac{\rho_l}{\rho_g}\right) \left(\frac{\mu_g}{\mu_l}\right) \right] \quad (6.27)$$

6.2.2.2 The Upper Bound

Although the data points are in laminar-laminar flow, they cover different flow patterns such as bubble, stratified, and annular. As the mass flow rate of the gas in two-phase flow increases, the flow pattern changes from bubble until reaches annular at high mass flow rate of gas. As mentioned in the literature, the Lockhart-Martinelli correlation has a good accuracy for annular flow pattern. This is why it is taken as an upper bound. Chisholm [30] gave a theoretical basis for the Lockhart-Martinelli correlation for two-phase flow as:

$$\phi_l^2 = 1 + \frac{C}{X} + \frac{1}{X^2} \quad (6.28)$$

$$\phi_g^2 = 1 + CX + X^2 \quad (6.29)$$

For laminar-laminar flow ($C = 5$),

$$\phi_l^2 = 1 + \frac{5}{X} + \frac{1}{X^2} \quad (6.30)$$

$$\phi_g^2 = 1 + 5X + X^2 \quad (6.31)$$

In the context of the asymptotic model from chapter 5, Eqs. (6.30) and (6.31) are equivalent to Eqs. (5.36) and (5.38) with $p = 1/2.4$. The second term of right hand

side in Eqs. (6.30) and (6.31) shows that there is an increase in ϕ_l^2 and ϕ_g^2 due to the phase interaction. Equations (6.30) and (6.31) can be written as:

$$\left(\frac{dp}{dz}\right)_f = \left(\frac{dp}{dz}\right)_{f,l} + 5 \underbrace{\left[\left(\frac{dp}{dz}\right)_{f,l} \left(\frac{dp}{dz}\right)_{f,g}\right]^{0.5}}_{\text{interaction}} + \left(\frac{dp}{dz}\right)_{f,g} \quad (6.32)$$

Using Eq. (6.32), Eq. (6.25), Eqs. (6.5)-(6.6), Eq. (6.26), and Eq. (6.8), we obtain

$$\left(\frac{dp}{dz}\right)_{f,upper} = \frac{32G(1-x)\mu_l}{d^2\rho_l} \left[1 + 5 \left(\frac{x}{1-x}\right)^{0.5} \left(\frac{\rho_l}{\rho_g}\right)^{0.5} \left(\frac{\mu_g}{\mu_l}\right)^{0.5} + \left(\frac{x}{1-x}\right) \left(\frac{\rho_l}{\rho_g}\right) \left(\frac{\mu_g}{\mu_l}\right) \right] \quad (6.33)$$

6.2.2.3 Mean Model

A simple model may be developed by averaging the two bounds. This is defined as follows:

$$\phi_{l,av}^2 = 1 + \frac{2.5}{X} + \frac{1}{X^2} \quad (6.34)$$

or

$$\phi_{g,av}^2 = 1 + 2.5X + X^2 \quad (6.35)$$

and

$$\left(\frac{dp}{dz}\right)_{f,av} = \frac{32G(1-x)\mu_l}{d^2\rho_l} \left[1 + 2.5 \left(\frac{x}{1-x}\right)^{0.5} \left(\frac{\rho_l}{\rho_g}\right)^{0.5} \left(\frac{\mu_g}{\mu_l}\right)^{0.5} + \left(\frac{x}{1-x}\right) \left(\frac{\rho_l}{\rho_g}\right) \left(\frac{\mu_g}{\mu_l}\right) \right] \quad (6.36)$$

The equations of the mean model are equivalent to the Chisholm correlation with $C = 2.5$. However a more accurate prediction can be accomplished with Eq. (5.34) with $p = 1/2$.

This model can be applied for circular shapes using tube diameter, d as well as using hydraulic diameter, d_h for non-circular shapes. The Hagen-Poiseuille constant is 16 in Eq. (6.26) will be changed for non-circular shapes. For example, the Hagen-Poiseuille constant is 24 for a rectangular channel with the aspect ratio of 0 while the Hagen-Poiseuille constant is 14.23 for a rectangular channel with the aspect ratio of 1 (square channel).

6.2.3 Results and Discussion

Examples of two-phase frictional pressure gradient versus mass flux at constant mass quality from published experimental studies are presented to show the advantages of the bounds models. The published data include different working fluids such as R-12, R-22, Argon and R717 at different mass qualities with different pipe diameters. Also, examples of two-phase frictional multiplier (ϕ_l and ϕ_g) versus Lockhart-Martinelli parameter (X) using published data of different working fluids such as R-12, R-22, steam and air-water mixtures from other experimental work are presented to validate the bounds model in dimensionless form.

6.2.3.1 Two-Phase Frictional Pressure Gradient

Figures 6.1-6.4 show the frictional pressure gradient versus mass flux in turbulent-turbulent flow. Equation (6.9) represents the lower bound and Eq. (6.13) represents the upper bound, while Eq. (6.16) represents the average. Figure 6.1

compares the present approach with Bandel's data [12] for R 12 flow at $x = 0.3$ and $T_s = 0^\circ\text{C}$ in a smooth horizontal pipe at $d = 14$ mm. Figure 6.2 compares the present approach with Hashizume's data [79] for R 12 flow at $x = 0.8$ and $T_s = 50^\circ\text{C}$ in a smooth horizontal pipe at $d = 10$ mm. Figure 6.3 compares the present approach with Hashizume's data [79] for R 22 flow at $x = 0.8$ and $T_s = 39^\circ\text{C}$ in a smooth horizontal pipe at $d = 10$ mm. Figure 6.4 compares the present approach with Müller-Steinhagen's data [180] for Argon flow at $x = 0.4$ and reduced pressure of 0.188 in a smooth horizontal pipe at $d = 14$ mm. From Figs. 6.1-6.4, it can be seen that the published data can be well bounded. In Figs. 6.1-6.4, the mean model predicts the published data with the root mean square (RMS) error of 26.41%, 8.62%, 11.23%, and 21.42% respectively, while the asymptotic model gives the root mean square (RMS) error of 29.67%, 10.65%, 8.34%, and 15.75% respectively.

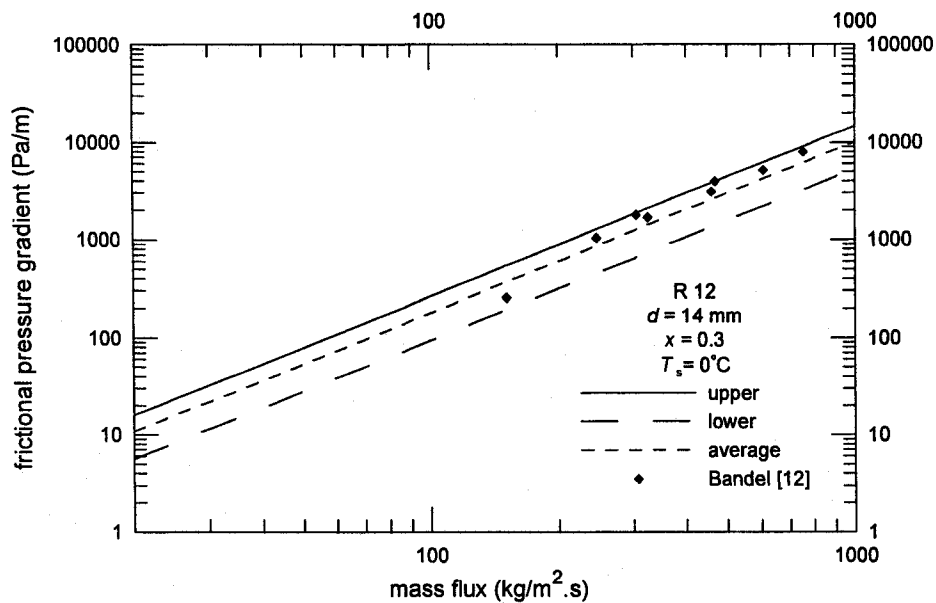


Figure 6.1 Comparison of the Present Model with Bandel's Data [12]

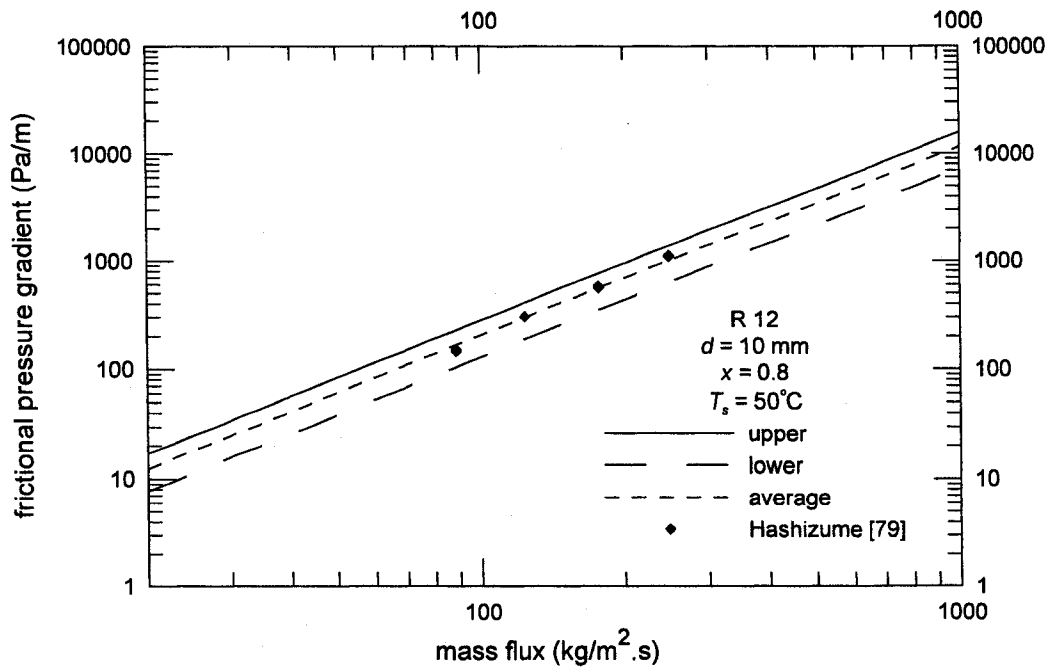


Figure 6.2 Comparison of the Present Model with Hashizume's Data [79]

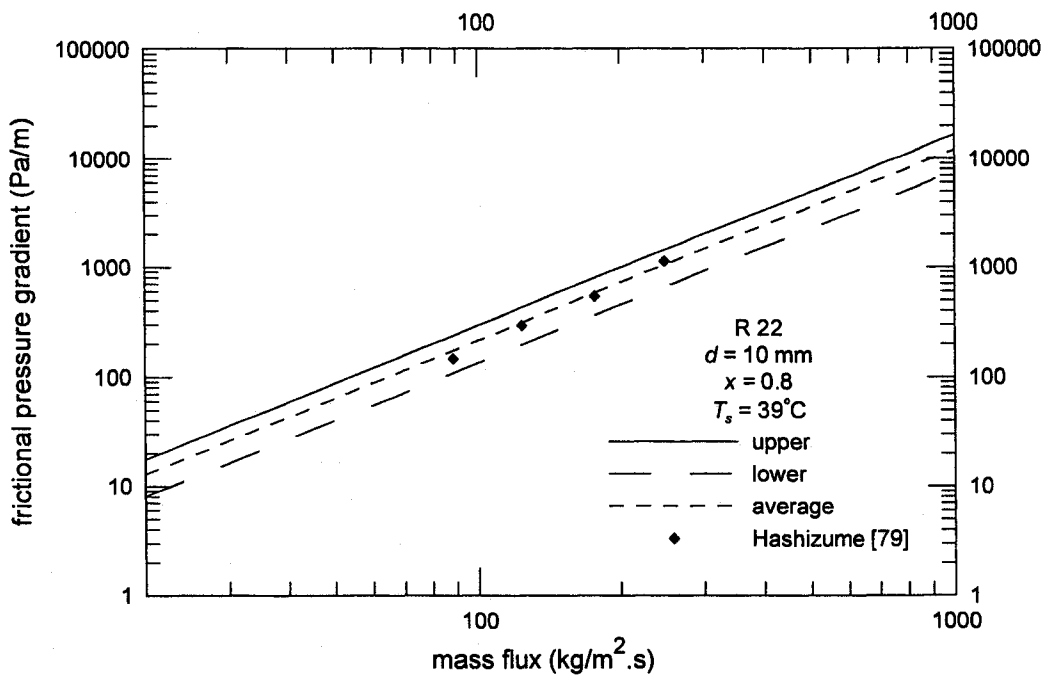


Figure 6.3 Comparison of the Present Model with Hashizume's Data [79]

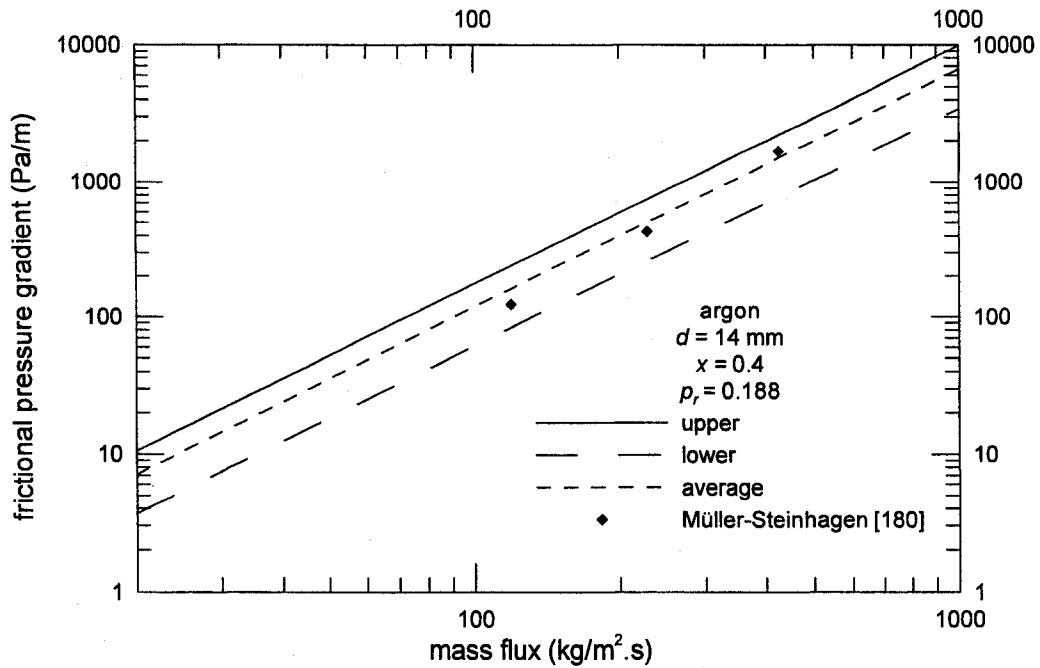


Figure 6.4 Comparison of the Model with Müller-Steinhagen's Data [180]

Figures 6.5 and 6.6 show the frictional pressure gradient versus mass flux in laminar-laminar flow. Equation (6.22) represents the lower bound and Eq. (6.33) represents the upper bound, while Eq. (6.36) represents the average. Figure 6.5 compares the present approach with Ungar and Cornwell's data [89] for R 717 flow at $x \approx 0.2$ and $T_s \approx 76^\circ\text{F}$ (168.8°C) in a smooth horizontal tube at $d = 0.0575 \text{ in.}$ (1.46 mm). Figure 6.6 compares the present approach with Ungar and Cornwell's data [89] for R 717 flow at $x \approx 0.1$ and $T_s \approx 76^\circ\text{F}$ (168.8°C) in a smooth horizontal tube at $d = 0.0701 \text{ in.}$ (1.781 mm). The mean model predicts the published data with the root mean square (RMS) error of 32.85%, and 29.48% respectively, while the asymptotic model gives the root mean square (RMS) error of 31.05%, and 36.72% respectively.

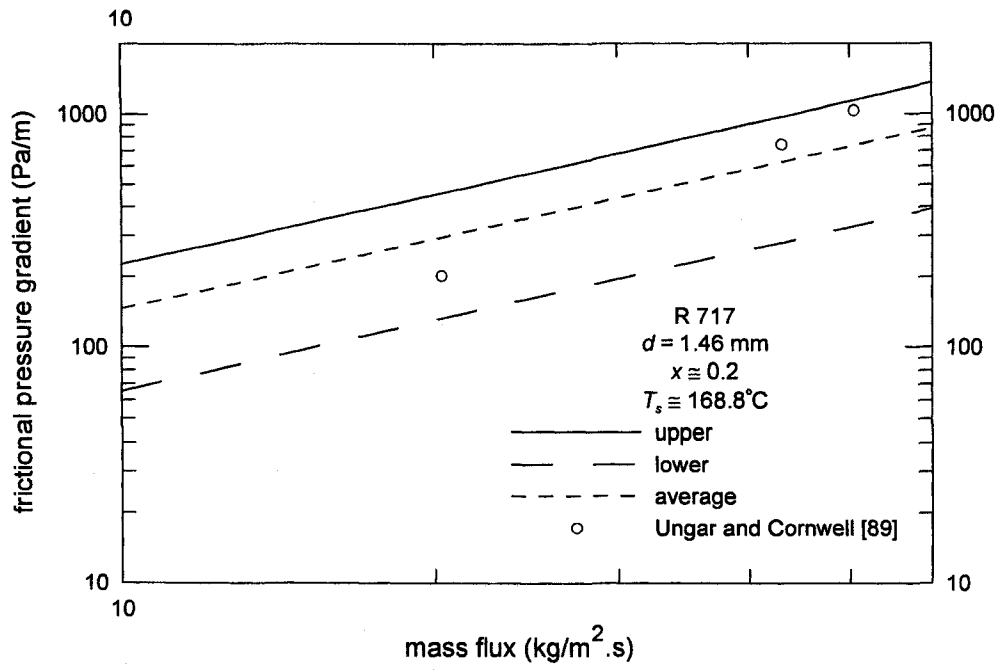


Figure 6.5 Comparison of the Model with Ungar and Cornwell's Data [89]

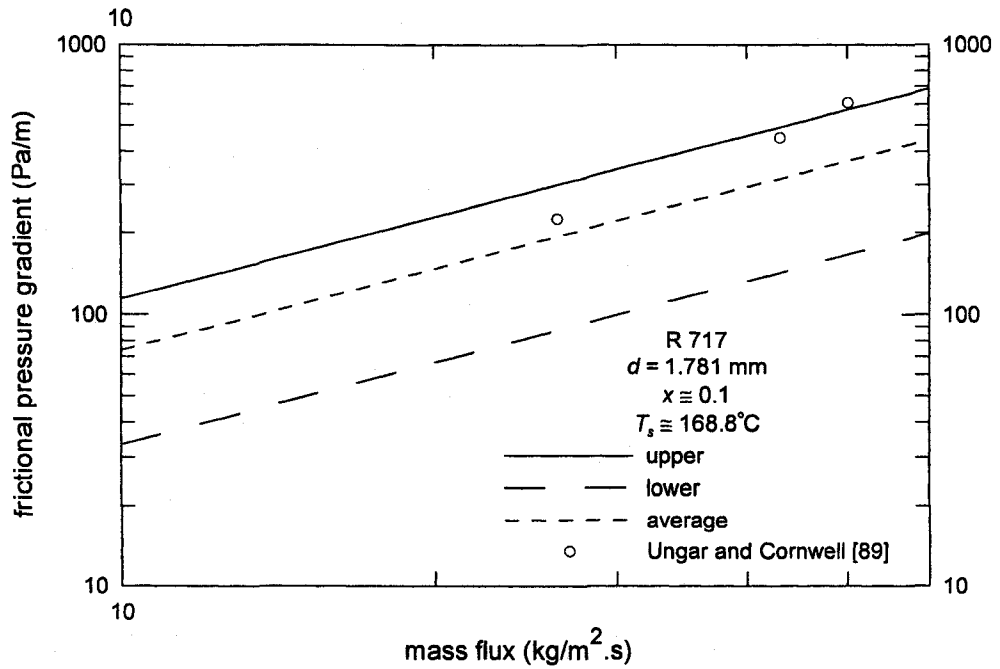


Figure 6.6 Comparison of the Model with Ungar and Cornwell's Data [89]

6.2.3.2 ϕ_l and ϕ_g versus Lockhart-Martinelli Parameter (X)

Figures 6.7-6.11 show ϕ_l versus Lockhart-Martinelli parameter (X) for turbulent-turbulent flow. Equation (6.2) represents the lower bound and Eq. (6.11) represents the upper bound, while Eq. (6.14) represents the average. Figure 6.7 compares the present model with Hashizume's data [79] for R 12 flow in a smooth horizontal pipe of $d = 10$ mm at $T_s = 20^\circ\text{C}$ and $x = 0.1, 0.3, 0.5$ and 0.8 respectively. Figure 6.8 compares the present model with Hashizume's data [79] for R 22 flow in a smooth horizontal pipe of $d = 10$ mm at $T_s = 20^\circ\text{C}$ and $x = 0.1, 0.3, 0.5$ and 0.8 respectively. Figure 6.9 compares the present model with Govier and Omer's data [203] for air-water mixtures in a smooth horizontal pipe of 1.026 in (26.06 mm) diameter while Fig. 6.10 compares the present model with Janssen and Kervinen's data [204] for steam-water flow in a smooth horizontal pipe at a pressure of 1 066 psia (73.5 bar) and $d = 0.742$ in (18.85 mm) for $G = 1.68 \times 10^6$ lb_m/ft².hr (2 278 kg/m².s). In Figs. 6.7-6.10, the mean model predicts the published data of ϕ_l with the root mean square (RMS) error of 14.41%, 21.47%, 16.19%, and 18.7% respectively, while the asymptotic model gives the root mean square (RMS) error of 10.8%, 16.68%, 19.87%, and 12.9% respectively.

Figure 6.11 shows ϕ_l versus Lockhart-Martinelli parameter (X) for turbulent-turbulent flow for all data in Figs. 6.7-6.10. It is clear that the bounds contain a vast majority of the data.

Figures 6.12-6.14 show ϕ_l versus Lockhart-Martinelli parameter (X) for laminar-laminar flow. Equation (6.22) represents the lower bound and Eq. (6.30) represents the upper bound, while Eq. (6.34) represents the average. Figure 6.12 compares the present model with Lee and Lee's data [206] for air-water mixture flow

in a smooth horizontal rectangular channels of 0.4×20 mm ($d_h = 0.78$ mm). Figure 6.13 compares the present model with Chung and Kawaji's data [207] for nitrogen-water mixture flow in a smooth horizontal circular channels of $d = 0.25$ mm at different mass fluxes between 30 and 5 758 kg/m².s. Figure 6.14 compares the present model with Kawaji et al.'s data [208] for nitrogen-water mixture flow in a smooth horizontal circular channels of $d = 0.1$ mm. The gas flow is in the main channel while the liquid flow is in the branch of T-junction. In Figs. 6.12-6.14, the mean model predicts the published data of ϕ_l with the root mean square (RMS) error of 17.91%, 19.29%, and 10.49% respectively, while the asymptotic model gives the root mean square (RMS) error of 14.07%, 16.09%, and 11.34% respectively.

Figure 6.15 shows ϕ_l versus Lockhart-Martinelli parameter (X) for laminar-laminar flow for all data in Figs. 6.12-6.14. Once again it is clear that a vast majority of the data lie within the bounds.

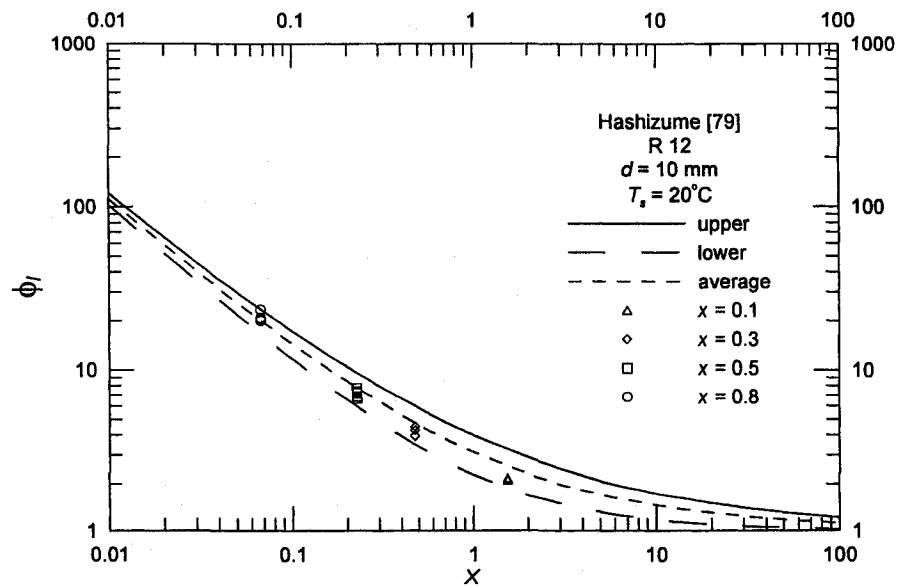


Figure 6.7 Comparison of the Present Model with Hashizume's Data [79]

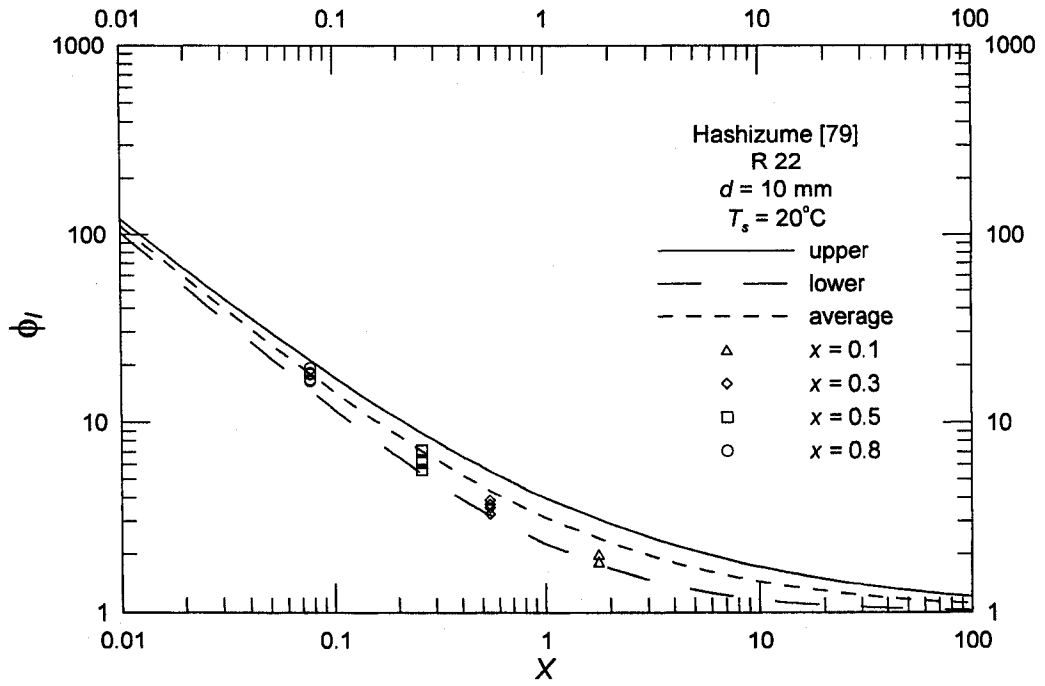


Figure 6.8 Comparison of the Present Model with Hashizume's Data [79]

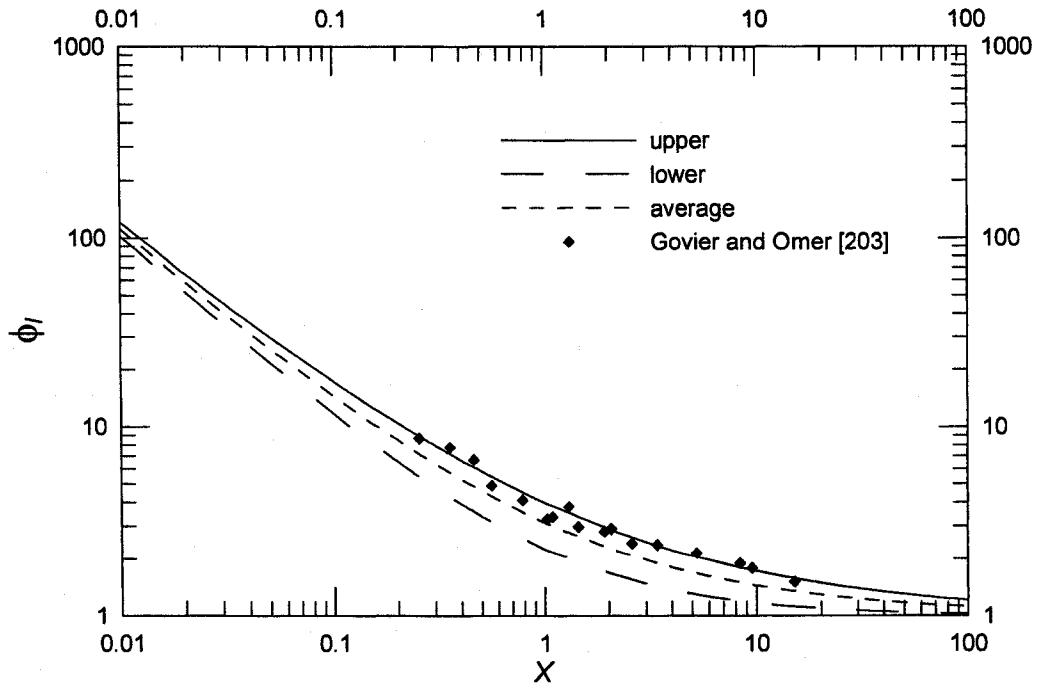


Figure 6.9 Comparison of the Present Model with Govier and Omer's Data [203]

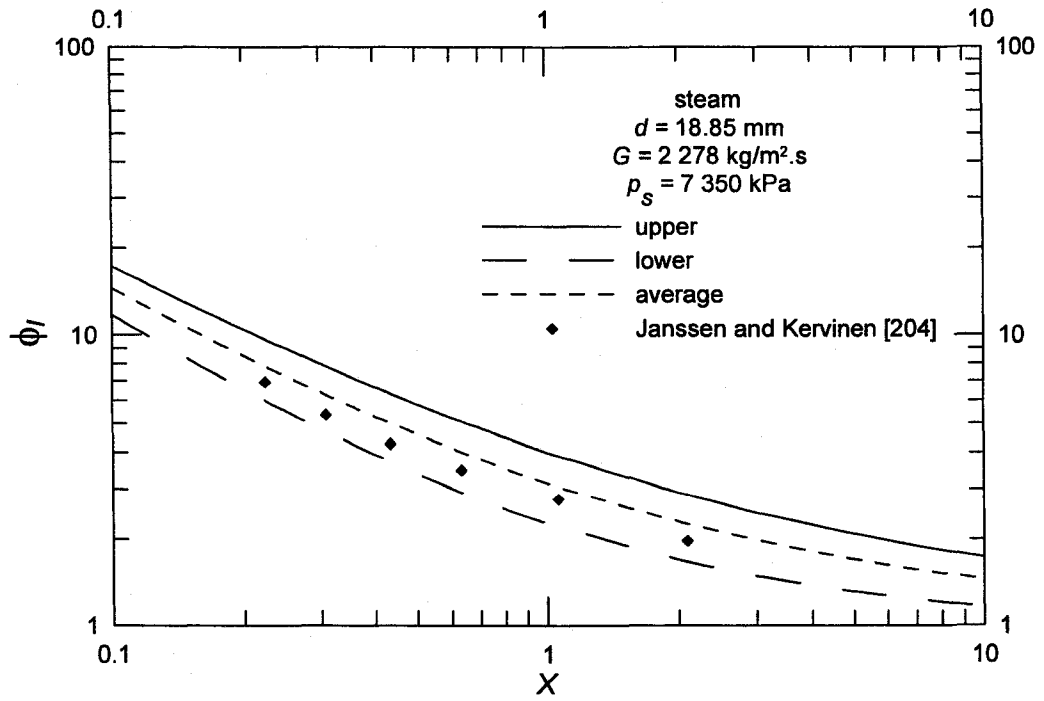


Figure 6.10 Comparison of the Model with Janssen and Kervinen's Data [204]

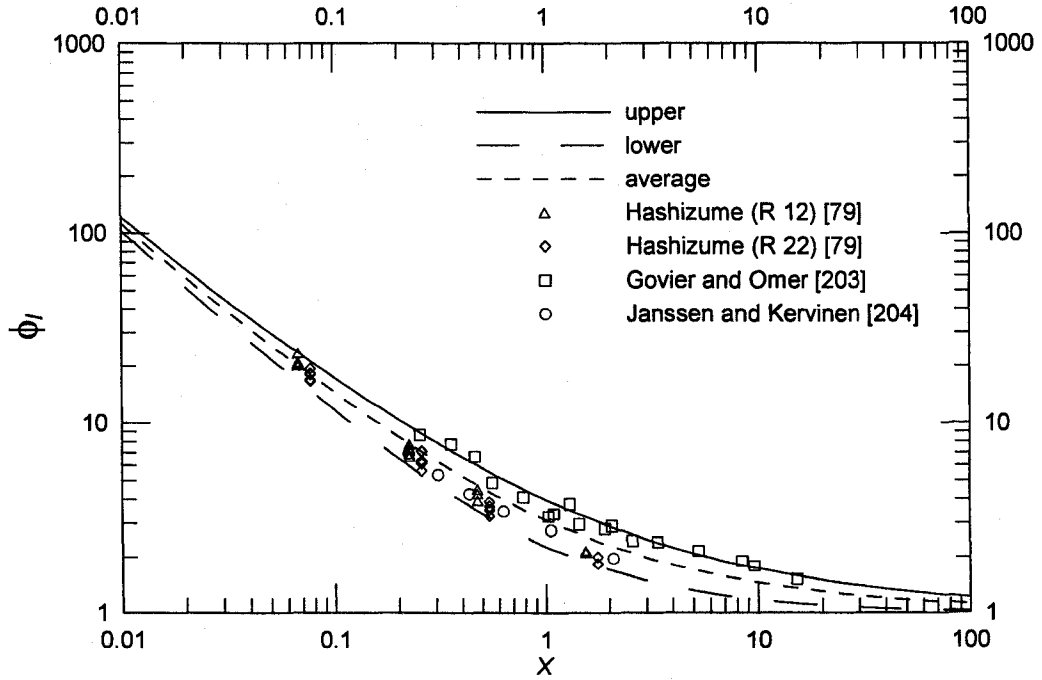


Figure 6.11 ϕ_1 versus X for Different Sets of Data

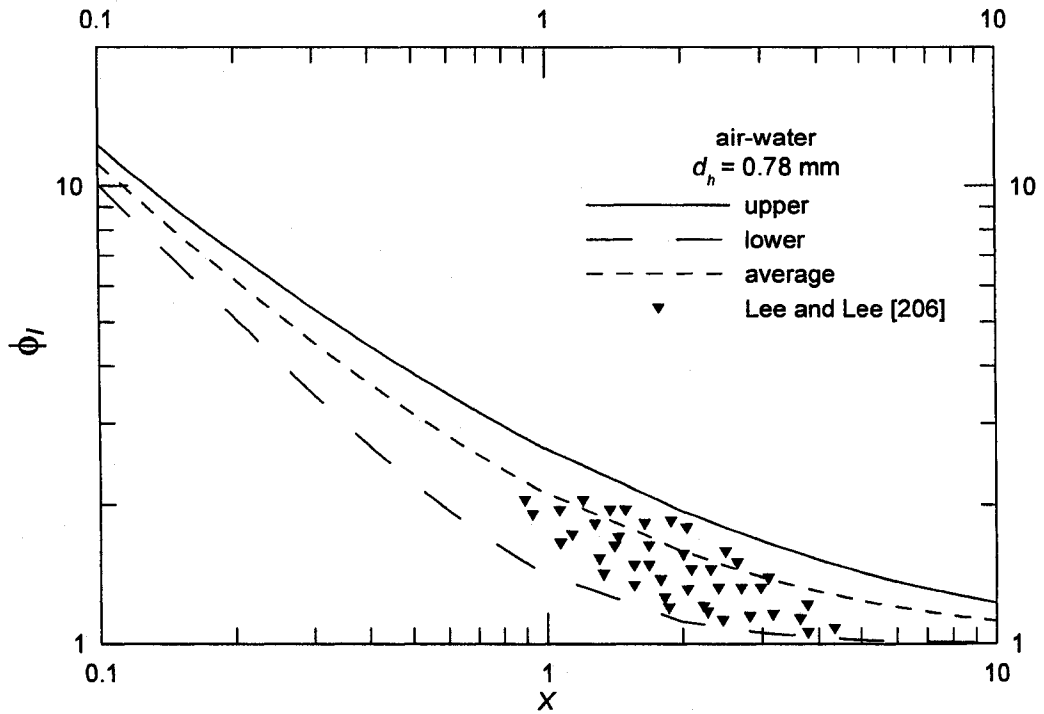


Figure 6.12 Comparison of the Present Model with Lee and Lee's Data [206]

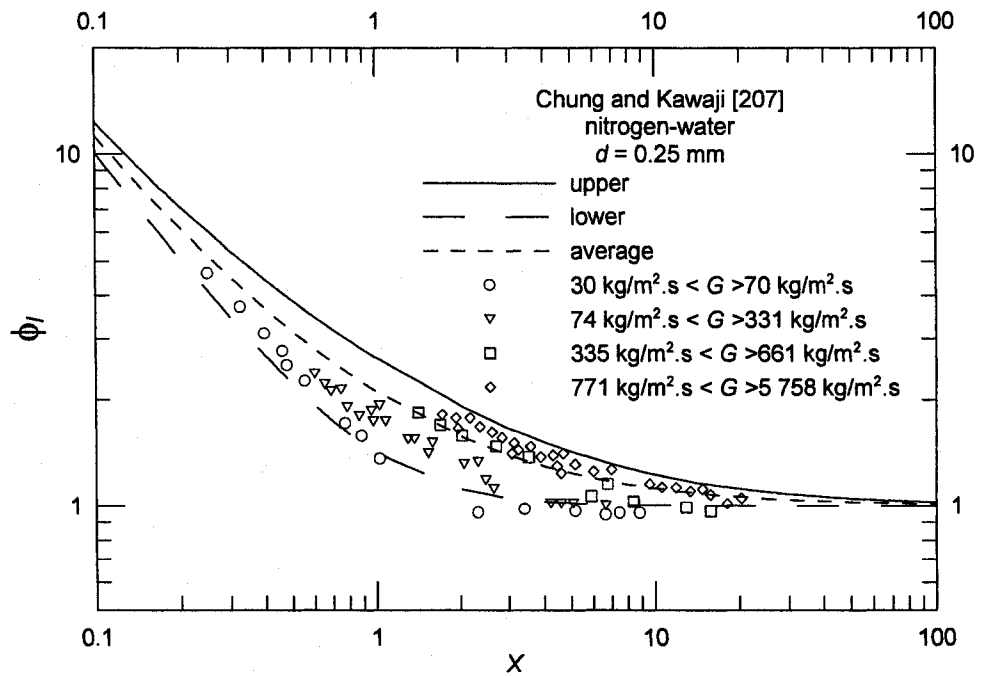
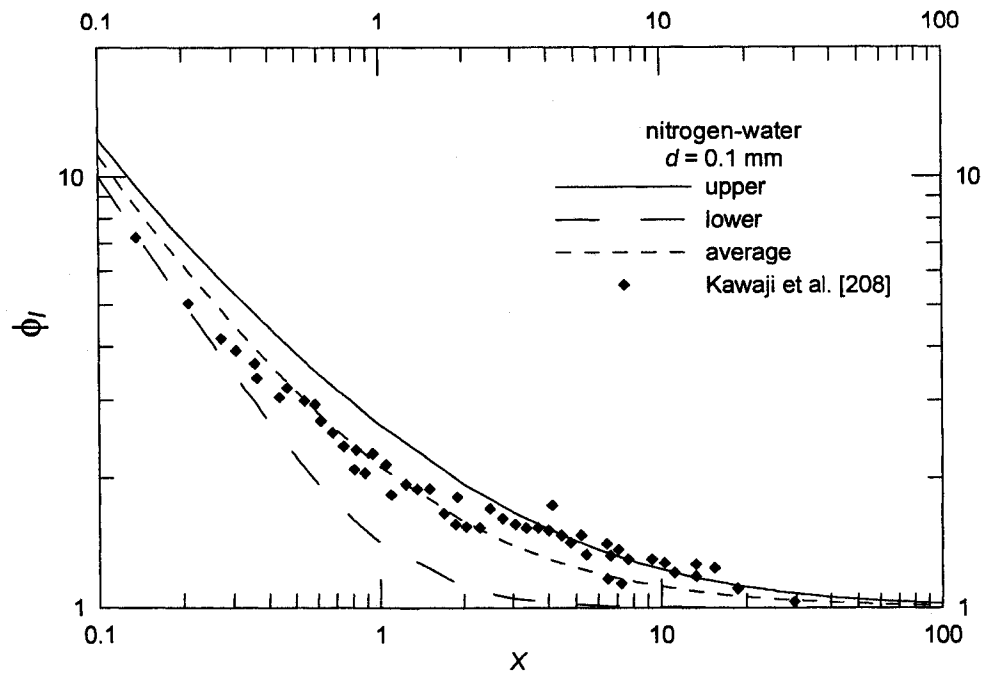


Figure 6.13 Comparison of the Model with Chung and Kawaji's Data [207]



**Figure 6.14 Comparison of the Present Model with Kawaji et al.'s Data [208]
(Gas in the Main Channel and Liquid in the Branch)**

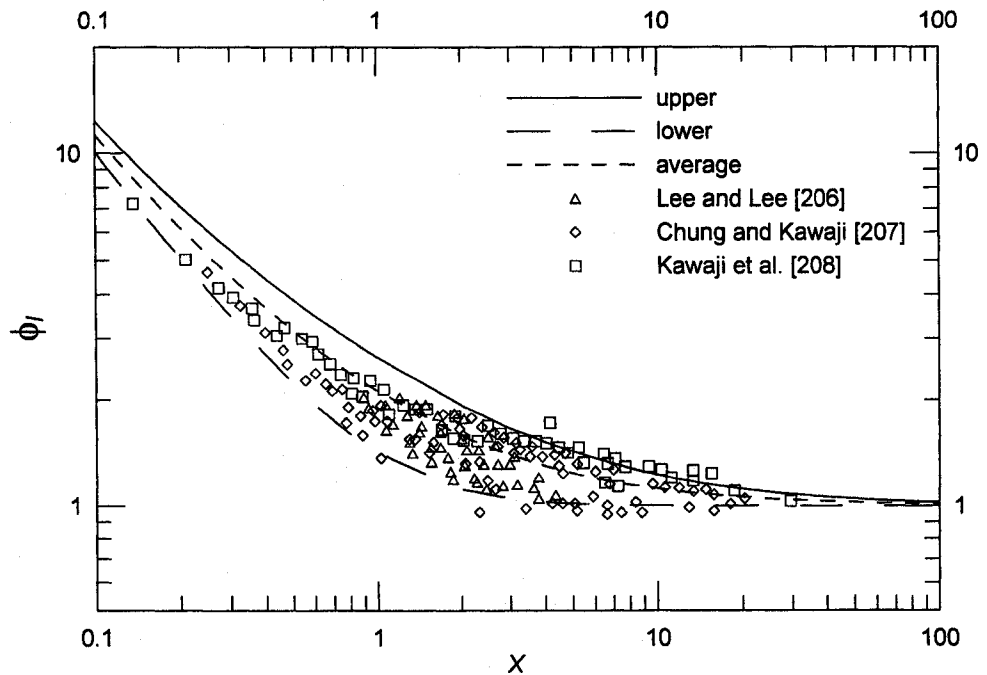


Figure 6.15 ϕ_l versus X for Different Sets of Data

Figures 6.16 and 6.17 show ϕ_g versus Lockhart-Martinelli parameter (X) for turbulent-turbulent flow. Equation (6.3) represents the lower bound and Eq. (6.12) represents the upper bound, while Eq. (6.15) represents the average. Figure 6.16 compares the present model with Cicchitti et al.'s data [46] for adiabatic flow of steam in a smooth pipe of 5.1 mm diameter at a pressure of 30-60 kg/cm² (29.4-58.8) bar. Cicchitti et al. [46] mentioned that their steam data for turbulent-turbulent flow (ϕ_g versus X) fall in the strip bounded by the Martinelli and Nelson lines drawn up for atmospheric and critical pressures. The advantages of the present bound models over the Martinelli and Nelson lines [8] at atmospheric and critical pressures are:

i. The Martinelli and Nelson lines [8] at atmospheric and critical pressures were presented in a graphical manner while the present bound models are presented in the form of simple equations.

ii. The Martinelli and Nelson lines [8] at atmospheric and critical pressures can be used only when steam is the working fluid while the present bound models can be used for other working fluids such as steam, R12, R22, etc.

Figure 6.17 compares the present model with Cheremisinoff and Davis's [205] for stratified flow of air-water mixtures in a smooth horizontal pipe of 63.5 mm diameter. In Figs. 6.16 and 6.17, the mean model predicts the published data of ϕ_g with the root mean square (RMS) error of 12.84% and 22.03% respectively, while the asymptotic model gives the root mean square (RMS) error of 9.56% and 18.51% respectively.

Figure 6.18 shows ϕ_g versus Lockhart-Martinelli parameter (X) for turbulent-turbulent flow for all data in Figs. 6.16 and 6.17. It is clear that the bounds contain a vast majority of the data.

Figures 6.19 and 6.20 show ϕ_g versus Lockhart-Martinelli parameter (X) for laminar-laminar flow. Equation (6.23) represents the lower bound and Eq. (6.31) represents the upper bound, while Eq. (6.35) represents the average. Figure 6.19 compares the present model with Kawaji et al.'s data [208] for nitrogen-water mixture flow in a smooth horizontal circular channels of $d = 0.1$ mm. The liquid flow is in the main channel while the gas flow is in the branch of T-junction. Figure 6.20 compares the present model with Ohtake et al.'s data [209] for Argon-water mixture flow in smooth horizontal rectangular channels of 0.18×1.87 , 0.26×4.28 , 0.26×9.87 and 0.25×19.9 mm ($d_h = 0.32$, 0.49 , 0.42 and 0.49 mm) respectively. The mean model predicts the published data of ϕ_g with the root mean square (RMS) error of 14.87%, and 28.04% respectively, while the asymptotic model gives the root mean square (RMS) error of 17.36% and 24.16% respectively.

In Fig. 6.20, if the two lower points of 0.18×1.87 , and 0.26×9.87 mm ($d_h = 0.32$ and 0.42 mm) respectively are not taken into account, the root mean square (RMS) error will be 21.77% instead of 28.04% while the asymptotic model gives the root mean square (RMS) error of 18.24% instead of 24.16%. These outlying points are likely affected by experimental error.

Figure 6.21 shows ϕ_g versus Lockhart-Martinelli parameter (X) for laminar-laminar flow for all data in Figs. 6.19 and 6.20. Once again it is clear that a vast majority of the data lie within the bounds.

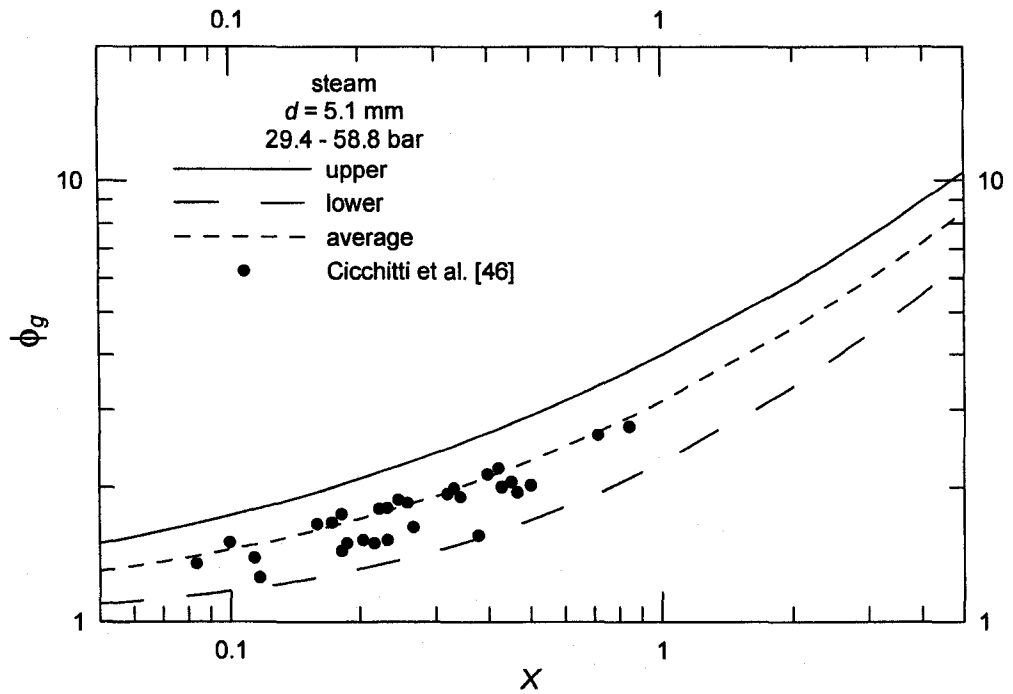


Figure 6.16 Comparison of the Present Model with Cicchitti et al.'s Data [46]

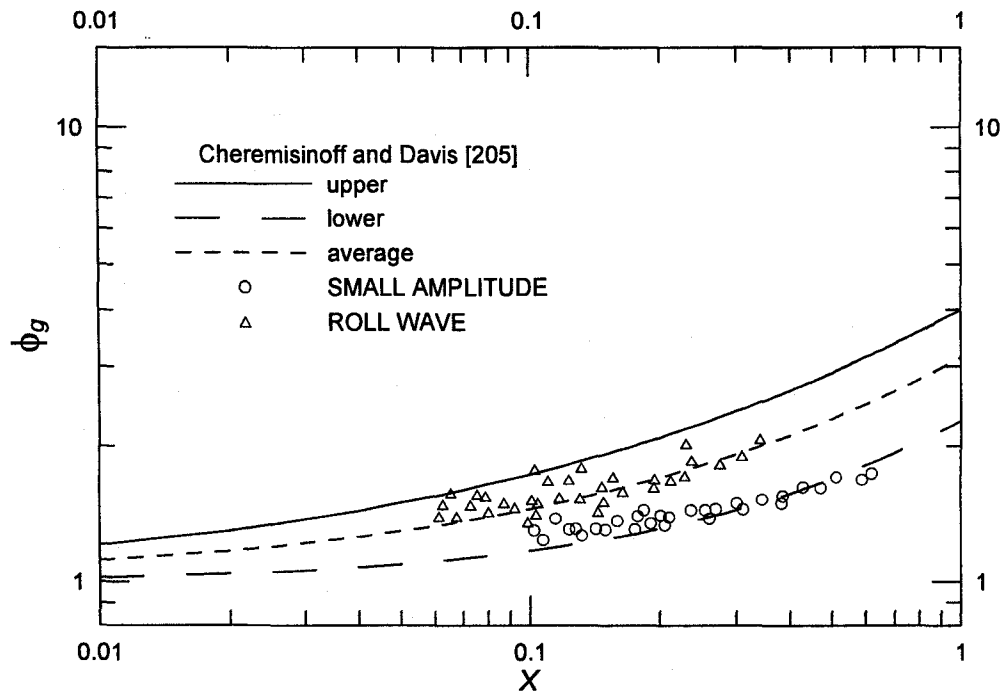


Figure 6.17 Comparison of the Present Model with Chermisinoff and Davis's Data [205]

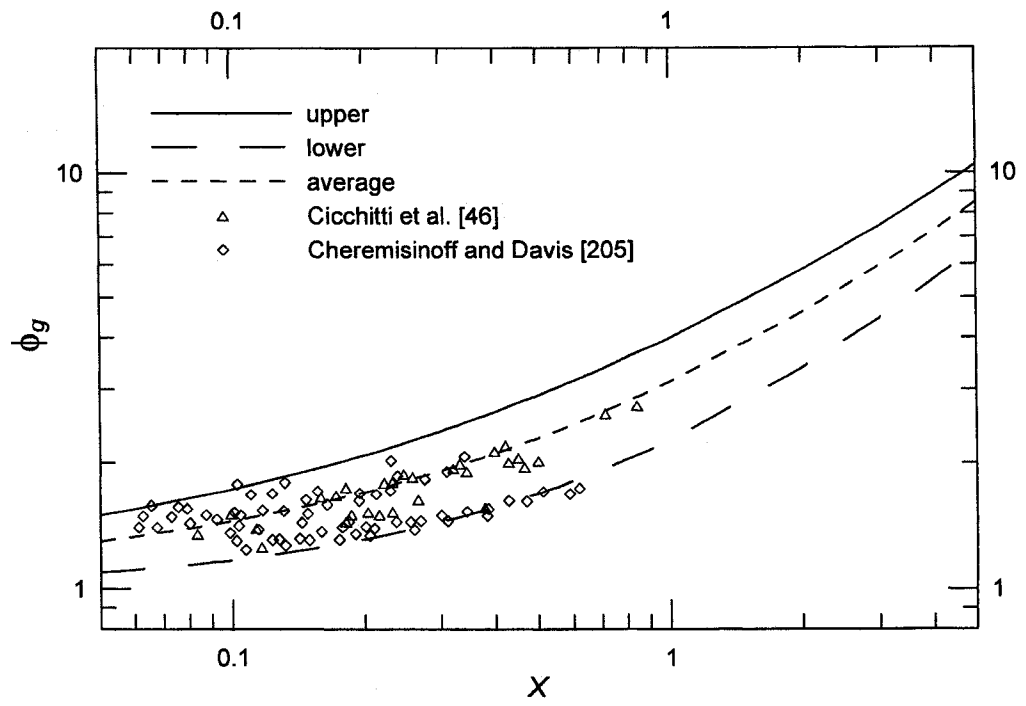


Figure 6.18 ϕ_g versus X for Different Sets of Data

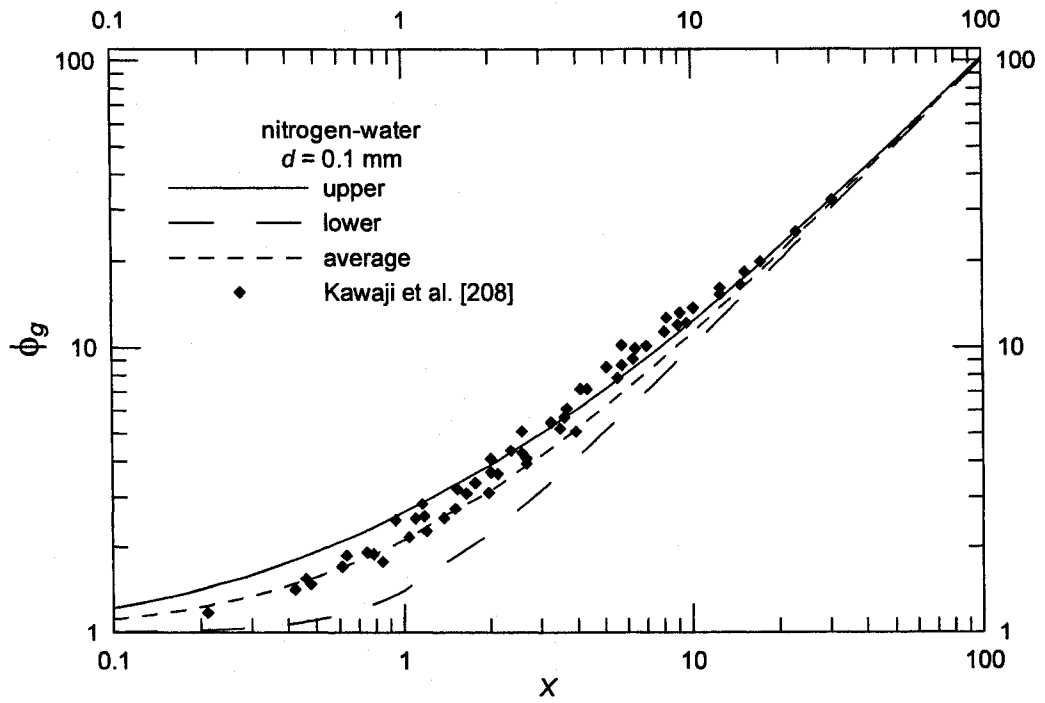


Figure 6.19 Comparison of the Present Model with Kawaji et al.'s Data [208]
(Liquid in the Main Channel and Gas in the Branch)

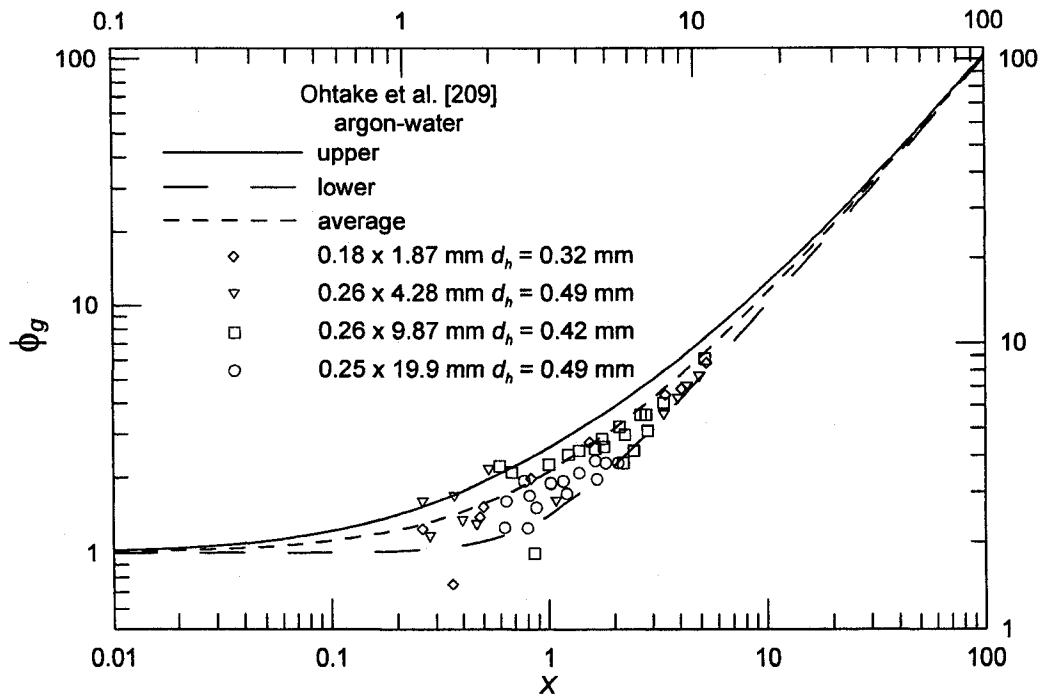


Figure 6.20 Comparison of the Present Model with Ohtake et al.'s Data [209]

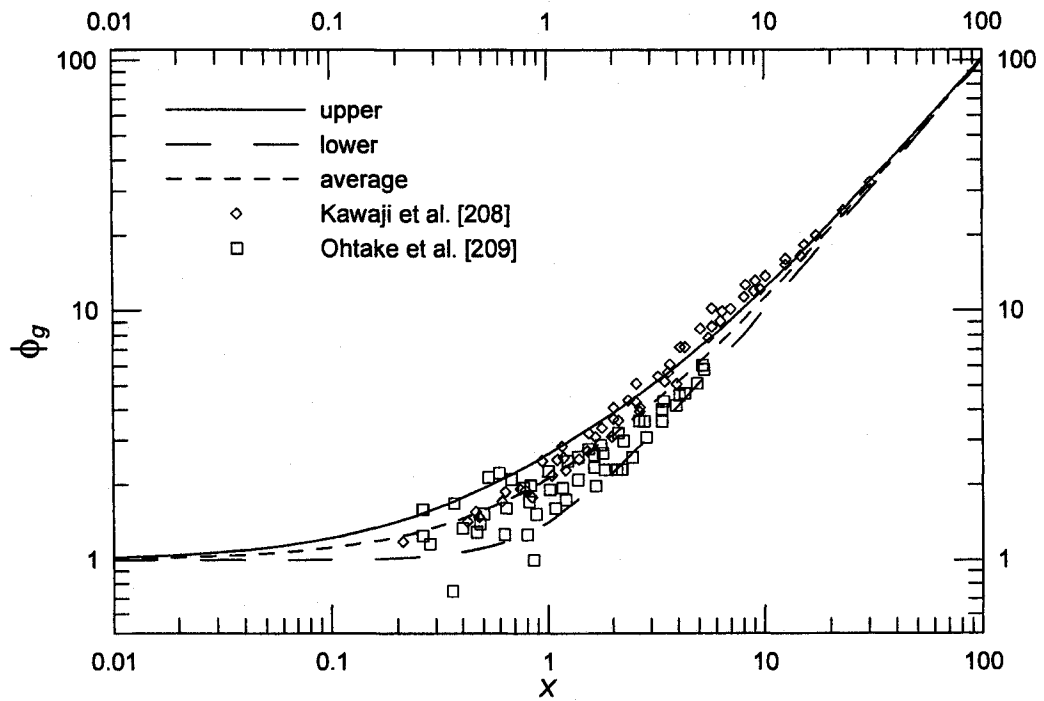


Figure 6.21 ϕ_g versus X for Different Sets of Data

6.3 Development of Bounds on Two-Phase Void Fraction in Circular Pipes

In this section, rational bounds for two-phase void fraction in circular pipes will be developed. These bounds may be used to determine the maximum and minimum values that may reasonably be expected in a two-phase flow. Further, by averaging these limiting values an acceptable prediction for the void fraction is obtained which is then bracketed by the bounding values:

$$\alpha_{lower} \leq \alpha \leq \alpha_{upper} \quad (6.37)$$

The bounds model will be in the form of two-phase void fraction against mass quality at constant mass flow rate. The bounds model may also be presented in the form of void fraction against the Lockhart-Martinelli parameter (X).

For the case of large circular pipes, the bounds method is based on turbulent liquid-turbulent gas assumption [210,211]. This assumption is suitable because, in practice, both Re_l and Re_g are most often greater than 2 000 in large circular pipes.

Both the lower and upper bounds are based on the separate cylinders formulation. The reasons of choosing lower and upper bounds are mentioned before in Section 6.2.1.

6.3.1 The Lower Bound

In chapter 5, the separate cylinders analysis [29] was utilized and introduced the Blasius equation [10] to represent the Fanning friction factor for turbulent-turbulent flow. From Table 5.3, expression of α for turbulent-turbulent flow is

$$\alpha = \frac{I}{I + X^{16/19}} \quad (6.38)$$

For turbulent-turbulent flow, the Lockhart-Martinelli parameter (X) can be expressed as [86]:

$$X = \left(\frac{1-x}{x} \right)^{7/8} \left(\frac{\rho_g}{\rho_l} \right)^{1/2} \left(\frac{\mu_l}{\mu_g} \right)^{1/8} \quad (6.39)$$

From Eqs. (6.38) and (6.39), we obtain

$$\alpha = \frac{I}{I + \left[\left(\frac{1-x}{x} \right)^{7/8} \left(\frac{\rho_g}{\rho_l} \right)^{1/2} \left(\frac{\mu_l}{\mu_g} \right)^{1/8} \right]^{16/19}} \quad (6.40)$$

6.3.2 The Upper Bound

In order to make the bounds model tight and present it in the form of void fraction (α) against the Lockhart-Martinelli parameter (X), the Lockhart-Martinelli correlation is chosen to represent the upper bound although the homogeneous model gives higher prediction of the void fraction (α) than the Lockhart-Martinelli correlation at same the mass quality (x) except at low values of the mass quality (x) as shown in Figs. 3.1-3.4.

Butterworth [141] represented the Lockhart-Martinelli correlation by the relation:

$$\alpha = \frac{I}{I + 0.28X^{0.71}} \quad (6.41)$$

From Eqs. (6.39) and (6.41), we obtain

$$\alpha = \frac{1}{1 + 0.28 \left[\left(\frac{1-x}{x} \right)^{7/8} \left(\frac{\rho_g}{\rho_l} \right)^{1/2} \left(\frac{\mu_l}{\mu_g} \right)^{1/8} \right]^{0.71}} \quad (6.42)$$

Since $(1-\alpha)$ represents the liquid fraction, the lower and upper bounds are reversed in the case of liquid fraction data.

6.3.3 Mean Model

A simple model may be developed by averaging the two bounds. This is defined as follows:

$$\alpha_{av} = \frac{0.5}{1 + X^{16/19}} + \frac{0.5}{1 + 0.28X^{0.71}} \quad (6.43)$$

or

$$\alpha_{av} = \frac{0.5}{1 + \left[\left(\frac{1-x}{x} \right)^{7/8} \left(\frac{\rho_g}{\rho_l} \right)^{1/2} \left(\frac{\mu_l}{\mu_g} \right)^{1/8} \right]^{16/19}} + \frac{0.5}{1 + 0.28 \left[\left(\frac{1-x}{x} \right)^{7/8} \left(\frac{\rho_g}{\rho_l} \right)^{1/2} \left(\frac{\mu_l}{\mu_g} \right)^{1/8} \right]^{0.71}} \quad (6.44)$$

6.3.4 Results and Discussion

Examples of two-phase void fraction versus mass quality at constant mass flow rate from published experimental studies are presented to show features of the

bounds. The published data include different working fluids such as steam, R-12, and R-22 at different pipe diameters, different pressures, and different mass flow rates. Also, the model is verified using published experimental data of void fraction (α) and liquid fraction ($1-\alpha$) versus the Lockhart-Martinelli parameter (X) for different working fluids such as R-12, R-22, and air-water mixtures in turbulent-turbulent flow.

6.3.4.1 Comparison of the Present Model with Data

Figures 6.22-6.25 show the void fraction versus mass quality. Equation (6.40) represents the lower bound and Eq. (6.42) represents the upper bound while Eq. (6.44) represents the average. Figure 6.22 compares the present model with Larson's data [216] for adiabatic flow of steam-water mixture at $p_s = 1\ 000$ psia (6 894.74 kPa). Figure 6.23 compares the present model with Hashizume's data [79] for R 12 flow at $T_s = 50^\circ\text{C}$ and $m = 25, 35, 50, 70$ and 100 kg/hr respectively in a smooth horizontal pipe at $d = 10$ mm. Figure 6.24 compares the present model with Hashizume's data [79] for R 22 flow at $T_s = 39^\circ\text{C}$ and $m = 25, 35, 50, 70$ and 100 kg/hr respectively in a smooth horizontal pipe at $d = 10$ mm. Figure 6.25 compares the present model with for Wojtan et al's data [217] R 410A flow at $T_s = 5^\circ\text{C}$ and $G = 70, 150, 200$ and 300 kg/m².s respectively in a smooth horizontal pipe at $d = 5/8$ in. (15.875 mm). In Figs. 6.22-6.25, the mean model predicts the published data of α with the root mean square (RMS) error of 12.17%, 9.04%, 7.39% and 26.86% respectively. In Fig. 6.25, if the two lower points at $G = 70$ kg/m².s are not included, RMS will be 10.6% instead of 26.86%.

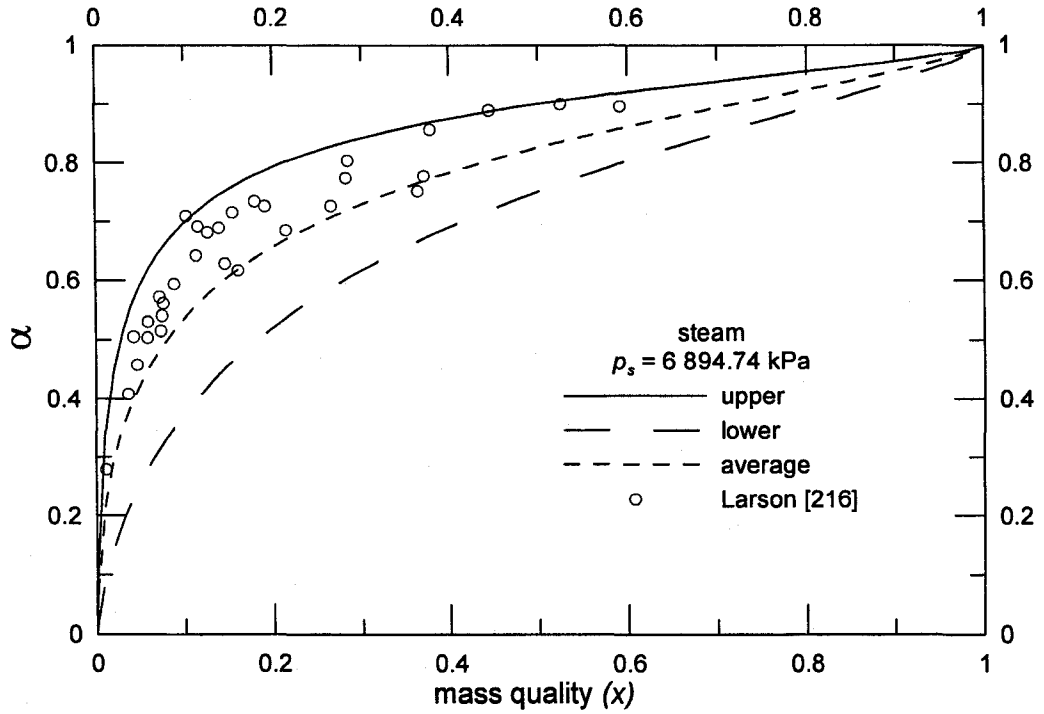


Figure 6.22 Comparison of the Present Model with Larson's Data [216]

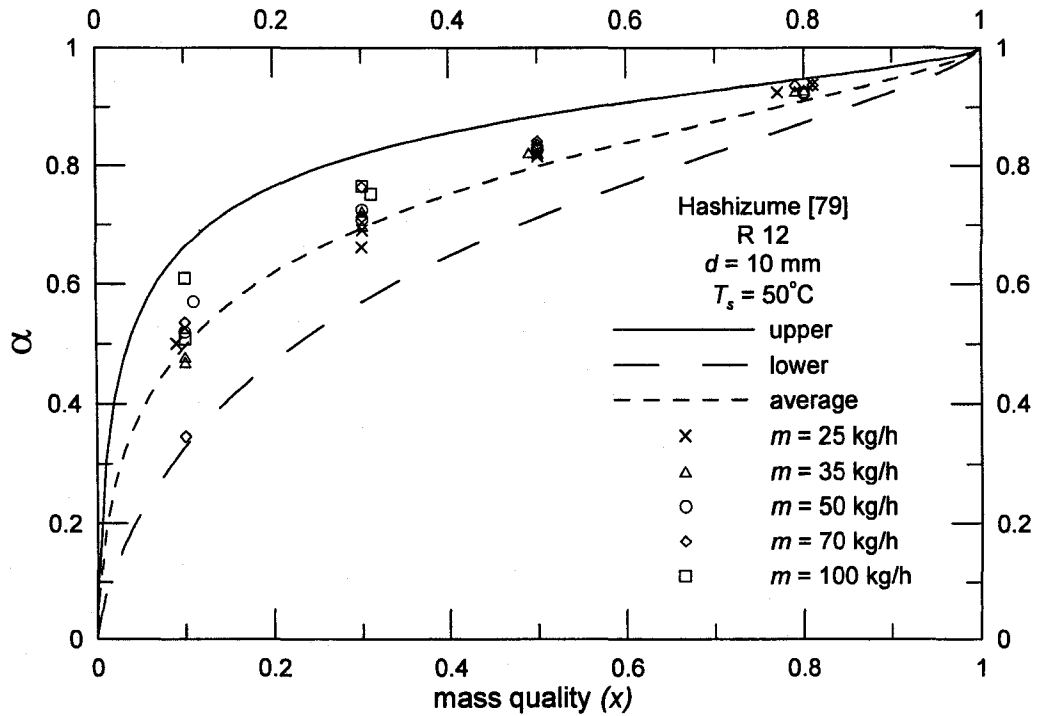


Figure 6.23 Comparison of the Present Model with Hashizume's Data [79]

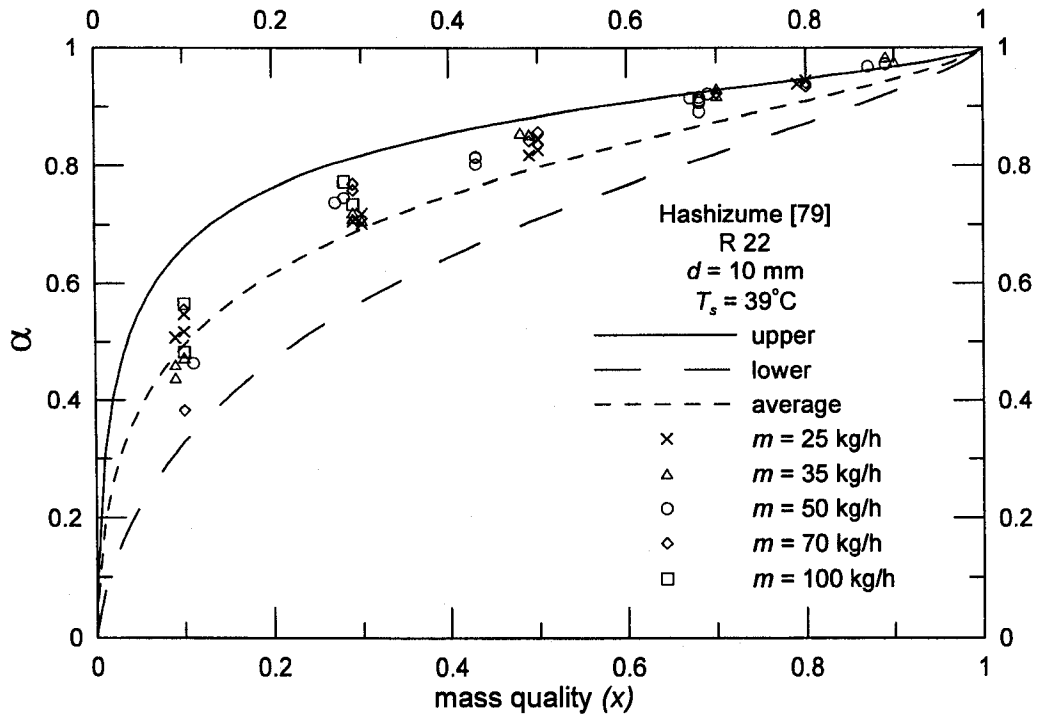


Figure 6.24 Comparison of the Present Model with Hashizume's Data [79]

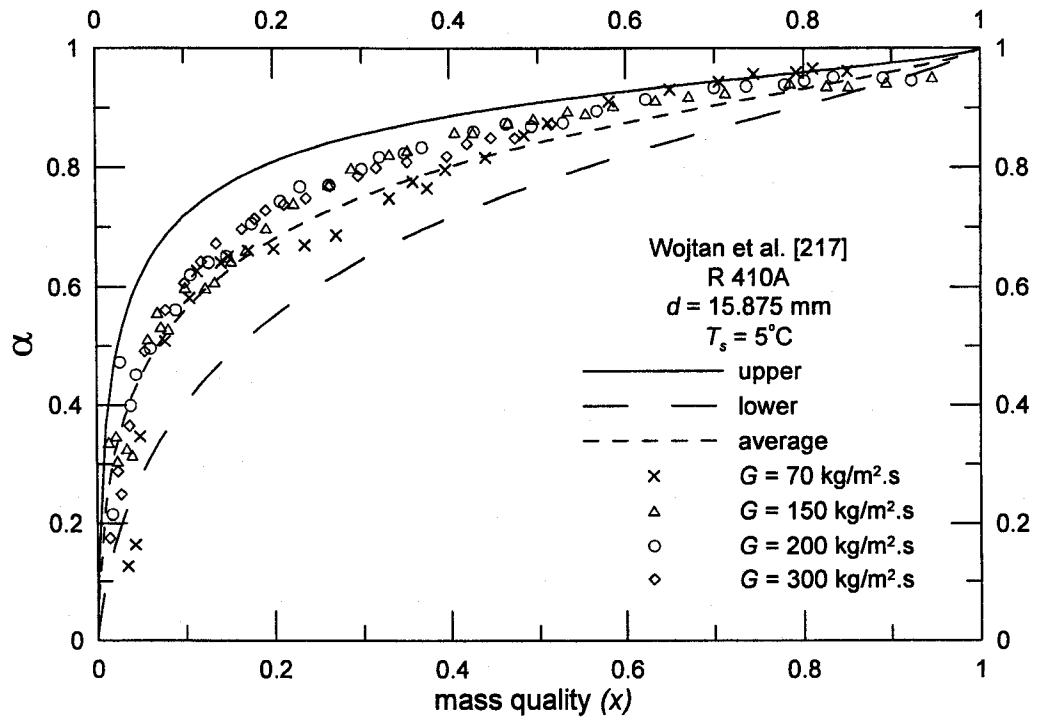


Figure 6.25 Comparison of the Present Model with Wojtan et al.'s Data [217]

6.3.4.2 α and $(1-\alpha)$ versus Lockhart-Martinelli Parameter (X)

Figures 6.26 and 6.27 show α versus Lockhart-Martinelli parameter (X) for turbulent-turbulent flow. Equation (6.38) represents the lower bound and Eq. (6.41) represents the upper bound, while Eq. (6.43) represents the average. Figure 6.26 compares the present model with Hashizume's data [79] for R 12 flow in a smooth horizontal pipe of $d = 10$ mm at $T_s = 39^\circ\text{C}$ and $x = 0.1, 0.3, 0.5$ and 0.8 respectively. Figure 6.27 compares the present model with Hashizume's data [79] for R 22 flow in a smooth horizontal pipe of $d = 10$ mm at $T_s = 50^\circ\text{C}$ and $x = 0.1, 0.3, 0.5$ and 0.8 respectively. In Figs. 6.26 and 6.27, the mean model predicts the published data of α with the root mean square (RMS) error of 9.21% and 5.78% respectively.

Figure 6.28 shows α versus Lockhart-Martinelli parameter (X) for turbulent-turbulent flow for all data in Figs. 6.26 and 6.27.

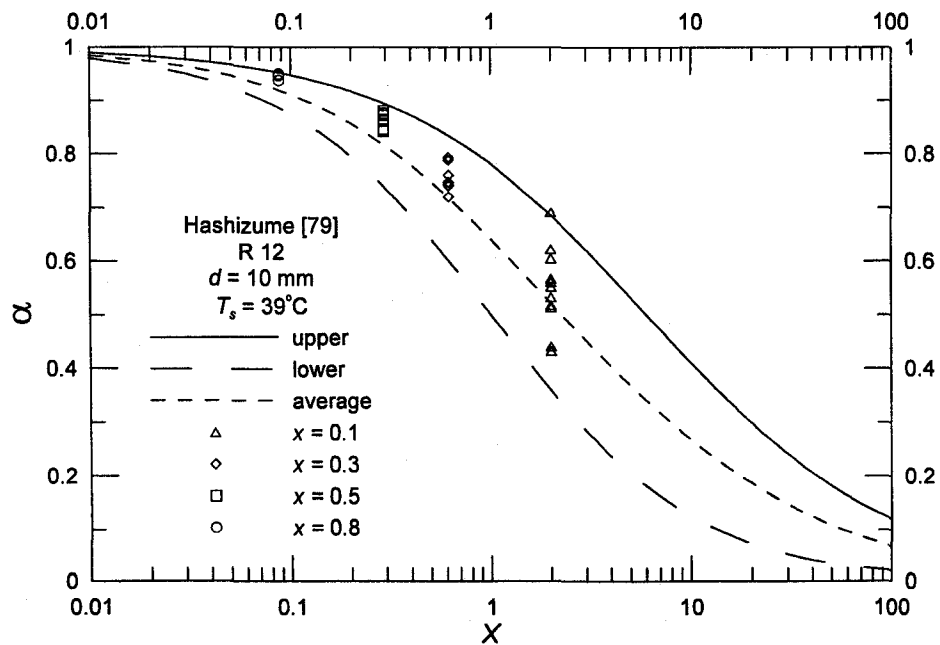


Figure 6.26 Comparison of the Present Model with Hashizume's Data [79]

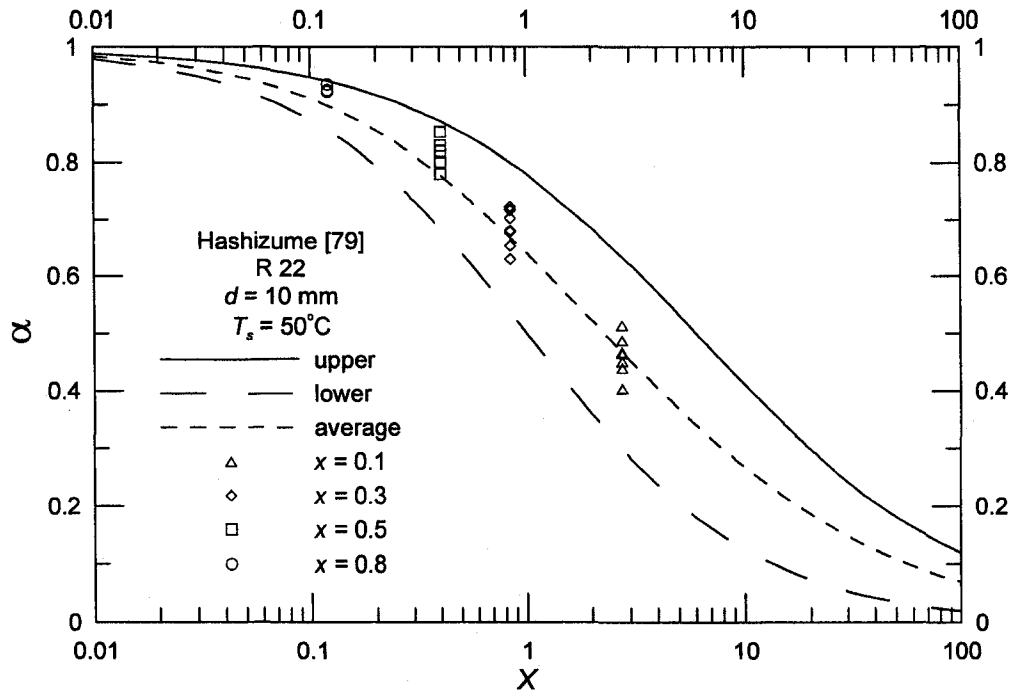


Figure 6.27 Comparison of the Present Model with Hashizume's Data [79]

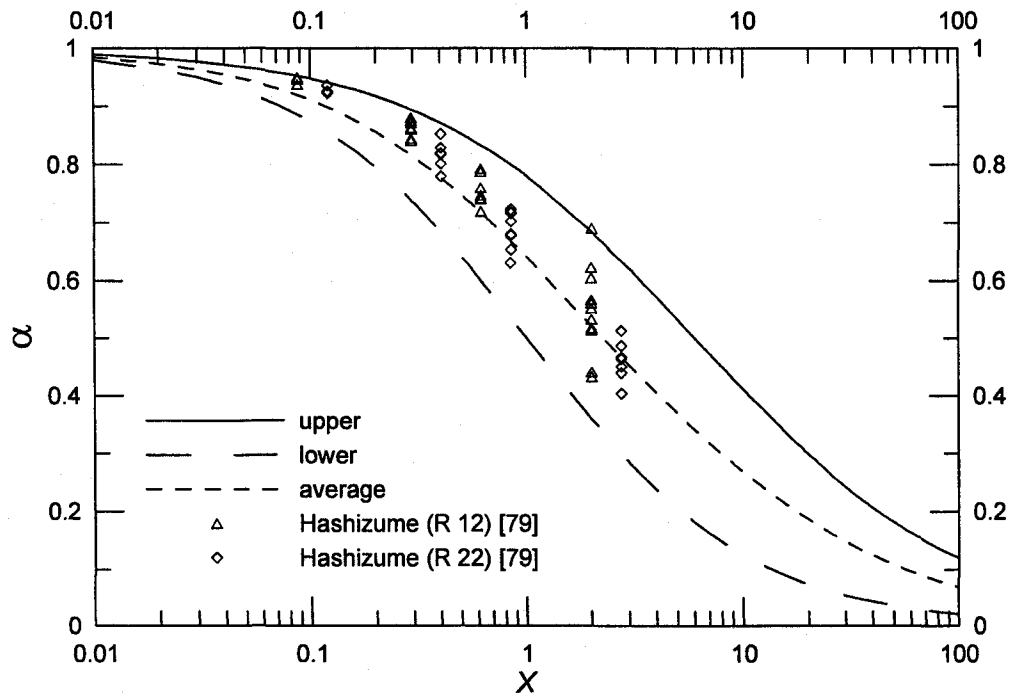


Figure 6.28 α versus X for Different Sets of Data

Figures 6.29 and 6.30 show $1-\alpha$ versus Lockhart-Martinelli parameter (X) for turbulent-turbulent flow. The lower bound is based on the Butterworth relation [141] for liquid fraction ($1-\alpha$). The upper bound is based on separate cylinders model [29] for liquid fraction ($1-\alpha$) for turbulent-turbulent flow. The average is based on the arithmetic mean of lower bound and upper bound for liquid fraction ($1-\alpha$). Figure 6.29 compares the present model with Bergelin and Gazley's data [218] for air-water flow in a smooth horizontal pipe at $m_t = 650, 1\ 070, 1\ 420, 1\ 830,$ and $2\ 275$ lb_m/hr (294.84, 485.352, 644.112, 830.088, and 1 031.94 kg/hr) respectively. Figure 6.30 compares the present model with Baker's data [3] for simultaneous flow of oil and gas in pipelines of $d = 8,$ and 10 in. (203.2 and 254 mm) respectively. In Figs. 6.29 and 6.30, the mean model predicts the published data of ($1-\alpha$) with the root mean square (RMS) error of 4.99% and 9.44% respectively.

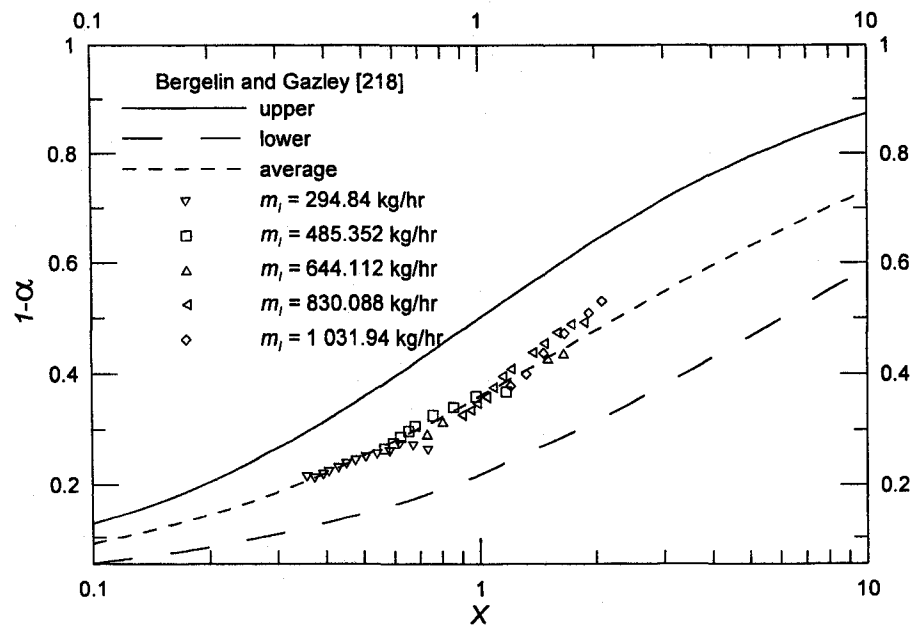


Figure 6.29 Comparison of the Model with Bergelin and Gazley's Data [218]

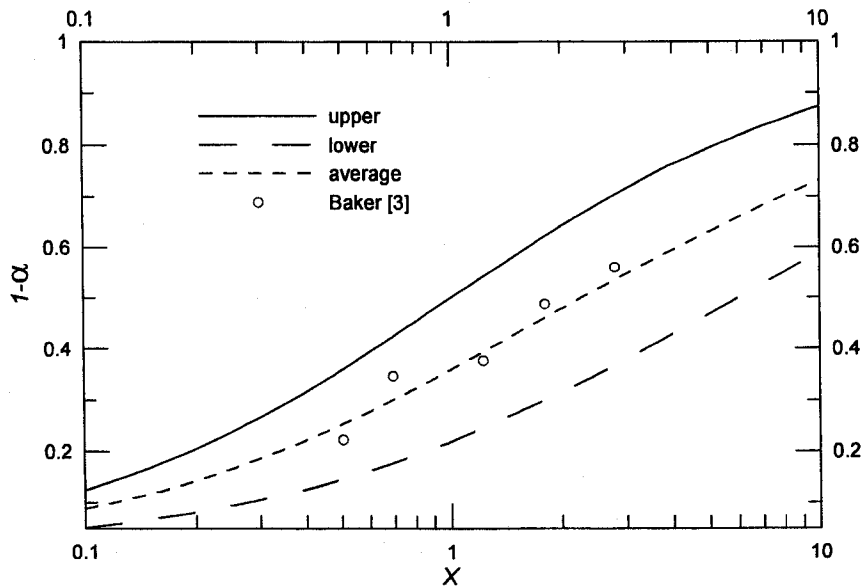


Figure 6.30 Comparison of the Present Model with Baker's Data [3]

Figure 6.31 shows $1-\alpha$ versus Lockhart-Martinelli parameter (X) for turbulent-turbulent flow for all data in Figs. 6.29 and 6.30.

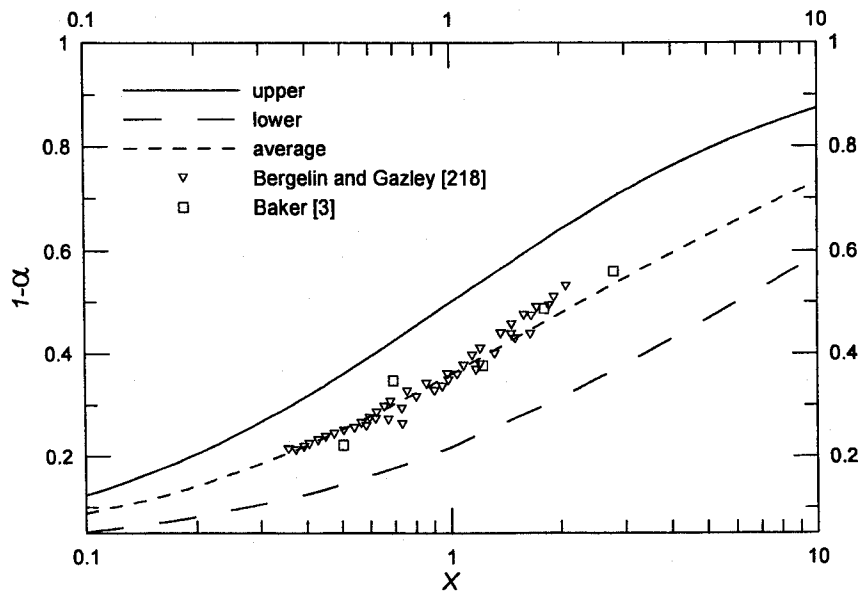


Figure 6.31 $1-\alpha$ versus X for Different Sets of Data

6.4 Summary

Tables 6.1-6.3 present summaries for bounds on two-phase frictional pressure gradient in large circular pipes, bounds on two-phase frictional pressure gradient in small circular pipes and bounds on two-phase void fraction in circular pipes.

Table 6.1 Bounds on Two-Phase Frictional Pressure Gradient in Large Circular Pipes

Assumption	Turbulent-Turbulent Flow
Lower Bound	Equation (6.2) for ϕ_l^2 Equation (6.3) for ϕ_g^2 Equation (6.9) for $(dp/dz)_f$
Upper Bound	Equation (6.11) for ϕ_l^2 Equation (6.12) for ϕ_g^2 Equation (6.13) for $(dp/dz)_f$
Mean Model	Equation (6.14) for ϕ_l^2 Equation (6.15) for ϕ_g^2 Equation (6.16) for $(dp/dz)_f$

Table 6.2 Bounds on Two-Phase Frictional Pressure Gradient in Small Circular Pipes

Assumption*	Laminar-Laminar Flow
Lower Bound	Equation (6.22) for ϕ_l^2 Equation (6.23) for ϕ_g^2 Equation (6.27) for $(dp/dz)_f$
Upper Bound	Equation (6.30) for ϕ_l^2 Equation (6.31) for ϕ_g^2 Equation (6.33) for $(dp/dz)_f$
Mean Model	Equation (6.34) for ϕ_l^2 Equation (6.35) for ϕ_g^2 Equation (6.36) for $(dp/dz)_f$

* Also suitable for the flow in minichannels and microchannels.

Table 6.3 Bounds on Two-Phase Void Fraction in Circular Pipes

Assumption	Turbulent-Turbulent Flow
Lower Bound*	Equation (6.38) for $\alpha (X)$ Equation (6.40) for $\alpha (x)$
Upper Bound*	Equation (6.41) for $\alpha (X)$ Equation (6.42) for $\alpha (x)$
Mean Model	Equation (6.43) for $\alpha (X)$ Equation (6.44) for $\alpha (x)$

*The lower and upper bounds are reversed in the case of liquid fraction data.

CHAPTER 7

SUMMARY AND CONCLUSIONS

7.1 Summary of Present Research

This thesis examined two-phase flow modeling in circular pipes. It introduced new analytical models to the field of two-phase flow such as new properties of two-phase flow, the asymptotic flow model and the bounds model. All of the models developed in this thesis fulfill the need for simple and accurate predictive techniques.

Three new definitions for two-phase viscosity are introduced using the analogy between thermal conductivity in porous media and viscosity in two-phase flow. These new definitions for two-phase viscosity are satisfying the following two conditions: namely (i) the two-phase viscosity is equal to the liquid viscosity at the mass quality = 0%, and (ii) the two-phase viscosity is equal to the gas viscosity at the mass quality = 100%. These new definitions of two-phase viscosity can be used to compute the two-phase frictional pressure gradient using the homogeneous model. Expressing of two-phase frictional pressure gradient in a dimensionless form as Fanning friction factor (f_m) versus Reynolds number (Re_m) can also be done as it is often desirable. Analysis of new properties of two-phase flow showed that the new definitions of two-phase viscosity might be used to analyze the experimental data of two-phase frictional pressure gradient in circular pipes.

The asymptotic modeling method in two-phase flow is proposed by taking into account the important frictional interactions that occur at the interface between liquid and gas because the liquid and gas phases are assumed to flow dependently of each

other in the same pipe. The values of the Reynolds number for the liquid and gas phases are not important because the Churchill model that spanned the entire range of laminar, transition, and turbulent flow in pipes is introduced to define the Fanning friction factor. The obtained expressions of ϕ_l^2 and ϕ_g^2 are explicit for all flow conditions. The only unknown parameter in the asymptotic modeling method in two-phase flow is the fitting parameter (p). The value of the fitting parameter (p) corresponds to the minimum root mean square (RMS) error, e_{RMS} for any data set. Analysis of a simple asymptotic compact model for two-phase frictional pressure gradient in horizontal pipes revealed that the present asymptotic model was very successful in representing the two-phase frictional pressure gradient in horizontal pipes for published data of different pipe diameters. In the present asymptotic model, the two-phase frictional pressure gradient for $x \cong 0$ was nearly identical to single-phase liquid frictional pressure gradient. Also, the two-phase frictional pressure gradient for $x \cong 1$ was nearly identical to single-phase gas frictional pressure gradient. Comparison with other existing correlations and experimental data for both ϕ_l and ϕ_g versus X showed good agreement with the present asymptotic model. To have a robust model, one value of the fitting parameter (p) is chosen as $p = 1/3.25$ for large diameter (macro scale) and $p = 1/2$ for small diameter (micro scale).

Bounds on two-phase frictional pressure gradient in large circular pipes, bounds on two-phase frictional pressure gradient in small circular pipes and bounds on two-phase void fraction in circular pipes are proposed. The assumption of turbulent-turbulent flow is used in large circular pipes while the assumption of laminar-laminar flow is used in small circular pipes. Simple expressions of lower and

upper bounds are presented for each case. A simple model may be developed by averaging the lower and upper bounds. For two-phase frictional pressure gradient, the bounds model is also presented in dimensionless form as two-phase frictional multiplier (ϕ_l^2 and ϕ_g^2). Analysis of bounds on two-phase frictional pressure gradient and void fraction in circular pipes revealed that the present model was very successful in bounding the two-phase frictional pressure gradient and void fraction well for different working fluids over a wide range of mass fluxes, mass qualities, pipe diameters and saturation temperatures. Also, the proposed mean model provided excellent prediction of two-phase flow parameters.

7.2 Areas for Future Research

Several areas for future research that would benefit from a similar modeling approach are outlined below.

1. Evaluate two-phase frictional pressure gradient data at different conditions such as microgravity two-phase flow that can be found in space applications, liquid-metal two-phase flow, and cryogenic two-phase flow using the new definitions of two-phase viscosity based on the homogeneous model.
2. Simple asymptotic compact models for two-phase frictional pressure gradient data at different conditions such as microgravity two-phase flow that can be found in space applications, liquid-metal two-phase flow, and cryogenic two-phase flow.
3. Simple asymptotic compact models for two-phase frictional pressure gradient in different engineering systems such as porous media, packed beds and fractures. For example, two-phase gas/liquid flow through porous media has

many applications in agricultural, biomedical, chemical, mechanical, and petroleum engineering. For example, chemical engineering application dealing with porous media includes multi-phase flow in packed columns and catalytic reactors. In all situations, it is necessary to predict design parameters such as frictional pressure drop to determine the desired operating conditions and the size of the equipment required for the specific purposes. As a result, accurate expressions are needed to predict the two-phase frictional pressure drop.

4. Bounds on two-phase flow in noncircular shapes like annulus. Two-phase flow in an annulus has many different applications in oil and gas industry. For example, to remove or unload undesirable liquids that can be accumulate at the bottom of gas wells; a siphon tube is often installed inside of the tubing string. The normal permanency of the siphon tube in the tubing string needs the fluids to flow upward through the tubing string-siphon tube annulus. Another example of two-phase flow in an annulus can be found in wells under different types of artificial lift. To connect the prime mover unit on the surface to the pump at the bottom of the sucker rod pumping wells; a rod string is often installed inside of the tubing string. The fluids are pumped upward through the tubing string-rod string annulus.
5. Bounds on two-phase flow in inclined pipes. Two-phase flow at inclined orientation has many different applications in oil and gas industry. Due to the search for petroleum moves into new unexplored areas, the number of inclined or directional wells is increasing. In offshore drilling, many directional wells are usually drilled from one platform with deviations of 35° - 45° for economic reasons. In the permafrost areas of Canada and Alaska, the cost of drilling rig

foundations and the difficulty of transportation need that many wells be directionally drilled from one location.

6. Bounds on two-phase void fraction in minichannels and microchannels. Two-phase void fraction in minichannels and microchannels is an important design parameter because it determines heat and mass transfer rates. For example, prediction of convective boiling heat transfer in microchannels requires the knowledge of void fraction because the local heat transfer coefficient in vapor slug sections is different from that in liquid slug sections as forced convective evaporation of a liquid film surrounding a vapor slug occurs.
7. Finally, new concepts like scale analysis can be introduced to the field of two-phase flow. The scale analysis concept can be used in the analysis of laminar-laminar stratified two-phase flow in a horizontal rectangular channel. Scale analysis is one of the simplest and most cost effective methods in many engineering applications such as fluid mechanics and heat transfer. It produces order-of-magnitude results and trends (scaling laws). Also, it reveals the correct dimensionless form to present more exact results produced by more complicated methods. Scale analysis is beneficial as a preliminary step. The results of scale analysis can serve as guide to tell the researchers what to expect before using more complicated methods, and how to report the results in dimensionless form.

REFERENCES

- [1] Alves, G. E., 1954, "Co-Current Liquid-Gas Flow in a Pipeline Contactor," *Chemical Engineering Progress Symposium Series*, **50** (9), pp. 449-456.
- [2] Hetsroni, G., 1982, "Handbook of Multiphase Systems," Hemisphere Publishing Corporation, Chap. 4.
- [3] Baker, O., 1954, "Simultaneous Flow of Oil and Gas," *Oil Gas J.*, **53**, pp.185-195.
- [4] Scott, D. S., 1963, "Properties of Co-Current Gas- Liquid Flow," In *Advances in Chemical Engineering*, **4**, pp. 199-277.
- [5] Whalley, P. B., 1987, *Boiling, Condensation, and Gas-Liquid Flow*, Clarendon Press, Oxford.
- [6] Hewitt, G. F., and Roberts, D. N., 1969, "Studies of Two-Phase Flow Patterns by Simultaneous Flash and X-Ray Photography," AERE-M2159.
- [7] ASHRAE, 1993, *Handbook of Fundamentals*, ASHRAE, Atlanta, GA, Chap. 4.
- [8] Martinelli, R. C., and Nelson, D. B., 1948, "Prediction of Pressure Drop during Forced-Circulation Boiling of Water," *Trans. ASME*, **70** (6), pp. 695-702.
- [9] Keilin, V. E., Klimenko, E. Yu., and Kovalev, I. A., 1969, "Device for Measuring Pressure Drop and Heat Transfer in Two-Phase Helium Flow," *Cryogenics*, **9** (2), pp. 36-38.
- [10] Blasius, H., 1913, "Das Ähnlichkeitsgesetz bei Reibungsvorgängen in Flüssigkeiten," *Forsch. Gebiete Ingenieurw.*, **131**.
- [11] Borishansky, V. M., Paleev, I. I., Agafonova, F. A., Andreevsky, A. A., Fokin, B. S., Lavrentiev, M. E., Malyus-Malitsky, K. P., Fromzel V. N., and Danilova, G. P.,

REFERENCES

- 1973, "Some Problems of Heat Transfer and Hydraulics in Two-Phase Flows," *Int. J. Heat Mass Transfer*, **16** (6), pp. 1073-1085.
- [12] Bandel, J., 1973, "Druckverlust und Wärmeübergang bei der Verdampfung siedender Kältemittel im durchströmten waagerechten Rohr," Doctoral Dissertation, Universität Karlsruhe.
- [13] Dukler, A. E., Moye Wicks and Cleveland, R. G., 1964, "Frictional Pressure Drop in Two-Phase Flow. Part A: A Comparison of Existing Correlations for Pressure Loss and Holdup," and "Part B: An Approach through Similarity Analysis" *AIChE Journal*, **10** (1), pp. 38-51.
- [14] Taitel, Y., and Dukler, A. E., 1976, "A Model for Predicting Flow Regime Transitions in Horizontal and Near Horizontal Gas-Liquid Flow," *AIChE Journal*, **22** (1), pp. 47-55.
- [15] Tribbe, C., and Müller-Steinhagen, H. M., 2000, "An Evaluation of the Performance of Phenomenological Models for Predicting Pressure Gradient during Gas-Liquid Flow in Horizontal Pipelines," *International Journal of Multiphase Flow*, **26** (6), pp. 1019-1036.
- [16] Lockhart, R. W., and Martinelli, R. C., 1949, "Proposed Correlation of Data for Isothermal Two-Phase, Two-Component Flow in Pipes," *Chemical Engineering Progress Symposium Series*, **45** (1), pp. 39-48.
- [17] Zivi, S. M., 1964, "Estimation of Steady-State Void Fraction by Means of the Principle of Minimum Energy Production," *J. Heat Transfer*, **86**, pp. 247-252.
- [18] Wallis, G. B., 1969, *One-Dimensional Two-Phase Flow*, McGraw-Hill Book Company, New York.

REFERENCES

- [19] Rouhani S. Z., and Axelsson, E., 1970, "Calculation of Volume Void Fraction in the Subcooled and Quality Region," *Int. J. Heat Mass Transfer*, **13** (2), pp. 383-393.
- [20] Lun, I., Calay, R. K., and Holdo, A. E., 1996, "Modelling Two-Phase Flows Using CFD," *Applied Energy*, **53** (3), pp. 299-314.
- [21] Osman, E. A., and Aggour, M. A., 2002, "Artificial Neural Network Model for Accurate Prediction of Pressure Drop in Horizontal and Near-Horizontal-Multiphase Flow," *Petroleum Science and Technology*, **20** (1-2), pp. 1-15.
- [22] Osman, E. A., 2004, "Artificial Neural Network Models for Identifying Flow Regimes and Predicting Liquid Holdup in Horizontal Multiphase Flow," *SPE Production and Facilities*, **19** (1), pp. 33-40.
- [23] Shippen, M. E., and Scott, S. L., 2004, "A Neural Network Model for Prediction of Liquid Holdup in Two-Phase Horizontal Flow," *SPE Production and Facilities*, **19** (2), pp 67-76.
- [24] Collier, J. G. and Thome, J. R., 1994, *Convective Boiling and Condensation (3ed Edn)*, Clarendon Press, Oxford.
- [25] Chenoweth, J. M., and Martin, M. W., 1955, "Turbulent Two-Phase Flow," *Petroleum Refiner*, **34** (10), pp. 151-155.
- [26] Thom, J. R. S., 1964, "Prediction of Pressure Drop during Forced Circulation Boiling of Water," *Int. J. Heat Mass Transfer*, **7** (7), pp. 709-724.
- [27] Haywood, R. W., Knights, G. A., Middleton, G. F., and Thom, J. R. S., 1961, "An Experimental Study of the Flow Conditions and Pressure Drop of Steam-Water Mixtures at High Pressures in Heated and Unheated Tubes," *Inst. of Mech. Engrs. Proceedings*, Vol. **175**, No. 13, pp. 669-748.

REFERENCES

- [28] Baroczy, C. J., 1966, "A Systematic Correlation for Two-Phase Pressure Drop," *Chemical Engineering Progress Symposium Series*, **62** (44), pp. 232-249.
- [29] Turner, J. M., 1966, "Annular Two-Phase Flow," Ph.D. Thesis, Dartmouth College, Hanover, NH.
- [30] Chisholm, D., 1967, "A Theoretical Basis for the Lockhart-Martinelli Correlation for Two-Phase Flow," *Int. J. Heat Mass Transfer*, **10** (12), pp. 1767-1778.
- [31] Chisholm, D., 1968, "The Influence of Mass Velocity on Friction Pressure Gradients during Steam-Water Flow," *Thermodynamic and Fluid Mechanics Group Convection, Inst. of Mech. Engrs. Proceedings*, Bristol, London, Vol. **182**, Pt. 3H, pp. 336-341.
- [32] Chisholm, D., 1970, "Pressure Gradients during the Flow of Evaporating Two-Phase Mixtures," NEL Report No. 470, National Engineering Laboratory, East Kilbride, Glasgow.
- [33] Chisholm, D., 1973, "Pressure Gradients due to Friction during the Flow of Evaporating Two-Phase Mixtures in Smooth Tubes and Channels," *Int. J. Heat Mass Transfer*, **16** (2), pp. 347-358.
- [34] Chisholm, D., 1978, "Influence of Pipe Surface Roughness on Friction Pressure Gradient during Two-Phase Flow," *J. Mechanical Engineering Science*, **20** (6), pp. 353-354.
- [35] Johannessen, T., 1972, "A Theoretical Solution of the Lockhart-Martinelli Flow Model for Calculating Two Phase Flow Pressure Drop and Holdup," *Int. J. Heat Mass Transfer*, **15** (8), pp. 1443-1449.

REFERENCES

- [36] Serizawa, A. and Michiyoshi, I., 1973, "Void Fraction and Pressure Drop in Liquid Metal Two-Phase Flow," *Journal of Nuclear Science and Technology*, **10** (7), pp. 435-445.
- [37] Russell, T. W. F., Etchells, A. W., Jensen, R. H., and Arruda, P. J., 1974, "Pressure Drop and Holdup in Stratified Gas-Liquid Flow," *AIChE Journal*, **20** (4), pp. 664-669.
- [38] Chen, J. J., and Spedding, P. L., 1981, "An Extension of the Lockhart-Martinelli Theory of Two Phase Pressure Drop and Holdup", *Int. J. Multiphase Flow*, **7** (6), pp. 659-675.
- [39] Taitel, Y., and Dukler, A. E., 1976, "A Theoretical Approach to the Lockhart-Martinelli Correlation for Stratified Flow," *Int. J. Multiphase Flow*, **2** (5-6), pp. 591-595.
- [40] Asali, J. C., Hanratty, T. J., and Andreussi, P., 1985, "Interfacial Drag and Film Height for Vertical Annular Flow," *AIChE Journal*, **31** (6), pp. 895-902.
- [41] Crowley, C. G., and Izenon, M. G., 1989, "Design Manual for Microgravity Two-Phase Flow and Heat Transfer," Final Report from Create Inc. to Air Force Astronautics Laboratory, Report No. AL-TR-89-027.
- [42] Barnea, D., 1986, "Transition from Annular Flow and from Dispersed Bubble Flow-Unified Models for the Whole Range of Pipe Inclinations," *Int. J. Multiphase Flow*, **12** (5), pp. 733-744.
- [43] Manzano-Ruiz, J. J., 1988, "Semi-Empirical Model to Predict Frictional Pressure-Drop in Annular/Wavy Two-Phase Flow through Horizontal Pipes," *Fundamentals of Gas-Liquid Flows*, Chicago, IL.

REFERENCES

- [44] Hemeida, A., and Sumait, F., 1988, "Improving the Lockhart and Martinelli Two-Phase Flow Correlation by SAS," *Journal of Engineering Sciences, King Saud University*, **14** (2), pp. 423-435.
- [45] McAdams, W. H., Woods, W. K. and Heroman, L. C., 1942, "Vaporization inside Horizontal Tubes. II -Benzene-Oil Mixtures," *Trans. ASME*, **64** (3), pp. 193-200.
- [46] Cicchitti, A., Lombaradi, C., Silversti, M., Soldaini, G., and Zavattarlli, R., 1960, "Two-Phase Cooling Experiments- Pressure Drop, Heat Transfer, and Burnout Measurements," *Energia Nucleare*, **7** (6), pp. 407-425.
- [47] Bo Pierre, 1964, "Flow Resistance with Boiling Refrigerants," *ASHRAE J.*, **70** (9), pp. 58-77.
- [48] Powley, M. B., 1965, "Two-Phase Flow," *15th Canadian Chemical Engineering Conference*, Chemical Institute of Canada, Université Laval, Quebec City.
- [49] Lombardi, E., and Pedrocchi, E., 1972, "A Pressure Drop Correlation in Two-Phase Flow," *Energia Nucleare*, **19** (2), pp. 91-99.
- [50] Beggs, H. D., and Brill, J. P., 1973, "A Study of Two-Phase Flow in Inclined Pipes," *Journal of Petroleum Technology*, **25** (5), pp. 607-617.
- [51] Moody, L. F., 1944, "Friction Factors for Pipe Flow," *Trans. ASME*, **66** (8), pp. 671-677.
- [52] Lombardi, C., and Ceresa, I., 1978, "A Generalized Pressure Drop Correlation in Two-Phase Flow," *Energia Nucleare*, **25** (4), pp. 181-198.
- [53] Bonfanti, F., Ceresa, I., and Lombardi, C., 1979, "Two-Phase Pressure Drops in the Low Flowrate Region," *Energia Nucleare*, **26** (10), pp. 481-492.

REFERENCES

- [54] Bonfanti, F., Ceresa, I., and Lombardi, C., 1982, "Two Phase Densities and Pressure Drops in the Low Flowrate Region for Different Duct Inclinations," Proceedings of the 7th International Heat Transfer Conference, Volume 5: General Papers: Condensation, Two-Phase Flow Nuclear Reactor Heat Transfer, pp. 271-276, Munich, Germany.
- [55] Beattie, D. R. H., and Whalley, P. B., 1982, "A Simple Two-Phase Frictional Pressure Drop Calculation Method," *Int. J. Multiphase Flow*, **8** (1), pp. 83-87.
- [56] Lombardi, C., and Carsana, C. G., 1992, "Dimensionless Pressure Drop Correlation for Two-Phase Mixtures Flowing Upflow in Vertical Ducts Covering Wide Parameter Ranges," *Heat and Technology*, **10** (1-2), pp. 125-141.
- [57] Selander, W. N., 1978, "Explicit Formulas for the Computation of Friction Factors in Turbulent Pipe Flow," AECL. 6354.
- [58] Reddy, D. G., Sreepada, S. R., and Nahavandi, A. N., 1982, "Two-Phase Friction Multiplier Correlation for High-Pressure Steam-Water Flow," Electric Power Research Institute (Report) EPRI NP-2522.
- [59] Sher, N. C. and Green, S. J., 1959, "Boiling Pressure Drop in Thin Rectangular Channels," *Chemical Engineering Progress Symposium Series*, **55** (23), pp. 61-73.
- [60] Awad, M. M., and Muzychka, Y. S., 2004, "A Simple Two-Phase Frictional Multiplier Calculation Method", *Proceedings of IPC2004, International Pipeline Conference*, IPC04-0721, Vol. 1, pp. 475-483, Calgary, Alberta.
- [61] Bankoff, S. G., 1960, "A Variable Density Single-Fluid Model for Two-Phase Flow with Particular Reference to Steam-Water Flow," *J Heat Transfer*, **82** (4), pp. 265-272.

REFERENCES

- [62] Wisman, R., 1975, "Analytical Pressure Drop Correlation for Adiabatic Vertical Two-Phase Flow," *Applied Scientific Research (The Hague)*, **30** (5) pp. 367-380.
- [63] Friedel, L., 1979, "Improved Friction Pressure Drop Correlations for Horizontal and Vertical Two Phase Pipe Flow," paper E2, *European Two Phase Flow Group Meeting*, Ispra, Italy.
- [64] Whalley, P. B., 1987, *Boiling, Condensation, and Gas-Liquid Flow*, Clarendon Press, Oxford.
- [65] Friedel, L., 1985, "Two-Phase Frictional Pressure Drop Correlation for Vertical Downflow," *German Chemical Engineering*, **8** (1), pp. 32-40.
- [66] Olujic, Z., 1985, "Predicting Two-Phase-Flow Friction Loss in Horizontal Pipes," *Chemical Engineering*, **92** (13), pp. 45-50.
- [67] Olujic, Z., 1981, "Compute Friction Factors Fast for Flow in Pipes," *Chemical Engineering*, **88** (25), pp. 91-93.
- [68] Müller-Steinhagen, H., and Heck, K., 1986, "A Simple Friction Pressure Drop Correlation for Two-Phase Flow in Pipes," *Chemical Engineering Process*, **20**, pp. 297-308.
- [69] Xiao, J. J., Shoham, O. and Brill, J. P., 1990, "A Comprehensive Mechanistic Model for Two-Phase Flow in Pipelines," SPE 20631, SPE 65th Annual Meeting, New Orleans, LA.
- [70] Crowley, C. J., 1988, "Contents of the A. G. A. Data Bank (August 1988 Release)," Creare.
- [71] Gomez, L. E., Shoham, O., Schmidt, Z., Chokshi, R. N., Brown, A., and Northug, T., "A Unified Mechanistic Model for Steady-State Two-Phase Flow in

REFERENCES

Wellbores and Pipelines,” SPE 56520, 1999 SPE Annual Technical Conference and Exhibition, Houston, Texas.

[72] García, F., García, R., Padrino, J. C., Mata, C., Trallero J. L., and Joseph, D. D., 2003, “Power Law and Composite Power Law Friction Factor Correlations for Laminar and Turbulent Gas-Liquid Flow in Horizontal Pipelines,” *Int. J. Multiphase Flow*, **29** (10), pp. 1605-1624.

[73] Bendiksen, K. H., Malnes, D., Moe, R., and Nuland, S., 2004, “The Dynamic Two-Fluid Model OLGA: Theory and Application,” *SPE Reprint Series*, **58**, pp. 52-61.

[74] Hoogendoorn, C. J., 1959, “Gas-Liquid Flow in Horizontal Pipes,” *Chemical Engineering Science*, **9**, pp. 205-217.

[75] Isbin, H. S., Larson, H. C., Moen, R. H., Mosher, R. D., and Wickey, R. C., 1959, “Two-Phase Steam-Water Pressure Drops,” *Chemical Engineering Progress Symposium Series-Nuclear Engineering*, **55** (23), pp. 75-84.

[76] Chawla, J. M., 1967, “Wärmeübergang und Druckabfall in waagerechten Röhren bei der Strömung von verdampfenden Kältemitteln,” *VDI-Forschungsheft*, **523**.

[77] Grønnerud, R., 1972, “Investigation of Liquid Hold-Up, Flow Resistance and Heat Transfer in Circulation Type Evaporators. Part IV: Two-Phase Flow Resistance in Boiling Refrigerants,” *Bull. de l’Inst. du Froid*, pp. 127-138.

[78] Rashid, H. A. and Edward, R., 1984, “Effect of Mass Flux and System Pressure on Two-Phase Friction Multiplier,” *Chemical Engineering Communications*, **27** (3-4), pp. 209-229.

REFERENCES

- [79] Hashizume, K., 1983, "Flow Pattern, Void Fraction and Pressure Drop of Refrigerant Two-Phase Flow in a Horizontal Pipe. Part I: Experimental Data," *Int. J. Multiphase Flow*, **9** (4), pp. 399-410.
- [80] Hashizume, K., Ogiwara, H., and Taniguchi, H., 1985, "Flow Pattern, Void Fraction and Pressure Drop of Refrigerant Two-Phase Flow in a Horizontal Pipe. Part II: Analysis of Frictional Pressure Drop," *Int. J. Multiphase Flow*, Vol. **11** (5), pp. 643-658.
- [81] Bandel, J., and Schlünder, E. U., 1973, "Druckverlust und Wärmeübergang bei der Verdampfung siedender Kältemittel im durchströmten Rohr," *Chem.-Ing.-Tech.*, **45**, pp. 345-350.
- [82] Bandel, J., and Schlünder, E. U., 1974, "Frictional Pressure Drop and Convective Heat Transfer of Gas-Liquid Flow in Horizontal Pipes," *5th Int. Heat Transfer Conference*, Vol. **4**, B5.2, pp. 190-194, Tokyo, Japan.
- [83] Jung, D. S., and Radermacher, R., 1989, "Prediction of Pressure Drop During Horizontal Annular Flow Boiling of Pure and Mixed Refrigerants," *Int. J. Heat Mass Transfer*, **32** (12), pp. 2435-2446.
- [84] McAdams, W. H., 1954, *Heat Transmission* (3rd Edition), McGraw-Hill Book Company, New York.
- [85] Souza, A. L., Chato, J. C., Wattlelet, J. P., and Christoffersen, B. R., 1993, "Pressure Drop During Two-Phase Flow of Pure Refrigerants and Refrigerant-Oil Mixtures in Horizontal Smooth Tubes," *ASME Heat Transfer With Alternate Refrigerants, HTD*, Vol. **243**, pp. 35-41, Atlanta, Georgia, U. S. A.
- [86] Souza, A. L., and Pimenta, M. M., 1995, "Prediction of Pressure Drop During Horizontal Two-Phase Flow of Pure and Mixed Refrigerants," *ASME Conference*

REFERENCES

Cavitation and Multi-Phase Flow, HTD, Vol. **210**, pp. 161-171, South Carolina, U. S. A.

[87] Anderson, S. W., Rich, D. G., and Geary, D. F., 1966, "Evaporation of Refrigerant 22 in a Horizontal $\frac{3}{4}$ in. OD Tube," ASHRAE Transactions, **72**, pp. 28-42.

[88] Chaddock, J. B., and Noerager, J. A., 1966, "Evaporation of Refrigerant 12 in a Horizontal Tube with Constant Wall Heat Flux," ASHRAE Transactions, **72**, pp. 90-113.

[89] Ungar, E. K., and Cornwell, J. D., 1992, "Two-Phase Pressure Drop of Ammonia in Small Diameter Horizontal Tubes," *17th AIAA Aerospace Ground Testing Conference*, AIAA 92-3891, Nashville, TN.

[90] Huang, X., and Van Sciver, S. W., 1995, "Pressure Drop and Void Fraction of Two-Phase Helium Flowing in Horizontal Tubes," *Cryogenics*, **35** (7), pp. 467-474.

[91] Wang, C-C., Kuo, C. S., Chang, Y-J., and Lu, D. C., 1996, "Two-Phase Flow Heat Transfer and Friction Characteristics of R-22 and R-407C," ASHRAE Transactions, **102** (1), pp. 830-838.

[92] Yang, C-Y., and Webb, R. L., 1996, "Friction Pressure Drop of R-12 in Small Hydraulic Diameter Extruded Aluminum Tubes with and without Micro-Fins," *Int. J. Heat Mass Transfer*, **39** (4), pp. 801-805.

[93] Akers, W. W., Deans, H. A., and Crosser, O. K., 1959, "Condensation Heat Transfer within Horizontal Tubes," *Chemical Engineering Progress Symposium Series*, **55** (29), pp. 171-176.

REFERENCES

- [94] Zhang, M., and Webb, R. L., 2001, "Correlation of Two-Phase Friction for Refrigerants in Small-Diameter Tubes," *Experimental Thermal and Fluid Science*, **25** (3-4), pp. 131-139.
- [95] Chen, I. Y., Yang, K-S., and Wang, C-C., 2001, "Two-Phase Pressure Drop of Air-Water in Small Diameter Horizontal Tubes," *39th AIAA Aerospace Sciences Meeting & Exhibit*, AIAA 2001-1046, Reno, Nevada.
- [96] Troniewski, L., and Ulbrich, R., 1984, "Two-Phase Gas-Liquid Flow in Rectangular Channels," *Chemical Engineering Science*, **39** (4), pp. 751-765.
- [97] Chen, I. Y., Yang, K-S., and Wang, C-C., 2002, "An Empirical Correlation for Two-Phase Frictional Performance in Small Diameter Tubes," *Int. J. Heat Mass Transfer*, **45** (17), pp. 3667-3671.
- [98] Ould Didi, M. B., Kattan, N., and Thome, J. R., 2002, "Prediction of Two-Phase Pressure Gradients of Refrigerants in Horizontal Tubes," *Int. J. Refrigeration*, **25** (7), pp. 935-947.
- [99] Kattan, N., Thome, J. R., and Favrat, D., 1998, "Flow Boiling in Horizontal Tubes. Part 1: Development of a Diabatic Two-Phase Flow Pattern Map," *J Heat Transfer*, **120** (1), pp. 140-147.
- [100] Kattan, N., Thome, J. R., and Favrat, D., 1998, "Flow Boiling in Horizontal Tubes. Part 2: New Heat Transfer Data for Five Refrigerants," *J Heat Transfer*, **120** (1), pp. 148-155.
- [101] Kattan, N., Thome, J. R., and Favrat, D., 1998, "Flow Boiling in Horizontal Tubes. Part 3: Development of a New Heat Transfer Model Based on Flow Patterns," *J Heat Transfer*, **120** (1), pp. 156-165.

REFERENCES

- [102] Yoon, S. H., Cho, E. S., Hwang, Y. W., Kim, M. S., Min, K., and Kim, Y., 2004, "Characteristics of Evaporative Heat Transfer and Pressure Drop of Carbon Dioxide and Correlation Development," *Int. J. Refrigeration* **27** (2), pp. 111-119.
- [103] Soliman, R., 1984, "Two Phase Pressure Drop Computed," *Hydrocarbon Processing*, **63** (4), pp. 155-157.
- [104] Churchill, S. W., 1977, "Friction Factor Equation Spans all Fluid Flow Regimes," *Chemical Engineering*, **84** (24), pp. 91-92.
- [105] Kern, R., 1969, "How to Size Process Piping For Two-Phase Flow," *Hydrocarbon Processing*, **48** (10), pp. 105-116.
- [106] Parlikar, R. N., Kulkarni, G., Kumar, A., and Rao, Y. B., 1993, "Program Calculates Two Phase Flow Pressure Drop," *Chemical Engineering World*, **28** (9), pp. 155-161.
- [107] Armand, A. A., 1946, "Resistance to Two-Phase Flow in Horizontal Tubes (in Russian)," *Izv. VTI*, **15** (1), pp. 16-23. English translation, NLL M882, Boston Spa, Yorks: National Lending Library.
- [108] Massena, W. A., 1960, "Steam-Water Critical Flow Using the Separated Flow Model," *Hanford Atomic Products Operation Report*, HW-65739.
- [109] Flanigan, O., 1958, "Effect of Uphill Flow on Pressure Drop in Design of Two-Phase Gathering Systems," *Oil Gas J.*, **56**, pp. 132.
- [110] Levy, S., 1960, "Steam Slip-Theoretical Prediction from Momentum Model," *J Heat Transfer*, **82** (3), pp. 113-124.
- [111] Jones, A. B., 1961, "Hydrodynamic Stability of a Boiling Channel," *Knolls Atomic Power Laboratory*, KAPL-2170.

REFERENCES

- [112] Hughmark, G. A., 1962, "Hold up in Gas-Liquid Flow," Chemical Engineering Progress Symposium Series, **58** (4), pp. 62-65.
- [113] Brill, J., and Beggs, H., 1988, *Two-Phase Flow in Pipes*, 6th Edition.
- [114] García, F., García, R., and Joseph, D. D., 2005, "Composite Power Law Holdup Correlations in Horizontal Pipes," *Int. J. Multiphase Flow*, **31** (12), pp. 1276-1303.
- [115] Grapher Version 3.01, 2000, Golden Software Inc., Colorado.
- [116] Hewitt, G. F., King, R. D., and Lovegrove, P. C., 1962, "Techniques for Liquid Film and Pressure Drop Studies in Annular Two-Phase Flow," AERE-R3921, London, UK, Harwell, Atomic Energy Research Establishment.
- [117] Nishino, H., and Yamazaki, Y., 1963, "A New Method of Evaluating Steam Volume Fractions in Boiling Systems," *J. Soc. Atom Energy Jpn.*, **5**, pp. 39-46.
- [118] Kowalczewski, J. J., 1964, "Two-Phase Flow in an Unheated and Heated Tube," Diss. ETH Zürich, Swiss.
- [119] Küttükçüoğlu, A. and Njo, Y., 1967, "Dampfvolumenanteil (void) beim Verdampfen," TM-IN-307, EIR Würenlingen.
- [120] Löscher, K. and Reingardt, H., 1973, "Der Schlupf bei ausgebildeter adiabater Einkomponenten-Zweiphasenströmung dampfförmig-flüssig im horizontellen Rohr," *Wiss. Zeitschrift T. U. Dresden*, **22** (5), pp. 813-819.
- [121] Friedel, L., 1975, "Modellgesetz für den Reibungsdruckverlust in der Zweiphasenströmung," VDI-Forsch.-Heft 572.
- [122] Marchaterre, J. F., Petrick, M., Lottes, P. A., Weatherhead, R. J., and Flinn, W. S., 1960, "Natural and Forced-Circulation Boiling Studies," ANL-5735, Chicago, Illinois, Argonne National Laboratory.

REFERENCES

- [123] Bae, S., Maulbetsch, J. S., and Rohsenow, W. M., 1969, "Refrigerant Forced-Convection Condensation inside Horizontal Tubes," DSR 79760-64, ASHRAE RP 63, Department of Mechanical Engineering, Massachusetts Institute of Technology, Cambridge, MA.
- [124] Soliman, M., Schuster, J. R., and Berenson, P. J., 1968, "A General Heat Transfer Correlation for Annular Flow Condensation," *J. Heat Transfer*, **90**, pp. 267-276.
- [125] Baroczy, C. J., 1965, "Correlation of Liquid Fraction in Two-Phase Flow with Applications to Liquid Metals," *Chemical Engineering Progress Symposium Series*, **61**, pp. 179-191.
- [126] Domanski, P. and Didion, D., 1983, "Computer Modeling of the Vapor Compression Cycle with Constant Flow Area Expansion Device," *NBS Building Science*, series 155.
- [127] Zuber, N., and Findlay, J. A., 1965, "Average Volumetric Concentration in Two-Phase Flow Systems," *J. Heat Transfer*, **87**, pp. 453-468.
- [128] Zuber, N., Staub, F. W., Bijwaard, G., and Kroeger, P., 1967, "Steady State and Transient Void Fraction in Two-Phase Flow Systems," GEAP-5417, San Jose, California, General Electric Co.
- [129] Guzhov, A., Mamayev, V., and Odishariya, G., 1967, "A Study of Transportation in Gas-Liquid Systems," *10th International Gas Conference*, Hamburg, Germany.
- [130] Eaton, B., Andrews, D., Knowles, C., Silberberg, I. and Brown, K., 1967, "The Prediction of Flow Patterns, Liquid Holdup and Pressure Losses Occurring During

REFERENCES

Continuous Two-Phase Flow in Horizontal Pipelines,” *J. Petroleum Technology*, **19** (6), pp. 815–828.

[131] Ros, N., 1961, “Simultaneous Flow of Gas and Liquid as Encountered in Well Tubing,” *J. Petroleum Technology*, **13** (10), pp. 1037–1049.

[132] Wallis, G. B., 1970, “Annular Two-Phase Flow. Part 1: A Simple Theory,” *ASME J. Basic Engineering*, **92** (1), pp. 59-72.

[133] Wallis, G. B., 1970, “Annular Two-Phase Flow. Part 2: Additional Effects,” *ASME J. Basic Engineering*, **92** (1), pp. 73-82.

[134] Premoli, A., Franceso, D. Di., and Prina, A., 1970, “An Empirical Correlation for Evaluating Two-Phase Mixture Density under Adiabatic Conditions,” paper B9, *European Two Phase Flow Group Meeting*, Milan, Italy.

[135] Smith, S. L., 1971, “Void Fractions in Two-Phase Flow: A Correlation Based Upon an Equal Velocity Head Model,” *Heat and Fluid Flow*, **1** (1), pp. 22-39.

[136] Bonnacaze, R., Erskine, W., and Greskovich, E., 1971, “Holdup and Pressure Drop for Two-Phase Slug Flow in Inclined Pipelines,” *AIChE J.*, **17** (5), pp. 1109–1113.

[137] Chisholm, D., 1973, “Void Fraction during Two-Phase Flow,” *J. Mechanical Engineering Science*, **15** (3), pp. 235-236.

[138] Mattar, L., and Gregory, G. A., 1974, “Air-Oil Slug Flow in an Upward-Inclined Pipe-I: Slug Velocity, Holdup and Pressure Gradient,” *J. Can. Petroleum Technology*, **13** (1), pp. 69–76.

[139] Madsen, N., 1974, “Void Fraction Correlation for Vertical and Horizontal Bulk-Boiling of Water,” *Proceeding of 5th International Heat Transfer Conference*, Vol. 4, paper B5.1, pp. 185-189, Tokyo, Japan.

REFERENCES

- [140] Moussalli, G. and Chawla, J. M., 1974, "Pressure Drop and Void Fraction in Bubble Flow," European Two-Phase Flow Group Meeting, Harwell.
- [141] Butterworth, D., 1975, "A Comparison of Some Void Fraction Relationships for Gas-Liquid Flow," *Int. J. Multiphase Flow*, **1** (6), pp. 845-850.
- [142] Nabizadeh, H., 1976, "Übertragungsgesetze für den Dampfvolumenanteil zwischen Freon and Wasser. EIR-Wurenlingen, Vortrag auf dem R12 Kolloquium im Inst. für Verahrenstechnik der T. U. Hanover, Germany.
- [143] Yamazaki, Y., and Yamaguchi, K., 1976, "Void Fraction Correlation for Boiling and Non-Boiling Vertical Two-Phase Flows in Tube," *J. Nuclear Science and Technology*, **13** (12), pp. 701-707.
- [144] Trimble, G. D., and Turner, W. J., 1977, "Characteristics of Two-Phase One-Component Flow with Slip," *Nuclear Engineering Design*, **42**, pp. 287-295.
- [145] Beattie, D. R. H., 1973, "A Note on the Calculation of Two-Phase Pressure Losses," *Nuclear Engineering Design*, **25**, pp. 395-402.
- [146] Ishii, M., 1977, "One-Dimensional Drift-Flux Model and Constitutive Equations Between the Phases in Various Two-Phase Flow Regimes," ANL77-47, Argonne National Laboratory, Argonne.
- [147] Gregory, G. A., Nicholson, M. K., and Aziz, K., 1978, "Correlation of the Liquid Volume Fraction in the Slug for Horizontal Gas-Liquid Slug Flow," *Int. J. Multiphase Flow*, **4** (1), pp. 33-39.
- [148] Hubbard, M. G., 1965, "An Analysis of Horizontal Gas-Liquid Slug Flow," Ph. D. Dissertation, the University of Houston, Houston, Texas.
- [149] Gardner, G. C., 1980, "Fractional Vapour Content of a Liquid Pool Through Which Vapour Is Bubbled," *Int. J. Multiphase Flow*, **6** (5), pp. 399-410.

REFERENCES

- [150] Chen, J. J. J., and Spedding, P. L., 1983, "An Analysis of Holdup in Horizontal Two-Phase Gas-Liquid Flow," *Int. J. Multiphase Flow*, **9** (2), pp. 147-159.
- [151] Spedding, P. L., and Chen, J. J. J., 1984, "Holdup in Two Phase Flow," *Int. J. Multiphase Flow*, **10** (3), pp. 307-336.
- [152] Tandon, T. N., Varma H. K., and Gupta, C. P., 1985, "A Void Fraction Model for Annular Two-Phase Flow," *Int. J. Heat Mass Transfer*, **28** (1), pp. 191-198.
- [153] Liao, L. H., Parlos, A., and Griffith, P., 1985, "Heat Transfer, Carryover and Fall Back in PWR Steam Generators during Transients," NUREG/CR-4376, EPRI NP-4298.
- [154] Spedding, P.L. and Chen, J.J.J., 1986, "Hold-up in Multiphase Flow," *Encyclopedia of Fluid Mechanics*, **3**, pp. 408-415.
- [155] Minami, K., and Brill, J., 1987, "Liquid Holdup in Wet-Gas Pipelines," *SPE Production Engineering*, **2** (1), SPE 14535, pp. 36-44.
- [156] Hart, J., Hamersma, P. J., and Fortuin, J. M. H., 1989, "Correlations Predicting Frictional Pressure Drop and Liquid Holdup during Horizontal Gas-Liquid Pipe Flow with a Small Liquid Holdup," *Int. J. Multiphase Flow*, **15** (6), pp. 947-964.
- [157] Huq, R., 1990, "An Analytical Two-Phase Flow Void Fraction Prediction Method," AIAA/ASME 5th Joint Thermophysics and Heat Transfer Conference, Paper No. 90-1738
- [158] Schmidt J., 1993, "Berechnung und Messung der Druckänderungen über plötzliche scharfkantige Rohrerweiterungen und -verengungen bei Gas/Dampf-Flüssigkeitsströmung," *Fortschr. Ber. VDI*, **7** (236).
- [159] Schmidt J., and Friedel, L., 1997, "Two-Phase Pressure Drop across Sudden Contractions in Duct Areas," *International J. Multiphase Flow*, **23** (2), pp. 283-299.

REFERENCES

- [160] Chexal, B., Horowitz, J. S., and Lellouche, G. S., 1991, "An Assessment of Eight Void Fraction Models for Vertical Flows," *Nuclear Energy and Design*, **126**, pp. 71-88.
- [161] Takeuchi, K., Young, M. Y., and Hochreiter, L. E., 1992, Generalized drift flux correlation for vertical flow, *Nuclear Science and Engineering*, **112** (2), pp. 170-180.
- [162] Steiner, D., 1993, "Heat Transfer to Boiling Saturated Liquids," *VDI-Warmeatlas (VDI Heat Atlas)*, Editor: Ingenieure, V. D., VDI-Gesellschaft Verfahrenstechnik und Chemie-in-genieurwesen (GCV), Translator: Fullarton, J. W., Dusseldorf, Germany.
- [163] El Hajal, J., Thome, J. R., and Cavallini, A., 2003, "Condensation in Horizontal Tubes, Part 1: Two-Phase Flow Pattern Map," *Int. J. Heat Mass Transfer*, **46** (18), pp. 3349-3363.
- [164] Thome, J. R., El Hajal, J., and Cavallini, A., 2003, "Condensation in Horizontal Tubes, Part 2: New Heat Transfer Model Based on Flow Regimes," *Int. J. Heat Mass Transfer*, **46** (18), pp. 3365-3387.
- [165] Abdul-Majeed, G., 1996, "Liquid Holdup in Horizontal Two-Phase Gas-Liquid Flow," *J. Petroleum Science Engineering*, **15** (2-4), pp. 271-280.
- [166] Spedding, P., Watterson, J., Raghunathan, S., and Ferguson, M., 1998, "Two-Phase Co-Current Flow in Inclined Pipe," *Int. J. Heat Mass Transfer*, **41** (24), pp. 4205-4228.
- [167] Graham, D. M., Kopke, H. P., Wilson, M. J., Yashar, D. A., Chato, J. C. and Newell, T. A., 1999, "An Investigation of Void Fraction in the Stratified/Annular Flow Regions in Smooth Horizontal Tubes," ACRC TR-144, Air Conditioning and Refrigeration Center, University of Illinois at Urbana-Champaign.

REFERENCES

- [168] Hulburt, E. T. and Newell, T. A., 1997, "Modeling of the Evaporation and Condensation of Zeotropic Refrigerants Mixtures in Horizontal Annular Flow," ACRC TR-129, Air Conditioning and Refrigeration Center, University of Illinois at Urbana-Champaign.
- [169] Gomeza, L. E., Shohama, O., and Taitel, Y., 2000, "Prediction of Slug Liquid Holdup: Horizontal to Upward Vertical Flow," *Int. J. Multiphase Flow*, **26** (3), pp. 517-521.
- [170] Sakaguchi, T., Tsubone, H., Sadatomi, M., Minagawa, H. and Shakutsui, H., 2003, "Correlations of Void Fraction of Gas-Liquid Two-Phase Flows in Vertical Pipes," Proceedings of 3rd European-Japanese Two-Phase Flow Group Meeting, Certosa di Pontignano, Italy, 7 pages in CD-ROM.
- [171] Yun-Long, Z., Bin, S., Wen-Peng, H., Wei, L., Jing, Y., and Ling, Z., 2005, "Mathematical Model of Void Fraction of Gas-Liquid Two-Phase Annular Flow in Vertical Tubes," *Journal of Engineering Thermophysics*, **26** (4), pp. 625-627.
- [172] Lin, S., Kwok, C. C. K., Li, R. Y., Chen, Z. H., and Chen, Z. Y., 1991, Local Frictional Pressure Drop during Vaporization for R-12 through Capillary Tubes," *Int. J. Multiphase Flow*, **17** (1), pp. 95-102.
- [173] Fourar, M. and Bories, S., 1995, "Experimental Study of Air-Water Two-Phase Flow Through a Fracture (Narrow Channel)," *Int. J. Multiphase Flow*, **21** (4), pp. 621-637.
- [174] Davidson, W. F., Hardie, P. H., Humphreys, C. G. R., Markson, A. A., Mumford, A. R., and Ravese, T., 1943, "Studies of Heat Transmission Through Boiler Tubing at Pressures from 500-3300 lbs," *Trans. ASME*, **65** (6), pp. 553-591.

REFERENCES

- [175] Owens, W. L., 1961, "Two-Phase Pressure Gradient," *ASME International Developments in Heat Transfer*, Part II, pp. 363-368.
- [176] Carson, J. K., Lovatt, S. J., Tanner, D. J., and Cleland, A. C., 2005, "Thermal Conductivity Bounds for Isotropic, Porous Materials," *Int. J. Heat Mass Transfer*, **48** (11), pp. 2150-2158.
- [177] Hashin, Z., and Shtrikman, S., 1962, "A Variational Approach to the Theory of the Effective Magnetic Permeability of Multiphase Materials," *J. Appl. Phys.*, **33**, pp. 3125-3131.
- [178] Landauer, R., 1952, "The Electrical Resistance of Binary Metallic Mixtures," *J. Appl. Phys.*, **23**, pp. 779-784.
- [179] Kirkpatrick, S., 1973, "Percolation and Conduction," *Rev. Mod. Phys.*, **45**, pp. 574-588.
- [180] Müller-Steinhagen, H., 1984, "Wärmeübergang und Fouling Beim Strömungssieden Von Argon und Stickstoff im Horizontalen Rohr," *Fortschr. Ber. VDI Z.* **6**.
- [181] Tran, T. N., Chyu, M.-C., Wambsganss, M. W., and France, D. M., 2000, "Two-Phase Pressure Drop of Refrigerants during Flow Boiling in Small Channels: An Experimental Investigation and Correlation Development," *Int. J. Multiphase Flow*, **26** (11), pp. 1739-1754.
- [182] Cavallini, A., Del Col, D., Doretti, L., Matkovic, M., Rossetto L., and Zilio, C., 2005, "Two-Phase Frictional Pressure Gradient of R236ea, R134a and R410A inside Multi-Port Mini-Channels," *Experimental Thermal and Fluid Science*, **29** (7), pp. 861-870.

REFERENCES

- [183] Field, B. S., and Hrnjak, P., 2007, "Adiabatic Two-Phase Pressure Drop of Refrigerants in Small Channels," *Heat Transfer Engineering*, **28** (8-9), pp. 704-712. Also presented at *The Fourth International Conference on Nanochannels, Microchannels and Minichannels (ICNMM 2006), Session: Two-Phase Flow, Experiments in Minichannels*, ICNMM2006-96200, Stokes Research Institute, University of Limerick, Ireland.
- [184] Carey, V. P., 1992, *Liquid-Vapor Phase-Change Phenomena : An Introduction to the Thermophysics of Vaporization and Condensation Processes in Heat Transfer Equipment*, Hemisphere Pub. Corp., Washington, D.C, Chap. 10.
- [185] MapleTM Release 9, 2003, Waterloo Maple Software, Waterloo, ON.
- [186] Churchill, S. W. and Usagi, R., 1972, "A General Expression for the Correlation of Rates of Transfer and Other Phenomena," *American Institute of Chemical Engineers*, **18** (6), pp. 1121-1128.
- [187] Churchill, S. W., 1988, *Viscous Flows: The Practical Use of Theory*, Butterworths, Boston, MA.
- [188] Kraus, A. D. and Bar-Cohen, A., 1983, *Thermal Analysis and Control of Electronic Equipment*, Hemisphere Publishing Corporation, New York.
- [189] Yovanovich, M. M., 2003, "Asymptotes and Asymptotic Analysis for Development of Compact Models for Microelectronic Cooling," *19th Annual Semiconductor Thermal Measurement and Management Symposium and Exposition (SEMI-THERM)*, San Jose, CA.
- [190] Churchill, S. W., and Ozoe, H., 1973, "Correlations for Laminar Forced Convection with Uniform Heating in Flow over a Plate and in Developing and Fully Developed Flow in a Tube," *J. of Heat Transfer*, **95** (1), pp. 78-84.

REFERENCES

- [191] Churchill, S. W., and Ozoe, H., 1973, "Correlations for Laminar Forced Convection in Flow over an Isothermal Flat Plate and in Developing and Fully Developed Flow in an Isothermal Tube," *J. of Heat Transfer*, **95** (3), pp. 416-419.
- [192] Raithby, G. D., and Hollands, K. G. T., 1998, *Handbook of Heat Transfer*, W. M. Rohsenow, J. P. Hartnett, and Y. I. Cho, eds., McGraw-Hill, New York, Chap. 4.
- [193] Yovanovich, M. M., Teertstra, P. M., and Culham, J. R., 1995, "Modeling Transient Conduction from Isothermal Convex Bodies of Arbitrary Shape," *Journal of Thermophysics and Heat Transfer*, **9** (3), pp. 385-390.
- [194] Teertstra, P. M., Yovanovich, M. M., and Culham, J. R., 1997, "Pressure Loss Modeling for Surface Mounted Cuboid-Shaped Packages in Channel Flow," *IEEE Transactions on Components, Packaging, and Manufacturing Technology, Part A*, **20** (4), pp. 463-471.
- [195] Muzychka, Y. S., 1999, "Analytical and Experimental Study of Fluid Friction and Heat Transfer in Low Reynolds Number Flow Heat Exchangers," Ph.D. Thesis, University of Waterloo, ON.
- [196] Muzychka, Y. S., and Yovanovich, M. M., 1998, "Modeling Friction Factors in Non-Circular Ducts for Developing Laminar Flow," *AIAA 98-2492, 2nd Theoretical Fluid Mechanics Meeting*, Albuquerque, NM.
- [197] Muzychka, Y. S., and Yovanovich, M. M., 1998, "Modeling Nusselt Numbers for Thermally Developing Laminar Flow in Non-Circular Ducts," *AIAA 98-2586, 7th AIAA/ ASME Joint Thermophysics and Heat Transfer Conference*, Albuquerque, NM.
- [198] Muzychka, Y. S., and Yovanovich, M. M., 2002, "Laminar Flow Friction and Heat Transfer in Non-Circular Ducts and Channels: Part I - Hydrodynamic Problem," *Compact Heat Exchangers: A Festschrift on the 60th Birthday of Ramesh K. Shah*, G.

REFERENCES

- P. Celata, B. Thonon, A. Bontemps, and S. Kandlikar, eds., Grenoble, France, pp. 123–130.
- [199] Muzychka, Y. S., and Yovanovich, M. M., 2002, “Laminar Flow Friction and Heat Transfer in Non-Circular Ducts and Channels: Part II - Thermal Problem,” *Compact Heat Exchangers: A Festschrift on the 60th Birthday of Ramesh K. Shah*, G. P. Celata, B. Thonon, A. Bontemps, and S. Kandlikar, eds., Grenoble, France, pp. 131–139.
- [200] Chisholm, D., 1983, *Two-Phase Flow in Pipelines and Heat Exchangers*, George Godwin in Association with Institution of Chemical Engineers, London.
- [201] Awad, M. M., and Muzychka, Y. S., 2004, “A Simple Asymptotic Compact Model for Two-Phase Frictional Pressure Gradient in Horizontal Pipes”, *Proceedings of IMECE 2004, Fluids Engineering, General Papers, FE-8 A Gen. Pap. : Multiphase Flows*, IMECE2004-61410, Anaheim, California.
- [202] Dukler, A. E., 1964, “Pressure Drop in Horizontal Conduits,” *Special Summer Program in Two-Phase Gas-Liquid Flow*, P. Griffith, and S. W. Gouse, Jr., eds., Massachusetts Institute of Technology, Massachusetts.
- [203] Govier, G. W. and Omer, M. M., 1962, “Horizontal Pipeline Flow of Air-Water Mixtures,” *The Canadian Journal of Chemical Engineering*, **40** (3), pp. 93-104.
- [204] Janssen, E., and Kervinen, J. A., 1964, “Two-Phase Pressure Losses,” Final Report, Report No. GEAP-4634, San Jose, California, General Electric Company.
- [205] Cheremisinoff, N. P. and Davis, E. J., 1979, “Stratified Turbulent-Turbulent Gas-Liquid Flow,” *AIChE J.*, **25** (1), pp. 48-56.

REFERENCES

- [206] Lee, H., J., and Lee, S., Y., 2001, "Pressure Drop Correlations for Two-Phase Flow within Horizontal Rectangular Channels with Small Heights," *Int. J. Multiphase Flow*, **27** (5), pp. 783-796.
- [207] Chung P. M.-Y., and Kawaji, M., 2004, "The Effect of Channel Diameter on Adiabatic Two-Phase Flow Characteristics in Microchannels," *Int. J. Multiphase Flow*, **30** (7-8), pp. 735-761.
- [208] Kawaji, M., Mori, K., and Bolintineanu, D., 2005, "The Effects of Inlet Geometry on Gas-Liquid Two-Phase Flow in Microchannels," *Proceedings of ICMM2005, 3rd International Conference on Microchannels and Minichannels, ICMM2005-75087*, Toronto, Ontario.
- [209] Ohtake, H., Koizumi, Y., and Takahashi, H., 2005, "Frictional Pressure Drops of Single-Phase and Gas-Liquid Two-Phase Flows in Circular and Rectangular Microchannels," *Proceedings of ICMM2005, 3rd International Conference on Microchannels and Minichannels, ICMM2005-75147*, Toronto, Ontario.
- [210] Awad, M. M., and Muzychka, Y. S., 2005 "Bounds on Two-Phase Flow. Part I. Frictional Pressure Gradient in Circular Pipes", *Proceedings of IMECE 2005, Session: FED-11 B Numerical Simulations and Theoretical Developments for Multiphase Flows-I*, IMECE2005-81493, Orlando, Florida.
- [211] Awad, M. M., and Muzychka, Y. S., 2005, "Bounds on Two-Phase Flow. Part II. Void Fraction in Circular Pipes", *Proceedings of IMECE 2005, Session: FED-11 B Numerical Simulations and Theoretical Developments for Multiphase Flows-I*, IMECE2005-81543, Orlando, Florida.

REFERENCES

- [212] Faghri, A., and Zhang, Y., 2006, *Transport Phenomena in Multiphase Systems*, Elsevier Inc., Chap. 11, pp. 874.
- [213] Awad, M. M., and Muzychka, Y. S., 2007, "Bounds on Two-Phase Frictional Pressure Gradient in Minichannels and Microchannels", *Heat Transfer Engineering*, **28** (8-9), pp. 720-729. Also presented at *The Fourth International Conference on Nanochannels, Microchannels and Minichannels (ICNMM 2006), Session: Two-Phase Flow, Numerical and Analytical Modeling*, ICNMM2006-96174, Stokes Research Institute, University of Limerick, Ireland.
- [214] Ali, M., Sadatomi, M., and Kawaji, M., 1993. "Adiabatic Two-Phase Flow in Narrow Channels between Two Flat Plates," *The Canadian Journal of Chemical Engineering*, **71** (5), pp. 657-666.
- [215] White, F. M., 2005, *Viscous Fluid Flow*, McGraw-Hill Book Co, 3rd edition, Chap. 3.
- [216] Larson, H. C., 1957, "Void Fraction of Two-Phase Steam-Water Mixture," M. S. Thesis, University of Minnesota.
- [217] Wojtan, L., Ursenbacher, T., and Thome, J. R., 2004, "Interfacial Measurements in Stratified Types of Flow. Part II: Measurements for R-22 and R-410A," *Int. J. Multiphase Flow*, **30** (2), pp. 125-137.
- [218] Bergelin, O. P. and Gazeley, C. Jr., 1949, "Cocurrent Gas-Liquid Flow. I. Flow in Horizontal Tubes," *ASME Proc. Heat Transfer and Fluid Mech. Inst.*, NY, pp. 5-18.

APPENDIX A**LIST OF RESEARCH PAPERS**

For reference purposes, list of research papers published from this thesis is given in this appendix.

A.1 Awad, M. M., and Muzychka, Y. S., 2004, "A Simple Two-Phase Frictional Multiplier Calculation Method", *Proceedings of IPC2004, International Pipeline Conference*, IPC04-0721, Vol. 1, pp. 475-483, Calgary, Alberta.

A.2 Awad, M. M., and Muzychka, Y. S., 2004, "A Simple Asymptotic Compact Model for Two-Phase Frictional Pressure Gradient in Horizontal Pipes", *Proceedings of IMECE 2004, Fluids Engineering, General Papers, FE-8 A Gen. Pap. : Multiphase Flows*, IMECE2004-61410, Anaheim, California.

A.3 Awad, M. M., and Muzychka, Y. S., 2005 "Bounds on Two-Phase Flow. Part I. Frictional Pressure Gradient in Circular Pipes", *Proceedings of IMECE 2005, Session: FED-11 B Numerical Simulations and Theoretical Developments for Multiphase Flows-I*, IMECE2005-81493, Orlando, Florida.

A.4 Awad, M. M., and Muzychka, Y. S., 2005, "Bounds on Two-Phase Flow. Part II. Void Fraction in Circular Pipes", *Proceedings of IMECE 2005, Session: FED-11 B Numerical Simulations and Theoretical Developments for Multiphase Flows-I*, IMECE2005-81543, Orlando, Florida.

A.5 Awad, M. M., and Muzychka, Y. S., 2007, "Bounds on Two-Phase Frictional Pressure Gradient in Minichannels and Microchannels", *Heat Transfer Engineering*,

28 (8-9), pp. 720-729. Also presented at *The Fourth International Conference on Nanochannels, Microchannels and Minichannels (ICNMM 2006), Session: Two-Phase Flow, Numerical and Analytical Modeling*, ICNMM2006-96174, Stokes Research Institute, University of Limerick, Ireland.

Papers A.3 and A.4 are published in the following book:

Faghri, A., and Zhang, Y., 2006, *Transport Phenomena in Multiphase Systems*, Elsevier Inc., Chap. 11.

